THE PHOTOCHEMISTRY AND PHOTOPHYSICS OF SOME STYRENES

by

Roger Leslie Brentnall

B.Sc. in Chemistry, Southampton University

A dissertation submitted in partial
fulfilment of the requirements for the degree of
Doctor of Philosophy at the University of Southampton

August 1981

UNIVERSITY OF SOUTHAMPTON

ABSTRACT

FACULTY OF SCIENCE

CHEMISTRY

Doctor of Philosophy

THE PHOTOCHEMISTRY AND PHOTOPHYSICS OF SOME STYRENES

by Roger Leslie Brentnall

A range of styrenes has been shown to form fluorescent exciplexes on irradiation in the presence of tertiary amines. The results of a mechanistic study of the photochemical and photophysical consequences of these bimolecular interactions are presented here. The systems which have been examined in the greatest detail in this context are those involving interaction of triethylamine (Et_3N) with Styrene itself, trans-1-phenylprop-1-ene and Indene. Using principally the techniques of Single Photon Counting and Fluorescence Spectroscopy, under a variety of conditions of solvent and temperature, a detailed kinetic analysis of the processes of exciplex formation and decay has been carried out for these systems.

Due to the polar nature of the exciplexes, strong correlations of various experimental parameters with the electron accepting ability of the initially excited styrenes have been observed. Over the range of systems studied, the exciplex emission maxima, free energy for complex formation and the various individual rate parameters (including apparently the rate constant for photoproduct formation) were all found to vary systematically in this way. In the case of the trans-1-phenylprop-1-ene/Et_3N system, the fact that photoproduct formation (and geometric isomerisation) may occur via the exciplex intermediate was demonstrated using the technique of exciplex quenching.

As a background to the study of the styrene/amine interactions, the unimolecular photophysics of a range of compounds containing the styryl group, was examined. The results obtained support the view that the relative orientation of the phenyl and olefinic moieties is of particular importance in determining the photophysical characteristics of these compounds.

ACKNOWLEDGEMENTS

I am most grateful to the many friends I made during my time at Southampton for providing an informal and, at the same time, stimulating atmosphere. There really are too many names to list individually so I would just like to thank in particular the other members of the Photochemistry Group at Southampton. These were my supervisor, Kingsley Salisbury, together with Geoff Abbott, Geoff Mant, Dave Sadler, Ken Ghiggino, Robin Humphry-Baker, Paul Crosby, Aurelio Ferreira and those honorary photochemists, John Stibbard and Simon Jenny. This is not to mention three intakes of M.Sc. students who provided many hours of harmless entertainment and, of course, last but not least, Gail, for her expert typing and often strained patience.

[redacted]

R.L. BRENTNALL

CONTENTS

CHAPTER 1

INTRODUCTION

1.1 The Unimolecular Photophysical Characteristics of Styrenes

Styrene is the simplest conjugated aryl olefin and as such, its electronic absorption and emission characteristics have received considerable attention. In particular, it is the observation of fluorescence which has permitted an examination of the unimolecular photophysics of Styrene and its derivatives. Of the wide variety of compounds incorporating the styryl group, those which have been studied in detail in this context are principally the cyclic and acyclic derivatives, containing alkyl substituents. Table 1.1 provides an indication of the range of structural types examined and referred to during the course of this work, together with the nomenclature and abbreviations adopted, throughout.

In general, on excitation in both the gas phase[1] and in solution[2], under a variety of conditions of solvent and temperature, these compounds are observed to fluoresce. However, the quantum yields of fluorescence (Φ_F) recorded for the styrenes are often found to be substantially less than unity. This is apparently a result of the presence in each case of at least two radiationless decay processes which may compete effectively with the radiative relaxation route, particularly at room temperature. The involvement of both Internal Conversion (IC) and Intersystem Crossing (ISC) processes in relaxation from the first excited singlet state of styrenes has been postulated and, as with the closely related stilbenes[3], the importance of internal rotation in radiationless decay has been recognised.

It can be seen that for those styrenes containing two different substituents at the C-8 (β) position, rotation about the $C_{7,8}$ essential double bond on excitation, can lead to geometric isomerisation and indeed photoisomerisation has been observed for

Table 1.1

The Structure of the Styrenes Referred to and the Nomenclature and Abbreviations Adopted Throughout this Work

Structure	Nomenclature*	Abbreviation
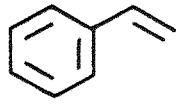	Styrene	St
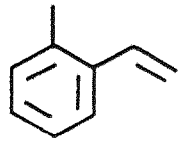	O-Methyl Styrene	OMe
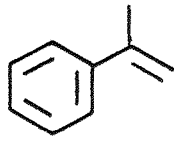	2-Phenylpropene (α-Methyl Styrene)	2PP
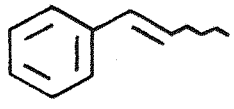	cis & trans 1-Phenylprop-1-ene (c,t-β-Methyl Styrene)	cPP,tPP
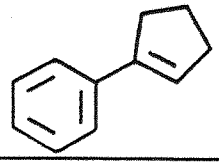	1-Phenylcyclopent-1-ene	PcP
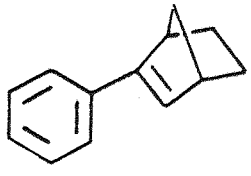	1-Phenylnorborn-1-ene	PNB
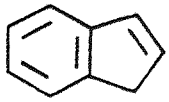	Indene	IND
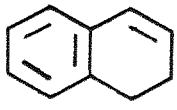	1,2 dihydronaphthalene	DHN

* - where applicable, the common trivial names are included, in parentheses

a number of such compounds, again in both the gas phase[1a)] and in solution[2a),4)]. From the angular dependence of the potential energy of the first excited singlet (S_1) and triplet (T_1) states of St itself, it has been shown that isomerisation may be possible via both these states[5]. However, the question as to the relative importance of singlet and triplet isomerisation mechanisms remains unresolved and there is in fact evidence to support the existence of both these routes. For example, twisted excited singlet states have been detected spectroscopically[6] for a number of styrenes in the gas phase, under 'isolated molecule' conditions. On the other hand, in the case of trans 1-phenyl prop-1-ene (tPP), it has been reported that on sensitised irradiation in solution, internal rotation about the $C_{7,8}$ bond provides the only significant decay route available to the triplet excited species[7].

Population of the T_1 state of styrenes via ISC following direct irradiation, is thought to provide one possible mode of radiationless decay from S_1, although it has been suggested[8] that the efficiency of this process may be relatively low. It seems likely that it is a combination of a relatively low ISC efficiency with an efficient non-radiative relaxation route from T_1 (i.e. internal rotation) which accounts for the lack of detectable phosphorescence from the simple, alkyl substituted styrenes[9]. The only reported observation of phosphorescence for such a compound, the benzocycloalkadiene, Indene[10], has since been ascribed to the presence of impurities[11]. In fact, to date, only in the case of the C-8 (β) nitro-substituted styrenes has phosphorescence been unequivocally demonstrated to occur[12].

For a number of styrenes, unimolecular processes which result in photochemical change (other than geometric isomerisation) have been demonstrated to be important[13]. The relative efficiencies of these processes are found to be strongly structure dependent[14], as in the case, of a series of 3-substituted-3-methyl-1-phenylbut-1-enes, as exemplified below in Fig. 1.1.

Within a series of substituents (R), the rate constant for photoreaction to form the corresponding phenylcyclopropanes is observed to increase in the order:

$$R = CH_3 < H < Ph$$

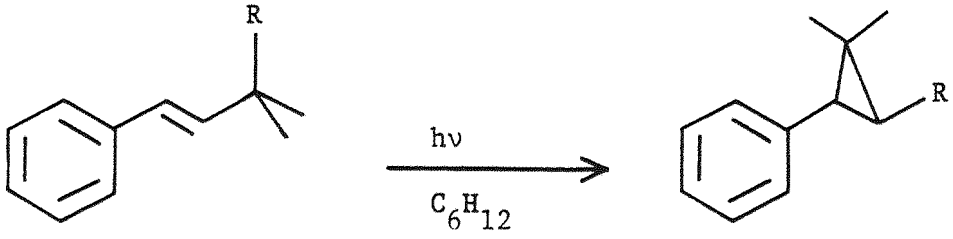

Figure 1.1
Phenylcyclopropane Formation as a Means of Non-Radiative Decay

Initially, it was proposed[2a] that a tendency for the substituted styrenes to undergo a photorearrangement of this type could account for the observed variation in the sum of the non-radiative rate constants for these compounds. However, in view of more recent experimental results[4a], the general correlation which appeared to exist between the efficiency of ring closure as a means of decay and the number of substituent C-H bonds, is no longer found to hold.

In the case of a number of benzocycloalkadienes also, photochemically induced skeletal rearrangements have been reported. These compounds appear to represent a special class of styrenes in that they are aryl olefins in which the conjugated double bond is present as part of a fused ring system. This distinction is reflected to some degree in the photophysical properties of these compounds, e.g. in the relatively small radiative rate constant observed for IND and also in the rather uncharacteristically broad room temperature absorption spectrum[15] of 1,2 dihydronaphthalene (DHN). On irradiation of DHN in solution, products due to oxidation and reduction are observed[16], together with the formation of a tricyclic compound, benzobicyclo [3.1.0] -hex-2-ene, as is illustrated in Fig. 1.2.

It has been proposed that the tricyclic product formed here is derived via ring opening to produce a non-aromatic pentaene intermediate, followed by ring closure:

Figure 1.2 - Photochemistry Observed for DHN in Solution

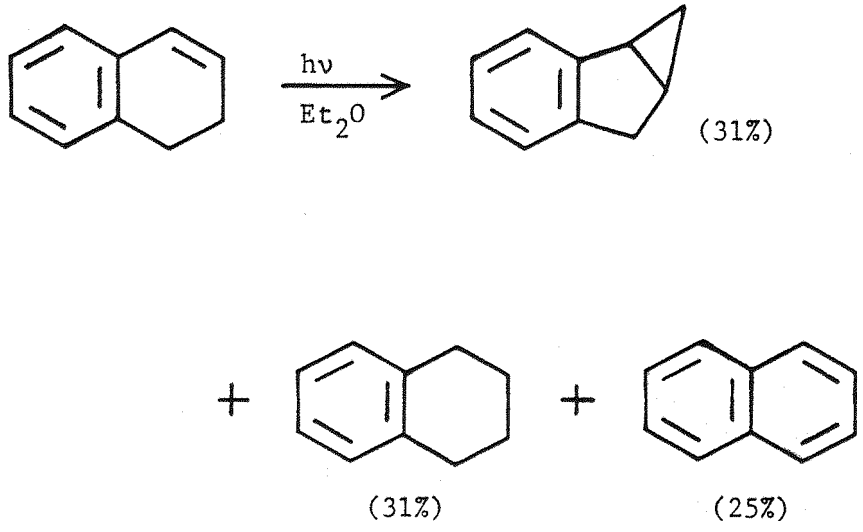

Similarly, skeletal rearrangements on excitation have been reported[17] for a range of alkyl, aryl and perfluoro substituted Indenes (but not IND itself) and here too, a mechanism involving the formation of non-aromatic intermediates has been suggested. Firm evidence supporting such a mechanism here, was obtained in the case of 1,1 dimethylindene by Diels Alder trapping of the intermediate 2,2 dimethylisoindene formed on irradiation, as is shown in Fig. 1.3 below.

Figure 1.3 - Trapping of the Intermediate Tetraene in the Rearrangement of 1,1 dimethylindene

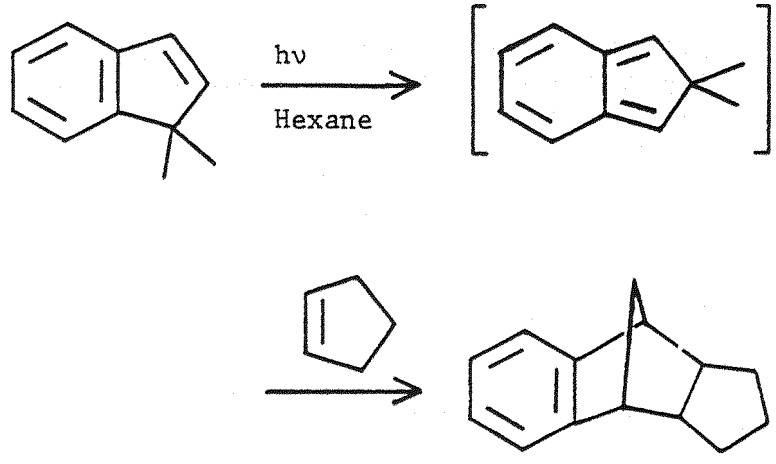

For those styrenes in which geometrical or structural rearrangements occur on excitation, it can be seen that these processes provide a 'handle' on at least one of the non-radiative decay routes available to these compounds. However, even when such processes are observed, it has often proved difficult to determine the precise nature of the primary decay pathways involved, as is the case e.g. with geometric isomerisation, in which the multiplicity of the state(s) involved is still uncertain. In fact, it is rather surprising that conclusive information regarding the decay characteristics of the simple styrenes is somewhat lacking. A survey of the principle conclusions from previous studies of the unimolecular photophysics of the acyclic styrenes, phenylcycloalkenes and benzocycloalkadienes is presented in Chapter 2.

During the course of the present work, measurements were made of the quantum yields and fluorescence lifetimes for examples of each of these three classes of styrene, at room temperature in both degassed and aerated cyclohexane solution. This was in the hope that a breakdown of the overall decay characteristics into components due to radiative and non-radiative decay processes, might allow the unimolecular photophysics of these compounds to be rationalised in terms of their molecular structure. A discussion of the results of these studies, which complement and further extend the earlier reported work, in particular that of Crosby[4a], is also presented in Chapter 2.

1.2 Bimolecular Photoreactions Involving Styrenes

The principle sections of this present work are concerned with an examination of the bimolecular interactions of electronically excited styrenes with tertiary amines, in particular Triethylamine (Et_3N). These investigations were prompted by the reported observation of fluorescence from a Styrene/Et_3N excited state charge transfer complex (exciplex) and by the implication of exciplexes of this type in the processes of photopolymerisation[18] and photoaddition/-reduction[19]. Exciplex formation between aromatic hydrocarbons and amines (both aliphatic and aromatic) has been shown to be a pervasive phenomenon[20] and consequently, has received considerable attention over the past two decades.

However, it would appear that, in the case of the styrenes, bimolecular interactions involving charge transfer are by no means limited to the reactions of these compounds with amines. For instance, it has been observed[21] that on irradiation of styrenes in the presence of alcohols, products due to addition to and reduction of the olefinic double bond may once again be formed. In fact the styrene/alcohol systems are interesting in that they provide an illustration of the fact that the styrenes may be involved in charge transfer processes in the role of both electron acceptors and electron donors. This is exemplified in Fig. 1.4 below, in which the products derived from photolysis of mixtures of 1-phenylnorborn-1-ene (PNB) and methanol, in the absence and presence of 1-cyano-naphthalene (CNNp) are illustrated.

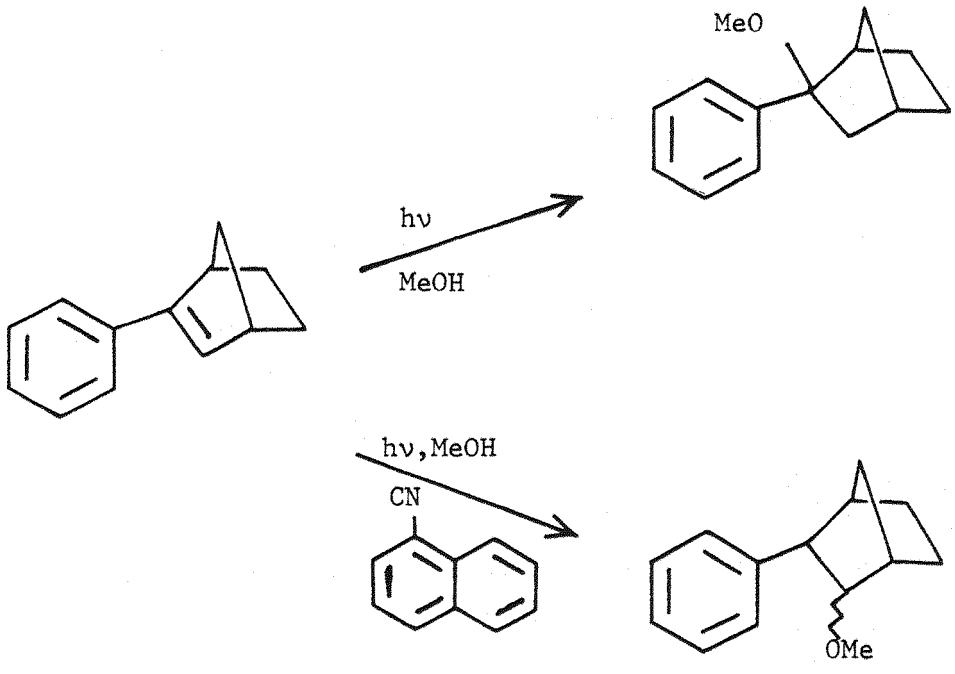

Figure 1.4 - Photoadduct Formation for the PNB/MeOH System in the Absence and Presence of CNNp

The product pattern here may be rationalised readily in terms of the nature of the charge transfer intermediates which are thought to be formed in each case[22]. It can be seen that on direct irradiation of PNB in MeOH solution, it should be possible for the

excited styrene to act as an electron acceptor. Hence, in this case, charge transfer from the donor alcohol would lead to formation of a styryl radical anion and a proton transfer and subsequent radical coupling would result in the observed (Markownikoff) addition product. On the other hand, in the presence of CNNp, charge transfer may be expected to occur preferentially from the ground state styrene to the initially excited 'electron transfer sensitiser' (i.e. ^{1}CNNp*), leading to the formation of a styryl radical cation. The observed photoadduct would then be formed, again via an intermediate benzylic radical, as a result of nucleophilic attack by the MeOH at the C-2(β) position of PNB$^{\cdot+}$

The process of electron transfer sensitised photoaddition has been extended to include other nucleophiles, as in the case of the synthetically useful route reported for the anti-Markownikoff cyanation of styrenes[23]. Similarly, photocyclodimerisation to form 1-aryl-1,2,3,4 tetrahydronaphthalenes has been observed[24] on photolysis of a number of styrenes in the presence of tetracyanobenzene (TCNB) as electron acceptor. This is in contrast to the direct and sensitised irradiation of Styrene itself, in the absence of TCNB, which has been shown to lead to the stereoselective formation of cis and trans 1,2 diphenylcyclobutane, respectively. Further examples of photocycloaddition involving styrenes, are to be found in the reactions of these compounds with olefins[25], aldehydes[26] and aromatic hydrocarbons[27] and it seems likely that for each of these systems, charge transfer intermediates are important. However, as in most such cases[28], it has proved to be difficult to establish whether the intermediacy of exciplexes is a necessary prerequisite for product formation or whether exciplex formation merely provides a competitive route for decay from the singlet excited monomer. For a number of systems it has been possible to demonstrate, using the technique of exciplex quenching[29], that the observed photoproducts are in fact formed via the fluorescent exciplexes, known to be present in solution. One such system for which photocycloaddition has been found to occur[30], with a high yield and high degree of stereospecificity, is that involving 9-cyanophenanthrene and trans-1-(4-methoxy) phenylprop-1-ene (trans anethole) as illustrated below in Fig. 1.5.

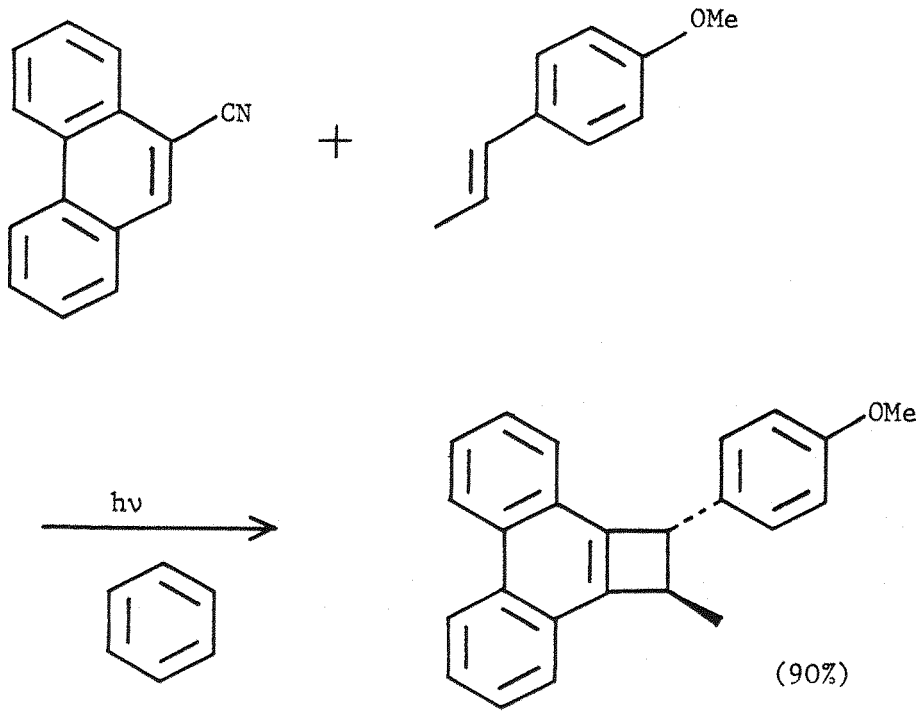

Figure 1.5 - The Photochemical Consequences of Exciplex Formation in a 9-cyanophenanthrene/styrene System

The fact that both exciplex fluorescence and product formation were quenched with equal efficiency here, on the addition of dimethyl-acetylene dicarboxylate, provided form evidence that in this case, the exciplex was indeed a necessary precursor to the observed photo-adduct.

In the case of the styrene/amine systems, as noted already, bimolecular interactions occurring on excitation have been shown to result in the formation of photoaddition and -reduction products[19], and here too, the involvement of exciplexes has been inferred. However, as is often found in the literature, while the product pattern observed may indeed be explained in terms of the intermediacy of exciplexes in photoreaction, no firm experimental evidence in support of this proposal was obtained. More recently, the observation of exciplex fluorescence has been reported[18], on irradiation of Styrene (St) itself in the presence of Et_3N and it was felt that an

examination of the mechanism of exciplex formation and decay for this and other related systems, might prove rewarding. During the course of the present work, therefore, a range of styrene/Et_3N systems, including a number of those for which photoproduct formation has been observed, were studied, using principally the techniques of Single Photon Counting and Fluorescence Spectroscopy. From the results of these studies, carried out under a variety of conditions of solvent and temperature, it was hoped that a detailed analysis of the kinetics and thermodynamics of the exciplex formation and decay processes could be constructed. The aim was then to combine this analysis with the results of an examination of the kinetics of photoproduct formation, under closely comparable experimental conditions, in order to try to assess the possible role of exciplex intermediates in photoreaction here. An attempt was made to examine this point further, using perhaps the most direct approach available, namely the technique of exciplex quenching and the principle conclusions from this and the other studies noted here are presented in some detail in Chapters 3 and 4.

REFERENCES - CHAPTER 1

1a) M.G. Rockley and K. Salisbury
J.C.S. Perkin II, 1582 (1973)

1b) K. Salisbury
J. Photochem., 2, 40 (1974)

2a) P.M. Crosby and K. Salisbury
J.C.S. Chem. Commun., 477 (1975)

2b) A.L. Lyons, Jr., and N.J. Turro,
J. Amer. Chem. Soc., 100, 3177 (1978)

2c) D.A. Condirston and J.D. Laposa
J. Lumin., 16, 47 (1978)

3a) G. Fischer, G. Seger, K.A. Muszkat and E. Fischer
J.C.S. Perkin II, 1569 (1975)

3b) J.B. Birks
Chem. Phys. Lett., 38, 437 (1976)

4a) P.M. Crosby
Ph.D. Southampton University (1979)

4b) C.S. Nakagawa and P. Sigal,
J. Chem. Phys. 58, 3529 (1973)

4c) A.A. Lamola and G.S. Hammond
J. Chem. Phys., 43, 2129 (1965)

5a) M.C. Bruni, F. Momicchioli, I. Baraldi and J. Langlet
Chem. Phys. Lett., 36, 484 (1975)

5b) M.H. Hui and S.A. Rice
J. Chem. Phys., 61, 833 (1974)

6a) R.P. Steer, M.D. Swords, P.M. Crosby, D. Phillips and K. Salisbury
Chem. Phys. Lett., 43, 461 (1976)

6b) K.P. Ghiggino, K. Hara, G.R. Mant, D. Phillips, K. Salisbury, R.P. Steer and M.D. Swords
J.C.S. Perkin II, 88 (1978)

7. R.A. Caldwell, G.W. Sovocool and R.J. Peresie
J. Amer. Chem. Soc., 93, 779 (1971)

8. H.E. Zimmerman, K.S. Kamm and D.P. Werthemann
J. Amer. Chem. Soc., 97, 3718 (1975)

9. P.M. Crosby, J.M. Dyke, J. Metcalfe, A.J. Rest, K. Salisbury and J.R. Sodeau
J.C.S. Perkin II, 182 (1977)

10. R.C. Heckman
J. Mol. Spectrosc. 2, 27 (1958)

11a) E.T. Harrigan and N. Hirota
Chem. Phys. Lett., 22, 29 (1973)

11b) B. Brocklehurst and D.N. Tawn
Spectrochim Acta, Part A, 30, 1807 (1974)

12. D.J. Cowley
J.C.S. Perkin II, 1576 (1975)

13a) H. Kristinsson and G.W. Griffin
J. Amer. Chem. Soc., 88, 378 (1966)

13b) S.S. Hixson and T.P. Cutler
J. Amer. Chem. Soc., 95, 3031 (1973)

13c) S.S. Hixson and T.P. Cutler
J. Amer. Chem. Soc., 95, 3032 (1973)

13d) H. Morrison and F. Scully
J.C.S. Chem. Commun., 529 (1973)

13e) J.M. Hornback
J. Amer. Chem. Soc., 96, 6773 (1974)

14. S.S. Hixson
J. Amer. Chem. Soc., 98, 1271 (1976)

15. See e.g. R.S. Becker, E. Dolan and D.E. Balke
J. Chem. Phys., 50, 239 (1969)

16a) R.C. Cookson, S.M. de B. Costa and J. Hudec
J.C.S. Chem. Commun., 1272 (1969)

16b) H. Kleinhuis, R.L.C. Wijting and E. Havinga
Tet. Lett, 255 (1971)

17a) J.J. McCullough
Canad. J. Chem., 46, 43 (1968)

17b) J.J. McCullough and M.R. McClory
J. Amer. Chem. Soc., 96, 1962 (1974)

17c) F.J. Palensky and H.A. Morrison
J. Amer. Chem. Soc., 99, 3507 (1977)

17d) W.J. Feast and W.C. Preston
J.C.S. Chem. Commun., 985 (1974)

18. K. Yokota, H. Tomioka and K. Adachi
Polymer, 14, 561 (1973)

19a) R.C. Cookson, S.M. de B. Costa and J. Hudec
J.C.S. Chem. Commun., 753 (1969)

19b) S.M. de B. Costa
Ph.D. Southampton (1969)

20a) B. Stevens
Adv. Photochem., 8, 161 (1971)

20b) 'The Exciplex'
M. Gordon and W.R. Ware (Ed.)
Academic Press N.Y., (1975)

20c) 'Organic Molecular Photophysics'
Chap. 4, H. Beens and A. Weller
(J.B. Birks, Ed.)
Wiley - Interscience N.Y. (1975)

20d) 'Molecular Association'
Vol. 1, R.S. Davidson (R. Foster, Ed.)
Academic Press, London (1975)

21a) P.J. Kropp
J. Amer. Chem. Soc. 95, 4611 (1973)

21b) S.S. Hixson
Tet. Lett., 277 (1973)

22. Y. Shigemitsu and D.R. Arnold
J.C.S. Chem. Commun., 407 (1975)

23. A.J. Maroulis, Y. Shigemitsu and D.R. Arnold
J. Amer. Chem. Soc., 100, 535 (1978)

24. T. Asanuma, M. Yamamoto and Y. Nishijima
J.C.S. Chem. Commun., 608 (1975)

25a) O.L. Chapman, R.D. Lura, R.M. Owens, E.D. Plank, S.C. Shimu,
D.R. Arnold and L.B. Gillis
Canad. J. Chem., 50, 1984 (1972)

25b) R.M. Bowman, J.J. McCullough and J.S. Swenton
Canad. J. Chem., 47, 4503 (1969)

25c) J.J. McCullough and C.W. Huang
Canad. J. Chem., 47, 757 (1969)

25d) D.R. Arnold
J.C.S. Chem. Commun., 351 (1979)

26. H.A.J. Carless, A.K. Maitra and H.S. Trivedi
J.C.S. Chem. Commun., 984 (1979)

27a) R.A. Caldwell and L. Smith
J. Amer. Chem. Soc., 96, 2994 (1974)

27b) B. Sket and M. Zupan
J.C.S. Chem. Commun., 1053 (1976)

28. See e.g. A. Lablache-Combier
Bull. Soc. Chim. Fr., 4791 (1972)

29. D. Creed, R.A. Caldwell and M. Mc.K.Ulrich
J. Amer. Chem. Soc., 100, 5831 (1978) and references therein.

30. R.A. Caldwell, N.I. Ghali, C.-K. Chien, D. De Marco and L. Smith
J. Amer. Chem. Soc., 100, 2857 (1978)

CHAPTER 2

THE UNIMOLECULAR PHOTOPHYSICS OF STYRENES

2.1 Introduction

This Chapter is intended to provide a brief examination of various aspects of the unimolecular photophysics of styrenes and thus to serve as a background to the rather more detailed study of styrene/amine interactions reported in Chapters 3 and 4. In a study of the photophysical characteristics of any compound, the electronic absorption and emission spectra of the compound are obviously of great importance, in providing a 'handle' on the ground and excited molecular states between which transitions may occur. The simply substituted styrenes are characterised by absorption and fluorescence in the near u-v region. Although the absorption spectra of styrenes have been studied fairly extensively[1], it is rather surprising that conclusive information regarding the radiative and non-radiative decay characteristics of the excited molecules is somewhat lacking.

In the case of Styrene (St) itself, the absorption spectrum in the region 230-300 nm. is composed of two principal absorption bands. These comprise a broad, intense absorption with λ_{max} = 248 nm. ($\varepsilon_{max} \simeq 18{,}000$) together with a weaker, more highly structured band observed in the region 270-300 nm. These are thought to correspond respectively to the ^1L_a and ^1L_b bands in benzene, both of which are bathochromically shifted on the introduction of conjugation with the ethylenic group in St. As is the case with benzene, the transition $S_0 \rightarrow S_1$, which gives rise to the ^1L_b band is formally forbidden and it would appear that this absorption is observed as a result of "intensity borrowing" from the nearby (allowed) ^1L_a band. This effect is reflected in the oscillator strengths (f),

which have been calculated[2] for excitation to the first and second excited singlet states of St:

$$S_0 \rightarrow S_1 \ (^1L_b), \quad f = 2 \times 10^{-2}$$

$$S_0 \rightarrow S_2 \ (^1L_a), \quad f = 0.34$$

The fluorescence spectrum of St in hydrocarbon solution at room temperature exhibits some structure and in particular, as with the ^1L_b absorption band, the 0-0 transition is well resolved. Fig. 2.1 illustrates this and other features of the fluorescence spectrum and the ^1L_b absorption band observed for St in cyclohexane solution. It may be noted that there exists an approximate mirror symmetry relationship between the spectra, when plotted on an energy scale, although the maximum in the fluorescence intensity appears as a doublet, while the corresponding absorption band shows no such structure. However, fig. 2.1 also illustrates the observation that on improving the resolution of the St absorption spectrum by employing a fluorinated solvent (perfluoromethylcyclohexane) further splitting does become apparent. The vibrational progression(s) in the ^1L_b absorption extend into and overlap the low energy tail of the ^1L_a band. It is interesting to observe that the fluorescence spectrum features a shoulder at $\sim$31,060 cm^{-1}, which may correspond to the 'submerged' transition appearing at $\sim$36,600 cm^{-1} in the absorption spectrum. The energy difference between the 0-0 bands of the absorption and fluorescence spectra is relatively small ($\sim$500 cm^{-1}) and may simply reflect the requirement for solvent reorganisation around the molecule on excitation. This lack of a significant Stokes shift, together with the approximate mirror symmetry relationship demonstrated in fig. 2.1, strongly suggests that the geometry of the molecule is very similar in both the S_0 and S_1 states.

It seems likely that the equilibrium configuration of St in its ground state is one in which the ethylenic C-atoms are essentially coplanar with those of the phenyl ring[1,3], i.e. the geometry which maximises the π-overlap possible between these two moieties. Hence, a planar geometry is also surmised for St in the S_1 state, a feature which appears to have important consequences as regards the decay characteristics of the excited molecule, as is discussed below.

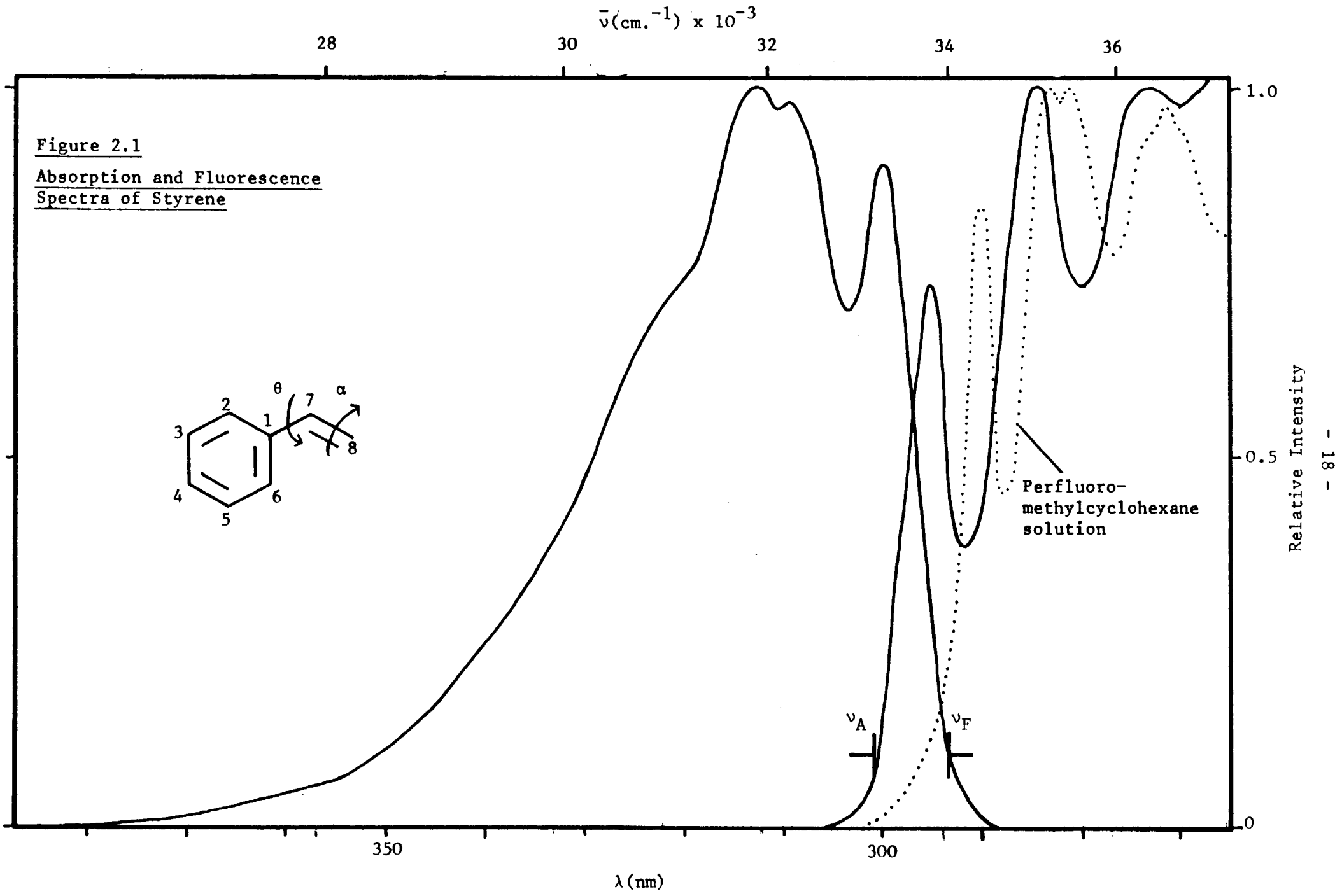

Figure 2.1

Absorption and Fluorescence Spectra of Styrene

2.2 Substituted Styrenes

The effects of molecular structure on the absorption spectra of a variety of simply substituted styrene derivatives have been examined by Suzuki and others[1]. An important general conclusion from these studies was that the introduction of substituents in the ortho, α or cis β positions (C-2, C-7 or cis C-8, see fig. 2.1) leads to the ^1L_a absorption band undergoing both a hypo- and hypsochromic shift. These effects are demonstrated in fig. 2.2 for the pair of isomeric styrenes, cis and trans 1-phenyl prop-1-ene (cPP, tPP). It can be seen that the trans isomer, which is thought to be planar in the ground state, is characterised by a more intense ^1L_a band, having an absorption maximum which is red shifted with respect to that of the cis isomer. For this latter compound, a value of 30° has been calculated[1e)] for θ, the dihedral angle in the ground state molecule (see fig. 2.1). Various attempts have been made, using M.O. techniques to correlate the observed effects on the absorption spectra with the magnitude of θ for the substituted styrenes. Correlation diagrams of the type presented as fig. 2.3 for St itself, are useful in this context in providing a qualitative interpretation of these effects. Such diagrams also serve as an aid to the description of the excited states of these molecules, in terms of electronic transitions between the various M.O.'s detailed. In this case, there is general agreement[2,4] that, while the wave function for the S_2 state of St is composed almost entirely of the HOMO-LUMO configuration [28,29], the S_1 state is in fact a linear combination of two principal electronic configurations ([27,29] and [28,30]).

The M.O. picture presented as fig. 2.3 is consistent with the Photoelectron (P.E.) spectrum of St[3] and this technique has been applied by Turner[5] to a number of substituted styrenes also. The effects of steric inhibition of resonance were apparent in the P.E. spectra of these compounds, principally in the form of a variation in the energy gap (ΔE_{1-3}) between the first and third ionisation energies. From fig. 2.3, it can be seen that any reduction in the interaction between the ethylene π-bonding M.O. and the benzene E_{1g} M.O. (A) should lead to a decrease in the energy splitting between the resulting M.O.'s in St (Ψ_{26} and Ψ_{28}). As illustrated

Figure 2.2 Electronic Absorption Spectra of cis and trans Phenyl-prop-1-ene

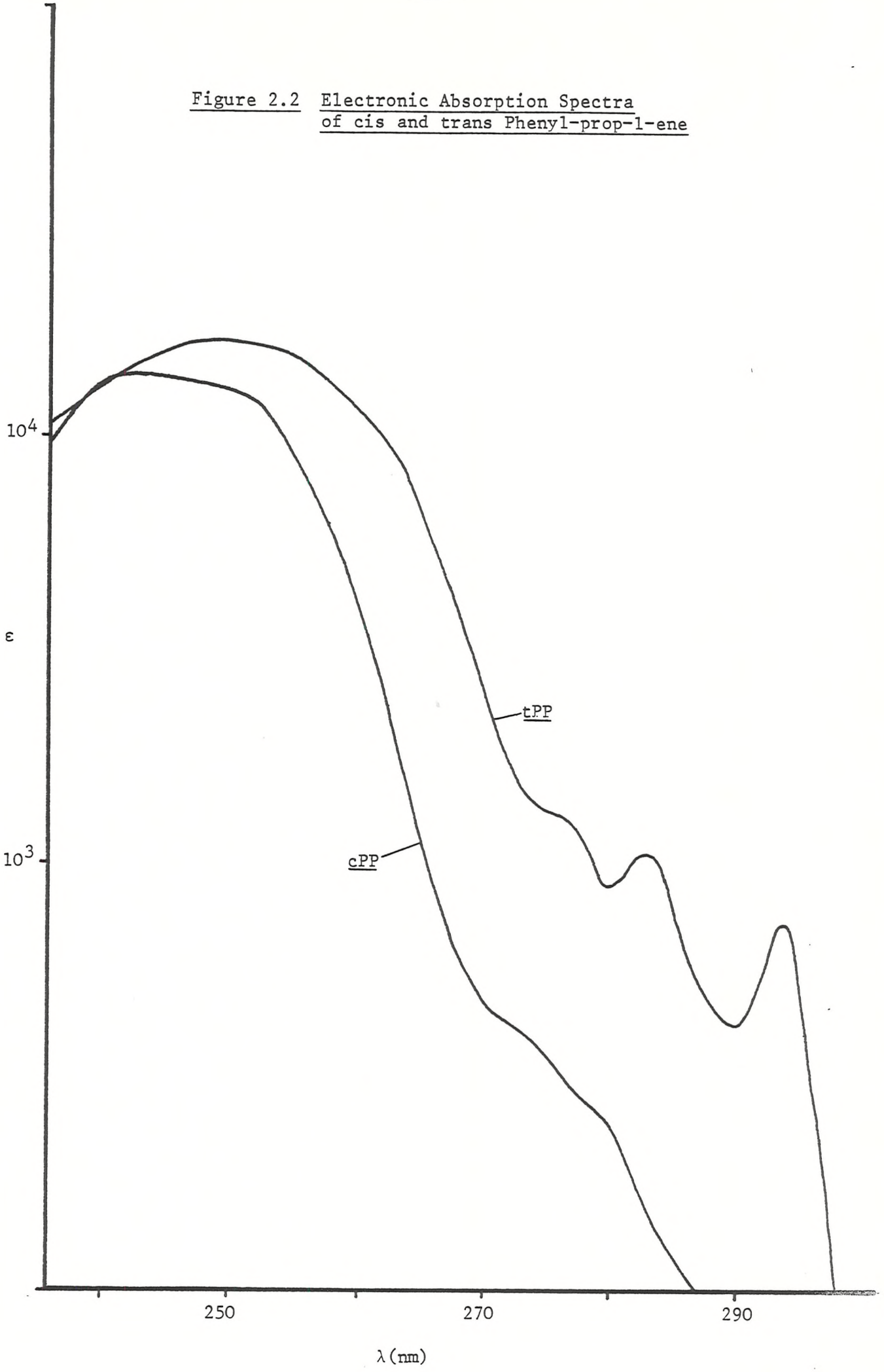

Figure 2.3 A Correlation Diagram of the Highest Occupied and Lowest Virtual MO's of Styrene with the MO's of Benzene and Ethylene (after ref.2)

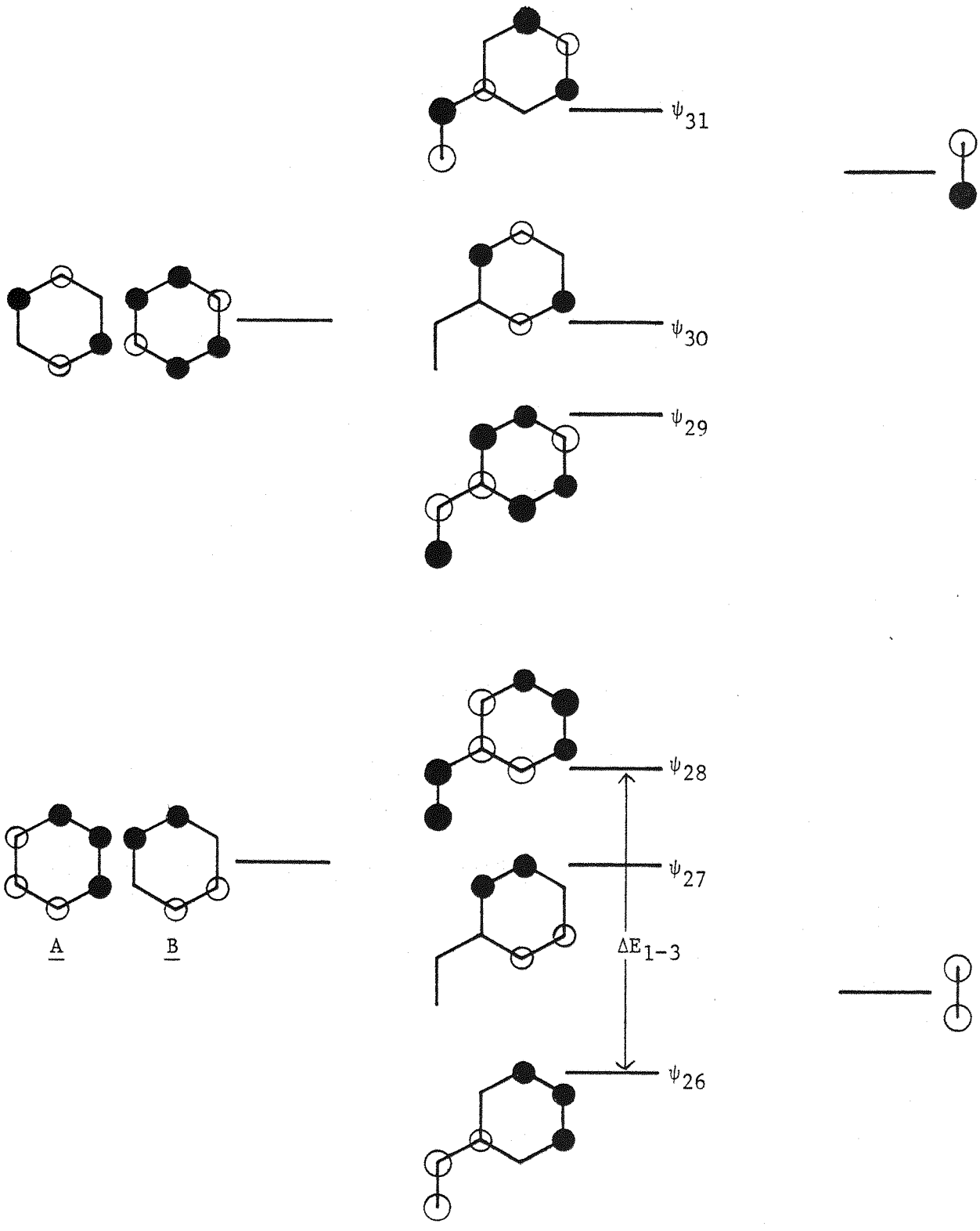

in Table 2.1 below, the introduction of steric constraints within the styryl nucleus, which inhibit the attainment of coplanarity, do indeed produce the expected decrease in ΔE_{1-3}. The magnitude of this splitting was used to estimate the expected dihedral angle, θ, within the ground state molecule and the results obtained for a series of methyl substituted derivatives are exemplified in Table 2.1 also.

Table 2.1

The Observed Difference in the First and Third Ionisation Energies (ΔE_{1-3}) and The Predicted Dihedral Angle (θ) for a Number of Styrenes[5]

	ΔE_{1-3} (eV.)	θ^{o}
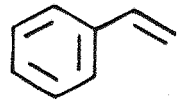	2.05	0
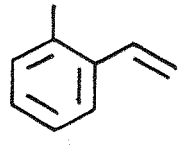	1.9	22
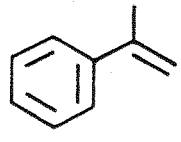	1.5	38
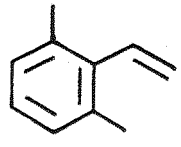	1.3	55

These results provide quantitative information concerning the influence of ground state geometry on a particular molecular parameter. They do have wider implications however, in that they serve to underline the more general observation that steric factors play an important role in controlling the overall reactivity of styrenes. For example, the importance of steric hindrance has also been recognised in studies of the i.r.[6] and n.m.r.[7] spectra, reaction[8] and polymerisation[9] rates and the molecular polarisability[10] of these compounds.

It would appear that the same may well be true with regard to both the electronic absorption and decay characteristics of the

styrenes, in that here too a correlation between these properties and their ground state molecular conformation may be noted. This same observation has been made by Crosby[11] from a study of a wide range of substituted styrenes and the results presented here serve to further substantiate this. As noted already, attempts have been made to relate the energy and the relative intensities of the ^1L_a absorption bands observed for these compounds to the magnitude of their ground state dihedral angle, θ. A similar correlation appears to exist in the case of the ^1L_b absorption band also. The planar styrenes are characterised by ^1L_b bands which, as for St itself, are structured and relatively intense by comparison to those of the derivatives which are forced, by steric constraints, to adopt a non-planar ground state equilibrium conformation. For these latter compounds, the ^1L_b absorption, if present at all, is often barely discernible and tends to be obscured by the tail of the ^1L_a band. These points are illustrated in fig. 2.2 (for the tPP:cPP pair) and it is interesting to compare the absorption spectra of these compounds with those observed for another pair of isomeric styrenes, oMe:2PP, as presented here in fig. 2.4. From an examination of their P.E. spectra[5] (see Table 2.1) and also from consideration of the position of the ^1L_a absorption band[1], both 2PP and oMe are predicted to be non-planar. However, as shown in fig. 2.4, oMe in fact exhibits a pronounced ^1L_b absorption and it is interesting to note that, in terms of its decay characteristics, it would appear that this compound should be classified along with other planar derivatives. This serves to illustrate the observation that in general, the decay properties of the styrenes may be predicted most readily (and not too surprisingly perhaps) from an examination of the appearance and relative intensities of their ^1L_b ($S_o \rightarrow S_1$) absorption bands.

During the course of this work, the fluorescence spectra were recorded for a variety of methylated and cyclic styrene derivatives, at room temperature in degassed cyclohexane solution. As was the case with the absorption spectra, there was a clear distinction between the appearance of the emission spectra observed for those compounds thought to be planar and those thought to be non-planar in the ground state. The planar derivatives were characterised by fluorescence

Figure 2.4 Electronic Absorption Spectra for the Isomeric Styrenes 2PP and oMe

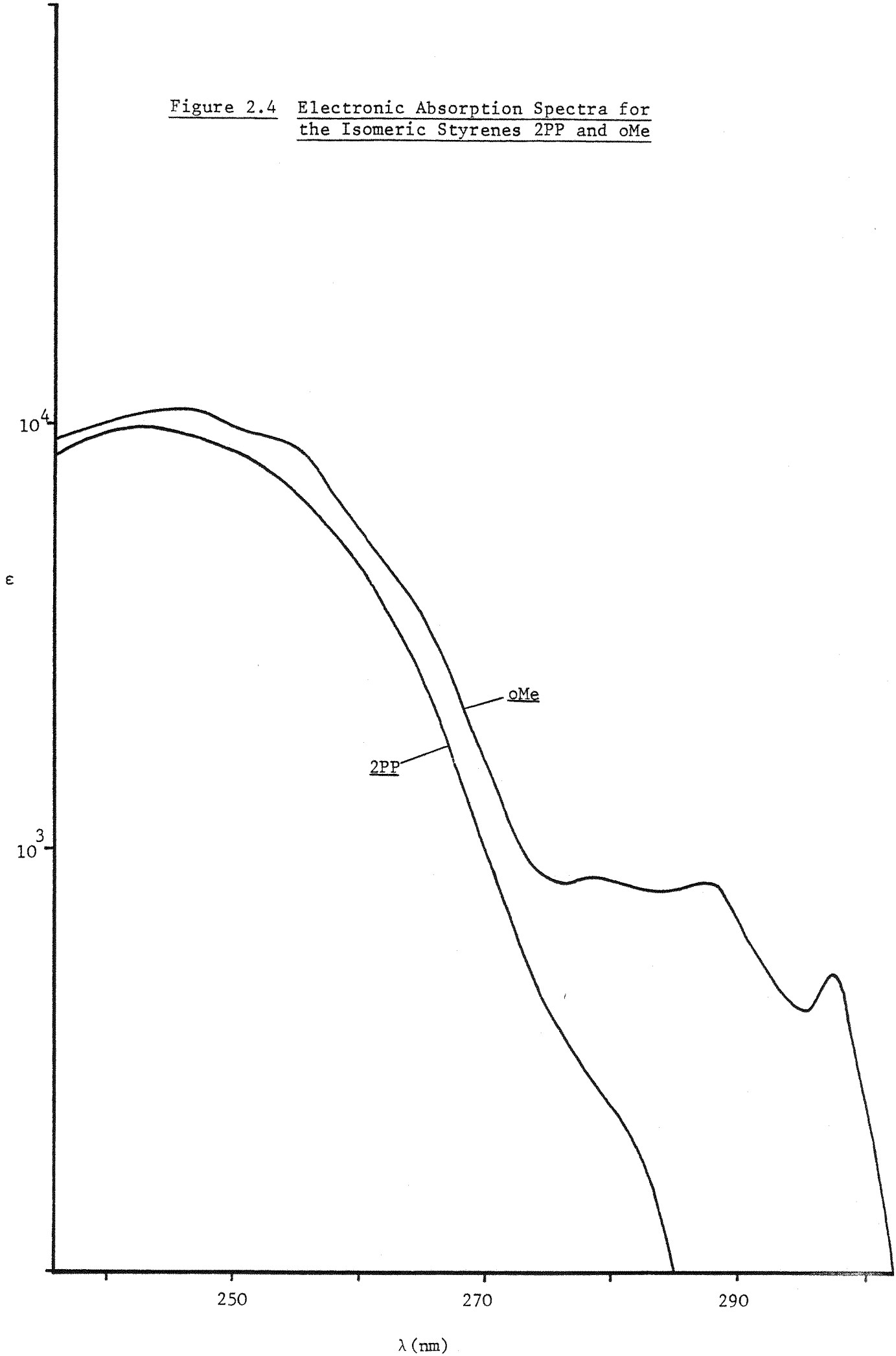

spectra similar in appearance to that of St itself. These spectra exhibited, in particular an intense, well-resolved 0-0 band; a doublet in the region of λ_{max} and a long wavelength shoulder. The fluorescence spectra for the non-planar styrenes were generally less well resolved and in particular, the 0-0 bands, although still discernible, had the appearance of a shoulder, rather than a definite peak. Also, it was generally observed that the integrated fluorescence intensity for the non-planar derivatives was appreciably reduced by comparison to that of the planar compounds. This point is illustrated in Table 2.2, in which the fluorescence quantum yields (Φ_F) observed experimentally for a number of styrenes, are recorded. The experimental values of τ_F, the fluorescence decay time, are also presented in Table 2.2, together with the values of the rate constants for the radiative (k_1) and the sum of the non-radiative (k_2) decay processes, for this series of compounds. In each case, the values of $k_{1,2}$ have been derived from the quantum yield and decay time data, according to the well-known expressions:

$$k_1 = \Phi_F/\tau_F \qquad (1)$$

$$k_2 = (\tau_F)^{-1} - k_1 \qquad (2)$$

(The notation $k_{1,2}$ is that employed by Ware[14] and is used here for consistency with that which has been adopted for the kinetic analyses, presented in the following Chapters).

This breakdown of the decay data into components due to radiative and non-radiative decay is most revealing in that, once again the distinction between the planar and non-planar derivatives becomes apparent:

a) <u>The Radiative Rate Constant (k_1)</u>

In the case of the planar styrenes listed here, the value of k_1 is observed to fall within a rather narrow range ($1.5 - 2.5 \times 10^7 s^{-1}$) with the exception of IND, for which k_1 is found to be anomalously low, although still within the region typical for a partially allowed $\pi\pi^*$ transition[12]. It can be seen that it is this rather low value for k_1 which leads to the fluorescence quantum yield of IND being

Table 2.2

Results Derived from Quantum Yield and Decay Time Measurements on a Number of Styrenes at Room Temperature in Degassed Cyclohexane Solution

Styrene	Φ_F	τ_F^D (ns)	k_1 (s^{-1}) $\times 10^7$	k_2 (s^{-1}) $\times 10^{-7}$	
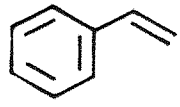	0.21	14.5	1.45	5.45	PLANAR
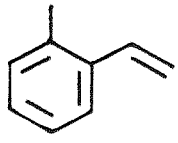	0.31	13.0	2.38	5.31	
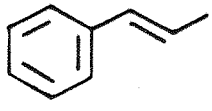	0.28	12.3	2.28	5.85	
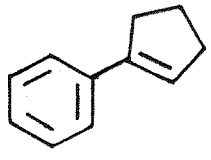	0.30	12.2	2.45	5.74	
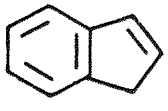	0.08	16.0	0.50	5.75	
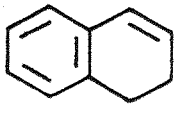	0.09	7.7	1.17	11.8	NON-PLANAR
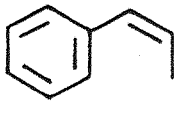	0.01(8)	2.2	0.82	44.6	
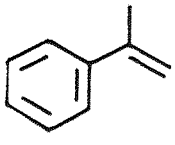	0.01(5)	2.2	0.68	44.7	

significantly reduced by comparison to the values of Φ_F recorded for the other planar derivatives. The anomalous behaviour of IND is also apparent in the fluorescence spectrum of this compound, which unlike the other planar styrenes, exhibits a comparatively weak 0-0 band. This may suggest that the molecular conformation of IND in the S_1 state differs in some way from that of ground state IND. The non-planar derivatives studied here (cPP, 2PP and DHN) are characterised by rather lower values of k_1 than their planar counterparts, e.g. the comparison may be made between the data presented for the isomeric pairs cPP:tPP and 2PP:oMe. Once again, the results presented here are in good agreement with observations made by Crosby from the study of a rather more extensive series of C-7 (α) and cis- and trans-C-8 (cis and trans β) alkylated styrenes. Also, it may be noted that for the styrenes in general, the magnitude of k_1 does appear to be roughly proportional to the integrated area under the ^1L_b absorption band. However, attempts to quantify this observation for example using the Strickler-Berg approximation, are hampered by the fact that, as mentioned already, for all these compounds, there is a significant degree of overlap between the ^1L_b and the tail of the ^1L_a absorption bands.

b) The Sum of the Non-Radiative Rate Constants (k_2)

It is perhaps on examination of the values of k_2 derived for these compounds that the correlation between ground state molecular conformation and the excited state decay characteristics is most striking. It can be seen from Table 2.2 that the magnitude of k_2 is observed to be identical, to within a reasonable experimental error of $\pm 5\%$, for all five planar styrenes studied. Furthermore, the average value of $k_2 = 5.6\ (\pm 0.3) \times 10^7 s^{-1}$ recorded here, is in excellent agreement with that reported by Crosby[11] for a number of other planar (trans-C-8 substituted) styrenes. In the case of the non-planar derivatives however, it would appear that the magnitude of k_2 increases with the ground state dihedral angle, θ, as is exemplified below for the series IND:DHN:cPP. These compounds are of interest, in that they may be considered as a series of benzocycloalkadienes of increasing ring size (cPP representing the case of an infinitely large ring):

	IND	DHN	cPP
θ^{o}	0	16	35
$k_2(s^{-1} \times 10^{-7})$	5.75	11.8	44.6

The unimolecular photophysics of a number of styrenes, and in particular the benzocycloalkadienes, have also been studied by Turro[13]. While the observations reported here are in general agreement with those in the literature, a discrepancy is apparent in the absolute values recorded for the fluorescence decay times (τ_F). This is illustrated in Table 2.3 below, in which the relevant values of Φ_F and τ_F reported by Turro are presented for comparison with the data of Table 2.2. Such a comparison reveals that, while there is excellent agreement between the two sets of quantum yield data, the values reported for the fluorescence decay times are observed to differ by approximately 7-8 ns. for each compound studied. The fact that the τ_F values recorded in the literature are in each case greater than those derived from the present study suggested initially that this variation could have arisen as a result of a less efficient degassing procedure having been used here. However, these doubts were proved to be groundless on measurement of the fluorescence decay times (τ_F^A) of a number of the styrenes studied, in aerated cyclohexane solution. The results obtained are presented in Table 2.4, in which the comparison is made of the experimental decay times, $(\tau_F^A)^{EXPT}$, with the expected values $(\tau_F^A)^{CALC}$ calculated from the decay times obtained in degassed cyclohexane solution (τ_F^D), according to:

$$(\tau_F^A)^{CALC} = \frac{\tau_F^D}{1 + k_{O2} \cdot \tau_F^D \cdot [O_2]} \qquad (3)$$

(where k_{O2} = the rate for diffusion-controlled fluoresence quenching by oxygen in cyclohexane solution = $2.2 \times 10\ M^{-1}s^{-1}$[38], and $[O_2]$ = the concentration of oxygen present in aerated cyclohexane at 25°C = $2.3 \times 10^{-3}M$[38])

Table 2.3

Literature[13] Values of Φ_F and τ_F for Some Styrenes

Styrene	Φ_F^*	τ_F^* (ns)
St	0.22	21.7
IND	0.072	23.2
DHN	0.083	16.1

* - Recorded at room temperature, in degassed cyclohexane solution.

Table 2.4

Experimental and Calculated Values of τ_F^A for Some Styrenes in Aerated Cyclohexane Solution

Styrene	$(\tau_F^A)^{EXPT}$ (ns)	$(\tau_F^A)^{CALC}$ (ns)
St	8.4	8.36
oMe	7.8	7.84
tPP	7.6	7.58
IND	8.8	8.81

Equation (3) may be derived on the assumption that the interaction between the excited styrenes and ground state O_2 can be described kinetically as an additional, bimolecular, diffusion controlled quenching process. That such an assumption is valid has been demonstrated by Crosby[11] and is underlined by the excellent agreement between the experimental and calculated τ_F^A values recorded in Table 2.4. It would seem unlikely therefore, that the observed reduction in τ_F^D, by comparison to the data reported by Turro, could be accounted for by the presence of air in the 'degassed' samples used in the present study and hence, the reason for this discrepancy is not readily apparent. However, another possibility which may be suggested is that this may reflect the fact that different methods were employed in extracting the τ_F values from the experimental fluorescence decay curves (even though these were obtained in both cases using the Single Photon Counting technique). As is outlined in Chapter 5, during the course of this work the experimental fluorescence decay profiles were analysed using an iterative convolution procedure, as employed by Ware[14]. Using this technique, it is possible to take account of the fact that the exciting lamp pulse itself has a finite decay time. The data presented in Table 2.3 however, was apparently derived using the slope of plots of Log (Fluorescence Intensity) vs. Time in each case, rather than any computational technique. Provided that once again the decay characteristics of the exciting lamp pulse are compensated for, the former method should be perfectly adequate for compounds such as the styrenes, which decay from S_1 according to a single exponential decay law. Although it would seem unlikely that this effect should have been overlooked, it is interesting to note that low-pressure oxygen filled lamps of the type used by Turro typically exhibit decay times of the order of 8-10 ns[15]. Thus, failure to deconvolute the lamp decay from the total fluorescence decay profile could indeed provide an explanation for the variation of the τ_F values of Tables 2.2 and 2.3.

2.3 A Discussion of the Decay Pathways Available to the Excited Styrenes

2.3.1 Radiative Decay

As has been demonstrated in Table 2.2 above, it is possible to describe the overall decay characteristics of the excited styrenes in terms of contributions from both radiative and non-radiative

relaxation routes. The relative importance of these decay pathways is observed to vary with molecular structure and in the following, an attempt is made to rationalise these observations. It is of particular interest in this context, to examine in some detail, the route(s) by which it may be possible for the S_1 states of these compounds to relax non-radiatively. As noted already, it is to be expected that the rate constant, k_2, in fact represents the summation of the rates of a number of decay pathways and an attempt to further break down this sum into its components may prove rewarding.

However, with regard initially, to the radiative decay of the excited styrenes, it is important to note that a significant Stokes shift was not observed for any of the examples studied here. Owing to the fact that in some instances, the 0-0 bands of both the absorption and emission spectra of the styrenes were discernible as an inflexion only, it was felt that a more reliable indication as to the magnitude of these Stokes shifts could be derived from comparison of the onsets of the band envelopes, rather than their peak maxima. As is illustrated in the spectra of St, presented already as fig. 2.1, the onsets (ν_A and ν_F respectively) were defined arbitrarily as the energies at which the absorption and emission spectra had reached an intensity of approximately 10% of what was assumed to be the 0-0 peak height. For compounds in which there is a significant conformational change prior to radiative relaxation, it would be expected that the energy difference ($\nu_A - \nu_F$) should be relatively large. Such an observation has indeed been made in the case of a number of cis-substituted stilbene derivatives[16], for which large, positive values of the order of +2,000 to +6,000 cm^{-1} have been reported for the parameter ($\nu_A - \nu_F$). In the case of the styrenes, however, rather small, negative values in the region of -800 to -1,000 cm^{-1} were observed for this parameter, for all the examples studied here. Hence, unlike the cis stilbenes, it would appear that radiative decay from the S_1 state of styrenes (including the hindered cis and α substituted derivatives) occurs from a molecular conformation which is very similar to that of the ground state (S_0). It has been suggested[13] that for those styrenes thought to be non-planar in the ground state, the emission is more

structured than the absorption and that this is indicative of the fact that the emissive state is somewhat more rigid and closer to planarity than the ground state. However, it is difficult to justify such an observation in view of the fact that for these non-planar compounds, any vibrational structure which may be present in the ^1L_b absorption band is most likely to be 'buried' in the tail of the more intense ^1L_a band. What seems to be more likely here is that conformational changes, similar to those observed in the stilbenes, do take place on excitation but that they do so in competition with, rather than prior to, radiative decay from S_1.

2.3.2 Non-Radiative Decay

The most common routes by which molecules in their first excited singlet state relax non-radiatively, involve dissipation of their excess energy into thermal energy via the processes of Internal Conversion (IC) and/or Intersystem Crossing (ISC). The efficiency with which these radiationless transitions may occur is governed principally by the magnitude of the energy gap between the two states involved, which in turn determines the extent to which vibrational overlap is possible between the zeroth vibrational level of the initial state and an upper level of the final state. The rates of singlet decay in general show an inverse dependence on the singlet energy of the compound (E_s) which may be derived readily from the energy of the 0-0 absorption band. In the case of the simply substituted styrenes, the value of E_s is relatively large ($\geq$400 kJ.mol^{-1}) and by comparison with other aromatic hydrocarbons[12,17] it would appear that, for an energy gap of this magnitude, the efficiency of vertical IC ($S_1 \rightsquigarrow S_0$) would be expected to be relatively low (e.g. a rate constant k_{IC} of only $\sim 10^5$ s^{-1} might be predicted). In order to satisfy the requirement for degeneracy of the interacting vibrational levels of the upper and lower states, very high levels of the S_0 state would have to be involved here. Thus, if as suggested above, there is in fact little change in molecular geometry on excitation of the styrenes, then the vibrational overlap possible between the zeroth level of S_1 and the required, very high vibrational level of S_0, would be expected to be minimal. In other words, the Franck-Condon factor for this non-radiative transition should be

rather small, which again suggests that vertical IC (i.e. prior to any conformational change in S_1) between these states should be relatively inefficient.

With regard to the possibility of ISC from the singlet excited styrenes, similar arguments will apply, although the energy gap between the states involved (S_1 and T_1) will obviously be much smaller than the singlet energy. An examination of the oxygen-enhanced $S_0 - T_n$ absorption spectra of a number of styrenes[18], demonstrated that the $S_1 - T_1$ energy gap (as measured using the difference in energy between the onsets of the $S_0 - S_1$ and $S_0 - T_1$ absorptions) would appear to be of the order of $\sim$150 kJ.mol^{-1} in each case. However, although this energy gap is relatively small (by comparison to E_s) it should be noted that ISC of the type suggested here, $^1\pi\pi^* \rightsquigarrow {}^3\pi\pi^*$, is in fact formally forbidden according to EL Sayed's selection rules. Nevertheless, such transitions are observed, as in the case of aromatic hydrocarbons, in which it is thought that the rigorous symmetry restraints may be relaxed as a result of vibronic spin-orbit coupling. Also, it may be noted that M.O. calculations[11] have predicted that for the styrenes a number of higher triplets ($T_2 - T_5$) in fact lie intermediate in energy between S_1 and T_1. The presence of these triplet states could provide an important and efficient means of enhancing the transition to the T_1 state by partitioning the overall energy gap ($S_1 - T_1$) into smaller units.

In view of the preceding discussion, it would seem reasonable to postulate that non-radiative decay from the S_1 state of styrenes in the molecular conformation to which they are initially excited is more likely to occur via ISC than IC. There is some (rather circumstantial) evidence to support this view but, unfortunately, a direct, spectroscopic 'handle' on the triplet excited styrenes is not available as, none of the simple alkylated styrenes has been observed to phosphoresce (see Section 1.1). It seems likely that the lack of phosphorescence, on direct irradiation is due at least in part, to the presence of a non-radiative decay pathway from T_1, which can compete effectively with the radiative relaxation process. Indeed, although it has been demonstrated that the T_1 states of styrenes may be populated using a triplet energy transfer technique[18]

no $T_1 - S_0$ emission was observed, even though the styryl triplets produced in this way were 'frozen out' in a matrix of Argon at 10K.

It has been suggested that a non-radiative decay pathway which may be open to the styrenes in both the S_1 and T_1 states, could involve rotation about the $C_{7,8}$ essential double bond. Fig. 2.5 illustrates the dependence of the energies of these states (and the ground state, S_0) on α, the angle of rotation about this bond, as predicted from M.O. calculations on St, itself[11,19]. In the case of the T_1 state, calculations indicate that the $C_{7,8}$ bond in fact has little double bond character, such that rotation about this bond may indeed be expected to occur readily. As shown in fig. 2.5, it would appear that as the angle of rotation about the $C_{7,8}$ bond is increased from that of the planar ($\alpha = 0^o$) conformation, the energy of T_1 is reduced, reaching a minimum for $\alpha = 90^o$. Furthermore, it seems that for sufficiently large values of α, the T_1 state may actually become degenerate with the ground state, S_0. It can be seen that a state crossing of this type, which is facilitated by the large energy barrier to rotation in S_0 (thought to be of the order of $\sim$300 $kJ.mol^{-1}$[2]), would be expected to provide an effective means of depopulating T_1.

There has been some dispute in the literature[2,19] as to the detailed form of the dependence of the S_1 energy for the styrenes on the angle of rotation, α. It seems likely that, as with the corresponding state in both ethylene[20] and stilbene[21], there should be an energy minimum for the orthogonal ($\alpha = 90^o$) S_1 state. However, some calculations[19] have predicted that in the case of the styrenes, there should also exist a relative energy minimum within the S_1 state, for $\alpha = 0^o$. This relative minimum is thought to arise as a result of the presence of an initial energy barrier to rotation within S_1, caused by an avoided crossing with the S_2 state, which lies close in energy to S_1, for small values of α. As noted by Bruni and others[19], the presence of an energy minimum for $\alpha = 0^o$ is consistent with the results of a rotational band contour analysis, performed on the 0,0 absorption band of St[22]. Also, it can be seen that this minimum, if present, would correspond to the initially excited molecular conformation and could thus provide an explanation for the observed lack of a significant

Figure 2.5 The Predicted Dependence of the Energies of the Ground and First Excited Singlet and Triplet States of Styrene on the Angle of Rotation about the Ethylenic Bond

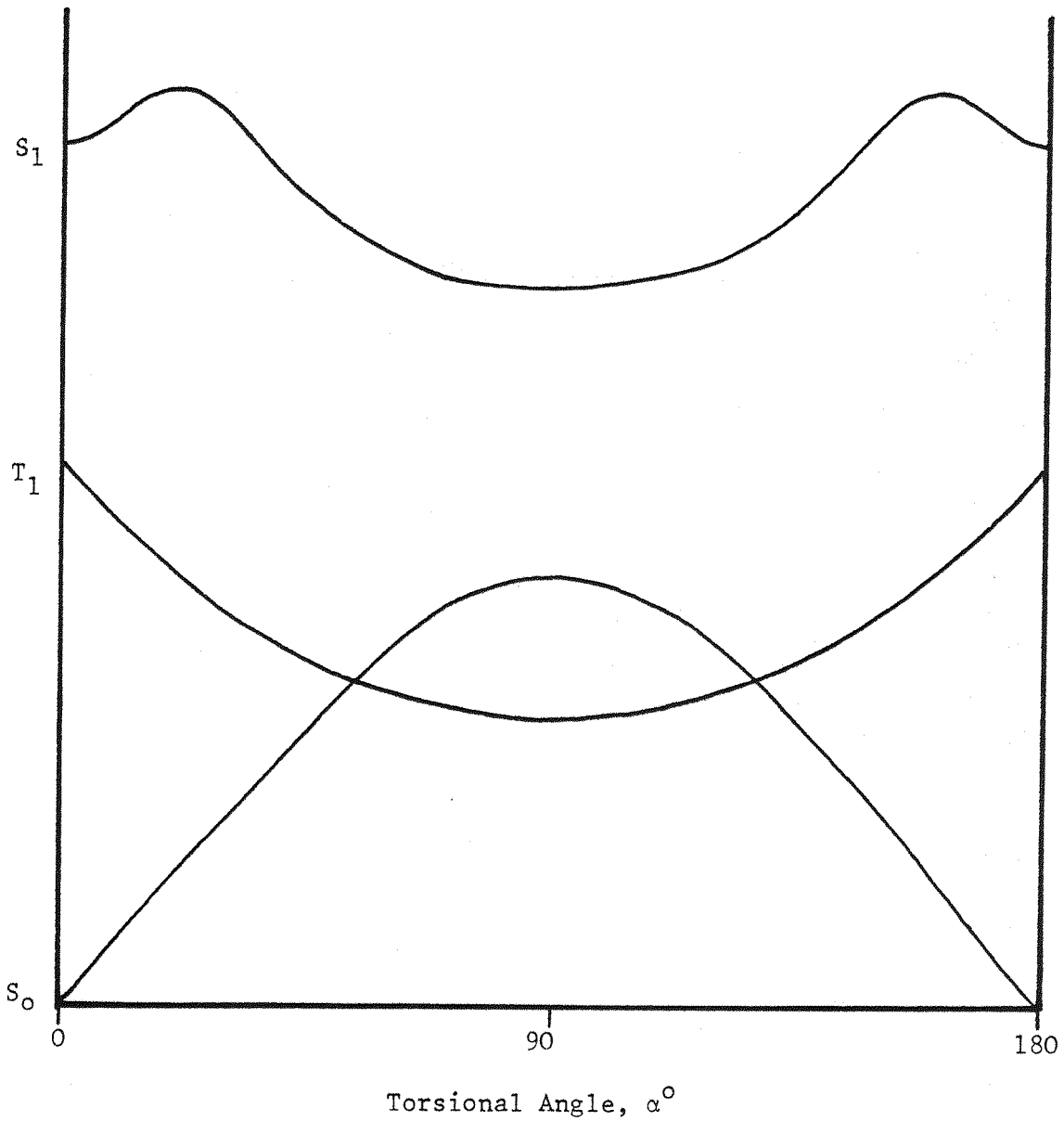

Stokes shift for the styrenes.

2.4 Geometric Isomerisation via the Excited Styrenes

In the case of styrenes possessing two different substituents at the C-8 (β) position, rotation about the $C_{7,8}$ bond on excitation may be expected to lead to geometric isomerisation. The process of photoisomerisation has been studied in most detail for the pair of isomeric styrenes, cis and trans phenylprop-1-ene (cPP and tPP respectively). The quantum yields for trans-cis (Φ_{cPP}) and cis-trans (Φ_{tPP}) isomerisation have been determined for this pair, on irradiation in both the gas phase[23] and in cyclohexane solution[11,24] and the values observed are presented below in Table 2.5.

Table 2.5

The Quantum Yields of Photoisomerisation Reported for the tPP, cPP System in the Gas Phase and in Cyclohexane Solution

	GAS	SOLUTION
Φ_{cPP}	0.22	0.24 (0.29)*
Φ_{tPP}	0.33	0.24

* The value in parentheses is Φ^{A}_{cPP}

According to fig. 2.5, it would appear that it may be possible for both singlet and triplet pathways to contribute to the process of photoisomerisation. Unfortunately, to date, attempts to determine the relative importance of these routes for the tPP, cPP pair[25] have proved inconclusive. Nevertheless, it may be useful at this point, to summarise some of the experimental observations reported in this context, in the hope that these may provide some insight into the question as to which non-radiative decay processes are important for the excited styrenes, in general. With this in mind, it may be noted that:

a) A triplet isomerisation mechanism may indeed be available here, since it has been observed[26] that on sensitised irradiation of tPP, rotation about the $C_{7,8}$ bond provides the only significant relaxation route for $^{3}tPP^{*}$.

b) On both direct[24] and sensitised[27] irradiation of tPP, it has been shown that the excited styrene may decay with equal efficiency to form ground state cPP and tPP, or in other words, a branching ratio of 1.0 has been determined for the isomerisation process. However, as illustrated in fig. 2.5, this observation does not in fact discriminate between the possibility of decay via the S_1 and T_1 states, since both these states are thought to possess an energy minimum for the orthogonal conformation, from which it is assumed that relaxation will occur. Hence, it would appear that in this case, partitioning between the products cPP and tPP should be governed principally by the form of the angular dependence of the S_o energy and a branching ratio of unity would thus be expected for decay from both S_1 and T_1.

c) From a comparison of Φ^D_{cPP} and Φ^A_{cPP}, the quantum yields of photoisomerisation of tPP in degassed and aerated cyclohexane respectively, it has been shown that an all singlet mechanism (i.e. internal rotation followed by IC from the twisted S_1 state) may in fact be ruled out as being the only isomerisation route available here. As has been illustrated in Table 2.4, the effects of ground state molecular oxygen on the decay characteristics of the singlet excited styrenes, may be described in terms of a diffusion-controlled, bimolecular quenching interaction. In common with other aromatic molecules[28], it may be proposed that this quenching of the S_1 state occurs as a result of an enhancement of the efficiency of ISC to T_1. It is interesting to note therefore, that as shown in Table 2.5, in the presence of oxygen, the efficiency of trans-cis photoisomerisation is also enhanced in the case of tPP. In fact, it can be seen that if an isomerisation pathway involving T_1 were not available, then the expected value of Φ^A_{cPP} could be calculated using the experimental value of Φ^D_{cPP}, according to a Stern-Volmer analysis analogous to equation (3) above. Using the value of Φ^D_{cPP} reported in Table 2.5, such a calculation provides a value for $(\Phi^A_{cPP})^{CALC}$ of 0.15 only, compared to the experimental value of $\Phi^A_{cPP} = 0.29$, determined by Crosby[11].

d) Two compounds which are structurally related to tPP and which have also been shown to undergo isomerisation on excitation are t-Stilbene (tSB) and t-β-Styryl Naphthalene (tStN). It is interesting

to compare the decay characteristics of these three compounds, in particular, in terms of the relative magnitudes of the rate constants (k_{ISOM}) which have been derived for the decay processes which result in isomerisation, in each case. The values of k_{ISOM} observed for these compounds at room temperature, in degassed, non-polar solvent are presented below in Table 2.6.

Table 2.6

The Values of the Rate Constant for trans-cis Photoisomerisation Reported for Three Related Compounds

	k_{ISOM} (s^{-1})
tPP	3.9×10^7
tStN[29]	2.0×10^7
tSB[30]	6.9×10^9

In the case of tPP, the experimental values of Φ^D_{cPP}, the quantum yield of formation of the cis isomer and τ_o, the fluorescence decay time of ^{1}tPP*, have been combined to yield a value for k_{ISOM}, according to:

$$k_{ISOM} = 2.\Phi^D_{cPP}.\tau_o^{-1} \qquad (4)$$

As a result of the fact that a branching ratio of unity has been reported for the isomerisation process here, a factor of 2 has been included in this expression, in order to take into account the fact that under these circumstances, k_{ISOM} should have a value equal to twice the rate of formation of the cis isomer ($\equiv\Phi^D_{cPP}.\tau_o^{-1}$).

From Table 2.6, it may be noted that the values of k_{ISOM} reported for tPP and tStN are very similar and that these are at least two orders of magnitude smaller than the corresponding value derived for tSB. In the case of the latter compound, it has been established that isomerisation occurs predominantly via a singlet mechanism[21,30], while tStN is thought to isomerise mainly via a route involving vertical ISC from S_1, followed by internal rotation

within T_1[29]. Hence, it may be that the relatively low value observed for k_{ISOM} in the case of tPP, is indicative of the fact that here too, such a triplet mechanism provides the principal non-radiative decay pathway. As is outlined briefly in the following, the results of a study of the temperature dependence of the decay characteristics of the excited styrenes are also compatible with this proposal.

2.5 The Effects of Temperature on the Decay of the Excited Styrenes

In general, the fluorescence quantum yields and decay times of the styrenes in degassed, non-polar solvents (such as the Methylcyclohexane/iPentane (MCHIP) system employed here) are observed to increase as the temperature is reduced. It has been shown[11] that these variations may be accounted for quantitatively, if it is assumed that at a given temperature (T), the sum of the rates of the non-radiative decay processes (k_2^T) comprises contributions from one temperature dependent and one temperature independent process (represented by k_{NR}^T and k_{NR}^{77}, respectively),

$$\text{i.e. } k_2^T = k_{NR}^T + k_{NR}^{77} \qquad (5)$$

The effects of temperature on the decay characteristics of the excited styrenes are typified in fig. 2.6, in which the fluorescence spectra recorded for IND at room temperature (290 K) and 77K are presented. Fig. 2.6 also illustrates the values which have been derived for the various rate parameters in this case, from quantum yield and decay time measurements at these temperatures. It can be seen that the increase in fluorescence intensity observed on reducing the temperature is accompanied by a marked improvement in the resolution of the fluorescence spectrum, as indeed is commonly observed[31].

The value reported here for k_{NR}^{77} has been corrected[32] for the effects of refractive index variation with temperature on the radiative decay rate (and hence Φ_F and τ_F), these effects being thought to become significant for temperatures below $\sim$200 K. The value of $3.8 \times 10^7 s^{-1}$, thus derived for k_{NR}^{77} is found to be typical of the styrenes in general and it is interesting to note that, even at room temperature, in the case of IND, this rate constant provides the major contribution to the observed value of k_2. This observation is characteristic of those styrenes which are thought to exist in a planar conformation in both

Figure 2.6 The Fluorescence Spectra of Indene Recorded at Room Temperature and 77K in Degassed Methylcyclohexane/i-Pentane Solution

$k_1^{290} = 5.0 \times 10^6 s^{-1} (k_1^{77})^{CALC} = 6.0 \times 10^6 s^{-1}$

$k_2^{290} = 5.75 \times 10^7 s^{-1}$ $k_{NR}^{77} = 3.78 \times 10^7 s^{-1}$

$k_{NR}^{290} = 1.95 \times 10^7 s^{-1}$

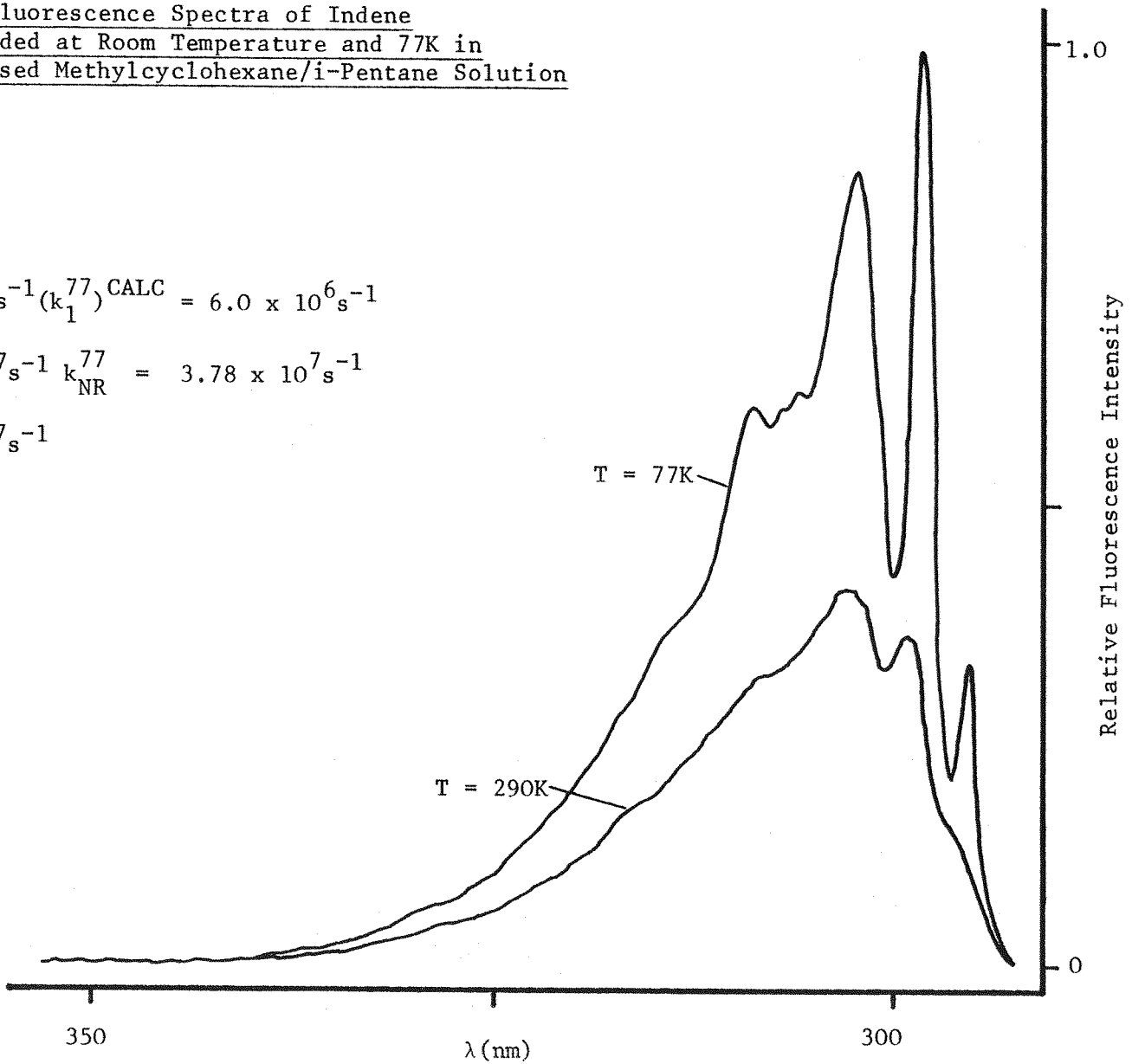

the ground and excited states, while in the case of the non-planar derivatives, the temperature dependent decay process, represented by k_{NR}^{T}, is found to increase markedly in importance as the temperature is increased (see e.g. Table 2.7 below). For all those styrenes examined so far, including the acyclic styrenes[11], phenyl cycloalkenes[33] and benzocycloalkadienes, as exemplified by IND studied in this work, it is remarkable that the value derived for k_{NR}^{77} falls within a very narrow range ($\sim$2-6 x $10^{7}s^{-1}$). The nature of the temperature independent decay process involved here is uncertain although the fact that rather low values have been observed for the ISC efficiencies in the case of the phenylcycloalkenes[33], has been taken to indicate that k_{NR}^{77} represents the rate of vertical IC ($S_1 \rightsquigarrow S_0$) for these compounds. However, these results were derived using a triplet energy transfer technique involving the use of biacetyl as acceptor. The applicability of this technique to compounds such as the styrenes, which are thought to be characterised by very short triplet lifetimes (possibly as low as 50-100 ns[34]) has been questioned. Furthermore, in view of the fact that as noted already, the S_1 - S_0 energy gap is relatively large for the styrenes (by comparison to other aromatic molecules for which IC is important) it may be more reasonable to suggest that k_{NR}^{77} is in fact associated with the process of vertical ISC ($S_1 \rightsquigarrow T_1$).

In the case of the temperature dependent decay pathway available to the styrenes, it would appear that the nature of this process is strongly dependent on the molecular structure of the compound under consideration. This is exemplified below in Table 2.7, for the pair of isomeric styrenes cPP and tPP, for each of which the room temperature value of the sum k_2^{290} has been broken down into components due to the temperature dependent and independent decay routes.

Table 2.7

The Effects of Temperature on the Non-Radiative Decay of cis and trans Phenylprop-1-ene

	k_2^{290} $s^{-1}(x10^{-7})$	k_{NR}^{290} $s^{-1}(x10^{-7})$	k_{NR}^{77} $s^{-1}(x10^{-7})$	$\Delta E_{NR}^{\dagger}$ $(kJ.mol^{-1})$	A_{NR}
tPP	5.85	1.85	4.0	3.65	9.8×10^{7}
cPP	44.6	40.2	4.4	14.78	9.1×10^{10}

Also presented in Table 2.7 are the values of the activation energies ($\Delta E^{\ddagger}_{NR}$) and Arrhenius A factors (A_{NR}) which have been derived[11] from plots of loge (k^{T}_{NR}) vs. T^{-1} for these compounds. It can be seen that the absolute value of k^{290}_{NR} here would appear to be determined principally by the magnitude of the A factor rather than the activation energy for the temperature dependent decay process. In the case of the planar trans isomer, although this process is characterised by a value of $\Delta E^{\dagger}_{NR}$ which is considerably lower than that observed for cPP, the thousand-fold increase in A_{NR} for the latter, results in the observation of a significantly larger value of k^{290}_{NR} than that derived for tPP. The fact that a relatively small A factor is observed for the temperature dependent non-radiative decay of ^{1}tPP* (and the other planar styrenes) may be taken to indicate that the process involved here is formally forbidden. It has been proposed that this process is in fact an activated ISC, involving promotion from S_1 to a higher triplet state T_n (where $n \geq 5$). This suggestion was made on the basis of a comparison of the magnitude of A_{NR} here with the corresponding parameter determined for the temperature dependent ISC process in other aromatics[35] (for which A factors of the order of 10^7 - $10^8 s^{-1}$ are typically observed). An alternative proposal as to the nature of the temperature dependent decay pathway here is that this could involve a crossover to a Doubly Excited (DE) state, although there is as yet no experimental evidence to support this view. However, in the case of St itself, the existence of a DE state, lying intermediate in energy between S_1 and S_2 has been predicted[2] and it could be that, as with the diphenylpolyenes[36], the presence of such a state could have important photophysical consequences.

As has been noted already in Table 2.2, those styrenes which are forced by steric constraints to adopt a non-planar ground state conformation, are characterised by rather larger values of k^{290}_{2} than their planar counterparts. From the data of Table 2.7, it would appear that in the case of the non-planar derivatives as exemplified by cPP, the principle contribution to k^{290}_{2} may be accounted for by the presence of a single, temperature dependent decay pathway. The relatively large Arrhenius A factor associated with this route suggests that the process involved is formally allowed and one such process

which might be envisaged here could involve internal rotation within the S_1 state. The steric hindrance to coplanarity of the aryl and olefinic moieties in the case of cPP, arises as a result of the non-bonded interactions between the phenyl protons and those protons attached to the terminal methyl group. It is interesting to note therefore that rotation (α) about the essential $C_{7,8}$ double bond may in fact alleviate these repulsive interactions, and thus allow freer rotation (θ) about the anyl-olefin ($C_{1,7}$) bond to occur. On excitation to the S_1 state, the $C_{1,7}$ bond is thought to shorten and gain some double bond character (cf. fig. 2.3). Hence, it can be seen that rotation about this bond should enable the aryl and olefinic groups to attain a conformation which is more favourable energetically, in terms of the greater degree of π-overlap then possible. A similar proposal has been made in the case of the closely related compound cis-Stilbene (cSB), for which an attempt has been made to quantify this effect by calculating the changes in the torsional angles α and θ which are predicted to occur, on excitation[16]. The values which have been derived for these parameters in the ground and first excited singlet states of cSB and also for the corresponding trans isomer (tSB) are illustrated in Table 2.8 below.

Table 2.8

The Calculated Values of the Torsional Angles α and θ for cis and trans Stilbene in the Ground and First Excited Singlet States

	tSB		cSB	
	S_o	S_1	S_o	S_1
α	180	180	10	37
θ	0	0	35	13

These results indicate that in the case of the hindered cis derivative, on excitation, the aryl-olefin bond angle θ is observed to decrease as rotation occurs about the essential double bond whereas under the same conditions, the conformation of the planar trans isomer is expected to remain unchanged. In other words, it would appear that the initially excited trans isomer already possesses

the extra stabilisation conferred by a planar geometry, while in the case of the cis derivative, internal rotation must occur prior to achieving such a conformation. It may be that the same is true for the styrenes and that it is the occurrence of this conformational change within the S_1 state, which provides the additional non-radiative decay pathway shown to be available to the hindered styrenes by comparison with the planar derivatives.

It is possible that such a process may also be responsible for the observed variation in the magnitude of k_2, the sum of the non-radiative rate constants, reported for a series of Phenylcycloalkenes[33] ($C_{(n)}$ - where n represents the number of ring C atoms). For these compounds it has been shown that at room temperature, the value of k_2 varies with ring size in the order:

$$C_{(4)}, C_{(5)} < (C_{(8)}) < C_{(6)} < C_{(7)}$$

Zimmermann has proposed that the important decay pathway here involves IC from the twisted S_1 state and that this ordering of the k_2 values reflects the relative ease of attainment of such a conformation. Indeed, it can be seen that within this series, the effects of ring strain imposed on rotation about the essential double bond, should be reduced as the ring size is increased. A decrease in the energy barrier to rotation within S_1 (and also T_1) would be expected to result from this and hence an increase in the value of k_2 with the ring size would be predicted. However, as shown in Table 2.2, the values of k_2 recorded at room temperature, for the planar acyclic derivatives such as tPP, for which there are no such structural restrictions to internal rotation, are found to be virtually identical to that derived for the highly constrained $C_{(5)}$ Phenylcycloalkene (PcP). This would appear to suggest once again, that the relative orientation of the aryl and olefinic groups may play an important role in determining the magnitude of k_2 for the styrenes, in general. Unfortunately, no quantitative information is available as to the values of the dihedral angles (θ) which might be expected for the phenylcyclo-alkenes. However, molecular models indicate that the extent to which non-bonded interactions between the phenyl and ring methylene protons can force the phenyl groups out of plane does vary with ring size.

Furthermore, these effects seem to mirror, qualitatively at least, the observed variation in k_2 with ring size noted above and may also provide an explanation for the apparently anomalous behaviour of the $C_{(8)}$ derivative, Phenylcyclooctene.

2.6 Summary

As has been demonstrated throughout this Chapter, structural effects appear to play an important part in governing the overall decay characteristics of the excited styrenes. In attempting to summarise the unimolecular photophysics of the styrenes in general, it is convenient to classify these compounds in terms of their ground state equilibrium configuration. The relative orientation of the aryl and olefinic moieties seems to be of particular importance and it is useful to categorise the styrenes as being either planar or non-planar in this respect. For each of these classes of compound, three routes which provide a significant contribution to the overall decay from the S_1 state have so far been identified and the nature and relative efficiencies of these processes are summarised briefly in Table 2.9.

In the case of the planar derivatives, the single most important decay pathway would appear to involve the temperature independent non-radiative decay process. It may be more than coincidental that in the case of tPP, the value of the rate constant for this process (k_{NR}^{77}) is in fact observed to be identical to that derived for the process(es) leading to geometric isomerisation, on excitation. On the basis of this observation and in view of the preceding discussions, it is tempting to suggest that k_{NR}^{77} in fact represents the rate constant for the primary decay process of vertical ISC from S_1 and that for the planar trans isomers in which isomerisation is possible, this occurs predominantly via the T_1 state. Although the magnitude of the rate constant for the temperature independent non-radiative decay of both the planar and non-planar derivatives is apparently the same, it can be seen that for the latter, the relative efficiency of this process is markedly reduced at room temperature. This is a result of the fact that at this temperature, the principle feature of the photophysics of the non-planar styrenes is the presence of a relatively efficient, temperature dependent non-radiative decay pathway (which would seem to be unimportant in the case of the planar

Table 2.9

A Summary of the Decay Pathways Thought to be Available to the Excited Styrenes at Room Temperature in Degassed, Non-Polar Solvents

PROCESS	PLANAR	NON-PLANAR
Radiative Decay	$\Phi_F \simeq 0.2 - 0.3$ - with the exception of IND, for which the relatively low k_1 value causes Φ_F to be reduced.	$\Phi_F \simeq 0.01 - 0.1$ - the efficiency here is reduced by comparison to the planar derivatives as a result of both a decrease in the value of k_1 and an increase in k_2
Temperature Independent Non-Radiative Decay	$\Phi_{NR}^{77} \simeq 0.5 - 0.6$ - with an average value for the rate constant associated with this process of:- $k_{NR}^{77} = 4.0 \times 10^7 s^{-1}$	$\Phi_{NR}^{77} \simeq 0.08 - 0.3$ - it may be noted that, as for the planar styrenes, a value of $k_{NR}^{77} = 4.0 \times 10^7 s^{-1}$ is generally observed.
Temperature Dependent Decay	$\Phi_{NR}^{290} \simeq 0.2 - 0.3$ - this process is apparently formally forbidden and may correspond to an activated ISC	$\Phi_{NR}^{290} \simeq 0.6 - 0.9$ - an allowed process possibly corresponding to a thermally activated conformational change within S_1, (followed by IC and/or ISC).

compounds). It is most interesting to note that from a study of a range of alkylbenzenes, similar observations, regarding structural effects on non-radiative decay have been reported[37]. For these compounds, the importance of α,β C-C bonds in the non-radiative decay process has been demonstrated and it has been shown that, as is apparently the case with the styrenes, these bonds are most effective in enhancing the decay rate, when out of the plane of the phenyl ring.

REFERENCES - CHAPTER 2

1a) H. Suzuki
Bull. Chem. Soc. Jpn., 33, 619 (1960)

1b) H. Suzuki
'Electronic Absorption Spectra and Geometry of Organic Molecules', Chap. 13
Academic Press, New York, (1967)

1c) A.M. Talati and B.V. Shah
Indian J. Chem. 11, 1328 (1973)

1d) G. Fischer, E. Fischer and H. Stagemeyer
Ber. Bunsenges Phys. Chem., 77, 687 (1973)

1e) T. Fueno, K. Yamaguchi and Y. Naka
Bull. Chem. Soc. Jpn., 45, 3293 (1972)

2. G.L. Bendazzoli, G. Orlandi, P. Palmieri and G. Poggi
J. Amer. Chem. Soc., 100, 392 (1978)

3a) J.W. Rabalais and R.J. Colton
J. Electron Spectrosc. Relat. Phenom, 1, 83 (1972)

3b) M.H. Palmer and S.M.F. Kennedy
J.C.S. Perkin II, 1893 (1974)

4. G.W. King and A.A.G. Van Putten
J. Mol. Spectrosc., 44, 286 (1972)

5. J.P. Maier and D.W. Turner
J.C.S. Faraday II, 196 (1973)

6. W.G. Fateley, G.L. Carlson and F.E. Dickson
Appl. Spectrosc., 22, 650 (1968)

7a) K.S. Dhami and J.B. Stothers
Can. J. Chem., 43, 510 (1965)

7b) Gurudata, J.B. Stothers and J.D. Tolman
Can. J. Chem., 45, 731 (1967)

7c) G.K. Homer, I.R. Peat and W.F. Reynolds
Can. J. Chem., 51, 915 (1973)

8. L.H. Schwartzmann and B.B. Corson
J. Amer. Chem. Soc., 78, 322 (1956)

9. e.g. G.B. Backman and R.W. Finholt
J. Amer. Chem. Soc., 70, 622 (1948)

10. P.L. Britton, C.L. Cheng, R.J.W. Le Fevre, L. Radom and G.L.D. Ritchie
J.C.S. (B), 2100 (1971)

11. P.M. Crosby
Ph.D. Thesis, Southampton (1979)

12. J.A. Barltrop and J.D. Coyle
'Excited States in Organic Chemistry', Chap. 3
John Wiley and Sons, London (1975)

13. A.L. Lyons, Jr. and N.J. Turro
J. Amer. Chem. Soc., 100, 3177 (1978)

14. W.R. Ware
Pure Appl. Chem., 41, 635 (1975)

15. W.R. Ware
'Creation and Detection of the Excited State', Chap. 5
(A.A. Lamola ed.), Marcel Dekker, New York (1971)

16. G. Fischer, G. Seger, K.A. Muszkat and E. Fischer
J.C.S. Perkin II, 1569 (1975)

17. J.B. Birks
'Photophysics of Aromatic Molecules'
Wiley, (1970) and references therein

18. P.M. Crosby, J.M. Dyke, J. Metcalfe, A.J. Rest, K. Salisbury and J.R. Sodeau
J.C.S. Perkin II, 182 (1977)

19a) M.C. Bruni, F. Momicchioli, I. Baraldi and J. Langlet
Chem. Phys. Lett., 36, 484 (1975)

19b) M.H. Hui and S.A. Rice
J. Chem. Phys., 61, 833 (1974)

20. A. Kaldor and I. Shavitt
J. Chem. Phys., 48, 191 (1968)

21. G. Orlandi and W. Siebrand
Chem. Phys. Lett., 30, 352 (1975)

22. A. Hartford Jr. and J.R. Lombardi
J. Mol. Spectrosc., 35, 413 (1970)

23. M.G. Rockley and K. Salisbury
J.C.S. Perkin II, 1582 (1973)

24. C.S. Nakagawa and P. Sigal
J. Chem. Phys. 58, 3529 (1973)

25. See e.g. ref. 11 and also the Xe quenching studies reported in:
G.R. Mant
Ph.D. Thesis, Southampton (1979)

26. R.A. Caldwell, G.W. Sovocool and R.J. Peresie
J. Amer. Chem. Soc., 93, 779 (1971)

27. A.A. Lamola and G.S. Hammond
J. Chem. Phys., 43, 2129 (1965)

28a) R. Potashnik, G.R. Goldschmidt and M. Ottolenghi
Chem. Phys. Lett., 9, 424 (1971)

28b) B. Stevens
J. Photochem., 3, 393 (1974)

29a) G.G. Aloisi, U. Mazzucato, J.B. Birks and L. Minuti
J. Amer. Chem. Soc., 99, 6340 (1977)

29b) P. Bartolus and G. Galiazzo
J. Photochem., 2, 361 (1974)

30a) D.J.S. Birch and J.B. Birks
Chem. Phys. Lett., 38, 432 (1976)

30b) J.B. Birks
Chem. Phys. Lett., 38, 437 (1976)

31a) See e.g. S. Hirayama
Bull. Chem. Soc. Jpn., 48, 2653 (1975)

31b) E.D. Cehelnik, R.B. Cundall, J.R. Lockwood and T.F. Palmer
J. Phys. Chem., 79, 1369 (1975)

32. For a discussion on the effects of refractive index variation on k_1, see:
J. Olmsted III
Chem. Phys. Lett., 38, 287 (1976)

33. H.E. Zimmerman, K.S. Kamm and D.P. Werthemann
J. Amer. Chem. Soc., 97, 3718 (1975)

34. R. Bonneau
Université Bordeaux
(Unpublished results)

35. J.B. Birks (ed.)
'Organic Molecular Photophysics', Vol. I
J. Wiley and Sons (1973)

36a) R.B. Birge, K. Schulten and M. Karplus
Chem. Phys. Lett., 31, 457 (1975)

36b) K. Schulten, I. Ohmine and M. Karplus
J. Chem. Phys., 64, 4422 (1976)

37. W.W. Schloman, Jr. and H. Morrison
J. Amer. Chem. Soc., 99, 3342 (1977)

38. S.L. Murov
'Handbook of Photochemistry'
(Marcel Dekker, 1977)

CHAPTER 3

PHOTOPHYSICAL ASPECTS OF EXCIPLEX FORMATION AND DECAY

3.1 Introduction

A study has been made of the bimolecular interactions between electronically excited styrenes and tertiary amines. This chapter provides an examination of some of the photophysical aspects of these interactions.

Fluorescent exciplexes have now been observed for a wide variety of systems[1], including those involving various combinations of condensed aromatic hydrocarbons with aliphatic and aromatic amines[2]. The appearance of exciplex emission has proved invaluable in a number of cases, in providing a means of analysing the kinetics of the quenching processes involved[3].

The styrene/tertiary amine systems were therefore examined in the hope that:

i) A bimolecular interaction of this sort might lead to formation of a fluorescent exciplex,

ii) Photophysical studies of such an interaction might then help to elucidate the mechanism of formation of the products observed[4] on photolysis of mixtures of these compounds.

Initially it was observed that addition of successive amounts of triethylamine (Et_3N) to a solution of Indene (IND) in cyclohexane, irradiated at a wavelength such that only the IND was absorbing, caused the intensity of the IND emission to be reduced. Associated with this quenching of the monomer fluorescence was the appearance, at longer wavelengths of a new, broad, structureless emission. Fig. 3.1 illustrates these features, the isosbestic point at 352 nm. being indicative of the presence of two emitting species.

U-v spectra of the amine/IND solutions gave no indication of any new absorption, which could be attributed to a ground state charge transfer complex. Furthermore, it was found that a corrected fluorescence excitation spectrum, recorded at the λ_{max} of the new emission, reproduced the absorption spectrum of the monomer, as is illustrated in fig. 3.2.

Figure 3.1

Fluorescence Spectra for the IND/Et_3N System in Degassed Cyclohexane

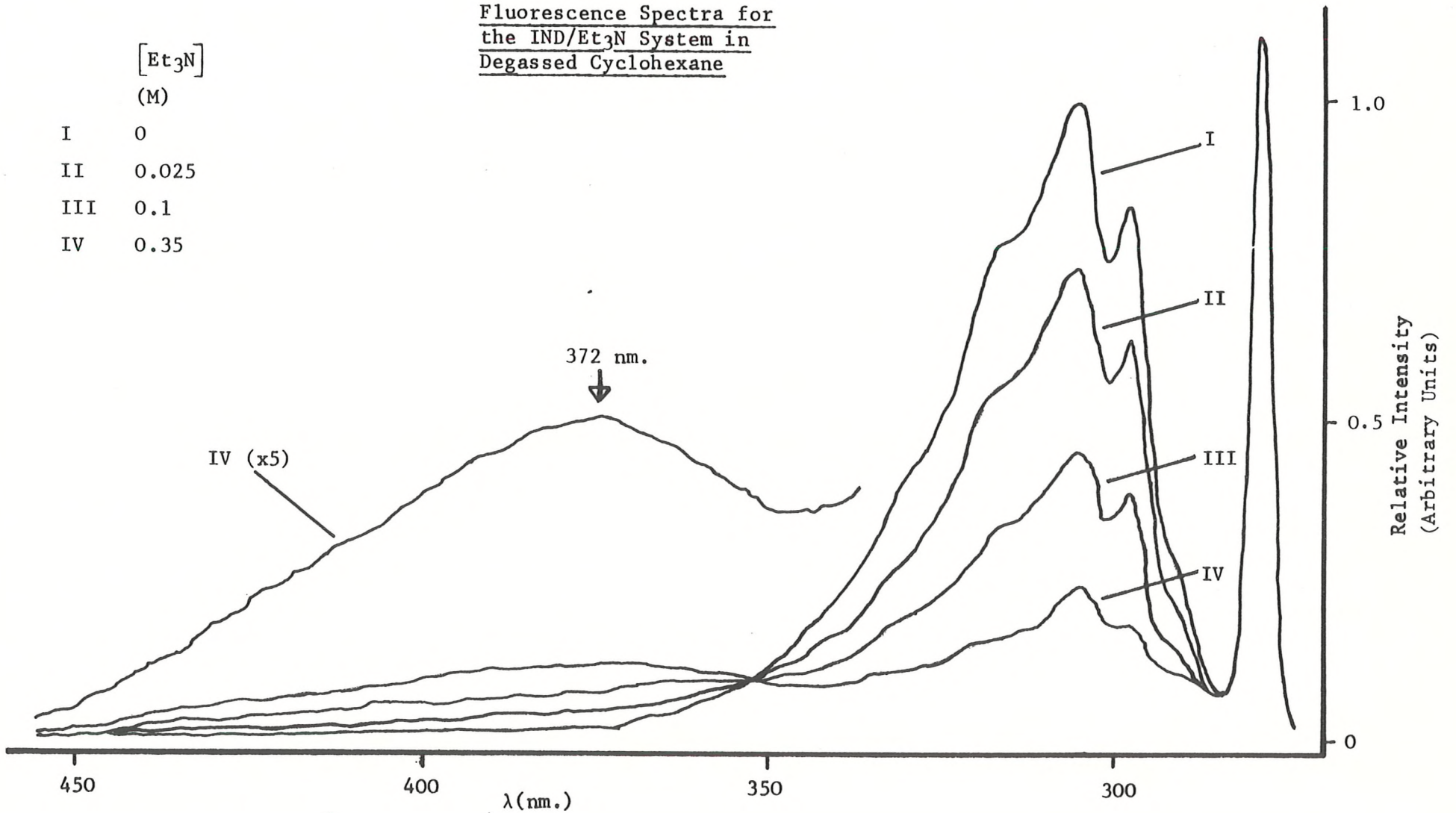

Figure 3.2

Comparison of Absorption and Fluorescence Excitation Spectra for the IND/Et_3N System

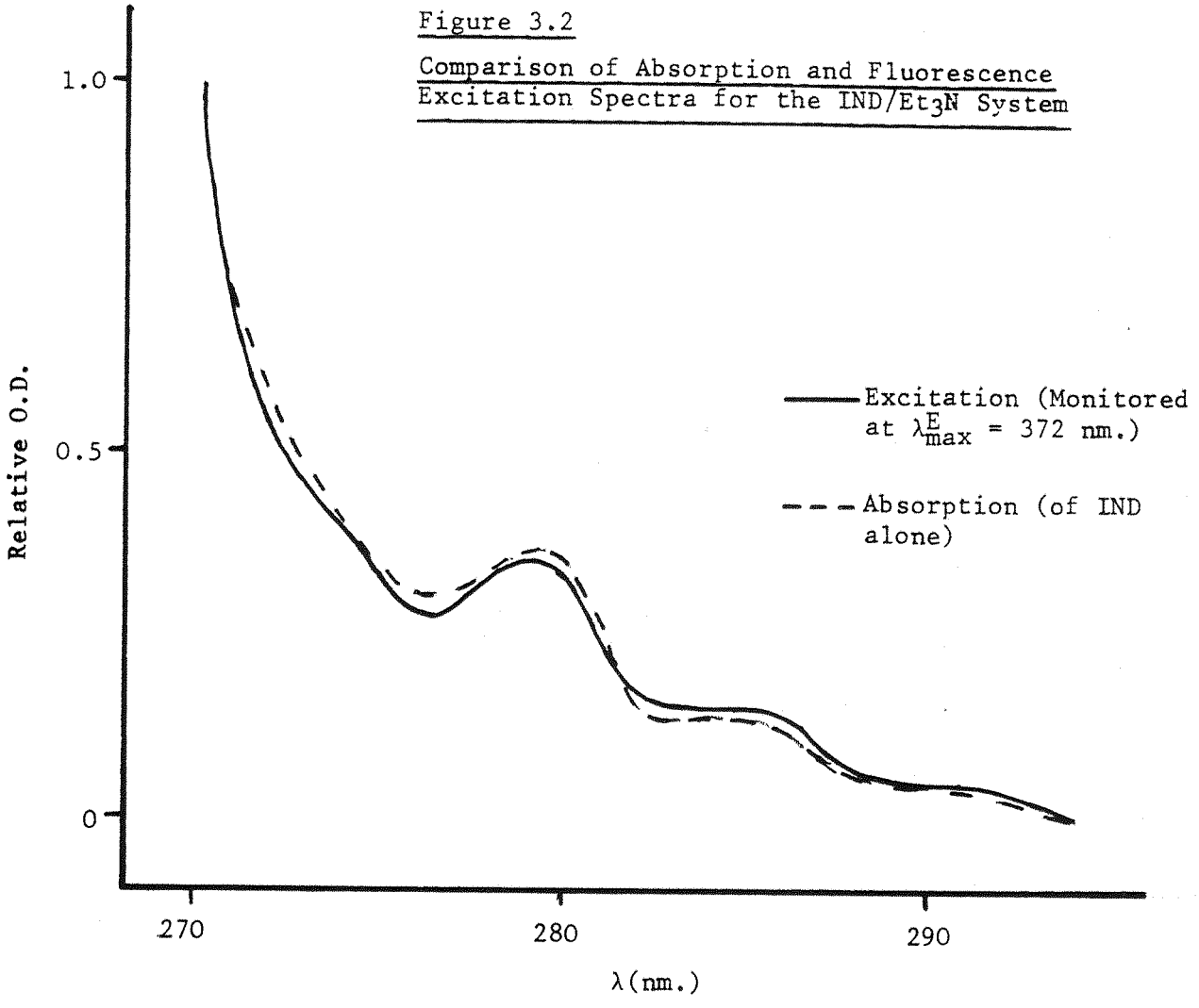

Further detailed investigation has now allowed the styrenes to be added to the growing list of exciplex-forming compounds.

3.2 Exciplex Emission Maxima (λ^E_{max})

The range of structural types, incorporating the styryl group, which have been studied with Et_3N as quencher, is detailed in Table 3.1. Also presented are the values of λ^E_{max}, the exciplex emission maximum observed in each case. The data of Table 3.1 indicates that even within such a series of closely related compounds, with a common quencher, the value of λ^E_{max} may vary quite considerably. As discussed in the following sections, these variations reflect the relative degree of Charge Transfer (CT) character within the excited state complexes.

Table 3.1

Exciplex Emission Maxima Observed for a Number of Styrene/Et_3N Systems in Cyclohexane

Styrene	λ^E_{max} (nm.)
St	399
oMe	409
2PP	391
tPP	387
cPP	385
IND	372
DHN	381
PNB[56]	375

The relative ordering of the molecular orbitals of the styrenes compared to Et_3N is such that the excited styrenes can act as electron acceptors ($^1A^*$) in the presence of a ground state electron donor (D), Et_3N. A simple M.O. treatment proposed by Weller[2a], provides a picture of the processes involved in such an interaction (see fig. 3.3). This suggests that in this case, a correlation might be expected between λ^E_{max} and the electron accepting ability of the styrenes, as ($^1A^*$) is varied.

It should be pointed out however, that such a treatment is an approximation in that it assumes a pure CT character for the interaction. The exciplex wavefunction however, comprises of contributions from both locally excited (LE) and CT configurations.

$$\text{i.e. } \psi_E = \underbrace{a\psi_{A^*D} + b\psi_{AD^*}}_{\text{LE}} + \underbrace{c\psi_{A^{\oplus}D^{\ominus}} + d\psi_{A^{\ominus}D^{\oplus}}}_{\text{CT}} \qquad (1)$$

Fig. 3.3 is thus equivalent to the case where all but the last term of this expression are neglected. That such an approximation is in

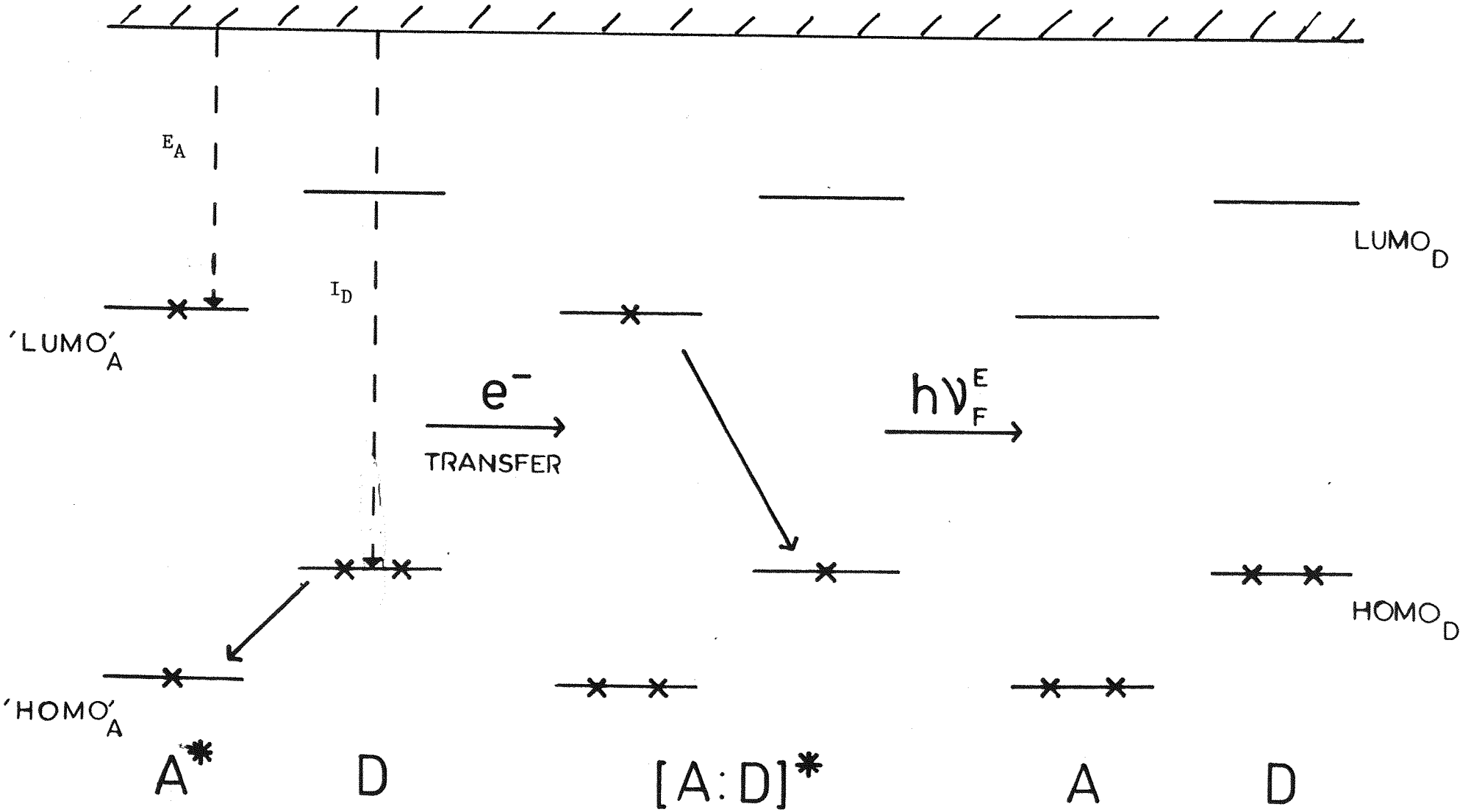

Figure 3.3 A Molecular Orbital Treatment of Exciplex Formation and Emission

fact not unreasonable, in the case of the styrene/Et_3N exciplexes, is demonstrated by the fact that relatively high dipole moments have been measured for a number of examples (see p.66). This is usually taken as an indication of a high degree of CT character in the complex.

3.3 Correlation of λ^E_{max} with Reduction Potential

From the model represented by fig. 3.3, it can be seen that the energy of the exciplex emission maximum (E^E_{max}) may be related to the donor Ionisation Potential (I_D) and the Electron Affinity of the acceptor (E_A). Neglecting solvation effects, this relation can be expressed in the form:

$$E^E_{max} = I_D - E_A + CONST \qquad (2)$$

which reduces to:

$$E^E_{max} = CONST - E_A \qquad (3)$$

- when a common donor is used (I_D = const.).

Hence, a linear relationship is expected between the energy of the exciplex emission maximum and the electron accepting ability (as measured by E_A) for a series of acceptors. Unfortunately, electron affinities are notoriously difficult to obtain experimentally and so recourse has been made to the more readily accessible half-wave reduction potentials ($E_{A^\ominus/A}$), which are assumed to be linearly related to E_A.

The work of Knibbe[6] provides an example of such a correlation between E^E_{max} and $E_{A^\ominus/A}$, where it was found that, for a series of aromatic hydrocarbon acceptors, with the common donor, N,N diethylaniline, the value of E^E_{max} obeyed the relation:

$$E^E_{max} = 1.17 - 0.65.E_{A^\ominus/A} \qquad (4)$$

The values of $E_{A^\ominus/A}$ were therefore measured for a number of the styrenes studied, using cyclic voltammetry in DMF solution. These values are given in Table 3.2, together with the corresponding energies of the exciplex emission maxima (in eV.).

Table 3.2

Exciplex Emission Maxima, Half-Wave Reduction Potentials and Calculated Electron Affinities[(a)] for a Number of Styrenes

Styrene	E^{E*}_{max} (eV.)	$-E_{A\ominus/A}$ ** (V.)	$-E_A^{CALC}$ *** (eV.)
St	3.11	2.48	0.36
OMe	3.03	2.46	0.36
tPP	3.20	2.63	0.23
IND	3.33	2.74	0.06
DHN	3.25	2.65	(-0.09)

* - with Et_3N as the quencher, in cyclohexane solution

** - measured by cyclic voltammetry in DMF

*** - from equation (8), using the I_A values given in Table 3.3

(a) - referred to in Section 3.4.

This data, plotted as in fig. 3.4, was found to give a least squares best fit to the relation:

$$E^E_{max} = 0.72 - 0.95\ E_{A\ominus/A} \qquad (5)$$

From the simple viewpoint of complete charge transfer within the exciplex, as illustrated by fig. 3.3, it would be expected that for a series of complexes, with a common donor, the slope of a plot of E^E_{max} versus E_A should be 1.0 (when both these terms are expressed in the same units). This is of course, providing that on formation of the exciplexes, there is little perturbation of the orbitals involved; or in other words, if the energy charges ΔE_{1-4} of fig. 3.5 are relatively small. The important orbital interactions, as shown here, are those between $'HOMO'_{A*}$ - $HOMO_D$ and $'LUMO'_{A*}$ - $LUMO_D$ and as the energy difference between each pair is rather small, these interactions will lead to first order perturbations. These, unlike the HOMO-LUMO interactions involved in ground state reactions, which lead to second order perturbations, are expected to be

Figure 3.4

A Plot of the Energy of the Styrene/Et_3N Exciplex Emission Maxima* vs. Half-Wave Reduction Potential for a Number of Styrenes

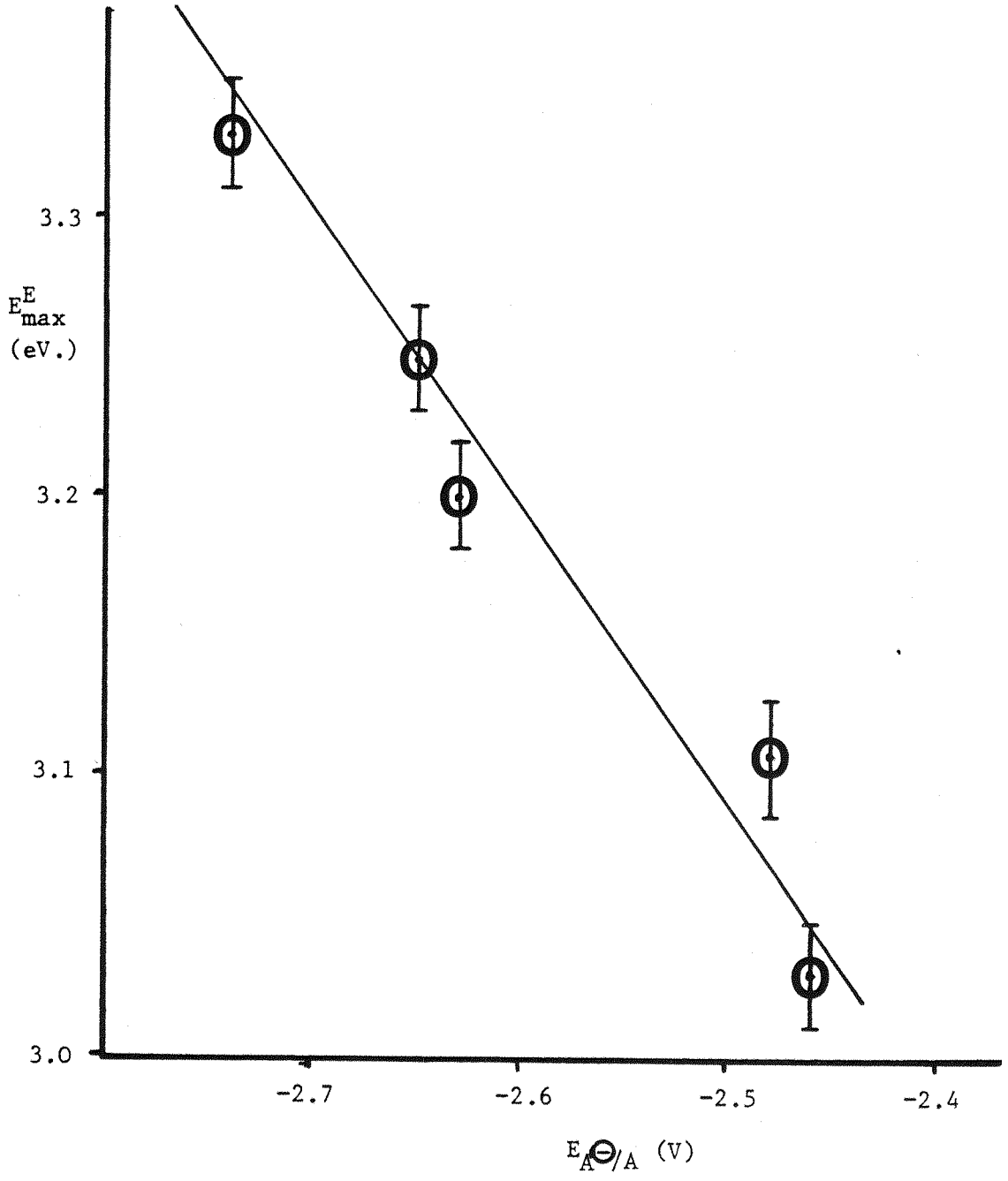

*The error bars represent ±2 nm. in the determination of λ^E_{max}

difficult to quantify[7]. In the case of the styrene/Et_3N systems, a comparison has been made between the energy of the exciplex emission maxima and the energy difference between the two orbitals involved in the radiative decay process (i.e. essentially $'LUMO'_{A*}$ and $HOMO_D$).

Figure 3.5 A Representation of the Principle Orbital Interactions Involved in Exciplex Formation

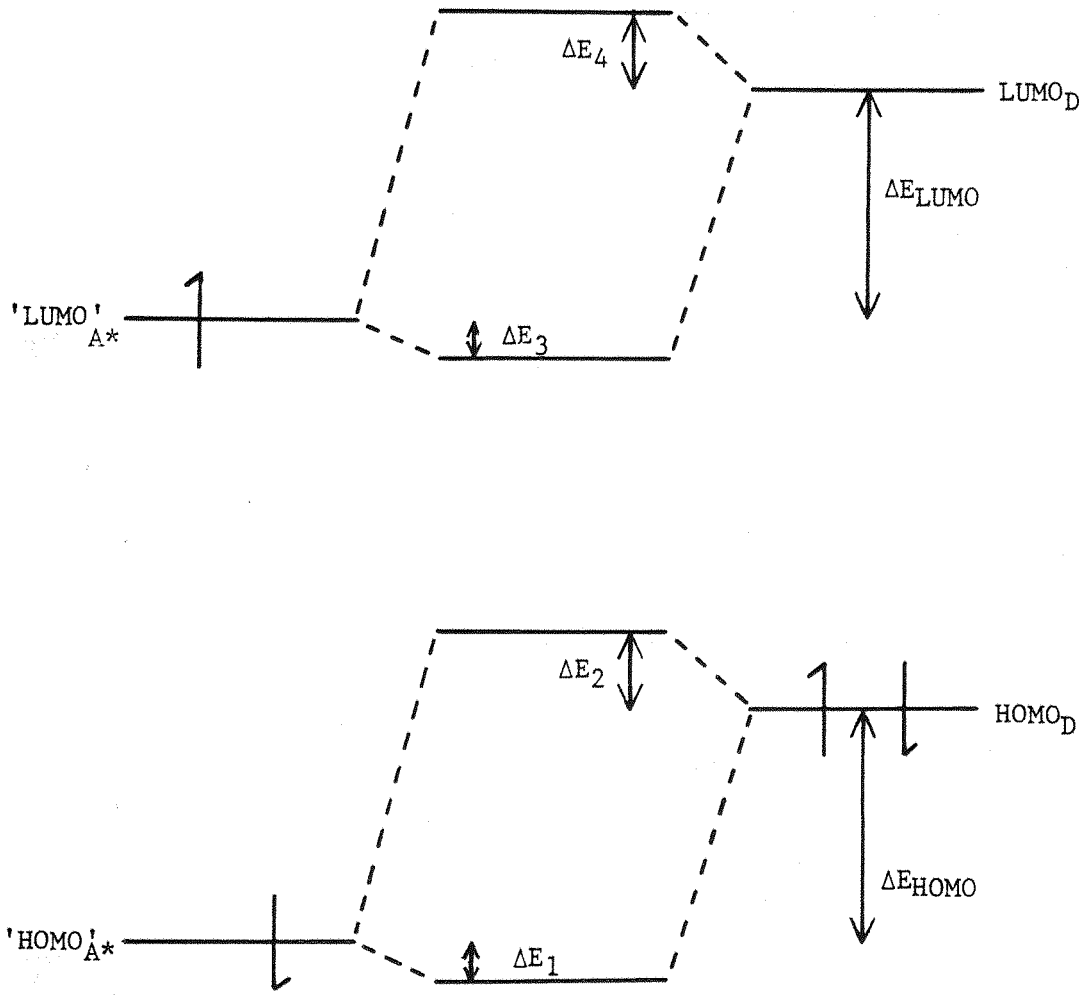

For this, the gas phase ionisation potentials for the donor (I_D) and the various acceptors (I_A) were used. The energy of $LUMO_{A*}$ was approximated to $(I_A - \Delta E_{o,o})$, where $\Delta E_{o,o}$, the energy of the o-o transition was obtained from absorption spectra. As shown in Table 3.3, this comparison revealed that in each case, the energy

of the exciplex emission maximum was only slightly less than the $'LUMO'_{A*}$ - $HOMO_D$ energy gap, measured in this way. This therefore suggests that for these systems, the perturbation of the various orbitals on exciplex formation, is indeed relatively small.

Table 3.3

Comparison of E^E_{max} and the $'LUMO'_{A*}$ - $HOMO_D$ energy gap for a number of styrene/Et_3N systems

Styrene	E^E_{max} (eV.)	$I_D-(I_A+\Delta E_{o,o})$ (eV.)	Difference (eV.)
St	3.11	3.22	0 .11
2Me	3.03	3.11	0.08
tPP	3.20	3.29	0.09
IND	3.33	3.60	0.27
DHN	3.25	3.57	0.32

Thus, as already stated, a plot of E^E_{max} versus the acceptor electron affinity here might be expected to have a slope of 1.0. However, the correlation of fig. 3.4 was obtained using $E_{A^\ominus/A}$ as a measure of the relative electron accepting abilities of the styrenes, rather than E_A. Hence the relationship between these two parameters is required before any comments may be made as to the meaning of the observed slope of fig. 3.4.

3.4 Electron Affinities of the Styrenes

It has been shown empirically by Brieglieb[8] that for a series of aromatic hydrocarbons, there is a linear relationship between $E_{A^\ominus/A}$ and E_A, taking the form:

$$E_A = 3.49 - 1.45\ E_{A^\ominus/A} \qquad (6)$$

However, more recently, E_A values for this same series of compounds were calculated using a SCFMO technique[9]. The values obtained were then found to correlate well with the experimental reduction potentials but giving a slope for the E_A vs. $E_{A^\ominus/A}$ plot of only -0.92. Styrene itself has been the subject of similar theoretical

calculations and these have predicted E_A values in the region of -0.29 to -0.55 eV[10].

The Pairing Theorem for alternant hydrocarbons as proposed by Pople[11] and others, predicts that:

$$I_A + E_A = \text{CONST.} \qquad (7)$$

(where I_A is the Ionisation Potential of molecule A)

and the value of the constant here has been determined to be 8.14 eV.[12], again from a study of a range of aromatic hydrocarbons. Therefore, it has been possible to calculate E_A for the styrenes studied here, using equation (7) and hence establish the relation between these values and the experimental reduction potentials. These results are presented in Table 3.2 and now, graphically, as fig. 3.6.

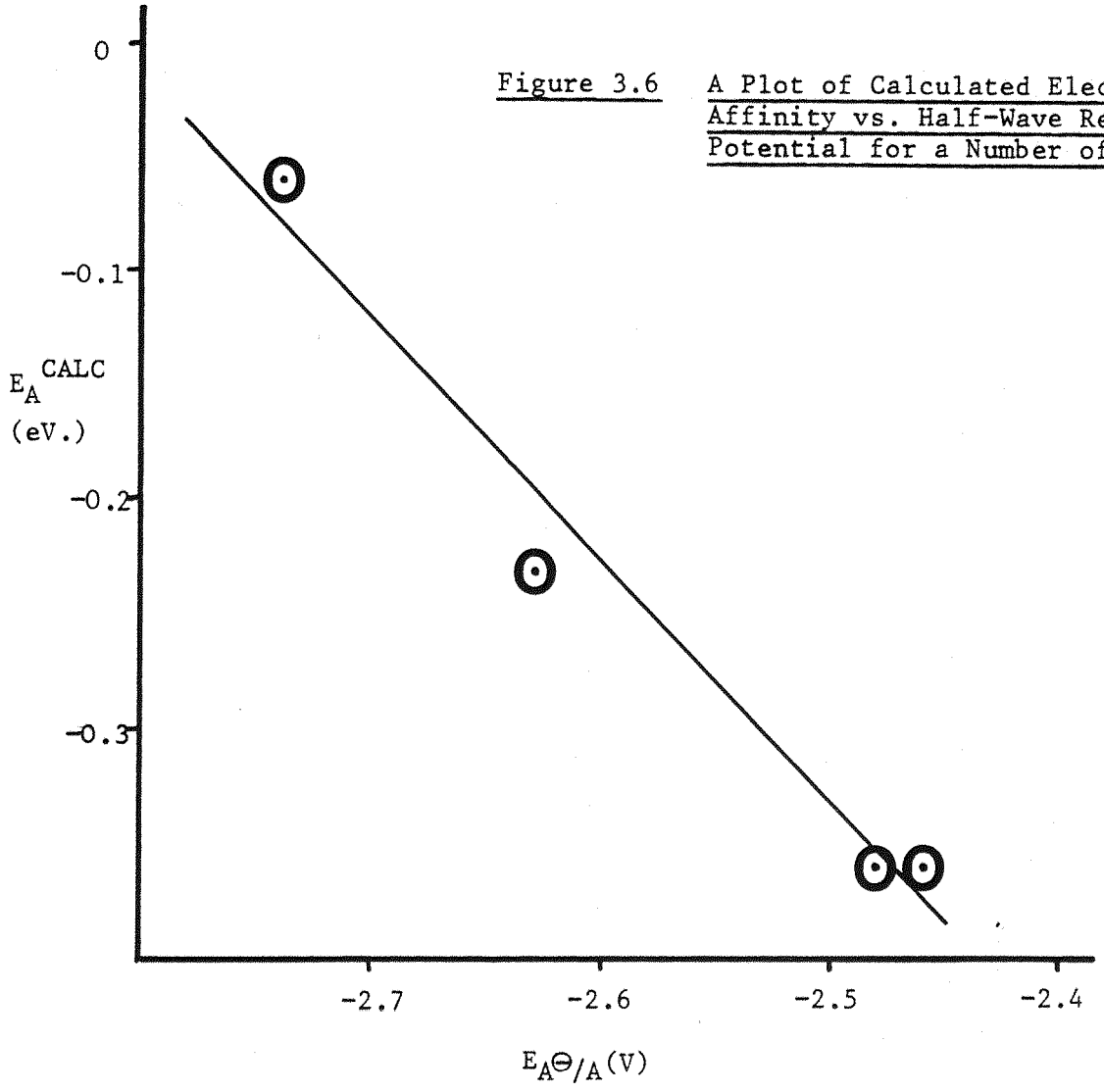

Figure 3.6 A Plot of Calculated Electron Affinity vs. Half-Wave Reduction Potential for a Number of Styrenes

It can be seen that, although there are relatively few data points accessible, a reasonable linear relationship does hold, with:

$$E_A^{CALC} = -2.93 - 1.04\ E_A^{\ominus}/A \qquad (8)$$

It is most interesting to observe that the slope of -1.04 obtained in this manner is in very close agreement with that of equation (5) above (-0.95), considering the number of approximations and experimental errors involved in each expression.

A notable exception here is that of DHN, where although the experimental values of I_A and $E_A^{\ominus}/A$ appear to correlate well with other photophysical data available (see e.g. figs. 3.4 and 3.11), this compound does not follow equation (8), which would predict an E_A^{CALC} of -0.18 eV as opposed to the 'observed' value of +0.09 eV. This inconsistency may be due to errors in the various measured quantities, in particular I_A. On the other hand, it may be another indication that the character of the excited monomer is less styrene-like for DHN than the other members of the series, as is proposed from the unimolecular photophysical studies of Chapter 2. Indeed, it may be noted here that the values of $E_A^{\ominus}/A$ obtained in this study are in good agreement with those of Laitinen[13] including the value of -2.65 V for DHN (Lit = -2.57 V). Also, the value of E_A^{CALC} obtained for styrene in this manner (-0.36 eV) is in reasonable agreement with an experimental value of -0.26 eV determined from a recent study using a low energy $e^{\ominus}$ scattering technique[14].

Thus, it appears that, with certain exceptions, E_A and $E_A^{\ominus}/A$ are indeed linearly related for the styrenes. The correlating factor here (i.e. the slope of fig. 3.6) approximates to the predicted value of -1.0 and hence, in this case, plots of E_{max}^{E} versus both these parameters are equivalent. It has been shown that for the styrene/Et_3N systems, a plot of E_{max}^{E} versus $E_A^{\ominus}/A$ also has a slope of approximately -1.0, this slope being less negative than that derived by Knibbe[6] from a similar plot for a series of aromatic hydrocarbon/N,N diethyl aniline exciplexes. This difference in behaviour can be rationalised using the FMO picture of fig. 3.5. In particular, if one considers the energy difference, ΔE_{HOMO}, between $'HOMO'_{A*}$ and $HOMO_D$, it is apparent that this energy gap (as measured by $(I_A - I_D)$) is relatively large for the styrene/Et_3N systems ($\geq$0.7 eV). However, for those exciplexes studied by

Knibbe, in all but the most favourable case, ΔE_{HOMO} is calculated to be less than 0.7 eV[15]. Therefore, for these systems, the perturbations of the various orbitals, as represented by ΔE_{1-4} of fig. 3.5, are expected to be that much greater. Also, as ΔE_{HOMO} is reduced at the same time as $E_A^{\ominus}/A$ becomes more negative within this series, so the magnitude of these perturbations will increase further. The effect of this will be that E^E_{max} will increase less rapidly with decreasing $E_A^{\ominus}/A$ (i.e. give a less negative slope for the $E^E_{max}/E_A^{\ominus}/A$ plot) for these exciplexes than for the styrene/Et_3N systems. For the latter, as shown already, ΔE_{HOMO} would appear to be large enough to cause only relatively small perturbations of these orbitals, leading to the observed, monotonic variation of E^E_{max} with $E_A^{\ominus}/A$. It may be of interest to note here, that a similar conclusion, regarding the importance of ΔE_{HOMO} was reached from a study of exciplex quenching[16]. In that case it was again suggested that ΔE_{HOMO} was required to be relatively small ($\lesssim$0.8 eV) before interaction of these orbitals was able to provide an important perturbation effect.

3.5 The Electron Accepting Ability of Ground State Styrene

As something of an aside, it may be noted here that the ability of styrene to act as an electron acceptor in the ground state has been demonstrated. It was found that N,N dimethylaniline (DMA) fluorescence was quenched by styrene at the diffusion controlled rate in cyclohexane (i.e. with a measured quenching rate constant, $k_q = 1.2 \times 10^{10} 1.mol.^{-1}s.^{-1}$). However, no exciplex emission could be detected in this case. In an attempt to observe such emission by using a less polar solvent, perfluoromethyl cyclohexane (Fluorochem PPII), it was interesting to find that the DMA fluorescence was in fact quenched by the PPII itself ($k_q = 3.9 \times 10^9$ $1.mol.^{-1}s.^{-1}$).

The quenching of amines by halogenated hydrocarbons in both the gas phase and in solution has been reported previously[17]. During the course of this work, the effects of such compounds on the photophysics of the styrenes and their exciplexes (Sect. 3.15) have been studied briefly. In particular, it was found that methylene chloride (CH_2Cl_2) quenched IND fluorescence, with $k_q = 6.25 \times 10^6$ $1.mol.^{-1}s.^{-1}$. However, whether this represents electron transfer type quenching of the monomer excited state or merely a solvent induced change in the electronic character of $^1IND^*$ is not obvious. The former is favoured as being the case here, since the ionisation

potential of CH_2Cl_2 (11.4 eV)[10] is such that it could possibly act as a weak electron donor in the presence of $^1IND^*$. CT type quenching here is also inferred from the observation of the fluorescence lifetime of IND (T_F) as a function of solvent polarity. In both cyclohexane and the highly polar solvent, acetonitrile, T_F (IND) is found to be similar at approximately 16 ns. However in methylene chloride solution (ε = 9.3), T_F (IND) = 5.6 ns. only.

3.6 Solvent Effects on Exciplex Emission

3.6.1 Measurement of Exciplex Dipole Moments

It is now well known that the spectral distribution and intensity of the emission from an exciplex are both strongly dependent on the properties of the solvent medium and in particular on the dielectric constant (ε) and refractive index (n) of the solvent. This dependence has been predicted, theoretically[18], to be of the form:

$$\bar{\nu}_{CT} = \bar{\nu}^{0}_{CT} - \frac{2\mu^2_{CT}}{hca^3}\left[\frac{\varepsilon - 1}{2\varepsilon + 1} - \tfrac{1}{2}\left(\frac{n^2-1}{2n^2+1}\right)\right] \qquad (9)$$

(where h = Planck's constant, c = speed of light and a = radius of the complex volume, or 'cavity radius').

The dipole moment, μ_{CT} can be extracted by plotting the value of the exciplex emission maximum in wave numbers, ν_{CT} for a range of solvents versus the expression in parentheses, which will be denoted here as $f(\varepsilon,n)$. Such plots were constructed for three of the styrene/Et_3N exciplexes studied and these are presented in fig. 3.7. Mixed solvent systems of cyclohexane/methylene chloride were used as this simplified $f(\varepsilon,n)$ somewhat since, while the dielectric constants (ε) of the two solvents vary from 2.023 (C_6H_{12}) to 9.3 (CH_2Cl_2), their refractive indices (n) are virtually identical at 1.425. Values for μ_{CT} which have been derived from these plots are given in Table 3.4 below.

The μ_{CT} values obtained in this way are seen to be in the region which has previously been associated with predominant CT within the exciplex and show the expected trend of reduction in μ_{CT} with the electron accepting ability of the styrenes. However, the absolute magnitude of the dipole moments obtained from such studies has been questioned recently, following an electro-optical study of a number of exciplexes[19]. This technique is thought to provide a method of determining μ_{CT} rather accurately and independent of solvent effects.

Figure 3.7 A Plot of the Energy of the Exciplex Emission Maximum as a Function of the Solvent Parameter $f(\varepsilon,n)$ for Three Styrene/Et_3N Systems

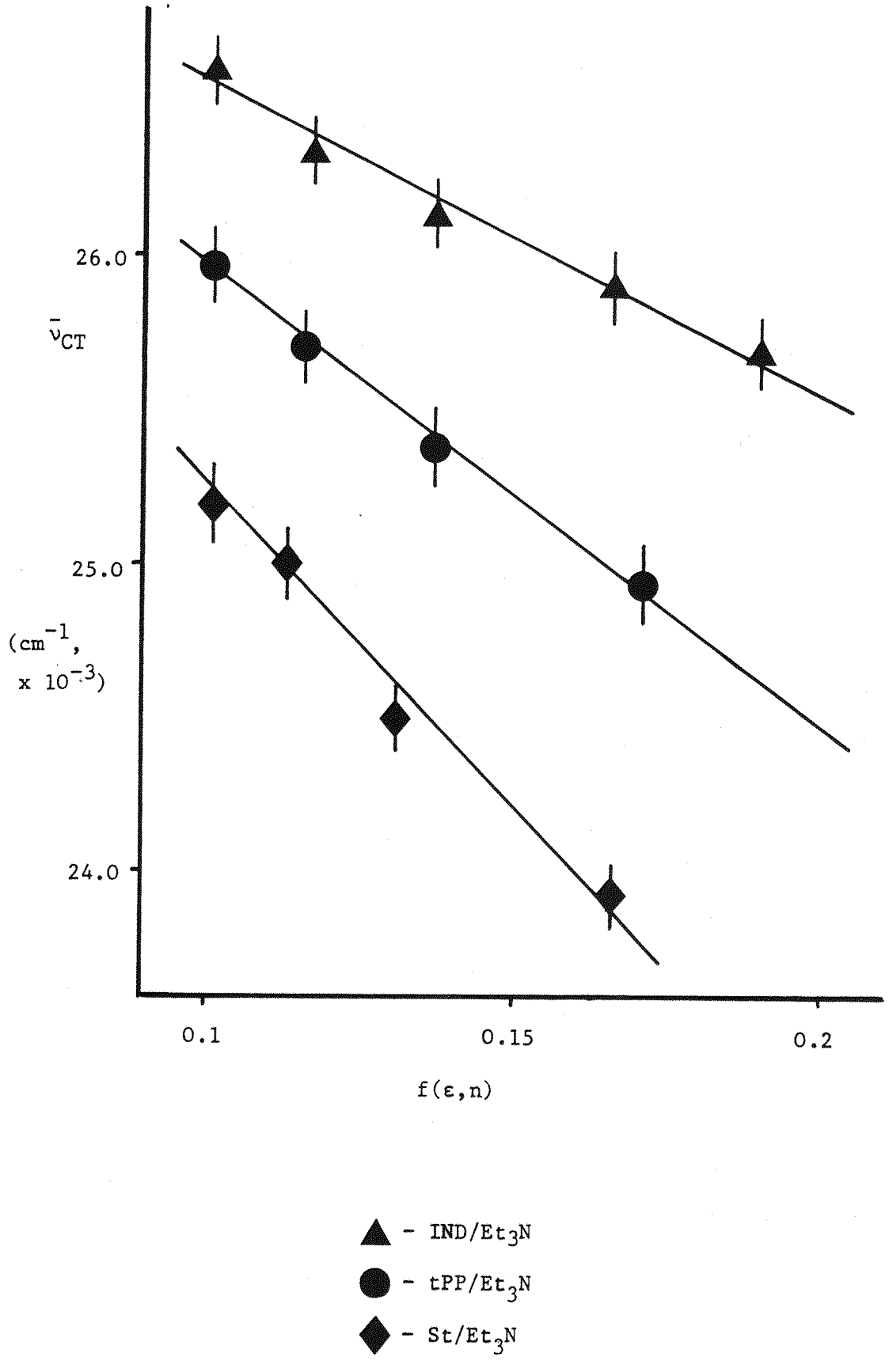

Table 3.4

Dipole Moments Calculated for Three Styrene/Et_3N Systems

EXCIPLEX	$\frac{2\mu_{CT}^2}{hca^3}$	μ_{CT} (D)	
		a = 4.2Å	a = 5.0Å
St/Et_3N	19,750	12.06	15.66
tPP/Et_3N	13,900	10.11	13.14
IND/Et_3N	8,830	8.06	10.47

It was found that the μ_{CT} values obtained were consistently lower than those derived for the same exciplexes by the solvent shift technique. These lower dipole moments suggested, therefore, that the contribution to the exciplex wave function from locally excited configurations should not be neglected.

Indeed, M.O. calculations on the 9,10 dicyanoanthracene/hexamethyl benzene (DCA/HMB) system confirmed that the wave function of the fluorescent state here, involved both CT and LE terms, giving:

$$\psi = 0.81\psi(D^{\oplus}A^{\ominus}) - 0.56\psi(DA^*) + \ldots \qquad (10)$$

The discrepancies in the μ_{CT} values obtained by the two methods were thought to arise from the difficulties associated with the accurate determination of the cavity radius, a. As shown by the data of Table 3.4, appreciable variations in μ_{CT} are observed on changing a, due to the a^3 dependence of equation (9) above. The values chosen for a of 4.2 and 5Å allow comparison with earlier dipole moment data; e.g. using a = 5Å, μ_{CT} values in the region of 8-12D were recorded for a range of aromatic hydrocarbon/heterocycle exciplexes[20], while typical aromatic hydrocarbon/amine exciplexes[2a] gave values of 10-14D. The work of Groenen[19] on the other hand, required that a = 4.2Å in order to correlate the μ_{CT} values obtained by the electro-optical and solvent shift methods. Dipole moments in the region of 6-10D were thus obtained and specifically, the DCA/HMB exciplex gave μ_{CT} = 9.8D, whilst still apparently having an appreciable contribution to the exciplex wave function from the LE states (equation (10)).

In the absence of accurate diffusion coefficients, which would be required to calculate a, and without the aid of any electro-optical data on the styrene/Et_3N exciplexes, the dipole moments measured must be regarded as being subject to errors of at least approximately ±1.D. However, given the data of Table 3.4, it is felt that it is still reasonable to classify the St/Et_3N and probably the tPP/Et_3N exciplexes as cases involving virtually complete charge transfer within the complex. The IND/Et_3N exciplex would appear to be at or near the borderline where locally excited states may be expected to become important.

3.6.2 The Effect of Solvent on the Quantum Yield of Exciplex Emission (Φ_E)

Accompanying the observed red shift of exciplex emission with increasing solvent polarity, there was a decrease in the intensity of this emission. This effect is clearly demonstrated in fig. 3.8 for the tPP/Et_3N exciplex in mixed cyclohexane/methylene chloride solvent systems.

In the case of a highly polar solvent, acetonitrile, no exciplex emission could be detected for any of the systems studied, although the monomer quenching rate was found to be enhanced, e.g. in the case of the IND/Et_3N system:

$k_q(C_6H_{12}) = 0.74 \times 10^9$ 1.mol.$^{-1}$s.$^{-1}$

$k_q(MeCN) = 4.6 \times 10^9$, but with no exciplex emission.

The variation of the measured quantum yield of exciplex emission (Φ_E) with the dielectric constant/refractive index parameter, f(ε,n) is presented in Table 3.5 for three exciplex systems.

Table 3.5

The Variation of Exciplex Fluorescence Quantum Yield (Φ_E) as a Function of Solvent Polarity

f(ε,n)	Φ_E*		
	St/Et_3N	tPP/Et_3N	IND/Et_3N
0.101	0.058	0.074	0.017
0.113	0.043	-	-
0.117	-	0.053	0.013
0.131	0.025	-	-
0.138	-	0.037	0.010
0.166	0.011	0.026	0.007

*recorded for Io/I values of approximately 2.5 in each case.

Figure 3.8 Fluorescence Spectra for the tPP/Et_3N System in Cyclohexane/Methylene Chloride Mixed Solvents

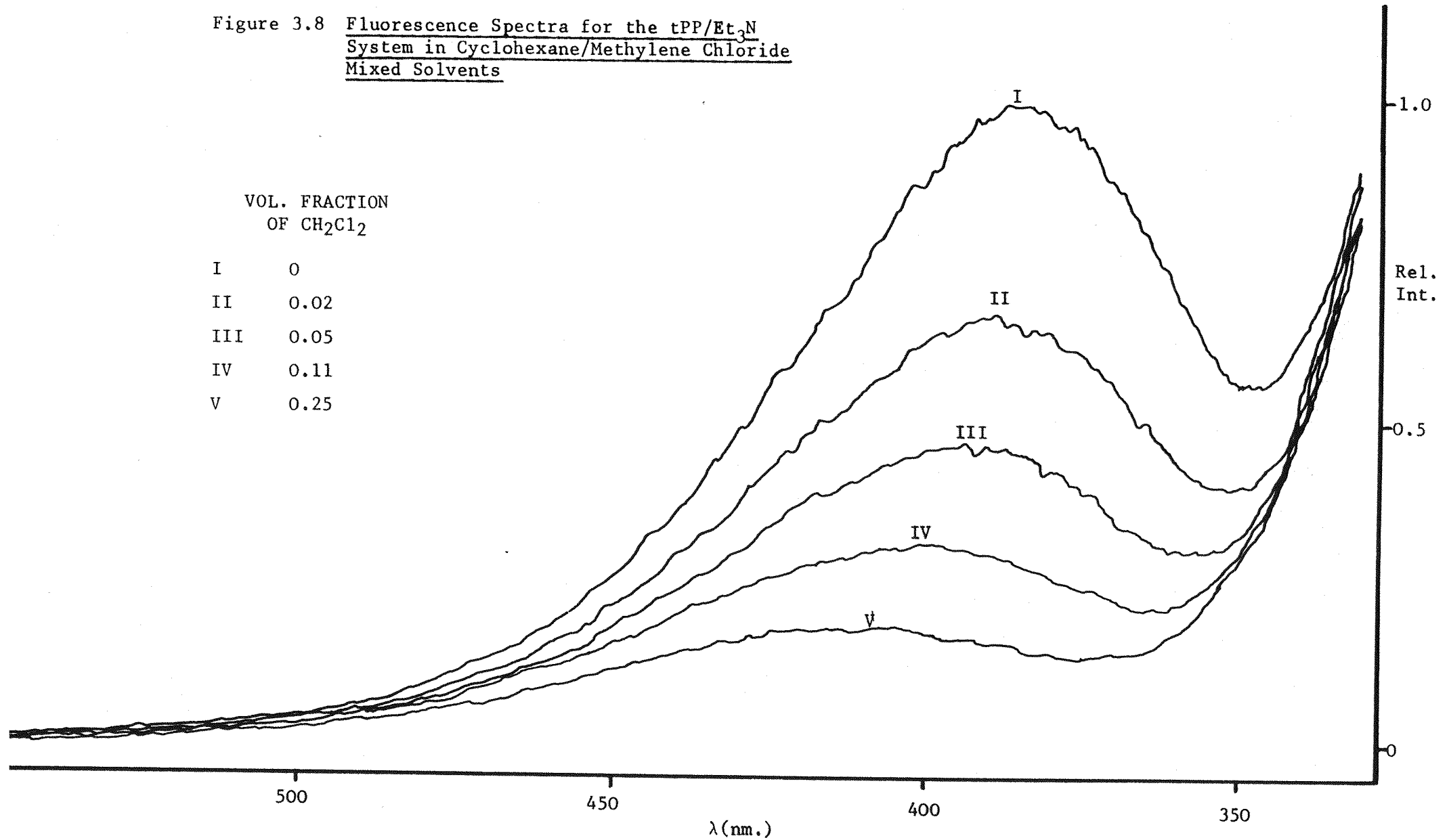

The effect of CH_2Cl_2 quenching of the monomer emission, as observed for IND (p.63) was thought to be of negligible importance in these studies. The magnitude of the quenching rate constants obtained was such that, even at the greatest volume fraction of CH_2Cl_2 used, the efficiency of quenching by Et_3N was an order of magnitude greater than that for quenching by the CH_2Cl_2 present. A consistent decrease in Φ_E is observed with increasing $f(\varepsilon,n)$ in these cases. However, no simple correlation between these functions would be expected as Φ_E is itself a complex function of the various rate constants involved in the quantum efficiency terms q_E and q_{EX} in the expression:

$$\Phi_E = q_E \cdot q_{EX} \qquad (11)$$

(where q_E = quantum efficiency of exciplex emission
and q_{EX} = quantum efficiency of exciplex formation).

As such, increases or decreases in Φ_E with increasing solvent polarity may be possible and indeed, both have been reported[21].

In the case of the tPP/Et_3N exciplex, a brief transient study of the exciplex and quenched monomer decay constants has been carried out. The rates of the various processes deactivating this exciplex were found to increase with increasing $f(\varepsilon,n)$, with the exception of the exciplex radiative rate constant. This rate constant was found to be relatively small and to decrease with increasing $f(\varepsilon,n)$, a fact which is discussed later (Section 3.15) in terms of a solvent induced change in the electronic structure of the complex.

It is felt that this combination of factors, together with the relatively large quencher concentrations, chosen for these experiments are the causes of the observation, presented in fig. 3.9, that Φ_E^{-1} is apparently linearly dependent on $f(\varepsilon,n)$ for this system. A similar, linear dependence is observed for the IND/Et_3N exciplex, while the plot for the St/Et_3N system shows some curvature. Taking into account the constraints noted above, such a linear correlation would not be expected to be a general phenomenon and apparently has not been examined previously. However, for a closely related exciplex system, that of Pyrene/N,N Diethylaniline, for which Φ_E data is available in a range of solvents[22], it may be significant that, with a number of exceptions, the data plotted in this form also adheres to a straight line. The exceptions here may well arise as a consequence of specific

Figure 3.9 A Plot of Φ_E^{-1} vs. the Solvent Parameter f(ε,n) for Three Styrene/Et N Exciplexes

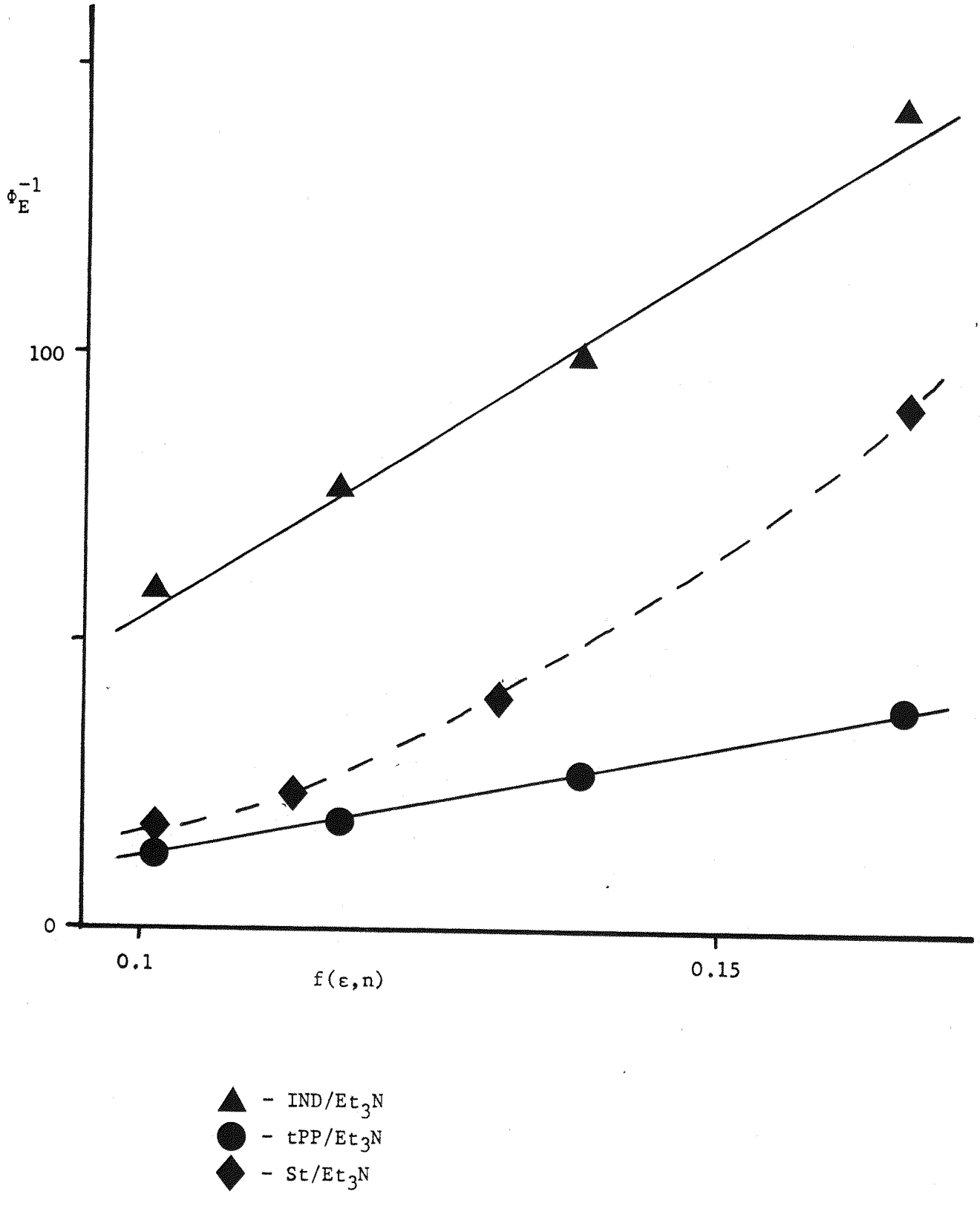

solvent interactions with the exciplex state, such interactions apparently being eliminated in the present study by the use of the cyclohexane/methylene chloride mixed solvent systems. Also, as pointed out in ref. (22), the effects of varying the solvent dielectric relaxation times may be important in this context. This variation would tend to affect the dissociation of the complex into a solvent separated radical ion pair, a significant exciplex decay route in more polar solvents.

3.7 The Rate Constant for Fluorescence Quenching

For the various styrene/Et_3N systems in cyclohexane and over the range of quencher concentrations used, the quenching of monomer fluorescence was observed to follow the familiar Stern-Volmer expression:

$$\frac{I_o}{I} = 1 + K_{sv}\,[Q] \qquad (12)$$

(where $K_{sv} = k_q \tau_o$)

The observed quenching rate constants, k_q, were thus obtained from the slope of plots of I_o/I (the ratio of monomer fluorescence intensity in the absence and presence of Q) versus [Q], using the known monomer fluorescence lifetime in the absence of Q, τ_o. A typical plot is presented as fig. 3.10, for the IND/Et_3N system and shows the effect on K_{sv} of degassing the solutions. The results obtained for a range of exciplex forming systems are presented in Table 3.6. Once again, these results may be expected to reflect the CT nature of the complex-forming step in a correlation between k_q and the electron accepting ability of the excited monomers. The free energy of formation of an $^1(AD)^*$ complex may be expressed as[23]:

$$\Delta G_A = I_D + E_A - \Delta E_{o,o} + \text{CONST} \qquad (13)$$

(see fig. 3.4)

Thus a linear relationship is predicted between loge k_q and $(E_A - \Delta E_{o,o})$ or as shown previously $(E_A^{\ominus}/A + \Delta E_{o,o})$, with I_D constant. However, only a rather limited range of $E_A^{\ominus}/A$ values were accessible for the styrenes and therefore, their ionisation potentials (I_A) were examined as another useful measure of their relative electron accepting abilities. This allowed expansion of the range of styrenes studied to include the p-methoxystyrene (pMeO)/and p-cyanostyrene (pCN)/Et_3N systems. Fig. 3.11 shows the result of plotting loge k_q vs. I_a for

Figure 3.10 Stern Volmer Plots for Quenching of Indene Fluorescence by Et_3N in Cyclohexane

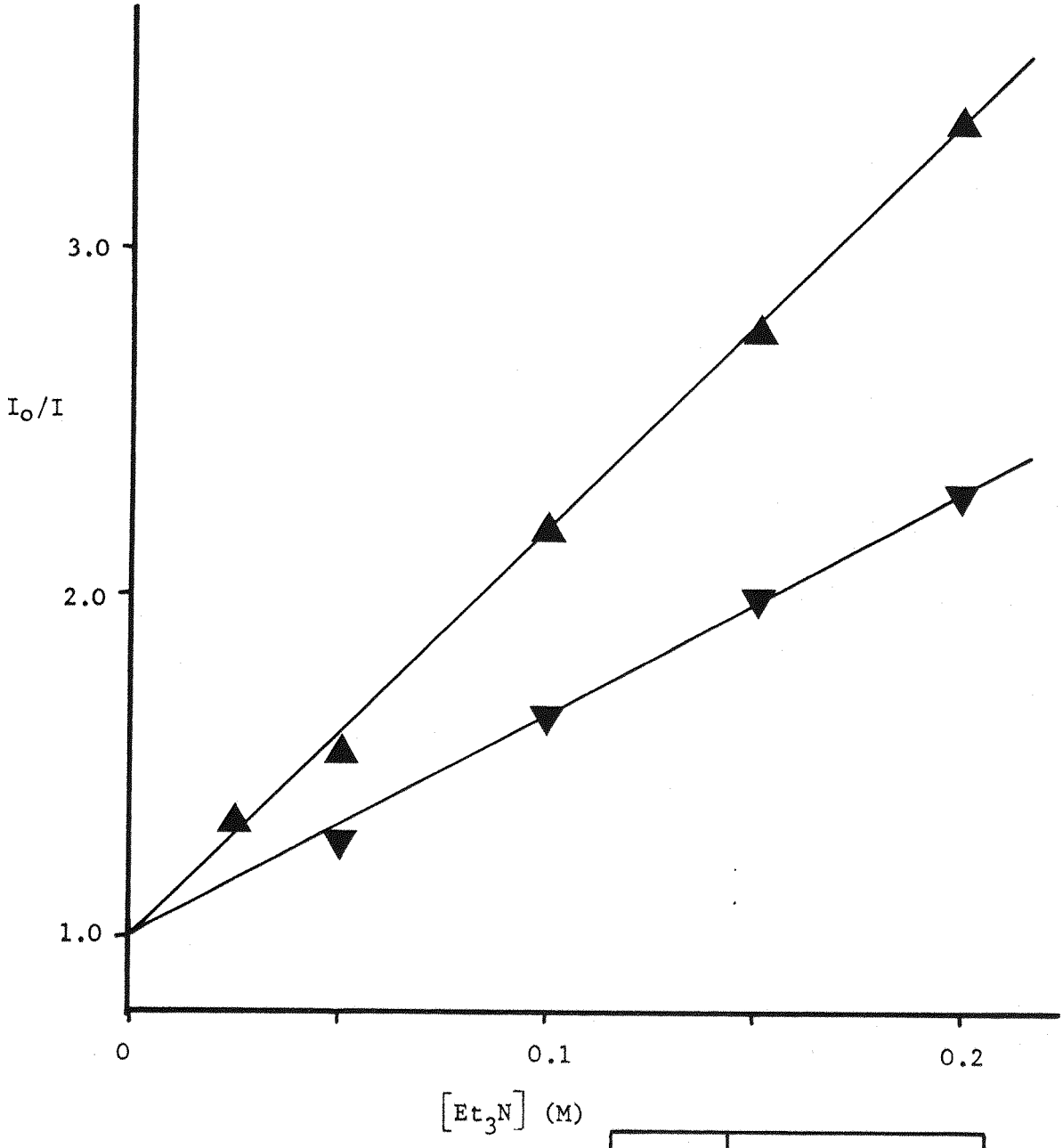

	K_{sv} (M^{-1})	k_q ($1.mol.^{-1}s.^{-1}$)
▲ - Degassed	11.8	0.74×10^9
▼ Non-Degassed	6.5	"

the data of Table 3.6.

Table 3.6

Fluorescence Quenching Data for a Number of Styrene/Et_3N Systems in Cyclohexane

Styrene	k_q ($l.mol.^{-1}s.^{-1}$) ($\times 10^{-9}$)	I_A (eV)
pCN	15.0	9.0[24]
2PP	13.0	8.5[25]
St	8.4 8.0*	8.5[11]
oMe	8.3	8.5[11]
tPP	4.8 4.6*	8.37[11]
cPP	8.5	-
DHN	0.88	8.05
IND	0.74 0.74*	8.20[26]
pMeO	0.14	7.5[24]

*Non-degassed solutions

A reasonable linear correlation is seen to exist over the region of $I_A \simeq 7.5 - 8.5$ eV and to higher I_A values, the plot levels off to a value approaching the diffusion controlled rate, k_{diff}, as given by the Debye equation:

$$k_{diff}(C_6H_{12}) = \frac{8RT}{2000\eta} = 1.2 \times 10^{10} l.mol.^{-1}s.^{-1} \qquad (14)$$

Similar plots have now been reported for quite a variety of exciplex-forming systems, e.g. Pyrene/amine[27] and Naphthalene/diene systems[28]. Indeed in the absence of exciplex emission, such a correlation is often taken as prima facie evidence for a fluorescence quenching mechanism involving charge transfer. In a number of such cases[29], where the slope of the linear portion of these plots has been observed to be relatively shallow, this has been interpreted in terms of a relatively minor CT contribution to the fluorescence

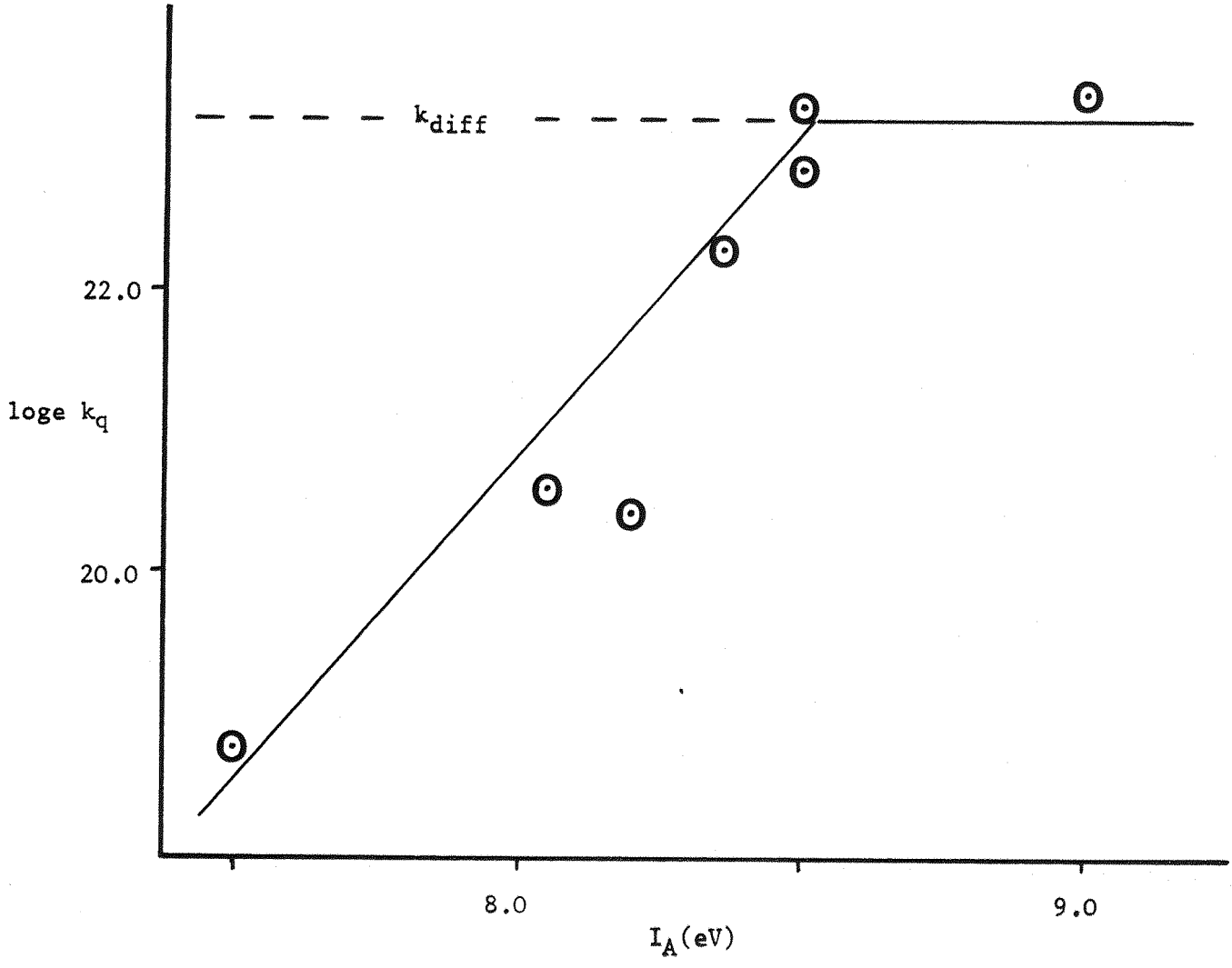

Figure 3.11 A Plot of loge k_q vs.the Monomer Ionisation Potential (I_A) from the Data of Table 3.6

quenching. However, in the case of the styrene/Et_3N exciplexes, the shallow slope of fig. 3.11 (4.4 eV^{-1}) compared to the theoretical value of 40 eV^{-1} (RT^{-1}) appears to contradict the findings of the previous section, in which solvent effects on λ^{E}_{max} seemed to indicate a high degree of CT character within these complexes. One is thus led to question the implications of the values of the slope of plots such as fig. 3.11.

3.8 The Free Energy of Complex Formation (ΔG_A)

In an attempt to examine this point further, the values of ΔG_A were calculated for a number of the styrene/Et_3N systems studied, according to the empirically derived expression of Weller[15]:

$$\Delta G_A = 23.06 \left[E(D/D^-) - (E(A^-/A) + \Delta E_{o,o})\right] - T\Delta S + 12.6 \ (kJmol^{-1}) \quad (15)$$

- where the values of the various terms were taken from ref. 15 as:

$E(D/D^+)Et_3N = 0.98$ V

$T\Delta S = 290$ (K) x -75.3 ($J.deg^{-1}mol^{-1}$)
$= 21.84$ $kJ.mol^{-1}$

The values of ΔG_A calculated for the styrenes, using equation 15 are presented in Table 3.7 below.

Table 3.7

ΔG_A Values for a Number of Styrene/Et_3N Exciplexes in Cyclohexane Calculated According to Equation 15

Styrene	$-\Delta G_A$ ($kJ.mol^{-1}$)
St	38.5
oMe	29.7
tPP	18.0
IND	20.9
DHN	11.3

The range of ΔG_A data thus obtained appears to show some correlation with k_q although by comparison with Weller's study of aromatic hydrocarbon/aromatic amine exciplexes, the magnitude of these ΔG values are such that k_q's in the region of k_{diff} are predicted for all but the 1,2 dihydronaphthalene/Et_3N system. Also, it should be noted that the ΔG_A's derived in this way suggest that $k_{q(IND/Et_3N)}$ should be greater than $k_{q(tPP/Et_3N)}$. Clearly, this is not observed experimentally (see Table 3.6). Interestingly, as illustrated in Table 3.8, these same observations apply to the styrene/Et_3N systems in acetonitrile solution.

Table 3.8

Calculated ΔG_A and Observed k_q Values for Three Styrene/Et_3N Systems in Acetonitrile

Styrene	$-\Delta G_A^{CALC}$ (kJ mol^{-1})	k_q^{OBS} ($l.mol^{-1}s^{-1}$)
St	78.7	1.0×10^{10}
tPP	58.6	5.8×10^{9}
IND	61.5	4.6×10^{9}

No exciplex emission was observed in these cases and thus radical ion pair formation is inferred. However, as was the case in cyclohexane solution, the calculated ΔG_A values[30] predict that the fluorescence quenching should be diffusion controlled here ($k_q^{CALC} = 1.34 \times 10^{10}$ $l.mol^{-1}s^{-1}$).

3.9 Transient Studies of Exciplex Formation and Decay

3.9.1-The Kinetics of Exciplex Formation and Decay

Fluorescence lifetime data, in terms of exciplex and quenched monomer fluorescence decay times under a variety of conditions of quencher concentration, solvent and temperature, has been obtained for three of the exciplex-forming systems studied. Analysis of this data provides a route to the individual rate constants involved in the processes of formation and decay of these exciplexes. This type of analysis has been used to great effect, in particular, by Ware and co-workers[3] to gain an understanding of the kinetics of these processes. Their studies have shown that the classical excimer type kinetic scheme is applicable also to exciplex formation and decay.

The basic form of such a kinetic scheme is outlined below as fig. 3.12 for the case of the interaction between an excited $e^{\ominus}$ acceptor ($^1A^*$) and a ground state donor (D).

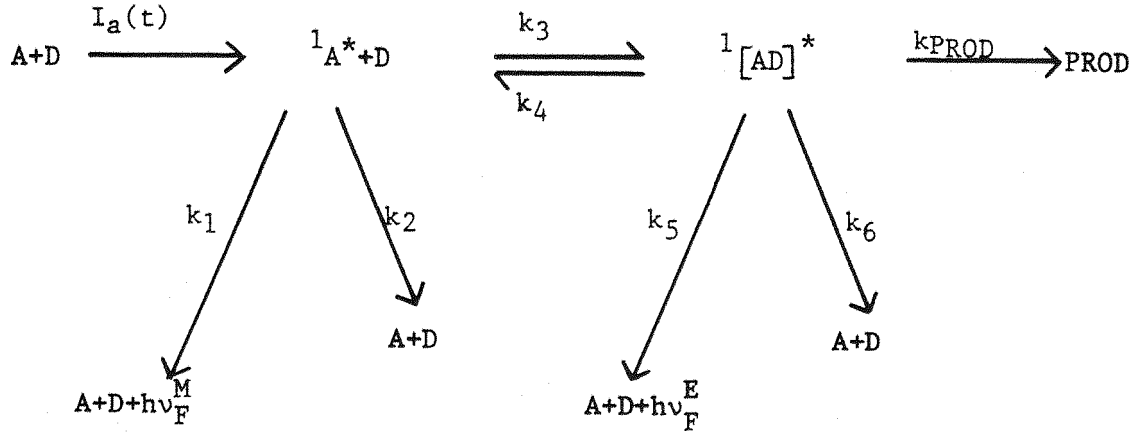

Figure 3.12 A Kinetic Scheme Depicting the Basic Processes Involved in Exciplex Formation and Decay

This scheme provides the relationships between the concentrations of the excited species and the various rate constants, in the form of a pair of coupled differential equations involving:

$$\frac{d[A^*]}{dt} \quad \text{and} \quad \frac{d[AD^*]}{dt}$$

Detailed transient and steady state analyses of these equations are presented in Appendix I. As outlined by Ware, a transient analysis provides a number of important relations involving the experimental decay constants for the monomer and exciplex (λ_1 and λ_2 respectively). In particular, it is found that the decay constants are given by solution of the quadratic auxiliary equation, which leads to the expression:

$$\lambda_{1,2} = \tfrac{1}{2}\Big[k_1 + k_2 + k_3[D] + k_4 + k_p \pm \Big[(k_1 + k_2 + k_3[D] - (k_4 + k_p))^2 + 4k_3k_4[D]\Big]^{\frac{1}{2}}\Big] \qquad (16)$$

Then, from this it can be seen that the sum of the decay constants at a particular quencher concentration, [D] is given by:

$$\lambda_1 + \lambda_2 = k_1 + k_2 + k_3 [D] + k_4 + k_p \qquad (17)$$

- while the product of the decay constants is:

$$\lambda_1 \cdot \lambda_2 = (k_1 + k_2)(k_4 + k_p) + k_3 k_p [D] \qquad (18)$$

Thus, it can be seen that plots of both -

Ⓐ $\lambda_1 + \lambda_2$ vs. [D] and

Ⓑ $\lambda_1 \cdot \lambda_2$ vs. [D]

should be linear and that the values of the slopes and intercepts of such plots should yield a number of the required rate constants.

Table 3.9

Rate Constants for the Processes of Exciplex Formation and Decay and How They May be Derived from Photophysical Studies

RATE CONSTANT		HOW DERIVED
$k_1 + k_2$	Sum of the radiative (k_1) and non-radiative (k_2) rate constants for the monomer in the absence of D	Unquenched monomer fluorescence decay time $\lambda_o = (\tau_o)^{-1}$
k_3	Rate constant for $e^{\ominus}$ transfer $^1A^* \longrightarrow D$	Slope Ⓐ
$k_4 + k_p$	Sum of all the rate constants depleting $^1AD^*$	a) Intercept Ⓐ $-(k_1 + k_2)$ b) $\frac{\text{Intercept Ⓑ}}{(k_1 + k_2)}$
k_p	Reciprocal of the exciplex fluorescence lifetime in the absence of k_4 or: Exciplex decay time at infinite quencher concentration.	$\frac{\text{Slope Ⓑ}}{k_3}$
k_4	Rate constant for the reverse dissoc. to regenerate A^*	$(k_4 + k_p) - k_p$
k_5	Exciplex radiative rate constant	Slope of a plot of Φ_E/Φ_m vs. [D] (see later p.99)

Table 3.9 lists these individual rate constants and how they may be derived. Thus, all but the exciplex radiative rate constant, k_5, can be obtained without recourse to steady state data. However, it should be noted that the sum $(k_1 + k_2)$ can be further broken down using Φ_m^o, the monomer fluorescence quantum yield in the absence of D, as has been examined in Section 2.2.

The decay constants λ_1 and λ_2 were obtained experimentally using the Single Photon Counting technique under conditions such that the monomer and exciplex decay profiles could be observed separately (as is explained in the experimental section (5.1). The variation of these decay constants with quencher concentration was examined for the St/,tPP/ and IND/Et_3N systems, initially at room temperature in degassed cyclohexane. The decay data thus obtained was analysed using an iterative convolution procedure based on a non-linear least squares curve-fitting technique, as employed by Ware[35] and others.

The form of the decay laws predicted for the quenched monomer and the exciplex are as follows:

$$[{}^1A^*] = A_1 e^{-\lambda_1 t} + A_2 e^{-\lambda_2 t} \qquad (19)$$

$$[{}^1AD^*] = A_3(e^{-\lambda_1 t} - e^{-\lambda_2 t}) \qquad (20)$$

Thus the fluorescence decay profile of the quenched monomer should appear as the sum of two exponential terms.

The exciplex decay profile on the other hand should show an initial rise followed by decay according to the difference of two exponential terms. This behaviour is a consequence of the reversible nature of the exciplex-forming step. The ability to observe such effects is strongly dependent on the magnitude of the dissociative, 'feedback', process as represented by k_4, in relation to the rates of the other processes depleting $^1AD^*$.

In the case of the styrene/Et_3N exciplexes studied under the conditions mentioned above, the exciplex decay profiles could indeed be characterised by an expression of the form of equation (20). As predicted, the pre-exponential terms associated with the two decay constants were found to be opposite in sign and were almost equal in magnitude. The negative pre-exponential (A_3) associated with the larger decay constant, λ_1 was found to be consistently slightly smaller than that for λ_2. ((A_3') - see Table 3.10 below). This same

observation has been made by O'Connor[31] for the 1-Cyanonaphthalene/1,2 Dimethyl Cyclopent-1-ene (CNNp/DMCP) exciplex system.

Attempts to analyse the styrene monomer decay profiles, in the presence of Et_3N at various concentrations, using a double exponential decay law, were unsuccessful. This was not too surprising though, as from a visual analysis of these decay profiles in the form of semi-log plots, it could be seen that such plots were essentially linear over most of the time region of the decay. This contrasts with much of the data in the literature and again one may take the CNNp/DMCP system as an example, showing a monomer decay profile exhibiting two distinct regions coresponding to a double exponential decay law.

A typical set of monomer and exciplex decay profiles obtained in this work is presented in fig. 3.13 for the St/Et_3N (0.012M) system, and these may be compared with figs. 1 and 2 of ref. (31). It may be noted that, while in both systems, the exciplex and quenched monomer fluorescence lifetimes derived are quite widely separated ($\tau_2 - \tau_1 \simeq$ 13-15 ns.), the St monomer decay does not show the sharp discontinuity observed for the CNNp monomer. This apparent discrepancy can be explained quite readily in terms of the relative magnitudes of the various rate constants involved in these two cases.

One may consider the expression for the monomer fluorescence quantum yield in the presence of a quencher at a concentration, [D] as:

$$\Phi_m = \frac{k_1}{(k_1 + k_2) + k_q [D]} \qquad (21)$$

$$\text{where } k_q = \frac{k_3 k_p}{k_4 + k_p}$$

From this, two factors which can affect the observation of a two component monomer decay profile may be recognised, i.e.

a) The relative magnitudes of the rate constants k_4 and k_p, since as the importance of k_4 is diminished such that $k_4 << k_p$, this tends towards the limiting case:

$$\frac{k_3 k_p [D]}{k_4 + k_p} \longrightarrow k_3 [D]$$

which would lead to single exponential monomer decay.

b) The relative importance of the components $(k_1 + k_2)$ and $k_q[D]$ to equation (21). As the unquenched monomer fluorescence lifetime is decreased ($k_1 + k_2$ increased) so the contribution to the quenched

Figure 3.13

Characteristic Exciplex and Quenched Monomer Fluorescence Decay Profiles for the St/Et_3N System

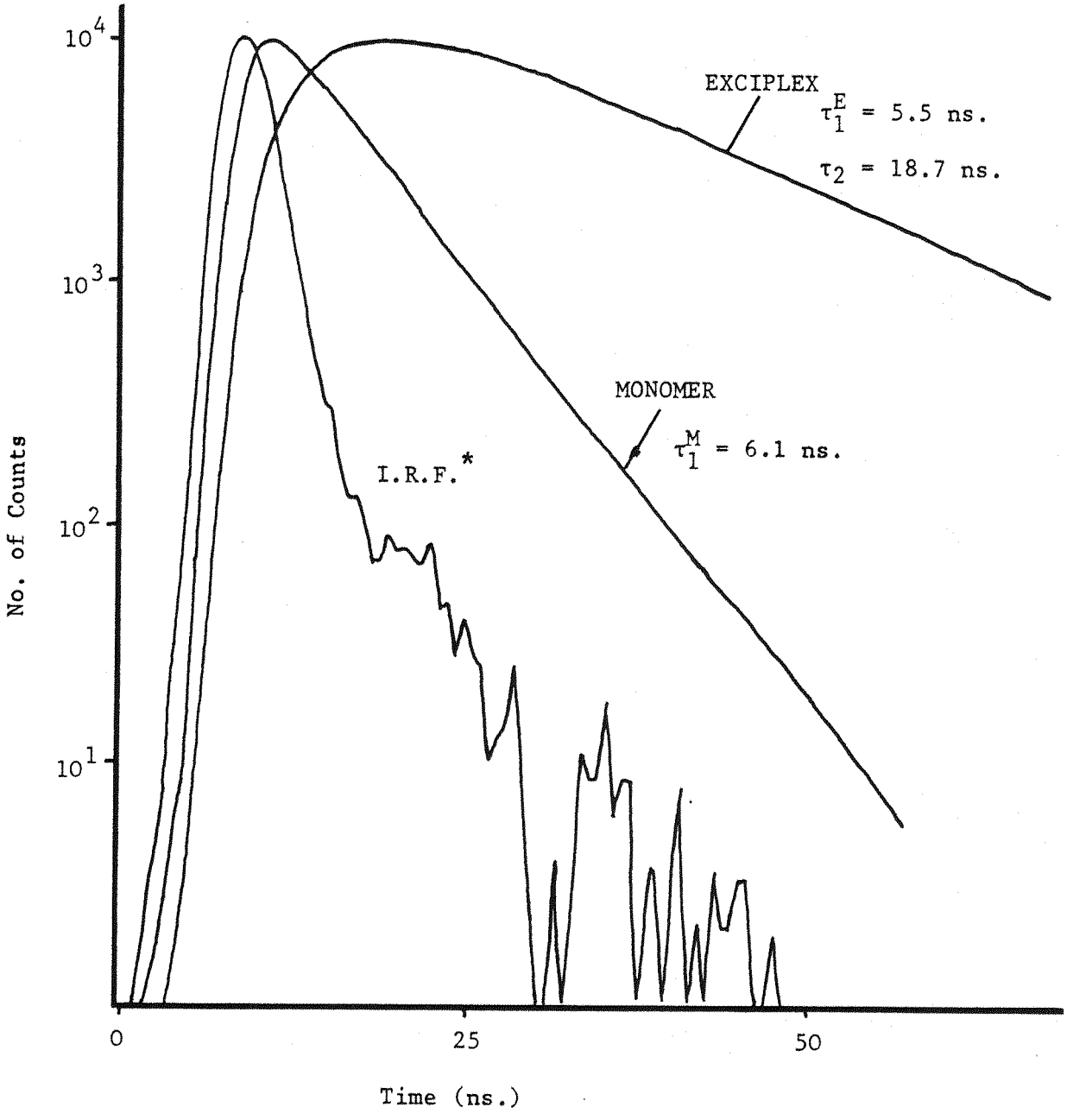

*I.R.F. - Instrument Response Function
or 'Lamp Profile' - see Sect. 5.1.

monomer fluorescence intensity from $^1A^*$ regenerated by reverse dissociation from an exciplex will be decreased for a given $k_q[D]$.

Now, while the St/(and tPP/Et_3N) exciplexes are not limiting cases in terms of either a) or b), it does seem that both these factors combine with the relatively low [D] used throughout to make observation and analysis of the monomer decays as double exponential difficult.

The CNNp/DMCP system on the other hand has a greater unquenched monomer fluorescence lifetime (~20 ns.), together with a significantly more important k_4 term than the styrene/Et_3N exciplexes, thus enhancing the possibility of observing two component monomer decay for the former.

The IND/Et_3N system required a somewhat different approach and is treated separately below as, at room temperature, it exhibits the properties of a system at or near the 'rapid equilibrium' limit.

3.9.2 - Analysis of Exciplex and Quenched Monomer Decay Times

A typical set of decay data is presented for the St/Et_3N system as Table 3.10. The λ_1 values derived from the monomer decay were obtained by analysing these profiles according to a single exponential decay law. This analysis was limited to the portion of the decay curves recommended by Hui and Ware[32], i.e. from a point 2-3 ns. after the maximum. This was done in order to minimise the effects of a time dependence of k_3. These so-called transient effects of diffusion controlled reactions have been shown to produce artificially high λ_1 values and a poor fit between the calculated and experimental decay curves if not taken into account in this way. The criteria taken as a measure of the goodness of fit between the calculated and experimental profiles[33] were that there should be a χ^2 value in the region of 1.0, together with a random distribution of the residuals ($I^{CALC}_{(t)} - I^{EXP}_{(t)}$).

The exciplex decay curves were analysed over the whole of the time region studied, in order to involve λ_1 in the rising edge, according to the difference of two exponentials (equation (20)). Therefore, in this case no account is taken of the transient effects and this can lead to a significantly increased λ_1 value being recovered from the exciplex decay compared to the monomer decay, at a particular [D]. Again this effect, shown clearly in Table 3.10, has been reported previously; for the Anthracene/N,N Dimethylaniline (An/DMA) system[32]. In that case, it was found that if λ_1 derived from the exciplex decay data was used to construct plots of $(\lambda_1 + \lambda_2)$ and $\lambda_1.\lambda_2$ vs. [D], various inconsistencies resulted, in some cases leading to negative rate constants being derived.

Table 3.10

Decay Characteristics of the Exciplex and Quenched Monomer as a Function of the Quencher Concentration for the St/Et_3N System in Degassed Cyclohexane

$[Et_3N]$ (M)	λ_1^M (s^{-1}) ($x10^{-8}$)	A_3	λ_1^E (s^{-1}) ($x10^{-8}$)	A_3'	λ_2 (s^{-1}) ($x10^{-7}$)
0	0.69	-	-	-	-
0.005	1.10	-0.179	1.39	0.182	5.52
0.008	1.32	-0.192	1.46	0.198	5.35
0.010	1.45	-0.169	1.70	0.170	5.38
0.012	1.64	-0.169	1.82	0.171	5.35

Therefore in constructing such plots for the St/ and tPP/Et_3N exciplex systems, the smaller λ_1 values derived from the monomer decay were used, together with λ_2 obtained, of necessity, from the exciplex decay.

These plots are presented as fig. 3.14 and as can be seen, they are linear as predicted. The values of the various rate constants which have been derived from these plots, by the methods outlined in Table 3.9, are given in Table 3.11.

Table 3.11

Rate constants calculated for the St/ and tPP/Et_3N Exciplexes at Room Temperature in Degassed Cyclohexane

Styrene	(k_1+k_2) (s^{-1}) ($x10^{-7}$)	k_3 ($lmol^{-1}s^{-1}$) ($x10^{-9}$)	$(k_4 + k_p)$ (s^{-1}) ($x10^{-8}$) a)	b)	k_4 (s^{-1}) ($x10^{-6}$)	k_p (s^{-1}) ($x10^{-8}$)
St	6.9	7.4	0.58	0.59	7.0	0.52
tPP	8.13	4.14	1.21	1.20	7.5	1.13

a) Derived using Intercept (A), see Table 3.9

b) Derived using Intercept (B), see Table 3.9.

Figure 3.14

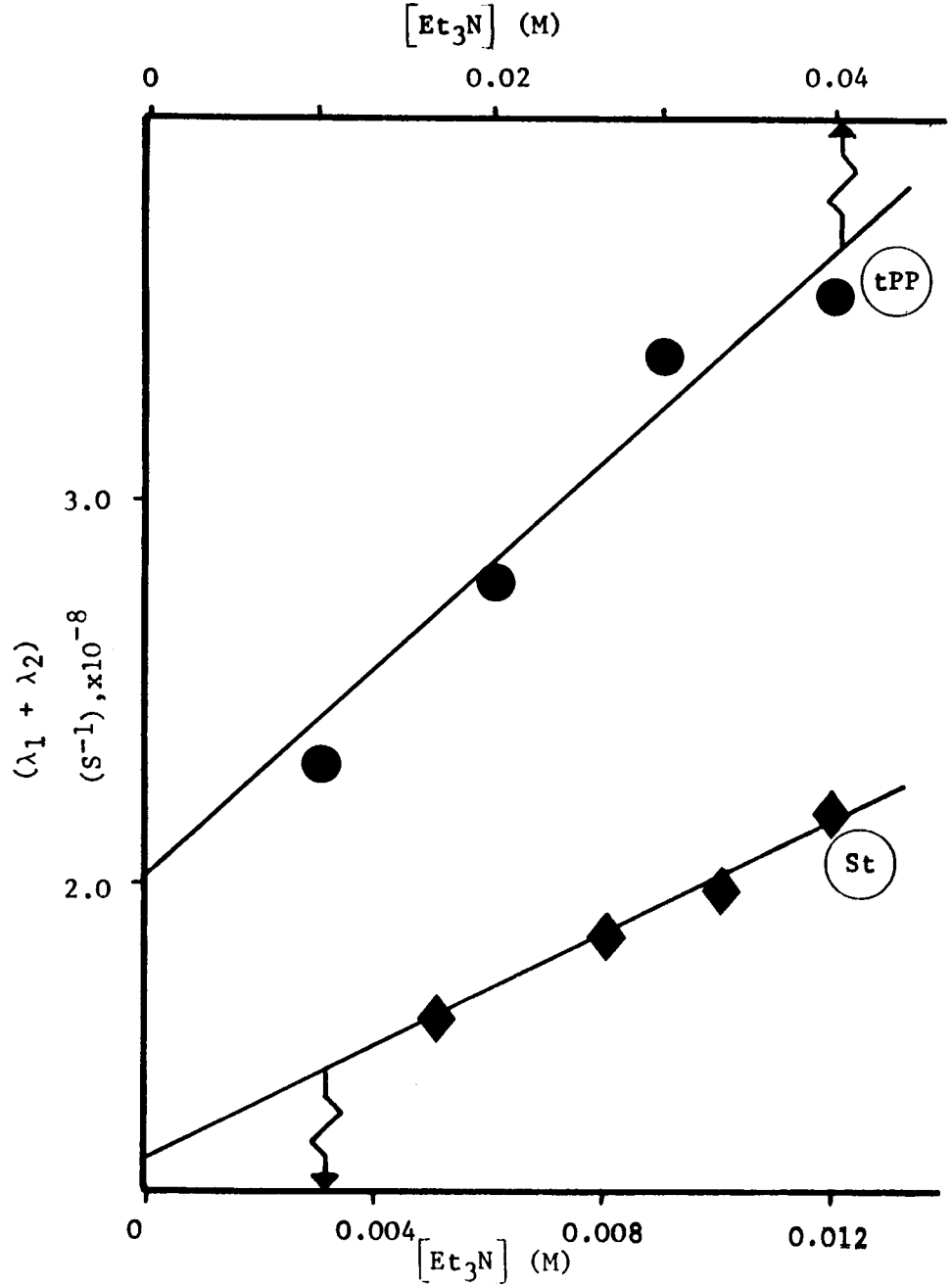
[Et3N] (M)
0
0.02
0.04
tPP
St
3.0
2.0
(λ1 + λ2) (s-1), x10-8
0
0.004
0.008
0.012
[Et3N] (M)

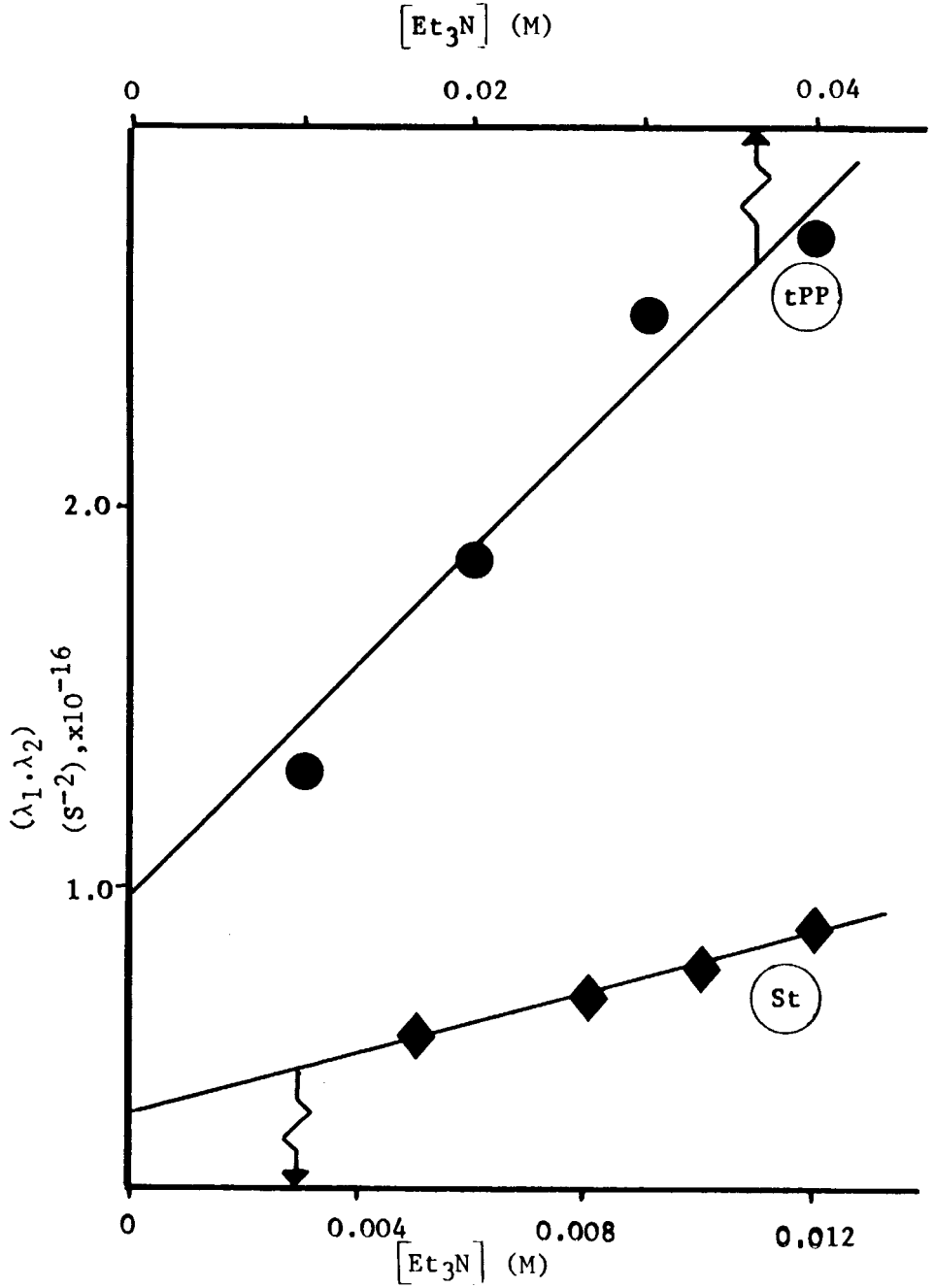
[Et3N] (M)
0
0.02
0.04
tPP
St
2.0
1.0
(λ1.λ2) (s-2), x10-16
0
0.004
0.008
0.012
[Et3N] (M)

As a test of the validity of the kinetic scheme proposed for exciplex formation and decay in this case, a comparison has been made of the experimental λ_1 and λ_2 values with values calculated by substitution into equation (16) of the various rate constants presented in Table 3.11. That there is good agreement between the calculated and experimental data for both these exciplex-forming systems, is apparent from fig. 3.15, where the comparison is made for λ_1 and λ_2 as a function of [D] in each case. This therefore adds further weight to the conventional kinetic scheme of fig. 3.12, above.

A number of points, characteristic of such plots are illustrated by figs. 3.15, namely:

a) Considering the variation of λ_1 with [D]:

In both these systems, λ_1 shows a slight curvature initially, followed by a linear portion as [D] is increased. It is interesting to note that the slopes of the linear portion of both plots approach k_3. This appears to be a consequence of the relatively small k_4 values observed here in that equation (16) reduces to give the approximation:

$$\lambda_1 \simeq k_1 + k_2 + k_3 [D] \qquad (22)$$

when the relative importance of the components X and Y of the square root term of equation (16) are such that:

$$\left[\underbrace{(k_1 + k_2 + k_3[D] - (k_4 + k_p))^2}_{X} + \underbrace{4k_3k_4[D]}_{Y}\right]^{\frac{1}{2}} \simeq k_1 + k_2 + k_3[D] - (k_4 + k_p) \qquad (23)$$

Substitution of the values of the various rate constants for the St/ and tPP/Et$_3$ N systems into (22) reveals that this approximation holds to within about 20%, i.e. $\sqrt{X}/\sqrt{X + Y} \geq 0.8$ for values of the ratio X/Y as low as 2.0. More importantly, even with this relatively small difference between the components X and Y, it is found that this leads to a difference of only approximately 5% in the values of λ_1 calculated using the two expressions (16) and (22). In fact, in this case, as the quencher concentration is increased to the region in which λ_1 is a linear function of [D], the X/Y ratio is increased to >3.0. At this point, the λ_1 values calculated using these two expressions rapidly converge to become equal to within $\lesssim$2% (i.e. within the errors involved in measuring λ_1 experimentally).

Figure 3.15

Comparison of the Calculated and Observed Values of $\lambda_{1,2}$ for the St/ and tPP/Et_3N Exciplex Systems

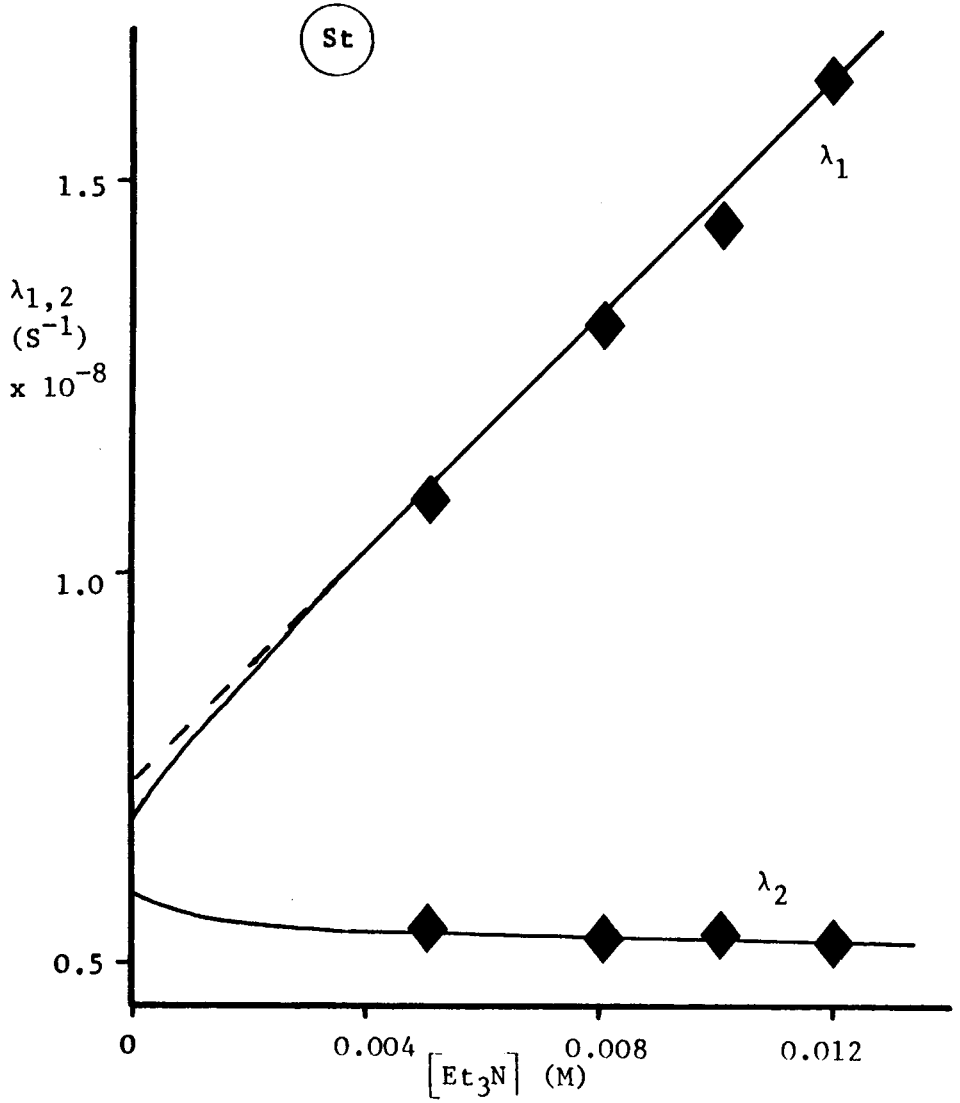

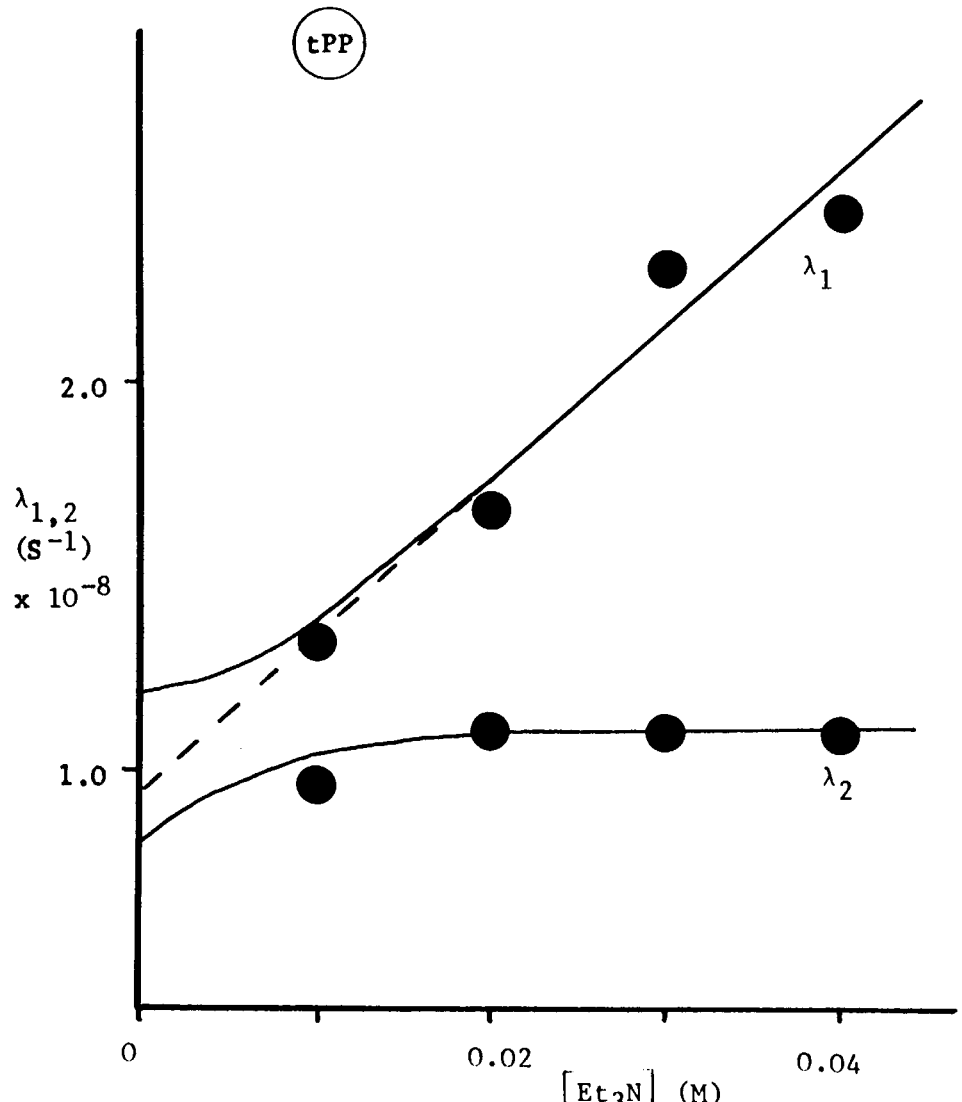

The form of λ_1 can be seen to be strongly dependent on both the absolute and relative values of the various rate constants and in particular on k_3 and k_4. In the case of the St/ and tPP/Et_3N exciplexes studied here, it appears that even though the k_3 values are high (approaching k_{diff}), k_4 in each case is relatively small by comparison. These exciplexes can thus be thought of as being formed essentially irreversibly, the almost negligible k_4 values leading directly to the observation that the expression (22) provides a good approximation to λ_1 over the range of [D] examined. Hence, it follows that the low k_4 values are also the factors governing the lack of discernible longer-lived components corresponding to λ_2, in the monomer decay curves.

Having stated that the k_4 values are negligible here, the significance and validity of their absolute values might be questioned. The method of determining k_4 is outlined in Table 3.8 and from this it can be seen that recovery of a measurable k_4 is dependent on the observation that:

$$\frac{\text{Slope (B)}}{k_3} < \frac{\text{Intercept (B)}}{k_1 + k_2} \quad \left(\text{or } \frac{\text{Intercept (A)}}{-k_1 + k_2}\right)$$

i.e. $\quad k_p \quad < \quad (k_4 + k_p)$

by an amount which is significantly greater than the errors involved in the measurement of the various parameters. The values of the sum $(k_4 + k_p)$ derived from the intercepts of the two plots; (A) $\lambda_1 + \lambda_2$ and (B) $\lambda_1.\lambda_2$ vs. [D] in this case, are shown in Table 3.11 to be in very close agreement and their average values were therefore taken to determine k_4. However, the k_p values recovered from the slopes of plots (B) are shown to represent ≥90% of the total rate of decay from these exciplexes. Thus in view of the cumulation of errors involved in constructing these plots, it is felt that the absolute values should be regarded with some caution. However, they are useful in giving an idea of the order of magnitude and relative lack of importance of the process of reverse dissociation from these exciplexes.

b) Variation of λ_2 with [D]

As with λ_1, it is found that for the St/ and tPP/Et_3N exciplexes, the process of reverse dissociation only has a marked effect at very low [D]. In this concentration region, the plots show a slight curvature with λ_2 initially decreasing for the St/Et_3N system but increasing for tPP/Et_3N. In both cases, the plots level out quite

rapidly such that λ_2 takes on its limiting value of:

$$\lambda_2 ([D] \rightarrow \infty) = k_p$$

c) Limiting values of λ_1 and λ_2 as $[D] \rightarrow 0$.

The two exciplex systems studied here are examples of the two possible sets of limiting conditions for λ_1 and λ_2 as $[D]$ approaches 0. The behaviour of λ_1 and λ_2 at this point is governed by the square root term in equation (16) in that, with $[D] = 0$:

1) For the St/Et_3N exciplex, having $(k_1 + k_2) > (k_4 + k_p)$, this leads to the obvious limits:

$$\lambda_1([D] \rightarrow 0) = k_1 + k_2$$

$$\lambda_2([D] \rightarrow 0) = k_4 + k_p$$

2) For the tPP/Et_3N system, on the other hand, $(k_1 + k_2) < (k_4 + k_p)$ and the effect of taking the square root of the squared term in equation (16) i.e.

$$\left[(k_1 + k_2 - (k_4 + k_p))^2\right]^{\frac{1}{2}}$$

is that the negative root here is disregarded. The outcome of this is to reverse the limits for λ_1 and λ_2 relative to case 1) above and give in this case:

$$\lambda_1([D] \rightarrow 0) = k_4 + k_p$$

$$\lambda_2([D] \rightarrow 0) = k_1 + k_2$$

Examples of both these limiting cases are to be found in the literature and the CNNp/DMCP system[31] mentioned already, is interesting in that it exhibits the properties of both cases 1) and 2) depending on the temperature.

From the data of Table 3.11, it can be seen that the main contribution to the reversal in behaviour observed on going from the St/ to the tPP/Et_3N system, in fact comes from a substantial increase in k_p. This, together with an increased k_4 value, is seen to more than offset the increase in $(k_1 + k_2)$ for the tPP monomer.

d) τ_o/τ_1 vs. [D]

A further point of interest which becomes apparent from plots such as fig. 3.16 concerns the use of Stern-Volmer type plots of τ_o/τ_1 vs. [D]. Any curvature in λ_1 should be reflected in this type of plot although in the cases studied here, this curvature is slight and lifetime data was not obtained at sufficiently low [D] to allow its observation experimentally. What did appear from plots of τ_o/τ_1 vs. [D] was a slight deviation of the intercepts from unity, having effectively extrapolated λ_1 from the linear portions of the curves of fig. 3.15. Such an effect has been reported already; however, as pointed out by Saltiel,[34] such a deviation could be due simply to errors in the unquenched monomer lifetimes (τ_o), which would imply again that in these cases, k_4 is effectively zero.

Conversely, in systems in which k_4 is important, curvature of these plots and deviation of their intercepts from unity should be observable as a general rule. Indeed, this is found to be the case for systems at and near the rapid equilibrium limit, such as the CNNp/olefin exciplexes studied by Ware et al[35]. Thus it is to be expected that plots of τ_o/τ_1 vs. [D] will be of value in yielding k_3 directly only for exciplexes which are formed essentially irreversibly.

3.10 Transient Effects of Diffusion Controlled Reactions

The rate constant for the forward electron transfer within the styrene/Et_3N exciplexes (k_3) derived from lifetime studies, has so far been assumed to be time independent. This is a reasonable approximation considering the method of analysis which has been used to extract λ_1 from the monomer decay curves (i.e. by fitting to only that portion of the curve $\geq$2 ns. after the maximum). As shown by Hui and Ware[32], this should greatly reduce any errors in the rate constants obtained, which might have been due to the transient effects of diffusion controlled reactions. These effects can arise in fluorescence quenching studies as a result of the time evolution of a concentration gradient of the two interacting species. Thus, in this case, acceptor molecules which have a ground state donor molecule in close proximity to them at the instant of excitation, may be quenched very rapidly as little or no diffusion is necessary to bring the two together. This leads to a value of k_3 which is initially very high ($>k_{diff}$) but which falls rapidly during the first 100-200 psec. after excitation. This type of effect has been clearly demonstrated, in studies using picosecond

laser techniques to follow the growth in fluorescence intensity of both inter- and intra-molecular aromatic hydrocarbon/amine exciplexes[36].

In general, 2-3 ns. after excitation, k_3 is observed to have decreased to within a few percent of its limiting value, $k_3(t \to \infty)$. Hence, it is essentially this limiting value which is derived from transient data such as that of the preceding section. However, no account is taken of transient effects in steady state quenching studies. These studies yield k_q^{SS}, the observed quenching rate constant. Transient effects, if present, can strongly influence the values obtained, tending to produce anomalously high k_q^{SS} values due to the rapid initial quenching. Therefore, a comparison is made below (Table 3.12) between the quenching rate constants derived from steady state and transient (k_q^{TR}) studies for the St/ and tPP/Et_3N exciplexes.

Table 3.12

Comparison Between Steady State and Transient Quenching Rate Constants for the St/ and tPP/Et_3N Systems at Room Temperature in Degassed Cyclohexane

Styrene	k_q^{SS} $(l.mol^{-1}s^{-1})$	k_q^{TR} $(l.mol^{-1}s^{-1})$	% Difference
St	8.4×10^9	6.54×10^9	22
tPP	4.8×10^9	3.88×10^9	19

As can be seen, when k_q^{TR} is calculated using the various individual rate constants, according to:

$$k_q^{TR} = \frac{k_3 . k_p}{(k_4 + k_p)} \qquad (24)$$

the value obtained is substantially less than k_q^{SS}, derived from a plot of I_o/I vs. [D], in each case. Similar discrepancies have been reported for the Anthracene (An)/N,N dimethylaniline (DMA) system[32]. In that case, it was suggested that as the unquenched monomer fluorescence lifetime is increased, so the effects of transient terms on k_q^{SS} should be reduced. However, even though τ_o for the styrene monomers are substantially greater than that of anthracene (τ_o = 5.3 ns. at room temperature) it does appear from the data of Table 3.12 that transient effects are by no means negligible here.

Numerical methods of correcting steady state data to take account of these effects have been studied quite extensively by Ware and co-workers[37]. It appears that the steady state and transient quenching rate constants may be related according to:

$$k_q^{SS} = k_q^{TR} \left(1 + \frac{R'}{\sqrt{\tau_o D}}\right) \qquad (25)$$

(in which D is the mutual diffusion coefficient and R' is related to the critical distance at which reaction can occur).

Further, it has been shown that the limiting value of $k_3(t)$ as $t \to \infty$, may be adequately represented by:

$$k_3(t \to \infty) = 4\pi R'DN' \qquad (26)$$

(where N' is the number of molecules $mmole^{-1}$).

Thus equations (25) and (26) have been utilised to obtain values for the parameters R' and D for three styrene/Et_3N systems. These values are listed below in Table 3.13.

Table 3.13

Calculated Values for the Parameters D and R' for Three Styrene/Et_3N Exciplex Systems

Styrene	D ($cm^2.s^{-1}$) ($x10^6$)	R' * (Å)
St	9.4	10.5
tPP	7.6	7.2
IND	3.1	5.2

* - R' is related to the critical distance (R) at which reaction takes place by[37a]:

$$R' = \frac{R}{1 + (D/KR)}$$

in which: $K = k_{gas}/4\pi R^2$

It may be noted that results for the IND/Et_3N exciplex are included here. These have been derived on the assumption that in this case k_q^{SS} and k_q^{TR} differ by an amount similar to that observed for the other two systems (i.e. $k_q^{TR} \simeq 0.8\ k_q^{SS}$).

From the data of Table 3.13, it can be seen that trends are apparent within these parameters. Both R' and D tend to decrease as the electron accepting ability of the styrene monomer is reduced. The values obtained for the St/ and tPP/Et_3N systems are of similar magnitude to those recorded for the An/DMA exciplex (R' = 7Å, $D = 1.75 \times 10^{-5}$ $cm^2.s^{-1}$). The IND/Et_3N system on the other hand, compares closely to the CNNp/DMCP exciplex[37a] (R' = 4Å, $D = 4.0 \times 10^{-6}$ $cm^2.s^{-1}$) and it may be noted that both these systems exhibit the properties of the rapid equilibrium limit, at room temperature.

3.11 Transient Studies on the Indene/Et_3N System

The lifetime data obtained for the exciplex and quenched monomer in the case of the IND/Et_3N system at room temperature in degassed cyclohexane could not be analysed successfully in the manner outlined in the foregoing sections. A typical set of this data is presented, for a range of quencher concentrations, as Table 3.14.

Table 3.14

Lifetime Data Obtained from the Exciplex and Quenched Monomer Fluorescence Decay Curves for the IND/Et_3N System at Room Temperature, in Degassed Cyclohexane

$[Et_3N]$ (M)	τ_1^M (ns)	τ_1^E (ns)	τ_2^E (ns)
0.05	10.8	0.77	11.4
0.1	7.6	0.55	8.0
0.15	6.0	0.80	6.6
0.2	5.1	0.81	5.7

From this, perhaps the most striking difference between IND/Et_3N and the other two systems studied is apparent, in that the lifetimes derived from the monomer fluorescence decay (τ_1^M) and the rising edge of the exciplex decay (τ_1^E) are no longer comparable. Instead, at each $[Et_3N]$, τ_1^E has now become very small (<1ns) such that its absolute value probably has little significance. This leads to the exciplex

decay appearing as a close approximation to a single exponential. Thus, in contrast to the other systems studied, it is the τ_2^E value which is in close agreement with τ_1^M in this case. In other words, both the monomer and exciplex are decaying according to essentially the same single exponential decay law, an observation which places this system at or near the so-called 'rapid equilibrium limit'.

A number of conditions has been quoted[38], which should be fulfilled by such a system, i.e.

$$k_4,\ k_3[D] \gg k_1,\ k_2,\ k_p$$

and these have been expanded further by Ware[35], to yield a simplified expression for the dependence of the decay constant, λ (taken as $(\tau_2^E)^{-1}$ in each case) on the quencher concentration:

$$\lambda = \lambda_0 + \frac{\dfrac{k_3 k_p [D]}{k_4}}{1 + \dfrac{k_3[D]}{k_4}} \qquad (27)$$

(where $\lambda_0 = k_1 + k_2$).

Thus it has been found that for systems at the rapid equilibrium limit, the various individual rate constants can often be derived successfully, utilising the slope and intercept of a plot of $(\lambda - \lambda_0)^{-1}$ vs. $[D]^{-1}$. Unfortunately, in the case of the IND/Et_3N system, although the function $(\lambda - \lambda_0)^{-1}$ appears to vary linearly, with respect to $[Et_3N]^{-1}$, as shown in fig. 3.16a), the intercept of this plot lies very close to zero. Hence an analysis of the type suggested by Ware was not possible for this system. However, fig. 3.16b) illustrates the observation that in fact, in this case, λ appears to be a linear function of $[Et_3N]$. This system therefore seems to represent a situation analogous to that described in ref.(35) for the 1-Cyano Naphthalene (CNNp)/1-Methyl Cyclopentene (MCP) exciplex.

In that case, λ was also found to be linearly related to $[D]$, with the slope, $d\lambda/d[D]$, having a value equal to the observed quenching rate constant, k_q^{SS}. For the IND/Et_3N system, k_q^{SS} has been determined to be:

Figure 3.16a) A Plot of $(\lambda-\lambda_0)^{-1}$ vs. $[Et_3N]^{-1}$ for the IND/Et_3N System

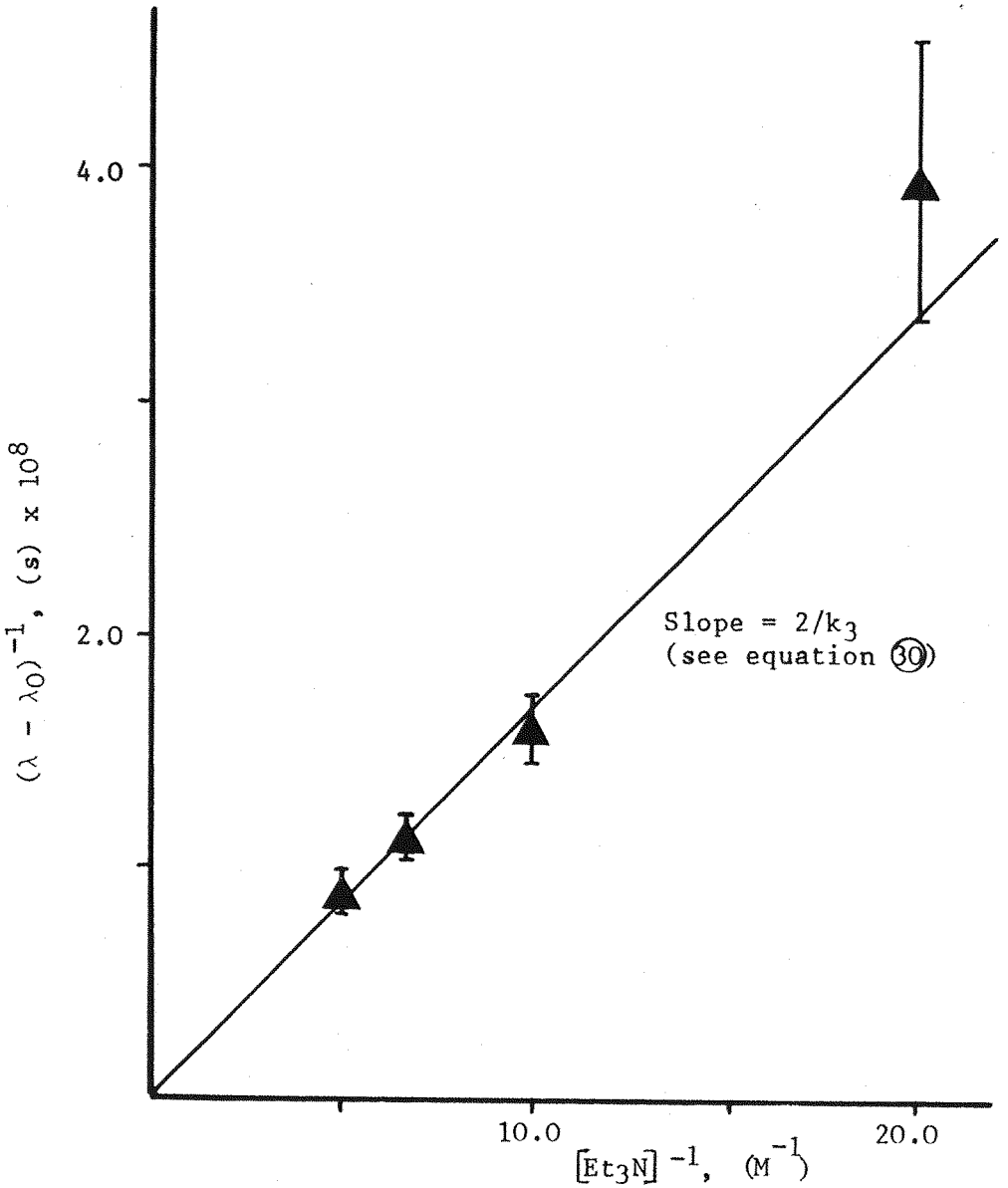

Figure 3.16b) A Plot of λ vs. $[Et_3N]$ for the IND/Et_3N System

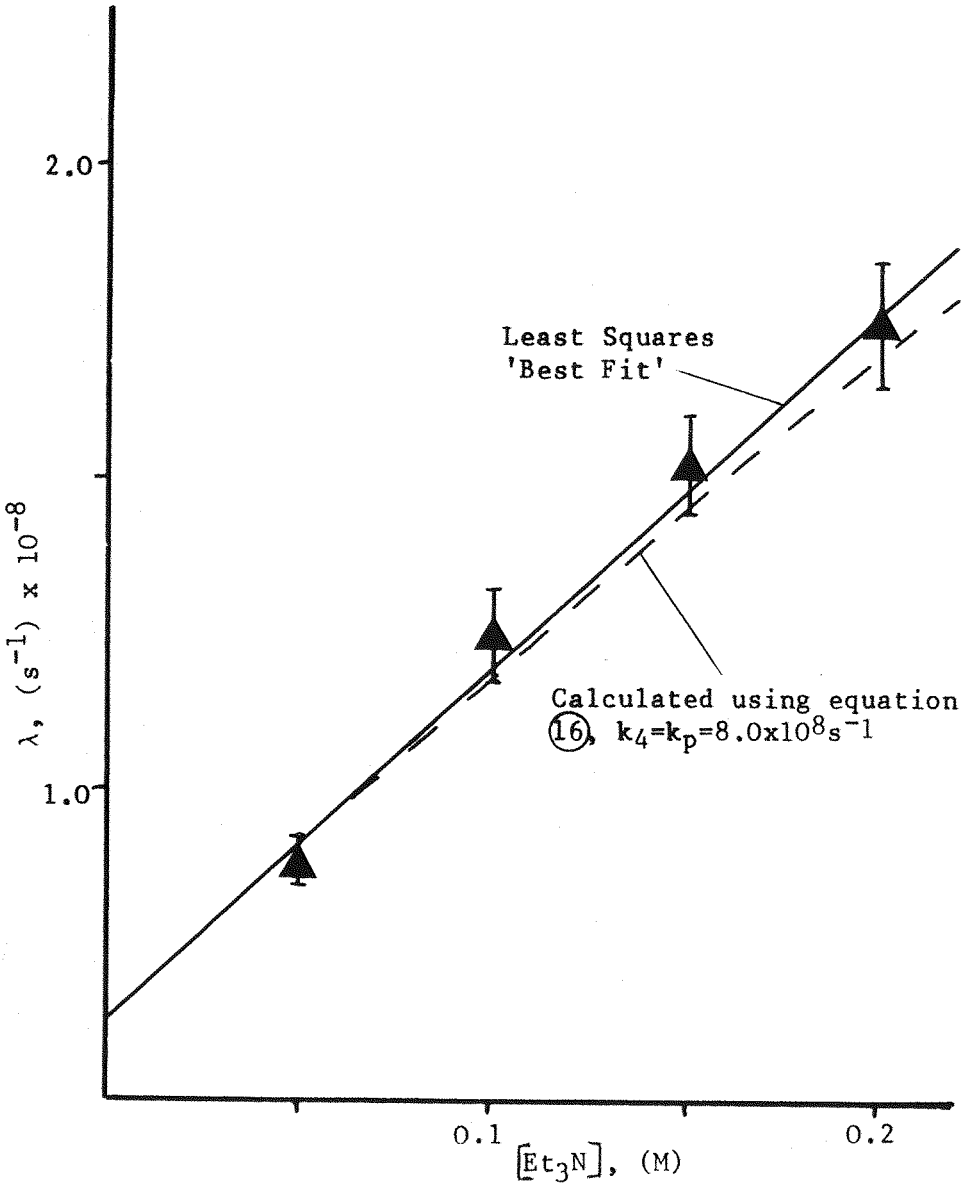

$$k_q^{SS} = 0.74 \times 10^9 \text{ l.mol}^{-1}.\text{s}^{-1}$$

- while as shown in fig. 3.16b), a linear least squares analysis of the transient data provides a value for the slope:

$$\frac{d\lambda}{d[D]} = 0.6 \times 10^9 \text{ l.mol}^{-1}.\text{s}^{-1}$$

However, as detailed already, a correction of the quenching rate constant observed under steady state conditions is often necessary, in order to take into account the transient effects of diffusion controlled reactions. In the case of the St/ and tPP/Et_3N systems, it was found that the time dependence of k_3 is such that $k_q^{TR} < k_q^{SS}$ by a factor of approximately 20%. If this same reduction is applied to k_q^{SS} for the IND/Et_3N system, then a value for k_q^{TR} of 0.6×10^9 $\text{l.mol}^{-1}.\text{s}^{-1}$ is obtained. This therefore suggests that here too, $d\lambda/d[D]$ is providing a measure of the transient effect corrected quenching rate constant, k_q^{TR}.

It was such an observation which prompted Ware to suggest that in the case of the CNNp/MCP exciplex, $k_4 >> k_3$ [35], such that the term $k_3[D]/k_4$ in equation (27) above, may be neglected. This would indeed explain the linear dependence of λ on $[D]$ observed for such systems. However this interpretation requires further, substantial approximations in order to extract the individual rate constants, in particular, a rather arbitrary choice of k_3 as being equal to k_{diff}. An alternative approach, which is derived from an examination of the relative importance of the rate constants k_4 and k_p for a particular system, is therefore suggested here.

It can be shown that the full expression for the decay constants $\lambda_{1,2}$ as a function of the individual rate constants, equation (16) is greatly simplified if k_4 and k_p happen to be approximately equal. The reduced form of this expression then becomes:

$$\lambda_{1,2} = \tfrac{1}{2}\left[k_1 + k_2 + k_3[D] + k_4 + k_p \pm (k_4 + k_p - (k_1 + k_2))\right] \qquad (28)$$

i.e.

$$\lambda_1 = k_4 + k_p + \frac{k_3[D]}{2} \qquad (29)$$

$$\lambda_2 = k_1 + k_2 + \frac{k_3[D]}{2} \qquad (30)$$

- predicting a linear dependence of both λ_1 and λ_2 on $[D]$. For a system at the rapid equilibrium limit, where only a single decay

constant is observable, this will correspond to λ_2. As is shown in fig. 3.16b), in the case of the IND/Et_3N system, a plot of λ vs. [D] has the predicted intercept of λ_0 (= $(k_1 + k_2)$), while the slope which may be derived from this plot, $d\lambda/d[D]$ appears to be equal to k_q^{TR}. This is again consistent with the proposition that k_4 and k_p are approximately equal here, since by definition:

$$k_q^{TR} = \frac{k_3 k_p}{(k_4 + k_p)} \qquad \left(\equiv \frac{k_3}{2} \right)$$

Furthermore, it can be seen that if λ may be represented by equation (30) then this also explains the observed form of the dependence of $(\lambda - \lambda_0)^{-1}$ on $[D]^{-1}$ for this system.

Hence, the value of k_q^{TR} derived from fig. 3.16b) was used directly to obtain a value for the rate constant k_3 for formation of the IND/Et_3N exciplex. An estimate was then made of k_4 and the value of λ_2 calculated at a number of quencher concentrations according to the full equation (16), assuming that k_4 and k_p were in fact equal. The chosen value of k_4 ($\equiv k_p$) was then varied until there was reasonable agreement between the experimental and calculated λ values over the whole range of [D] studied. As illustrated in fig. 3.16b), these conditions were met when the values of k_4 and k_p were taken as $8.0 \times 10^8 s^{-1}$. The values derived for the various rate constants for the IND/Et_3N system by this somewhat circuitous route are summarised in Table 3.15 below.

Table 3.15

The Individual Rate Constants Derived for the IND/Et_3N System at Room Temperature in Degassed Cyclohexane

$(k_1 + k_2)$ (s^{-1})	k_3 $(l.mol^{-1}.s^{-1})$	k_4, k_p (s^{-1})
6.25×10^7	1.2×10^9	8.0×10^8

These values may now be compared with those observed for the other styrene/Et_3N systems studied under the same conditions (see Table 3.11). Such a comparison reveals that the correlations of the various rate constants with electron accepting ability of the styrenes, which

might be expected simplistically, are in fact observed. Although these three systems cover a range of only 0.3 eV. in the gas phase ionisation potential (I_A), it can be seen that k_3, the rate constant for the electron transfer process $D \rightarrow {}^1A^*$ decreases with I_A. Those rate constants associated with the decay of the exciplexes also show a strong correlation, both k_4 and k_p increasing as I_A is reduced. For a similar series of exciplexes formed between CNNp and a range of olefins[35] only k_4 was seen to reflect systematically changes in the ionisation potential of the donor olefin. However, a greater degree of CT character is predicted (from solvent effects on λ^E_{max}) for the styrene/Et_3N exciplexes, compared to the less polar CNNp/olefin systems. Thus, it may be that simple correlations between the various rate constants and the electron accepting ability of the styrene monomers are more likely to be observed for the former.

In this context, Ware has loosely classified complexes as 'weak' or 'strong', depending on the relative importance of k_4. The St/ and tPP/Et_3N systems, in which the feedback process is relatively insignificant, would thus be termed 'strong'. For these, the variation in the observed quenching rate constant is caused by the differences in k_3. The IND/Et_3N system is an intermediate case here in that, while k_3 is reduced, along with I_A, k_4 has now become important. The value of k_4 recorded in this case, is still two orders of magnitude less than the rate constant expected for separation of two non-interacting species in a non-polar solvent[39] ($k_{diff} = 10^{11} sec^{-1}$). However, this value of k_4 is such that the observed value of k_q is substantially less than k_3 in this case.

3.12 ΔG_A Values Derived from Transient Studies

The ratio of the rate constants k_3 and k_4 has been used to calculate ΔG_A, the free energy change for the association process for these three systems, since:

$$\frac{k_3}{k_4} = e^{-\Delta G_A/RT} \qquad (31)$$

The ΔG_A values obtained are presented as Table 3.16a) and it is interesting to compare these with ΔG_A calculated for these same systems, according to the empirical equation (15) (see p.75). It can

be seen that only ΔG_A derived from transient studies predicts the correct ordering of the reactivity of the three styrene monomers with Et_3N. Also the absolute values of ΔG_A obtained in this way for the St/ and tPP/Et_3N systems are now of the same order as those observed for other aromatic hydrocarbon/amine exciplexes. Some such examples for which ΔG_A has been calculated from transient studies alone, are presented, for comparison, in Table 3.16b).

Table 3.16a)

ΔG_A Values for the Styrene/Et_3N Exciplexes, Calculated from Transient Studies

Styrene	$-\Delta G_A$ (kJ mol^{-1})
St	17.2
tPP	15.5
IND	0.84

Table 3.16b)

Typical ΔG_A Values for Aromatic Hydrocarbon/Amine Exciplex Systems

Exciplex*	$-\Delta G_A$ (kJ mol^{-1})
Anthracene/DMA[32]	20.1
Perylene/DMA[2b]	11.7
β-StyrylNaphthalene/DEA[40]	17.6
Pyrene/DEA[41]	13.4
Pyrene/TBA[41]	10.9

* - DMA = N,N Dimethylaniline
DEA = N,N Diethylaniline
TBA = Tri-n-Butylamine

On the other hand, a rather small negative ΔG_A value was recorded for the IND/Et_3N system. Once again, this system appears to be a typical example of the rapid equilibrium type, as the CNNp/olefin exciplexes[35], which show these same properties at room temperature, are characterised by similar ΔG_A values (in the region of -2.5 to -7.1 kJ mol^{-1}.)

3.13 The Exciplex Radiative Rate Constant (k_5)

As pointed out already, k_p is not expected to represent a single rate constant but rather a sum of two or more. This sum can be broken down into contributions from radiative (k_5) and non-radiative (k_p-k_5) processes, using a plot of Φ_E/Φ_M (the relative quantum yields of exciplex and quenched monomer fluorescence) versus [D], since:

$$\frac{\Phi_E}{\Phi_M} = \frac{k_5}{k_1} \cdot \frac{k_3}{(k_4 + k_p)} \cdot [D] \qquad (32)$$

Such plots are presented for three styrene/Et_3N systems as fig. 3.17. These plots are seen to be linear over the range of [D] studied, as predicted by the standard exciplex kinetic scheme. Deviations from linearity have been observed[34] for systems in which a termolecular process, involving quenching of the exciplex itself e.g. by ground state donor, is important. However, for the systems studied here, there is no reason to invoke this extra decay pathway and thus k_5 has been derived directly from the slopes of figs. 3.17. The values obtained are given below in Table 3.17 and interestingly, they again appear to show a correlation with the electron accepting ability of the styrene monomers (as measured by I_A).

Table 3.17

The Observed Values of the Exciplex Radiative Rate Constant, k_5, for Three Styrene/Et_3N Systems

Exciplex	k_5* (s^{-1}) x10^{-7}
St/Et_3N	0.46
tPP/Et_3N	1.29
IND/Et_3N	1.94

* - Calculated from the slopes of figs. 3.17 using the transient effect - corrected value of the photoassociation rate constant,

$$k_3^{SS} = k_3\left(1 + \frac{R'}{\sqrt{\tau_0 D}}\right)$$

Figure 3.17 The Observed Variation of the Ratio of the Quantum Yields of Exciplex and Quenched Monomer Fluorescence with Quencher Concentration for Three Styrene/Et_3N Systems

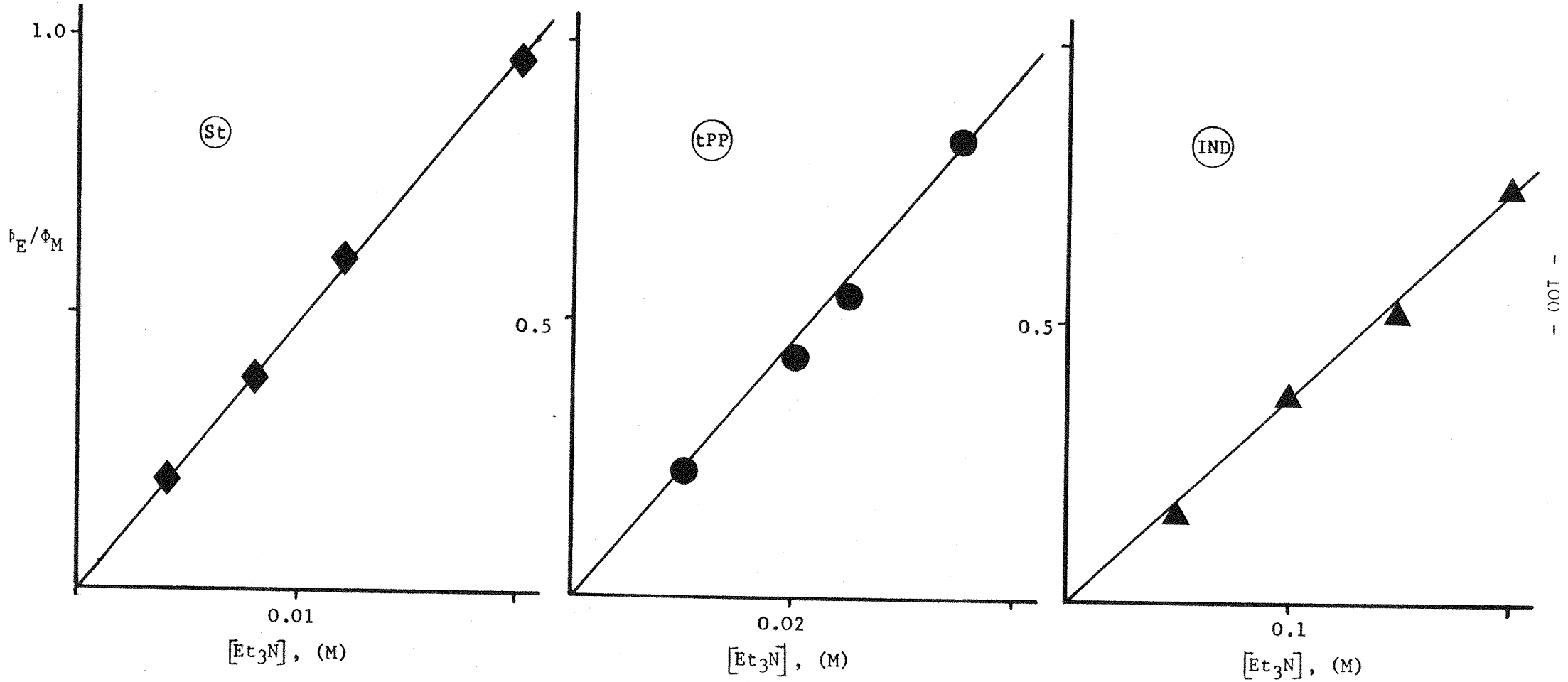

The magnitude of k_5 for a particular system will be determined by the various configurations both Locally Excited (LE) and Charge Transfer (CT), which are important in the description of the exciplex state. Thus, for systems in which both LE and CT configurations are important, the variety of transitions from which the exciplexes can derive oscillator strength is expected to make observation of a strong correlation between k_5 and I_A unlikely. It may be that the observations presented in Table 3.17 serve to further enforce the view that the styrene/Et_3N exciplexes exhibit a high degree of CT character.

It is suggested here that for these systems, the transition dipole moment for the exciplex emission, M^E, may be approximated as:

$$M_E \simeq a \langle \Psi(A^- D^+) | \mu_{op} | \Psi_o(AD) \rangle \qquad (33)$$

- involving only the dominant CT term. If this is so, then k_5 and I_A might be expected to be related in some way. The matrix element of equation (33) is thought to be approximately proportional to the degree of overlap between the donor orbital in D and the acceptor orbital in A[42]. Hence it may be more than coincidental that the value of k_5 is observed to increase as the critical distance at which reaction can occur, R', (see p.91) decreases within the series St > tPP > IND. Although many more examples are required, it is tempting to suggest from this that as the electron accepting ability of the monomer is reduced, so the two reaction partners must be brought closer together in order that complex formation can occur.

3.14 Time Resolved Fluorescence Spectra

The transient studies of the previous section provided a route to the various rate parameters for the processes of exciplex formation and decay. This same information has also been derived[41,43] from measurement of the Time Resolved Spectra (TRS) of a number of exciplex-forming systems. Although no such analysis is attempted here, fig. 3.18 illustrates the changes which occur in the fluorescence spectrum of a styrene/Et_3N system, with time. The system chosen for this brief study was oMe/Et_3N. This was one case in which the styrene monomer possessed a sufficiently large extinction coefficient at the excitation wavelength of the laser light source (310 nm).

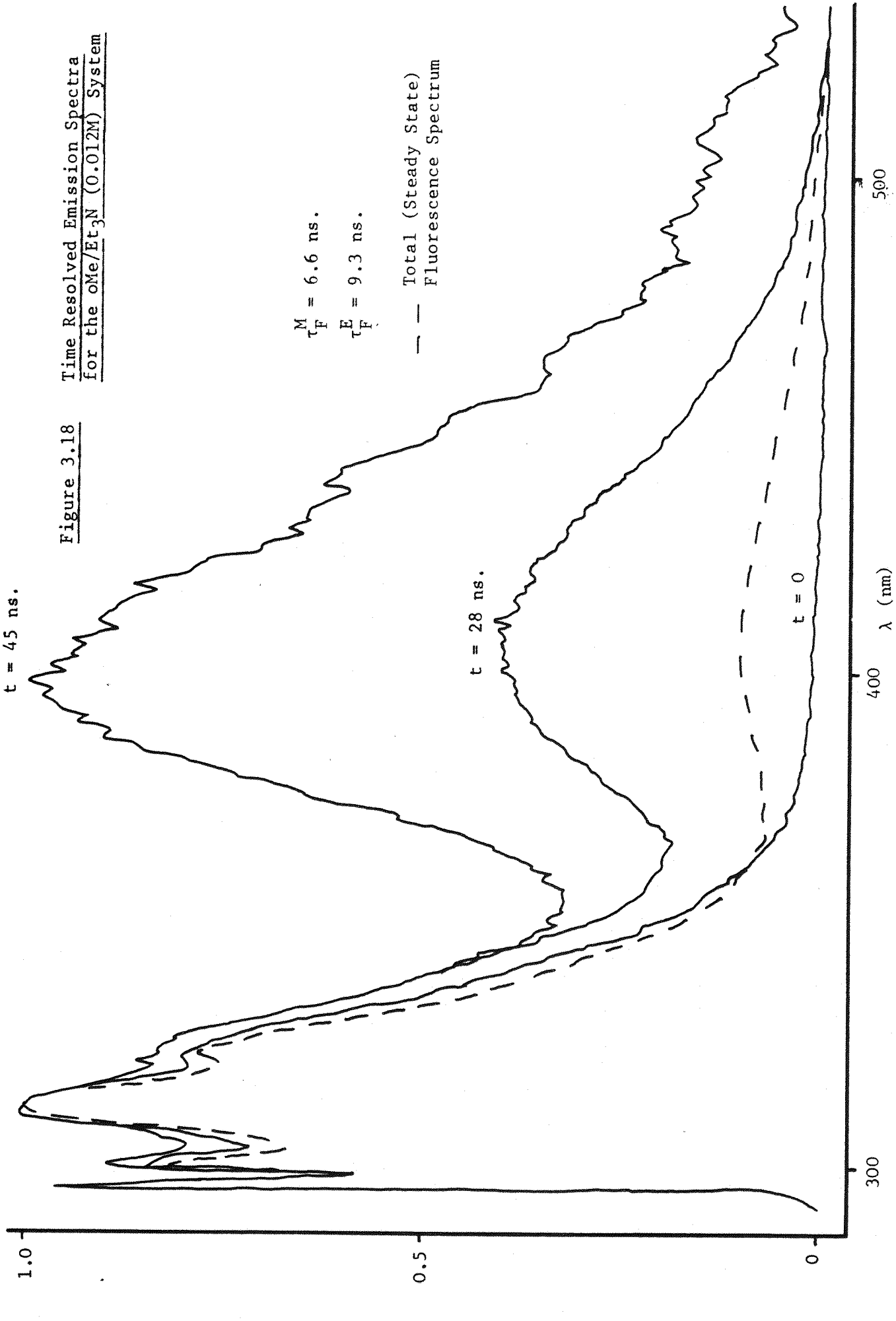

Figure 3.18 Time Resolved Emission Spectra for the oMe/Et_3N (0.012M) System

The total (Steady State) fluorescence spectrum observed under the same conditions is also presented in fig. 3.18 for comparison. From this it can be seen that even at the relatively high quencher concentration used (such that $I_M^0/I_M \simeq 2.5$) the exciplex emission intensity is weak, compared to the fluorescence due to the styrene monomer. However, as the fluorescence spectrum is recorded at increasing intervals after pulsed laser excitation, the broad, structureless exciplex emission grows in, at the expense of the monomer fluorescence. This provides further proof, if any were necessary, that the exciplex is being formed via the quenched monomer. The effect is clearly demonstrated in fig. 3.18, which shows the spectrum recorded at three time intervals relative to the peak of the laser excitation pulse (t = 0). Indeed, at t = 0 ns, the emission spectrum observed appears to be due solely to the oMe monomer. Subsequently, the exciplex emission appears and the ratio of the fluorescence intensities of the exciplex and quenched monomer (I_E/I_M) increases with time. However, even at t = 45 ns, residual monomer emission is still observable and the ratio I_E/I_M has a value of only approximately 2.5. This is despite the fact that the measured monomer fluorescence lifetime, τ_M, predicts that >99.9% of the initially excited monomer should have been quenched after this time. This would appear to indicate that in this case, the emitting species are not decaying independently. By comparison with the St/Et_3N system, it would be expected that here too, the process of reverse dissociation would be relatively insignificant. However, it does appear that, at long intervals after excitation, the effects of this feedback process may be observable.

3.15 Solvent Effects on Exciplex Kinetics

The effects of solvent polarity on exciplex photokinetics have been studied for relatively few systems. A recent paper[21] due yet again to Ware and co-workers, has presented perhaps the most detailed transient study so far on the effects of slightly polar solvents; on the photophysics of an aromatic hydrocarbon/olefin exciplex. In this case the importance of solvent participation in exciplex formation and decay was shown to account for the observed changes in the thermodynamic properties of the system. A brief study has been conducted in this work, on the effects of mixed cyclohexane/methylene chloride

solvent systems on the various rate constants associated with the tPP/Et_3N exciplex at room temperature.

Lifetime data for both the exciplex and quenched monomer was obtained for three such solvent systems in the range of dielectric constant, ε = 2-4. As noted already, as the solvent polarity is increased so the exciplex fluorescence maximum undergoes a red shift and the fluorescence quantum yield of the exciplex, Φ_E, is decreased. Transient studies indicate that the exciplex lifetime, τ_E, also decreases with increasing solvent dielectric, whilst the associated quenched monomer lifetime (at a given donor concentration) remains constant, within the experimental error. Two possible explanations have been proposed in order to account for this type of observation:[43a,44]

a) Competition between ionic dissociation and fluorescent exciplex formation within an encounter complex,

b) Solvent induced changes in the electronic and geometrical structure of the exciplex.

The processes involved in a) can be represented schematically as in fig. 3.19 below.

Figure 3.19

A Scheme Depicting the Competition Between Ionic Dissociation and Exciplex Formation via an Encounter Complex

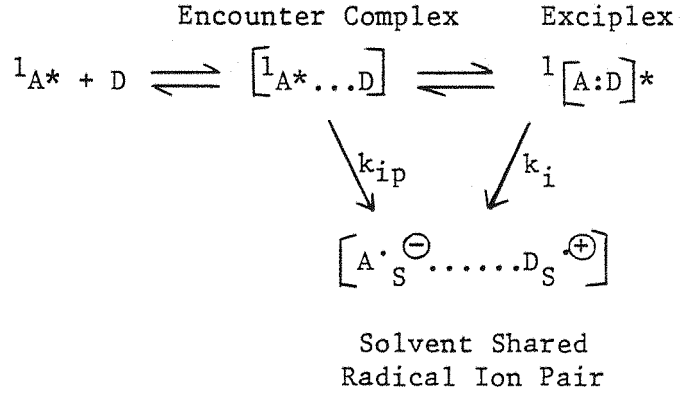

According to this scheme, a decrease in τ_E with increasing solvent polarity is explained in terms of an increase in the efficiency of radical ion pair formation via the exciplex (represented by k_i). Φ_E on the other hand, will be dependent on both k_i and the process k_{ip}, corresponding to formation of the solvent shared radical ion pair

directly from an encounter complex. Such complexes are thought to be formed prior to formation of the relaxed exciplex and may represent simply a non-relaxed state of the exciplex, requiring solvent reorganisation and/or a change in geometry in order to produce the fluorescent complex.

Evidence for the existence of the process k_{ip} has come from laser induced photoconductivity studies[45] carried out, for example, on the Pyrene/N,N Dimethylaniline exciplex. In solvents of moderate to high polarity, large photocurrents were recorded immediately after pulsed laser excitation of the Pyrene, whereas a growing in of the current, matching the decay of the exciplex would be expected if k_i represented the only route to the radical ion pair. For some systems, triplet formation has also been proposed to be an important deactivation pathway for the encounter complex[46] in both polar and non-polar solvents. Thus it can be seen that a complete description of the primary processes affecting a particular excited CT system is by no means straightforward to obtain.

Substantiation of the proposal that solvent induced changes in the electronic and geometrical structure of an exciplex can affect τ_E and Φ_E may be equally difficult. This will depend on the ease with which the various individual rate constants can be extracted, free from the interfering effects of decay from an encounter complex, noted above.

In the case of the tPP/Et_3N system, the conditions of this study of exciplex kinetics as a function of solvent polarity were chosen such that a relatively high quencher concentration was used, ($[Et_3N]$ = 0.04 M). As shown previously, at this point, λ_2 has effectively reached its limiting value of k_p, while λ_1 can be adequately represented by the sum ($k_1 + k_2 + k_3 [Et_3N]$). The observed lack of dependence of λ_1 on solvent is therefore indicative of the fact that k_3 is little affected by solvent polarity, within the rather narrow range studied. The effect of solvent on λ_2 however showed that k_p increases with ε and the values derived for this rate constant ($= \lambda_2^{-1}$) in each case are recorded in Table 3.18. However k_p is in fact a sum of the rate constants for the radiative (k_5) and non-radiative exciplex decay processes and in order to separate out these two contributions to k_p, steady state measurements must be used, of necessity. Therefore,

it is at this point that the assumption must be made that under these conditions, ionic dissociation and/or triplet formation within an encounter complex are not influencing the measured Φ_E values to an appreciable extent. If this is the case for the tPP/Et_3N system, then at the relatively high quencher concentrations used, Φ_E may be defined according to

$$\Phi_E = \frac{k_3[D]}{k_1 + k_2 + k_3[D]} \cdot \frac{k_5}{k_p} \qquad (34)$$

Hence, the observed k_p values may be combined with the measured quantum yields of exciplex fluorescence to derive a value for k_5 for each solvent system. This expression corresponds to the condition that the effects of reverse dissociation of the exciplex may be neglected here. As a test of the validity of this approximation, the value derived for k_5 in cyclohexane solution using equation (34) (presented in Table 3.18) may be compared with that obtained from a plot of Φ_E/Φ_M vs. $[Et_3N]$ and given already in Table 3.17. Such a comparison reveals that the agreement is indeed very good, provided that once again, it is the transient effect corrected value, k_3^{SS}, which is used in the calculation. Therefore, the k_5 values obtained directly from the measured exciplex fluorescence quantum yields, using equation (34) are presented for the mixed solvent systems also, in Table 3.18.

Table 3.18

The Observed Variation in the Radiative and Non-Radiative Rate Constants for the tPP/Et_3N Exciplex in Methylene Chloride/Cyclohexane Mixed Solvent Systems

$\%CH_2Cl_2$	ε	$f(\varepsilon,n)$*	k_p (s^{-1}) x10^{-8}	k_5 (s^{-1}) x10^{-6}	k_p-k_5 (s^{-1}) x10^{-8}	$\frac{k_p}{k_5}$
0	2.02	0.101	1.13	11.9	1.01	9.5
10	2.80	0.171	1.61	5.7	1.55	28.1
25	3.79	0.223	1.72	4.2	1.68	41.4

* As defined earlier (Section 3.6)

There appear to be no straightforward correlations between either k_p or k_5 and the solvent parameters ε or $f(\varepsilon,n)$, although the plot of Φ_E^{-1} vs. $f(\varepsilon,n)$ presented as fig. 3.9, does imply that for this system, the ratio k_p/k_5 should be a linear function of this parameter. As shown in fig. 3.20, this does appear to be the case here, although it is difficult to rationalise such a correlation and it would not be expected that this should be a general characteristic of exciplex-forming systems. However, fig. 3.20 illustrates the rather interesting observation that over a similar range of $f(\varepsilon,n)$, the CNNp/DMCP system studied by O'Connor[21] also shows a linear dependence of k_p/k_5 on this parameter. The slope of this plot is observed to be negative as a result of the fact that for this system, k_p decreases with increasing solvent polarity.

It is proposed here that for the tPP/Et_3N system, under the conditions noted above, the observed decrease in Φ_E with increasing solvent polarity may be accounted for solely by a variation in the rates of the processes deactivating the relaxed exciplex state. As illustrated in Table 3.18, the exciplex radiative rate constant k_5 is found to decrease as ε is increased, while the non-radiative rate constant $(k_p - k_5)$ increases. It may be that as with the CNNp/DMCP system, these observations can be explained in terms of specific solvent participation in the formation of the exciplex. Using the arguments proposed by Mataga[44b], it can be shown that increasing the solvent dielectric will tend to cause an increase in the polarity of the exciplex electronic structure. This is brought about by a decrease in the relative importance of the locally excited configurations to the exciplex wave function (ψ_E) and will lead to a decrease in the radiative transition probability and hence, k_5. However, if as postulated already, the tPP/Et_3N exciplex is a highly ionic species even in cyclohexane, this effect on ψ_E may be relatively small. What may be more important in this case is the possibility that as ε is increased, the polar solvent molecules will interact more strongly with the dipolar exciplex. Crowding of the solvent around this dipole may then influence the A-D distance within the complex, leading to an increased cavity radius. Then, as proposed in the explanation of the effects of variation of the styrene monomer

Figure 3.20 A Plot of the Ratio k_p/k_5 vs. $f(\varepsilon,n)$ for Two Exciplex Systems

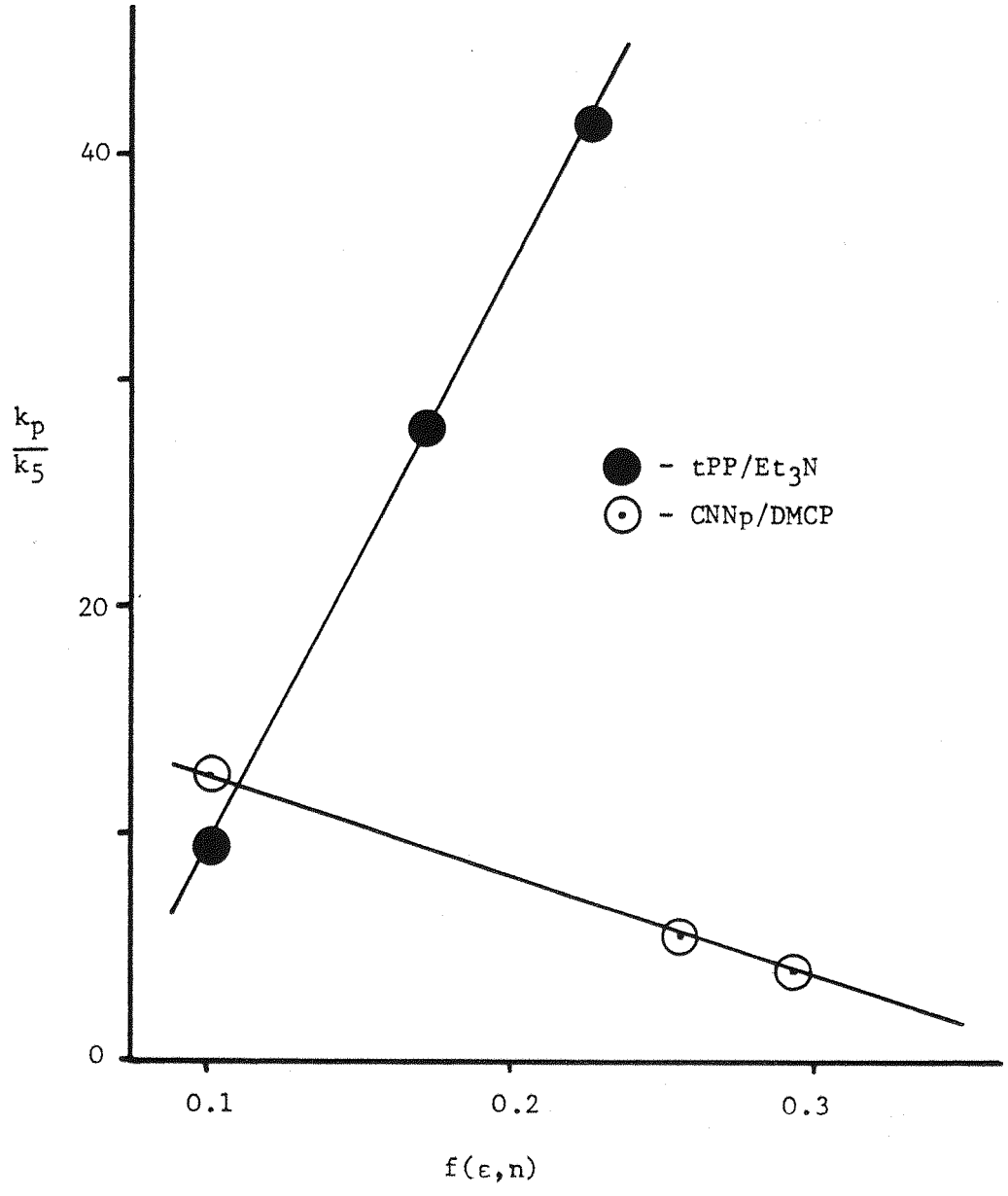

on k_5, this change in geometry could lead to a decrease in the transition dipole moment (M_E) and thus k_5, as ε is increased. The magnitude of this variation in k_5 would appear to be rather large, considering the narrow range of solvent dielectric studied. This would suggest that the value of k_5 for the tPP/Et_3N system is in fact highly sensitive to the intermolecular separation within the exciplex, since calculations predict that for highly polar exciplex systems, the equilibrium separation is affected only slightly by solvent polarity[47]. However, the three-fold decrease in k_5 here is not unreasonable, since it has been demonstrated by Prochorow[48], that an increase in the complex equilibrium separation of as little as 0.2-0.3 Å may be all that is required for such a decrease to be observed.

It has been claimed[49] that for highly polar exciplexes such as those formed between aromatic hydrocarbons and amines, solvent-induced changes in the electronic and geometrical structures of these complexes may be unimportant. This is most probably the case for solvents of moderate to high polarity. However, it is felt that the results presented here illustrate that for such a system, these effects can account for the observed variation in the exciplex radiative rate constant, over a range of relatively low ε values. The same may be true in the case of the non-radiative exciplex decay processes, although it may be more likely that the observed increase in the rates of these processes with ε is accounted for by an accompanying decrease in the height of the energy barrier to formation of a solvated radical ion pair via the exciplex. This is discussed in somewhat more detail later (Section 4.3), however, it may be noted at this point that as ε is increased to above the range studied here, the tPP/Et_3N exciplex fluorescence diminishes further.

Indeed in pure methylene chloride solution (ε = 9.3), no such emission is observable. This is most probably an indication that at this point, radical ion pair formation via either a relaxed or non-relaxed exciplex state has become a major deactivation pathway.

The solvent dependence of the energy of the various species involved in exciplex formation and decay has been represented schematically[50] as in fig. 3.21. This prompts the suggestion that solvent induced changes in electronic/geometrical structure may only be observable at ε values below which the transition occurs

Figure 3.21 A Schematic Representation of the Solvent Dependence of the Energy of the Various Species Involved in Exciplex Formation and Decay

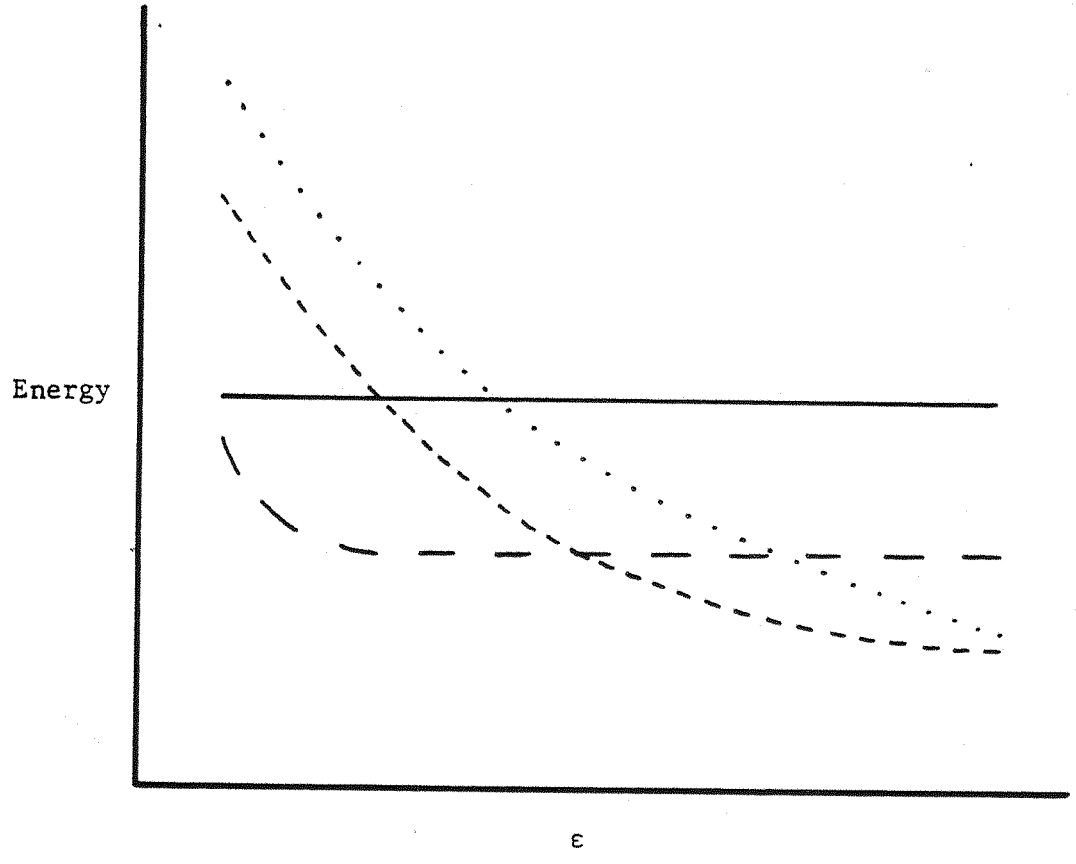

from exciplex to solvated radical ion pair as the more stable entity. The absolute value of ε at this point will presumably be determined for a particular system by the polarity of the exciplex. For highly polar systems such as tPP/Et_3N, this transition is thought to occur at relatively low ε values ($\lesssim$ 6-10). However, in the case of a less polar exciplex, that involving Diphenylvinylidene Carbonate and 1,5 Dimethylhexadiene[51], it has been suggested that an ε value greater than 20 is required for efficient radical ion pair formation to occur.

3.16 Temperature Dependence of Exciplex Photophysics

The effects of variation of temperature on the various rate parameters involved in exciplex formation and decay can be most valuable, in providing a measure of some of the important thermodynamic properties of a particular system. As illustrated in fig. 3.22, for the tPP/Et_3N exciplex in a non-polar solvent system (1:1 Methylcyclohexane/Isopentane), as the temperature is lowered in the region from room temperature to 250 K, the intensities of both the exciplex and quenched monomer fluorescence are increased. It is apparent from this figure that the exciplex fluorescence intensity is enhanced more rapidly than the corresponding monomer fluorescence. This type of effect has been explained in terms of a 'freezing-out' of the reverse dissociation process, represented here by k_4, and has been quantified using the familiar Stevens-Ban type of plot[52]. Such a plot of loge ($\Phi_E/\Phi_M[D]$) versus T^{-1} is presented as fig. 3.23 for the tPP/Et_3N system and shows the two distinct temperature regions usually observed. In the low temperature region, the reduction in the ratio $\Phi_E/\Phi_M[D]$ with T is thought to be due[1b] simply to a decrease in the encounter frequency between $^1A^*$ and D. This is a reflection of the increased solvent viscosity at lower temperatures, the temperature coefficient here being related to the activation energy for viscous flow of the solvent.

Analysis of the high temperature portion of plots such as fig. 3.23 has frequently been used[53] to determine ΔH_o, the photoassociation enthalpy, for a given exciplex formation process. However, as pointed out by Selinger[54] and others, the validity of this derivation is strongly dependent on the relative magnitude of the rate constants k_4 and k_p. The ratio of exciplex to quenched

Figure 3.22 The Effects of Temperature on the Fluorescence Spectrum of the tPP/Et_3N System

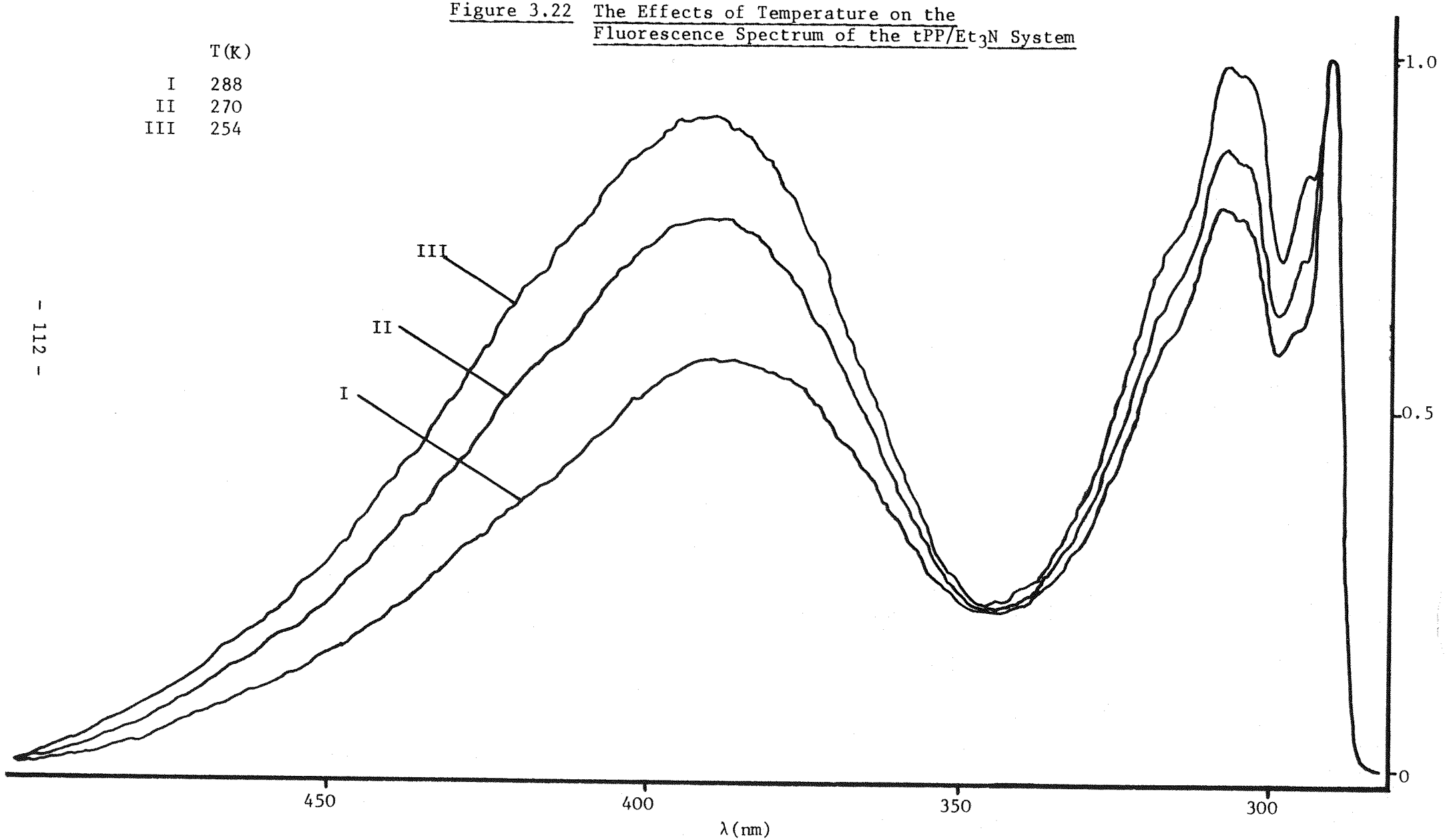

Figure 3.23 A Stevens-Ban Plot for the tPP/Et_3N System

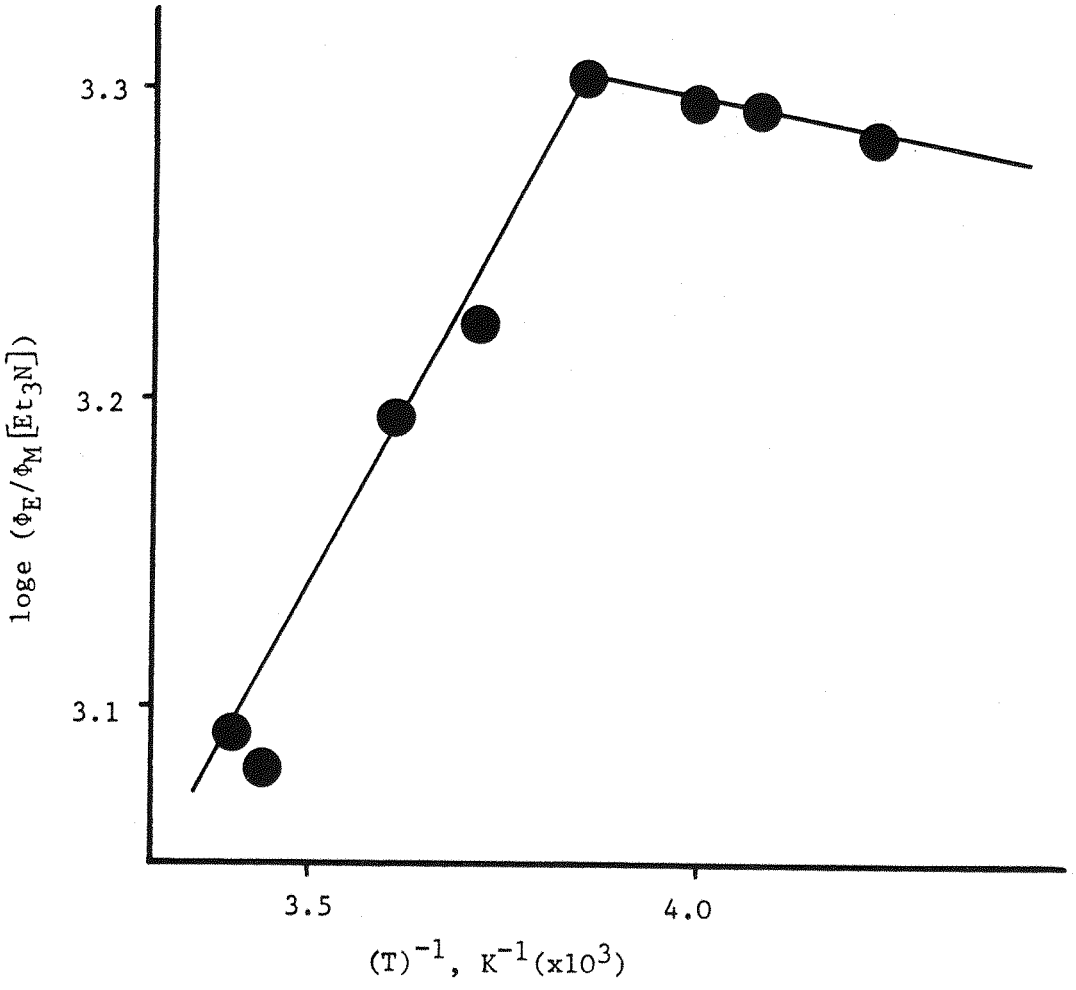

monomer fluorescence quantum yields can be defined as:

$$\frac{\Phi_E}{\Phi_M[D]} = \frac{k_5}{k_1} \cdot \frac{k_3}{(k_4 + k_p)} \qquad (35)$$

in which the two radiative rate constants k_1 and k_5 are assumed to be temperature independent. From equation (35), it can be seen that a plot of loge $(\Phi_E/\Phi_M[D])$ vs. T^{-1}, will only provide a measure of the temperature coefficient of the ratio k_3/k_4 and hence ΔH_o, for systems in which $k_4 >> k_p$. The tPP/Et_3N system clearly does not fall into this category and the apparent value of the enthalpy of complex formation, derived from fig. 3.23 ($\Delta H_o' = -4.6$kJ mol^{-1}) is not therefore a true reflection of the stability of this exciplex.

A more meaningful value for ΔH_o is accessible without recourse to the arguments implicit in a Stevens-Ban plot, by carrying out a study of the variation of the monomer and exciplex fluorescence decay times as a function of temperature. In this case, activation parameters for the individual rate constants may be derived and a transient study of this kind has been attempted in the present work, for the tPP/Et_3N system. The results obtained are presented in Table 3.19, showing the observed values of the various rate constants over a range of temperatures.

Table 3.19

Temperature Variation of the Rate Constants for the tPP/Et_3N System, as Derived from Transient Studies

T (K)	k_3 ($1.mol^{-1}s^{-1}$) (10^{-9})	$k_4 + k_p$ (s^{-1}) ($x10^{-7}$)	k_4 (s^{-1}) ($x10^{-6}$)	k_6 (s^{-1}) ($x10^{-7}$)
290	4.14	12.1	7.6	9.8
276	3.36	9.2	2.3	7.0
266	2.95	7.5	0.93	6.0
251	2.40	5.8	-	4.3
230	1.69	4.2	-	2.7

Given that the temperature dependence of each rate constant (k_i) may be expressed as:

$$k_i = A_i \, e^{\frac{-\Delta E_i^{\ddagger}}{RT}} \qquad (36)$$

then it can be seen that Arrhenius plots of loge k_i versus T^{-1} should provide values for the activation energy, $\Delta E_i^{\ddagger}$ for that process. Figs. 3.24 present the data of Table 3.19 in this form and it can be seen that the plots a) and b) for the rate constants k_3 and k_4 respectively are indeed linear. Loge k_p shows some curvature, when plotted against T^{-1} (plot c) of fig. 3.24), however this is not surprising as it should be remembered that k_p in fact represents a sum of rate constants. Interestingly though, it is found that plot c) can be linearised simply by taking the value of k_5 as a constant and subtracting this from the value of k_p at each temperature, as is shown in fig. 3.24d). This may suggest that there is a single major, temperature dependent, non-radiative process depleting the excited tPP/Et_3N complex. This process has been denoted here by the rate constant k_6. Its activation energy $\Delta E^{\ddagger}_6$, together with those for the processes of association and reverse dissociation for this exciplex, as derived from the slopes of figs. 3.24, are presented in Table 3.20.

Table 3.20

Activation and Thermodynamic Parameters Derived for the tPP/Et_3N System

$\Delta E^{\ddagger}_3$ ($kJ.mol^{-1}$)	$\Delta E^{\ddagger}_4$ ($kJ.mol^{-1}$)	$\Delta E^{\ddagger}_6$ ($kJ.mol^{-1}$)	ΔH_o ($kJ.mol^{-1}$)	ΔS_o ($J.deg^{-1}mol^{-1}$)
7.7	52.6	11.9	-44.8	-101.3

Also given in Table 3.20 are the values of the thermodynamic parameters ΔH_o and ΔS_o (the entropy of photoassociation) obtained using equations (37) and (38) respectively, i.e.

$$\Delta H_o = \Delta E^{\ddagger}_3 - \Delta E^{\ddagger}_4 \qquad (37)$$

$$\Delta S_o = \frac{\Delta H_o - \Delta G_o}{T} \qquad (38)$$

Figures 3.24 Arrhenius Plots for the Various Rate Constants Associated with the tPP/Et_3N Exciplex

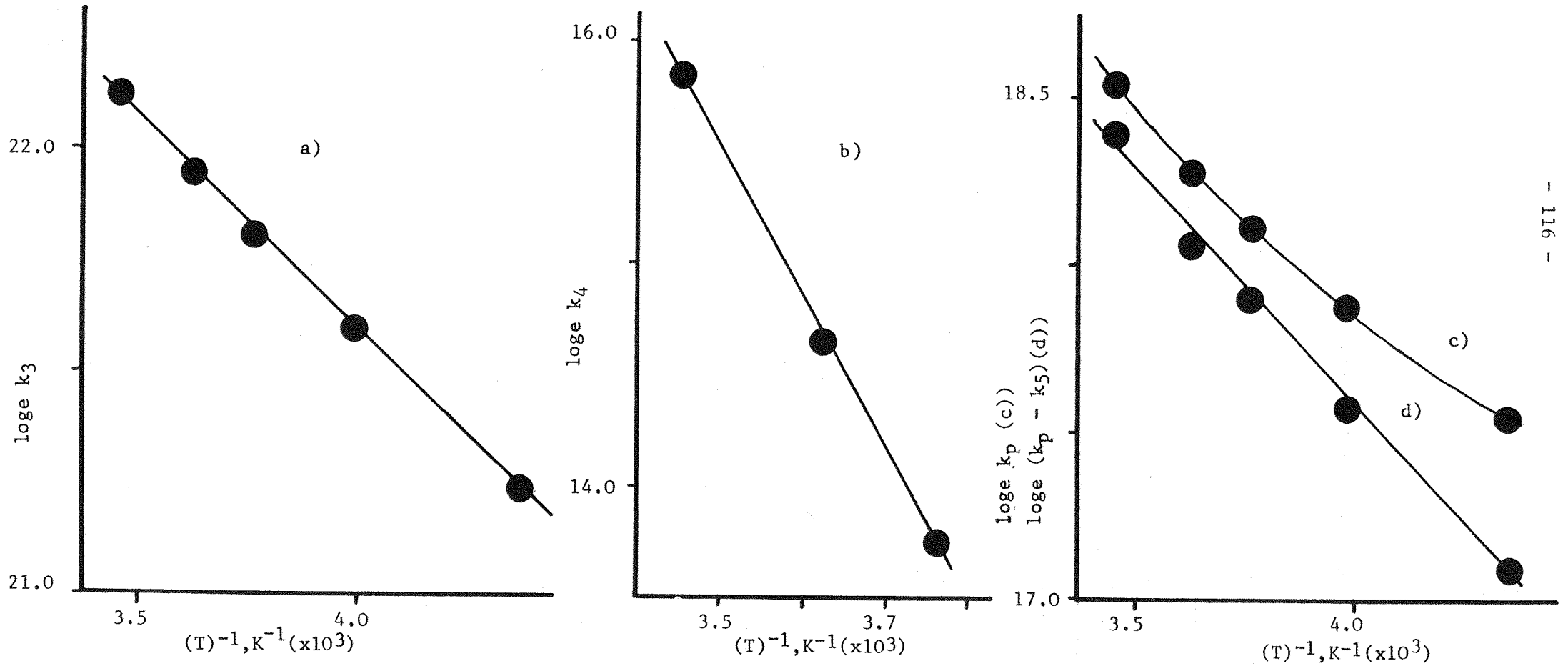

It can be seen that the activation energy, $\Delta E_3^{\ddagger}$, associated with the electron transfer process ($Et_3N \rightarrow {}^1tPP^*$) has a value close to that which might be expected for the temperature coefficient for viscous flow for this solvent system[32]. This can be taken as an indication of the importance of diffusion of the two interacting species together prior to complex formation. As indicated in Table 3.19, a measurable value for k_4 could only be derived over the temperature range from room temperature (290 K) to around 270 K. The activation energy $\Delta E_4^{\ddagger}$ for the reverse dissociation is found to be quite large (52.6 $kJ.mol^{-1}$) and thus k_4, which is already relatively small at 290 K, decays rapidly with decreasing temperature. Consequently, the Stevens-Ban expression, equation (35), is simplified such that the slope of the high temperature portion of fig. 3.23 provides an approximate measure of the temperature coefficient of the ratio k_3/k_p rather than k_3/k_4. This is borne out further by the observation that the apparent ΔH_o value derived from this plot is in close agreement with the difference between the activation energies for the formation (k_3) and non-radiative decay (k_6) of the complex, i.e.

$$\Delta H_o' \simeq \Delta E_3^{\ddagger} - \Delta E_6^{\ddagger} \qquad (39)$$

Once again, there are relatively few systems for which similar data to that of Table 3.20 has been extracted from transient studies alone. However, these results may be compared with the same parameters, obtained from such studies for a series of Cyanonaphthalene (CNNp)/olefin exciplexes[35] and also, the more closely related Anthracene (An)/N,N Dimethylaniline (DMA) system[32]. Such a comparison reveals that there are remarkable similarities in the thermodynamic properties of these systems. In all five cases it is observed that ΔH_o varies only slightly, within the rather narrow region of -38 to -50 $kJ.mol^{-1}$. This variation does not appear to be systematic, although in the case of the tPP/Et_3N system, the experimental ΔH_o value is reproduced remarkably well by Weller's empirical equation[1a]:

$$\begin{aligned} \Delta H_o &= \Delta E_{\frac{1}{2}} - \Delta E_{o,o} + 0.15 \text{ (eV)} \\ &= -0.47 \text{ eV } (= -45.4 \text{ kJ.mol}^{-1}) \end{aligned} \qquad (40)$$

(in which $\Delta E_{\frac{1}{2}}$, the difference between the donor Oxidation Potential and acceptor Reduction Potential = 3.61 V; and the singlet energy, $\Delta E_{o,o}$, as derived from the tPP absorption spectrum = 4.23 eV).

The ΔS_o values observed in each case are relatively large and negative, around -105 $J.deg^{-1}mol^{-1}$, suggesting that all these exciplexes have a quite ordered geometrical structure. Alternatively, these ΔS_o values may reflect, at least in part, the necessity for solvent reorganisation around the exciplex dipole[32].

Further important activation parameters may be derived from Arrhenius plots such as those of figs. 3.24. In particular, the pre-exponential term A_i may be used to provide a value for the entropy of activation ($\Delta S_i^{\ddagger}$) for each process, i, since:

$$A_i = \frac{kT}{h} e^{\frac{\Delta S_i^{\ddagger}}{R}} \qquad (41)$$

Then, combining $\Delta S_i^{\ddagger}$ obtained in this way with $\Delta H_i^{\ddagger}$, the enthalpy of activation at the same temperature, derived according to:

$$\Delta H_i^{\ddagger} = \Delta E_i^{\ddagger} - RT \qquad (42)$$

- a rather complete picture of the processes of exciplex formation and decay can be built up as the activation free energy, $\Delta G_i^{\ddagger}$ can then be obtained from:

$$\Delta G_i^{\ddagger} = \Delta H_i^{\ddagger} - T\Delta S_i^{\ddagger} \qquad (43)$$

The values of these parameters, determined thus for the processes of association and reverse dissociation, within the tPP/Et_3N system at 290 K, are presented as Table 3.21.

Table 3.21

Activation Parameters for the tPP/Et_3N Exciplex at 290 K

A_3	9.92×10^{10}	A_4	2.4×10^{16}
$\Delta S_3^{\ddagger}$ ($J.deg^{-1}mol^{-1}$)	-34.0	$\Delta S_4^{\ddagger}$ ($J.deg^{-1}mol^{-1}$)	69.0
$\Delta H_3^{\ddagger}$ ($kJ.mol^{-1}$)	5.36	$\Delta H_4^{\ddagger}$ ($kJ.mol^{-1}$)	50.2
$\Delta G_3^{\ddagger}$ ($kJ.mol^{-1}$)	15.2	$\Delta G_4^{\ddagger}$ ($kJ.mol^{-1}$)	30.3

These same calculations have been carried out for the systems mentioned above, for which the required data was available in the literature. As was the case with ΔH_o and ΔS_o, the corresponding activation parameters, A, $\Delta H^{\ddagger}_{3,4}$ and $\Delta S^{\ddagger}_{3,4}$ all fall within rather narrow ranges, the values of Table 3.21 being typical for each of these. No simple interpretation of the magnitude or variation of these parameters, within this series of exciplexes, was apparent. However, an examination of the calculated $\Delta G^{\ddagger}_{3,4}$ values for these systems, as set out below in Table 3.22, reveals a number of interesting points:

Table 3.22

Comparison of Free Energy Parameters for A Number of Exciplex-Forming Systems (at 290K)

EXCIPLEX	$-\Delta G_o$ (kcal.mol^{-1})	$\Delta G^{\ddagger}_3$ (kcal.mol^{-1})	$\Delta G^{\ddagger}_4$ (kcal.mol^{-1})
An/DMA [a]	4.77	3.26	8.03
tPP/Et_3N [b]	3.66	3.63	7.23
CNNp/ 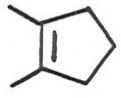 [c]	1.96	3.0	4.96
" /  [c]	1.02	3.05	4.10
" / 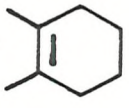 [c]	0.82	3.92	4.74
IND/Et_3N [b]	0.20	4.28	4.48

a) Cyclohexane solution

b) Methylcyclohexane/isopentane 1:1 solution

c) Hexane solution

1) The $\Delta G^{\ddagger}$ values appear to divide these exciplex systems into two separate categories. These may be defined as: a) those exciplexes formed essentially irreversibly (An/DMA and tPP/Et_3N and b) the rapid

equilibrium type systems (including the CNNp/olefin exciplexes and once again, the IND/Et_3N system).

2) Although more data is required here, it does appear that, within these two categories, the observed variation in ΔG_o is accounted for by systematic changes in both $\Delta G_3^{\ddagger}$ and $\Delta G_4^{\ddagger}$. Thus for both the type a) and b) systems, ΔG_o becomes less negative as a result of an increase in $\Delta G_3^{\ddagger}$, together with a decrease in $\Delta G_4^{\ddagger}$. This is made more obvious in the case of the type b) systems if the results for the CNNp/Tetramethylethylene exciplex are disregarded. The validity of the $\Delta G_{3,4}^{\ddagger}$ values recorded for this particular system is thought to be questionable in view of the very large negative ΔS_o value derived in this case (ΔS_o = -146 $J.deg^{-1}mol^{-1}$). This is well outside the narrow range observed for the other systems and may reflect errors in the experimentally determined k_4 and hence $\Delta S_4^{\ddagger}$ values.

3) The variation in ΔG_o with $\Delta G_3^{\ddagger}$ and $\Delta G_4^{\ddagger}$ noted above, is observed to be of the same form for the two types of complex. However, the decrease in $\Delta G_3^{\ddagger}$ is not continuous throughout the whole range of ΔG_o. In fact, the type a) systems appear to have much higher $\Delta G_3^{\ddagger}$ values than would be predicted by comparison with those of the type b) complexes. A similar discontinuity is also apparent in $\Delta G_4^{\ddagger}$ and again the values for the type a) systems are greater than might be expected. It is seen to be the dramatic increase in $\Delta G_4^{\ddagger}$ for these systems which more than outweighs the increase in $\Delta G_3^{\ddagger}$ and results in their observed larger negative values of ΔG_o. In other words, it appears that the type a) exciplexes are formed essentially irreversibly as a consequence of a rather large activation free energy for the reverse dissociation. The smaller $\Delta G_4^{\ddagger}$ values recorded for the rapid equilibrium type b) systems, leads to an increase in the importance of the feedback process in these cases.

The reasons for the observed changes in $\Delta G_{3,4}^{\ddagger}$ are not readily apparent and it might be useful at this point to examine more closely some of the other corresponding activation parameters. In particular, the activation energies $\Delta E_3^{\ddagger}$ and entropies $\Delta S_3^{\ddagger}$ are seen to be informative. The values of these parameters for this range of exciplex-forming systems are presented below as Table 3.23. For all the examples shown, as already noted for the tPP/Et_3N system, the value of $\Delta E_3^{\ddagger}$ is

Table 3.23

Association Energies and Entropies of Activation for a Number of Exciplex-Forming Systems

Exciplex	$\Delta E_3^{\ddagger}$ ($kJ.mol^{-1}$)	$-\Delta S_3$ ($J.deg^{-1}mol^{-1}$)
An/DMA	10.5	19.2
tPP/Et_3N	7.7	33.9
CNNp/ 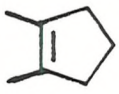	7.5	25.5
" / 	7.5	26.4
" / 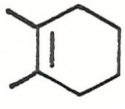	7.5	38.9
IND/Et_3N	8.3	41.8

close to that of the temperature coefficient for viscous flow ($\Delta E_{diff}^{\ddagger}$) for the various solvents used. $\Delta E_3^{\ddagger}$ is thus essentially independent of the exciplex-forming systems themselves. However, the value of the rate constant k_3 for a particular system at a given temperature is often observed to be less than the calculated value of k_{diff}, under those conditions. It would appear from the above that this reduction in k_3 is not due to an increased activation energy, $\Delta E_3^{\ddagger}$. Rather, it is the frequency factor A_3, appearing to have a smaller value than would be predicted on the basis of simple co-diffusion of the two interacting species, which is giving rise to this observation. The strong correlation of k_3 with the pre-exponential A_3 (and hence $\Delta S_3^{\ddagger}$) is demonstrated in Table 3.24. The ratio of the observed A_3 value to the calculated value, A_{diff} is used here to take into account variations in $\Delta E_{diff}^{\ddagger}$ for the different solvent systems.

Thus, as A_3 is reduced and the entropy of activation for the association process ($\Delta S_3^{\ddagger}$) becomes more negative within this series, so k_3 is observed to decrease systematically. The magnitude of $\Delta S_3^{\ddagger}$ provides an indication as to the extent to which freedom of motion of the reaction partners is lost on formation of the transition state. Hence, from the data of Table 3.24, it appears that in order to form 'weaker' complexes (as characterised by smaller k_3 values), there are more stringent requirements as to the nature of the transition state for complex formation.

Table 3.24

A Correlation Between the Photoassociation Rate Constant and the Arrhenius A Factor for that Process, for a Number of Exciplex-Forming Systems

Exciplex	k_3 ($l.mol^{-1}s^{-1}$) ($\times 10^{-9}$)	$\frac{A_3}{A_{diff}}$
CNNp/ 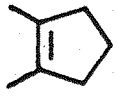	12.0	1.0
" / 	11.0	0.92
An/DMA	7.8	0.66
St/Et_3N	7.4	0.67*
tPP/ "	4.1	0.36
CNNp/ 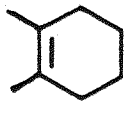	2.4	0.20
IND/Et_3N	1.2	0.14*

* calculated assuming $\Delta E_3^{\ddagger}$ = 1.85 $k_{cal}.mol^{-1}$

Two factors which might be expected to influence the value of $\Delta S_3^{\ddagger}$ for a given system are:

a) The critical distance at which electron transfer can take place;

b) The geometrical constraints placed on the system in order that exciplex formation can occur.

Unfortunately, as usual the nature of the transition state for exciplex formation is rather ill-defined. However, in the case of the CNNp/DMCP exciplex, it has been observed that over a range of solvents of different polarity, $\Delta E_3^{\ddagger}$ was dependent only on the solvent viscosity[21]. This was taken as an indication that charge separation occurs in the transition state only to a small extent. Also, the absolute values of $\Delta S_3^{\ddagger}$ presented in Table 3.23 are relatively small, i.e. less negative than the corresponding values of less than $-83.7\ J.deg^{-1}mol^{-1}$, commonly derived for second order gas phase reactions[55]. Thus, it is suggested that the transition state for the exciplex-forming systems here is a rather loosely bound, non-polar complex formed between the two reaction partners. It is interesting to note that this description corresponds closely to that normally applied to the collisional, encounter complex, thought to be formed prior to formation of the relaxed exciplex state.

3.17 Summary

1) A wide range of compounds, involving the styryl group have been observed to form fluorescent exciplexes with Et_3N.

2) These complexes have been characterised using techniques including:

a) Steady state fluorescence measurements, which yielded the parameters λ_{max}^{E} and k_q^{SS}, in particular.

b) Transient studies of the fluorescence decay times of both exciplex and quenched monomer, from which values for k_q^{TR} and the various individual rate constants were derived.

c) Time resolved fluorescence spectra.

3) The transient effects of diffusion controlled reactions appear to be important for these systems. It is thought that these effects give rise to the observation that, in each case, $k_q^{SS} > k_q^{TR}$.

4) The St/ and tPP/Et_3N exciplexes are found to be formed essentially irreversibly, while IND/Et_3N exhibits the properties of a system at

the rapid equilibrium limit (at room temperature).

5) Solvent effects, both steady state and transient appear to indicate a high degree of CT character within the three complexes studied in detail. Relatively large dipole moments (μ_{CT}) in the region characteristic of aromatic hydrocarbon/amine exciplexes, were recorded.

6) It is thought that it is the polar nature of these exciplexes which makes observation of correlations between the various experimental parameters and the electron accepting ability of the styrene monomers quite straightforward. The electron affinity (E_A), reduction potential ($E_{A^{\ominus}/A}$) and ionisation potential (I_A) were all useful in this context, i.e.

a) λ^E_{max} was found to be linearly related to $E_{A^{\ominus}/A}$ (and hence E_A)

b) For a range of styrenes, a characteristic plot of loge k_q^{SS} vs. I_A was obtained, having a linear portion but levelling off as $k_q^{SS} \rightarrow k_{diff}$ (fig. 3.11).

c) The various individual rate constants show a strong correlation with the electron accepting ability of the styrenes. k_3 was found to decrease, while the rate constants for the processes depleting the exciplex state, k_4, k_5 and k_p all increased systematically as I_A was reduced.

7) Low temperature transient studies were used to provide various thermodynamic and activation parameters, in particular for the processes of association and reverse dissociation. Over a range of systems, a number of points became apparent:

a) The overall kinetic behaviour of a given system appears to be strongly influenced by the activation free energy $\Delta G_4^{\ddagger}$.

b) The activation energy, $\Delta E_3^{\ddagger}$, is often comparable to the activation energy for viscous flow ($\Delta E_{diff}^{\ddagger}$).

c) The activation entropy term, $\Delta S_3^{\ddagger}$, seems to be of crucial importance in determining the value of k_3 for a particular system.

REFERENCES - CHAPTER 3

1a) 'The Exciplex'
M. Gordon and W.R. Ware Ed.,
Academic Press N.Y., 1975

1b) B. Stevens
Adv. Photochem., 8, 161 (1971)

2a) A. Weller,
Pure Appl. Chem., 16, 115 (1968)

2b) W.R. Ware and H.P. Richter
J. Chem. Phys., 48, 1595 (1967)

3. W.R. Ware
Pure Appl. Chem., 23, 635 (1975)

4. R.C. Cookson, S.M. de B. Costa and J. Hudec
J.C.S. Chem. Commun., 753 (1969)

5. R.L. Brentnall, P.M. Crosby and K. Salisbury
J.C.S. Perkin II, 2002 (1977)

6. H. Knibbe, D. Rehm and A. Weller
Z. fur Phys. Chem. (NF) 56, 95 (1967)

7. 'Frontier Molecular Orbitals in Organic Chemical Reactions'
I. Fleming
John Wiley and Sons, London

8. G. Brieglieb
Angew Chem., 76, 326 (1964)

9a) M.J.S. Dewar and N. Trinajstic
J.C.S.(A), 1220 (1971)

9b) M.J.S. Dewar et al
J. Amer. Chem. Soc., 92, 5555 (1970)

10. R.P. Blaunstein and G. Christophorou
Radiation Research Reviews, 3, 69, (1971)

11. N.C. Hush and J.A. Pople
J.C.S. Trans. Faraday Soc., 51, 600 (1955)

12. J.A. Pople
J. Phys. Chem., 61, 6 (1957)

13a) S. Wawzonek and H.A. Laitinen
J. Amer. Chem. Soc., 64, 1765 (1942)

13b) S. Wawzonek and H.A. Laitinen
J. Amer. Chem. Soc., 64, 2365 (1942)

14. P.D. Burrow, J.A. Micheljohn and K.D. Jordan
J. Amer. Chem. Soc., 98, 6392 (1976)

15. H. Knibbe, D. Rehm and A. Weller
Bev. Bunsenges. fur Phys. Chem., 73, 839 (1969)

16. D. Creed, R.A. Caldwell, H. Ohta and D.C. de Marco
J. Amer. Chem. Soc., 99, 277 (1977)

17. C.G. Cureton
Ph.D. Thesis, Southampton (1979)

18. H. Beens, H. Knibbe and A. Weller
J. Chem. Phys., 47, 1183 (1967)

19. E.J.J. Groenen and P.N. Th. van Velzen
Mo. Phys., 35, 19 (1978)

20. R.S. Davidson, A. Lewis and T.D. Whelan
J.C.S. Perkin II, 1280 (1977)

21. D.V. O'Connor and W.R. Ware
J. Amer. Chem. Soc., 101, 121 (1979) and references therein.

22. J. Prochorow
Chem. Phys. Lett., 35, 175 (1975)

23. 'Excited States in Organic Chemistry', chap. 4, p.108
J.A. Barltrop and J.D. Coyle
John Wiley and Sons, 1975

24. C. Coutts
M.Sc. Dissertation, Southampton Univ. (1978).

25. J.P. Maier and D.W. Turner
J.C.S. Faraday II, 196 (1973)

26. M.H. Palmer and S.M.F. Kennedy
J.C.S. Perkin II, 1893 (1974)

27. T. Okada, T. Mori and N. Mataga
Bull. Chem. Soc. Jpn., 49, 3398 (1976)

28a) D.A. Labianca, G.N. Taylor and G.S. Hammond
J. Amer. Chem. Soc., 94, 3679 (1972)

28b) T.R. Evans
J. Amer. Chem. Soc., 93, 2081 (1971)

29. P.A. Wagner and R. Leavitt
J. Amer. Chem. Soc., 95, 3672 (1973)

30. D. Rehm and A. Weller
Isr. J. Chem., 8, 259 (1970)

31. D.V. O'Connor and W.R. Ware
J. Amer. Chem. Soc., 98, 4706 (1976)

32. M.H. Hui and W.R. Ware
J. Amer. Chem. Soc., 98, 4718 (1976)

33. For a discussion on confidence in fluorescence lifetime determinations, see D.M. Rayner, A.E. McKinnon, A.G. Szabo and P.A. Hackett
Can. J. Chem., 54, 3246 (1976)
- and references therein.

34. J. Saltiel, D.E. Townsend, B.D. Watson, P. Shannon and S.L. Finson
J. Amer. Chem. Soc., 99, 884 (1977)

35. W.R. Ware, D. Watt and J.D. Holmes
J. Amer. Chem. Soc., 96, 7853 (1974)

36a) T.J. Chuang, R.J. Cox and K.B. Eisenthal
J. Amer. Chem. Soc., 96, 6828 (1974)

36b) K. Gnadig and K.B. Eisenthal
Chem. Phys. Lett., 46, 339 (1977).

37a) M.H. Hui and W.R. Ware
J. Amer. Chem. Soc., 98, 4712 (1976)

37b) T.L. Nemzek and W.R. Ware
J. Chem. Phys., 62, 477 (1975)

38. 'Photophysics of Aromatic Molecules'
J.B. Birks
Wiley - Interscience, N.Y. (1970)

39. C. Lewis and W.R. Ware
Mol. Photochem., 5, 261 (1973)

40. G.G. Aloisi, U. Mazzucato, J.B. Birks and L. Minuti
J. Amer. Chem. Soc., 99, 6340 (1977)

41. N. Nakashima, N. Mataga and C. Yamanaka
Internat. J. Chem. Kinet., V, 833 (1973)

42. 'Molecular Interactions and Electronic Spectra'
N. Mataga and T. Kubota
Marcel Dekker, N.Y., (1970)

43a) N. Nakashima, N. Mataga, F. Ushio and C. Yamanaka
Z. fur Phys. Chem., (NF), 79, 150 (1972)

43b) D. Creed, P.H. Wine, R.A. Caldwell and L.A. Melton
J. Amer. Chem. Soc., 98, 621 (1976)

44a) S. Masaki, T. Okada, N. Mataga, Y. Sakata and S. Misumi
Bull. Chem. Soc. Jpn., 49, 1277 (1976)

44b) N. Mataga, T. Okada and N. Yamamoto
Chem. Phys. Lett., 1, 119 (1967)

45a) M. Ottolenghi
Acc. Chem. Res., 6, 153 (1973)

45b) H. Masuhara, T. Hino and N. Mataga
J. Chem. Phys., 79, 994 (1975)

46. N. Orbach, R. Potashnik and M. Ottolenghi
J. Chem. Phys., 76, 1133 (1972)

47. 'Organic Molecular Photophysics', vol. 4 (J.B. Birks Ed.)
H. Beens and A. Weller
Wiley-Interscience N.Y. (1975)

48. J. Prochorow and E. Bernard
J. Lumin, 8, 471 (1974)

49. Y. Taniguchi and N. Mataga
Chem. Phys. Lett., 13, 596 (1972)

50. N. Mataga, Y. Taniguchi and Y. Nishima
Bull. Chem. Soc. Jpn., 45, 764 (1972)

51. F.D. Lewis and C.E. Hoyle
J. Amer. Chem. Soc., 99, 3779 (1977)

52. B. Stevens and M.I. Ban
J.C.S. Trans. Faraday. Soc., 60, 1515 (1964)

53a) T. Okada, N. Matsui, H. Oohari, N. Matsumoto and N. Mataga
J. Chem. Phys., 49, 4717 (1968)

53b) S. Murata, H. Kokubun and M. Koizumi
Z. Phys. Chem. (F. am M.), 70, 47 (1970)

54. R.J. McDonald and B.K. Selinger
Mol. Photochem., 3, 99 (1974)

55. 'Physical Chemistry', 2nd. Ed.
G.M. Barrow
McGraw-Hill (1966

56. G.R. Mant
Ph.D (Southampton), 1980

CHAPTER 4

PHOTOCHEMICAL ASPECTS OF EXCIPLEX FORMATION AND DECAY

4.1 Introduction

The intermediacy of exciplexes and excimers has been invoked to explain the course of many bimolecular photochemical reactions[1], and much indirect evidence for their involvement has now been accumulated. However, only for relatively few systems have exciplex fluorescence and photoproduct formation been observable concomitantly[2]. Exciplex emission is observed for a number of styrene derivatives, irradiated in the presence of Et_3N and the spectroscopic studies of the preceding Chapter have allowed characterisation of these complexes. These observations therefore prompted an investigation into the possible role of exciplexes in the formation of the photoproducts which are reported to be formed on irradiation of styrene/amine mixtures[3].

For a number of such systems, it has been shown that photolysis, using the amine as solvent, leads to reduction of the styrene, together with the formation of a styrene/amine adduct. This is exemplified in fig. 4.1, for the IND/Et_3N pair.

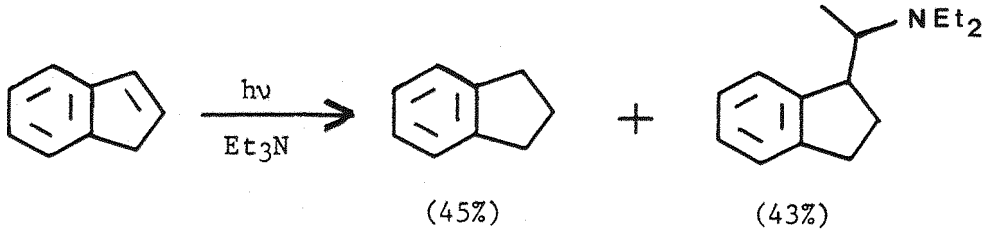

Figure 4.1: Photoproduct Formation in the IND/Et_3N System

This behaviour is similar to that observed for other aromatic hydrocarbon/amine systems such as Anthracene/N,N Dimethylaniline[4] and Stilbene/Et_3N[5].

However, no attempt was made during the course of this work, to repeat the earlier study of de Brito Costa[6]. Instead, the initial aim here was to reproduce as closely as possible the conditions of the photophysical studies but on a rather larger preparative scale. Consequently, dilute solutions of a number of styrenes in cyclohexane were irradiated in the presence of Et_3N at concentrations similar to those chosen for the work described in Chapter 3. In this way, it was ensured that the polarity of the solutions remained low. Also, as outlined in the experimental section, the photolyses were carried out using a filter solution as the cooling medium for the lamp. Thus, again the conditions of the photophysical studies could be reproduced in that absorption by the Et_3N was minimised.

Three styrene/amine pairs were studied under these conditions, namely the IND/, tPP/ and 2-phenylpropene/Et_3N systems. In each case, the styrene monomer was rapidly consumed with the formation of two major photoproducts. These were shown to be the expected products from reduction of and addition to the styrenes. The products were characterised by n.m.r. and mass spectral analysis, in the case of the photoadducts, and by g.l.c. comparison with authentic samples, in the case of the reduced hydrocarbons.

4.2 Photoadduct Formation

a) Indene/Triethylamine

This system was chosen in order to establish whether or not the photoadduct formed under the conditions outlined above was indeed the same as that reported from the earlier study. The rather complex n.m.r. spectrum obtained for the isolated compound here was shown to be comparable to that recorded by de Brito Costa[6]. An assignment was made in that instance, based on an examination of the spectra of adducts formed from various substituted indenes (e.g. the di- and tri-methyl, and deuterated derivatives). Further support for this characterisation of the structure of the IND/Et_3N adduct as that shown in fig. 4.1, is presented here in the form of a mass spectral

analysis. Mass spectral data for the three photoadducts synthesised in this work is given in the experimental section (5.3). The spectrum obtained for the IND/Et_3N adduct is seen to be characteristic of the series, having in particular, a very weak parent ion peak (at m/e = 217 in this case) together with a base peak at m/e = 100, assigned to the triethylamino radical ion ($CH_3-\dot{C}\overset{\oplus}{H}NEt_2$).

b) 2-Phenylpropene/Triethylamine

2-Phenylpropene (2PP) has been shown to form a fluorescent exciplex with Et_3N (see p.54) and it was therefore interesting to observe that here too, preparative scale photolysis allowed isolation of a single photoadduct. By analogy with the other systems studied, the structure of this product is proposed to be:

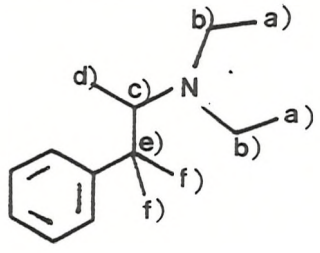

Figure 4.2: The 2PP/Et_3N Photoadduct

It may be noted that, unlike the adducts from the other systems studied, this compound has only a single asymmetric carbon (at position c)). It was hoped that this would result in this compound having a rather more straightforward n.m.r. spectrum than the other adducts. Fortunately, this did prove to be the case, as is illustrated below in fig. 4.4.

The two enantiomeric forms, which may be envisaged for this compound, can be represented as:

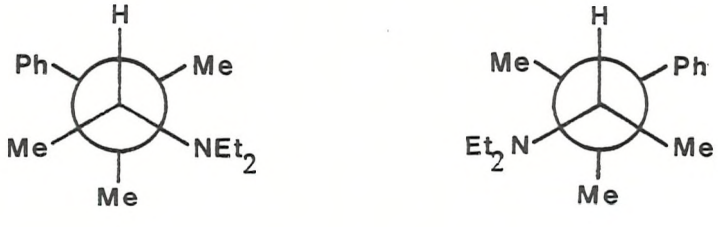

Figure 4.3: The Two Enantiomeric Forms of the 2PP/Et_3N Adduct

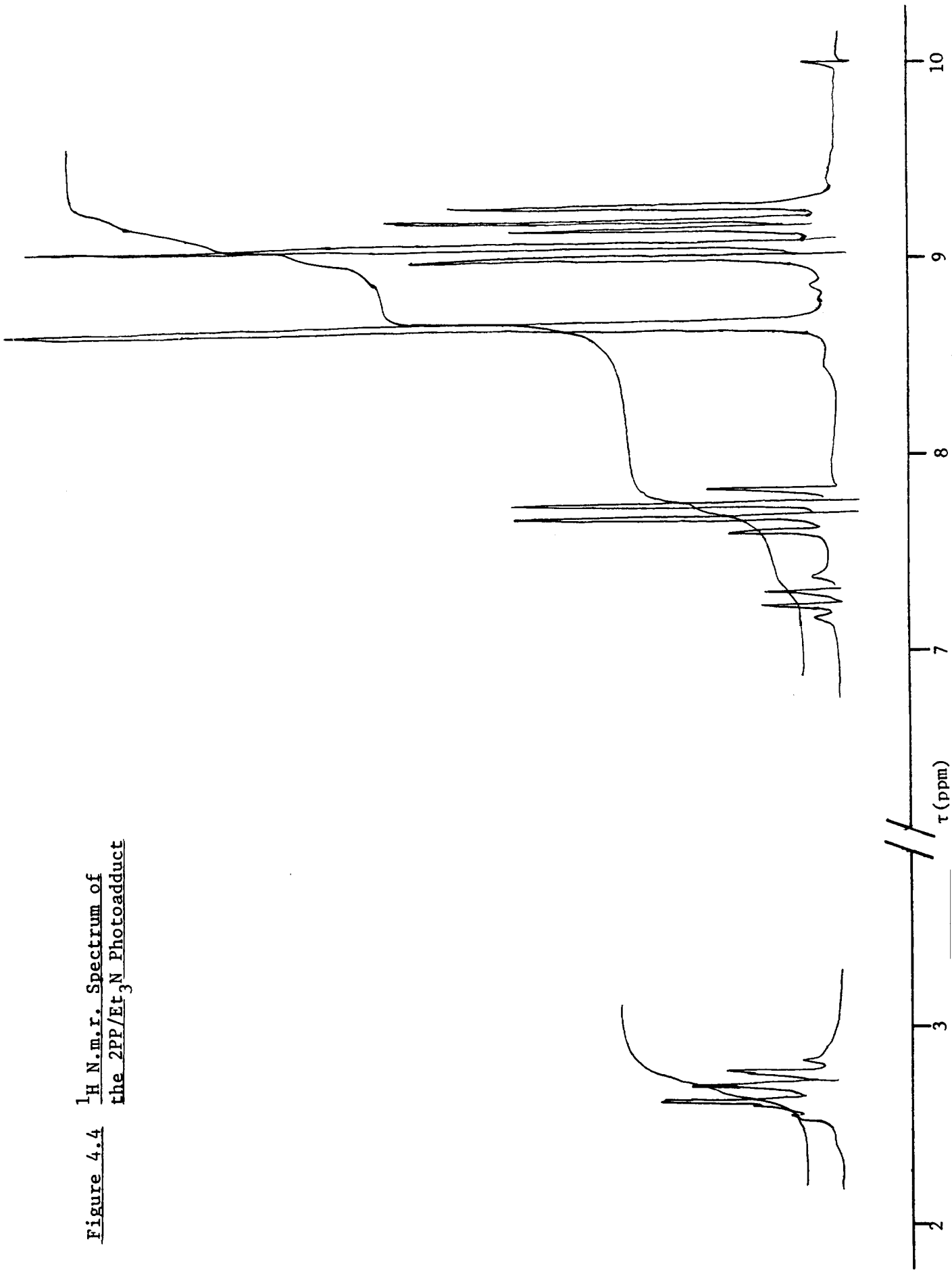

Figure 4.4 ^{1}H N.m.r. Spectrum of the 2PP/Et_3N Photoadduct

However, there is no reason to suggest that formation of either of these should predominate. Hence, it is likely that both forms are present but are in fact inseparable by n.m.r., as would be expected. An assignment of the spectrum of this compound is presented in Table 4.1.

Table 4.1

Assignment of the n.m.r.
Spectrum of the 2PP/Et_3N Photoadduct

Chemical Shift (p.p.m.)	Number of protons	Multiplicity(i)	Assignment(ii)
9.22	3	d	d)
9.05	6	t	a)
8.64	6	s	f)
7.72	4	q	b)
7.28	1	q	c)
2.5-2.9	5	m	Phenyl

(i) A coupling constant, J, of approximately 7Hz was observed for all absorbances other than those due to the phenyl group protons.
(ii) The positions of the various protons are denoted according to fig. 4.2.

c) Trans 1-Phenylprop-1-ene/Triethylamine

As with the other systems studied, it was observed that tPP, irradiated in cyclohexane solution, in the presence of Et_3N, afforded a single addition product, together with the reduced hydrocarbon (1-phenylpropane in this case). N.m.r. analysis of the photoadduct produced the spectrum presented as fig. 4.5. The rather complex nature of this spectrum is thought to be due to the presence of two chiral centres within the molecule, at positions c) and e).

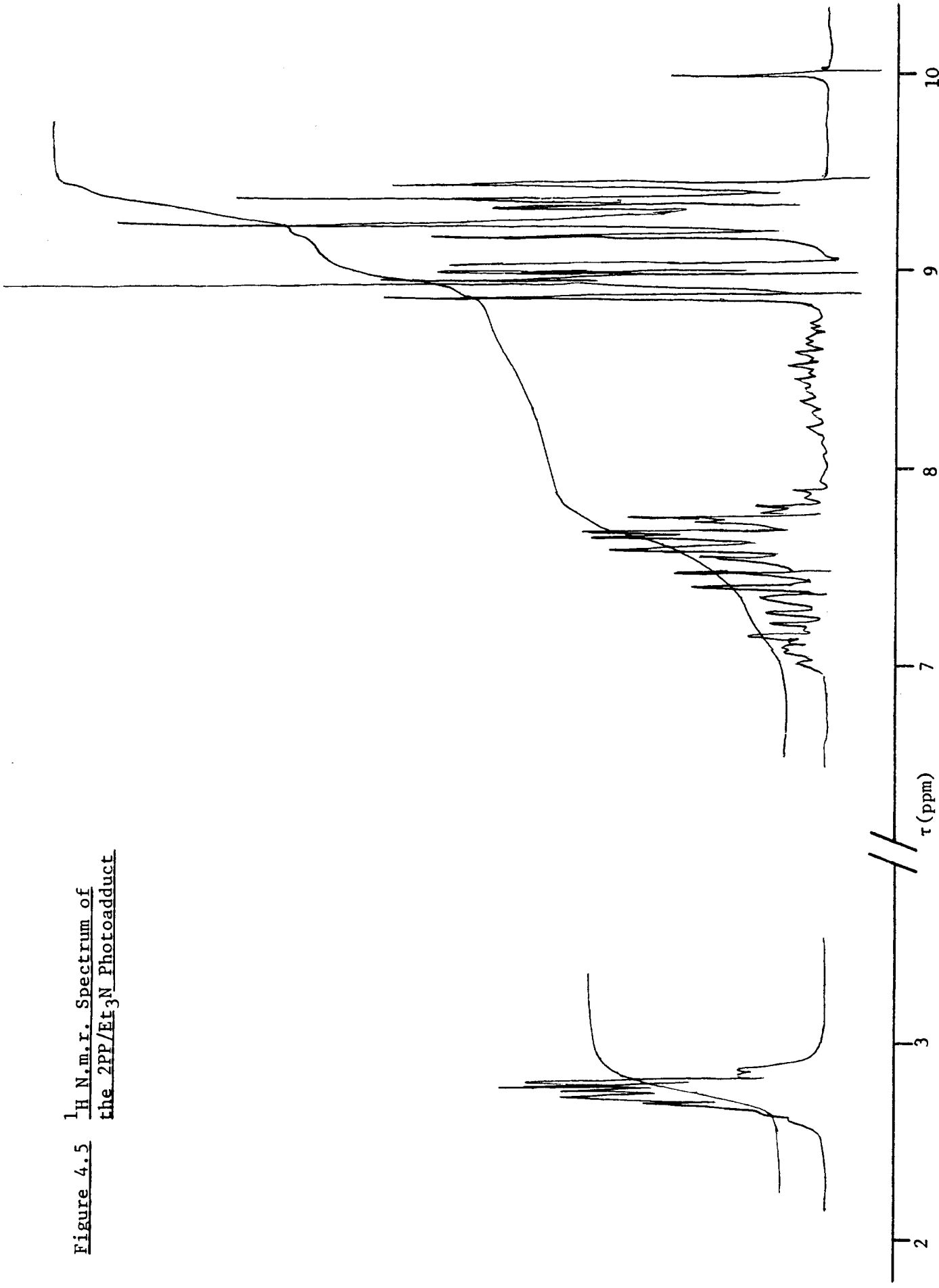

Figure 4.5 ^{1}H N.m.r. Spectrum of the 2PP/Et_3N Photoadduct

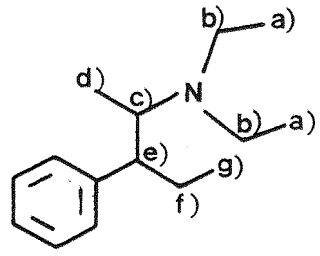

Figure 4.6: The tPP/Et_3N Photoadduct

These will give rise to two pairs of diastereoisomeric forms of this compound (A and B below).

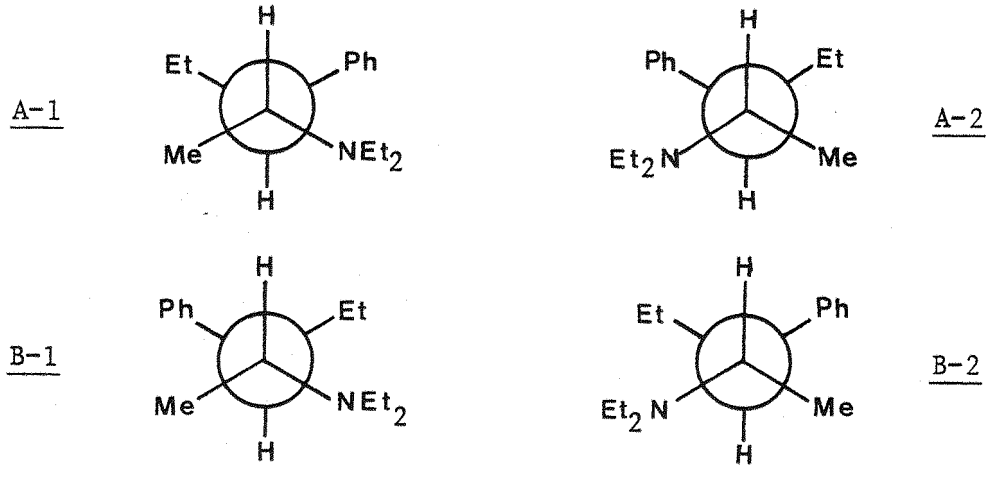

Figure 4.7: The Diastereoisomeric Forms of the tPP/Et_3N Adduct

By analogy with the 2PP/Et_3N adduct, it may be expected that each enantiomeric pair will possess the same n.m.r. spectrum. In other words, the spectra of A-1 and A-2 will be superimposable, as will those of B-1 and B-2. However, from fig. 4.7, it may be noted that the positions of the substituent groups at C-c) relative, in particular to the phenyl group at C-e) are rather different for the two pairs of

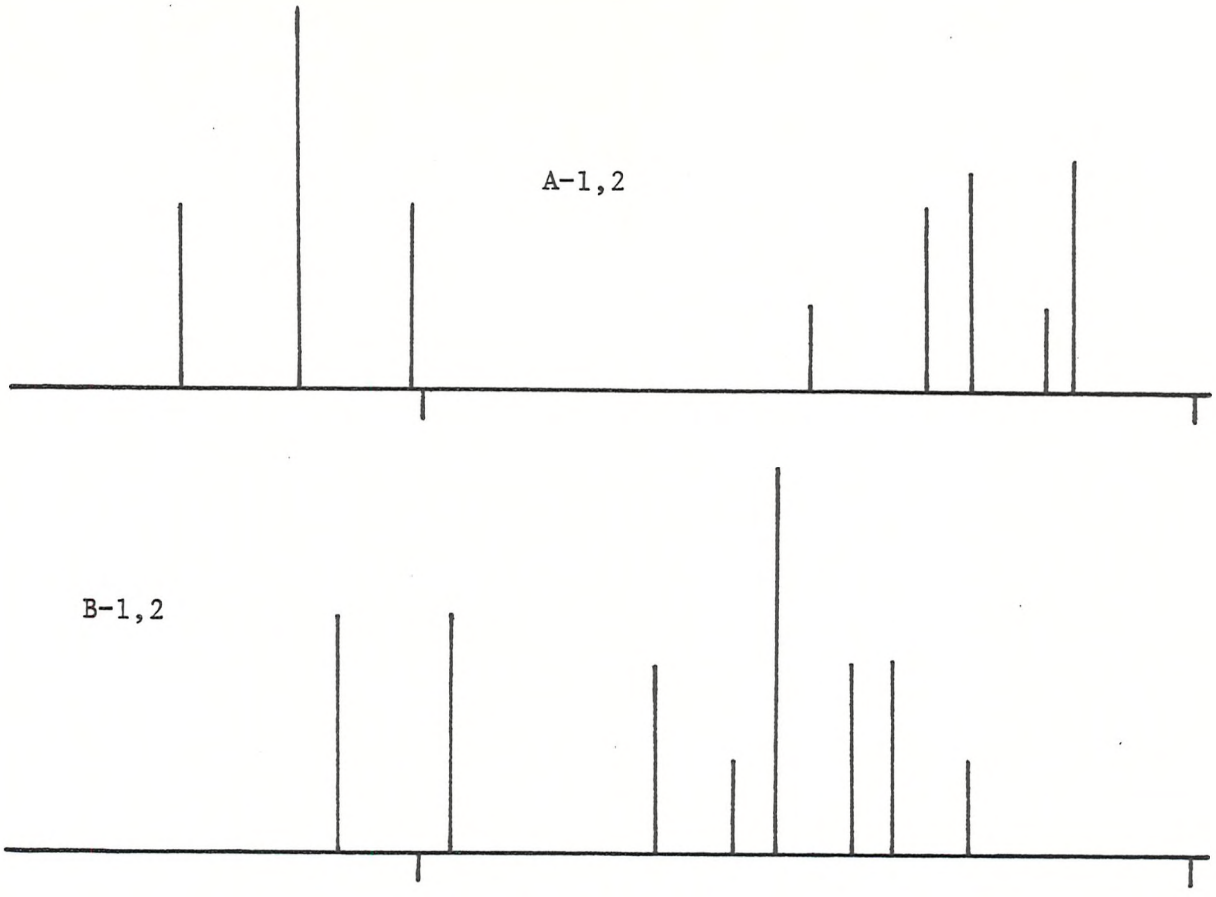

Fig. 4.8

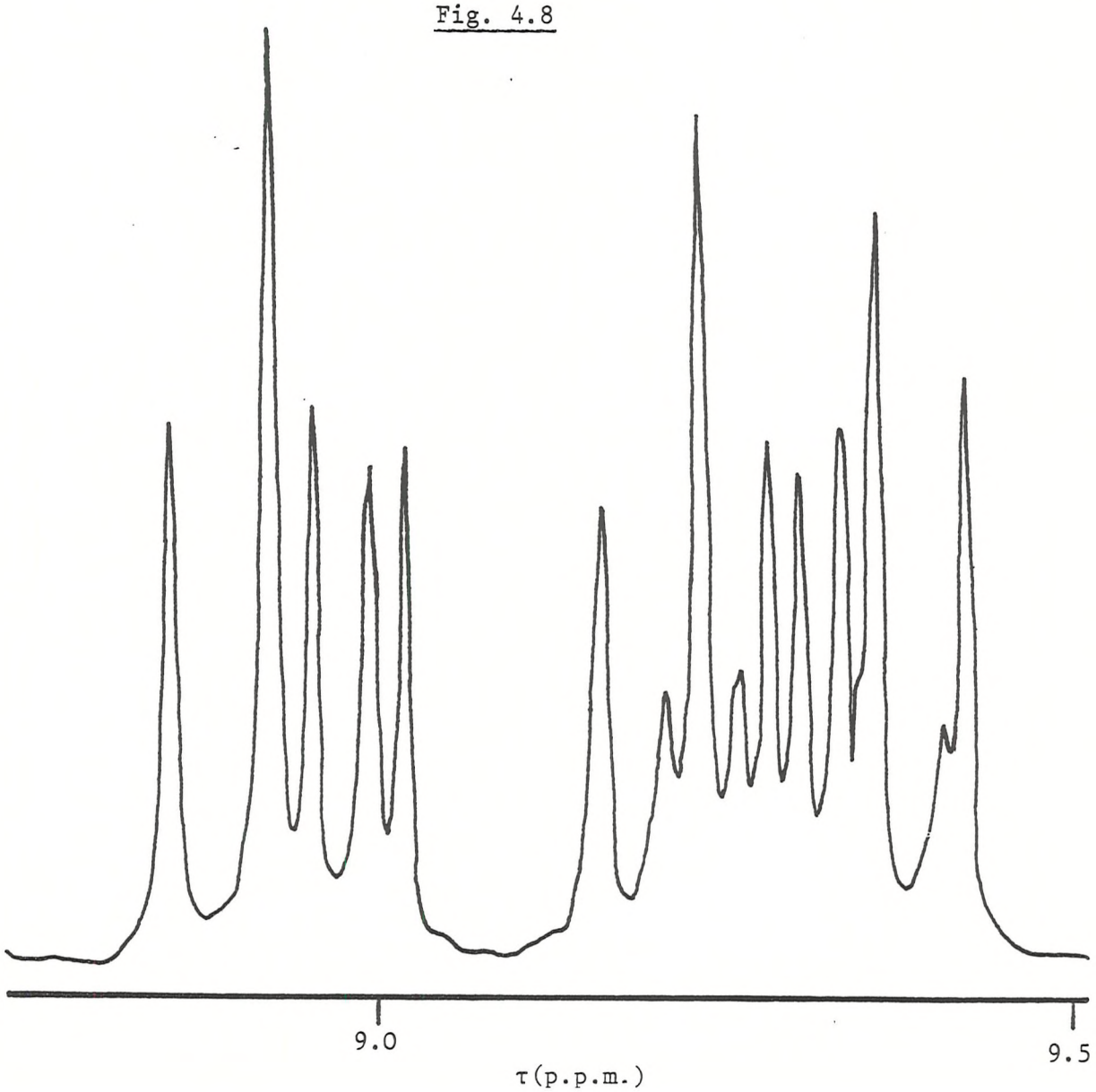

diastereoisomers. Thus, it would be expected that the deshielding influence of the phenyl ring on the protons in close proximity to this group, will cause the absorptions due to these protons to be shifted downfield. On this basis, a breakdown of the observed structure in the region 8.7-9.5 p.p.m. into contributions from the spectra of the two diastereoisomeric pairs, is suggested. An expansion of this region of the spectrum, together with a schematic representation of the proposed assignments, is presented in fig. 4.8. As for the remainder of the spectrum, the splitting patterns are rather complex but the chemical shift and integration of the various absorbances are consistent with the proposed structure.

4.3 The Mechanism of Photoproduct Formation

Having thus established that photoproduct formation is indeed observable for a number of styrene/Et_3N systems, under these conditions, the possible mechanisms by which these products are formed may be examined. Two principal mechanisms suggest themselves here, namely:

1) A direct, free radical H-atom abstraction process, or

2) An electron transfer/proton transfer mechanism, involving the exciplex as an intermediate.

For the former, it can be seen that abstraction of a hydrogen atom from the α-position of the amine by the excited styrene, would lead to formation of a pair of radicals, as is illustrated in fig. 4.9 below.

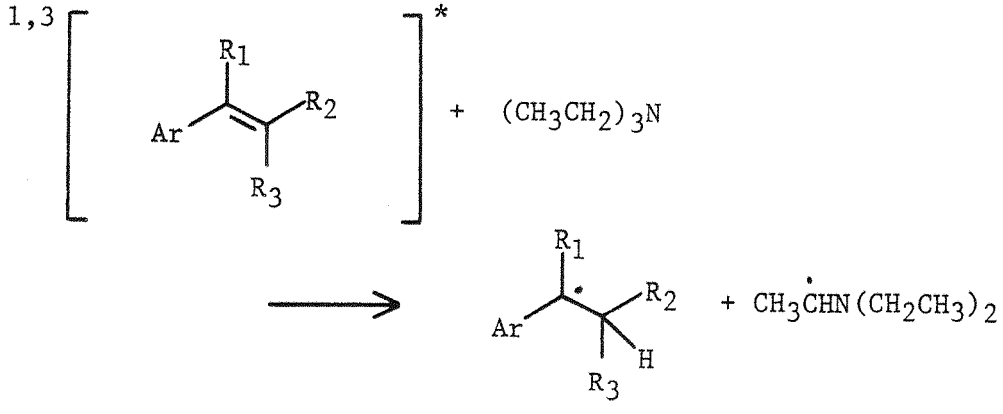

Figure 4.9: Radical Pair Formation via H-atom Abstraction

These radicals could then couple to form the observed photoadduct or alternatively, a further H-atom abstraction by the styryl radical

would lead to formation of the reduced hydrocarbon. This situation would then be analogous to that observed in the photoreduction of ketones by alcohols[7], which is thought to proceed via such a radical abstraction process.

However, in the case of the styrene/Et_3N systems, the observation of exciplex fluorescence obviously suggests that the alternative mechanism noted above may well be a valid proposition here. In this case, a general scheme for formation of the observed photoproducts may be represented as follows:

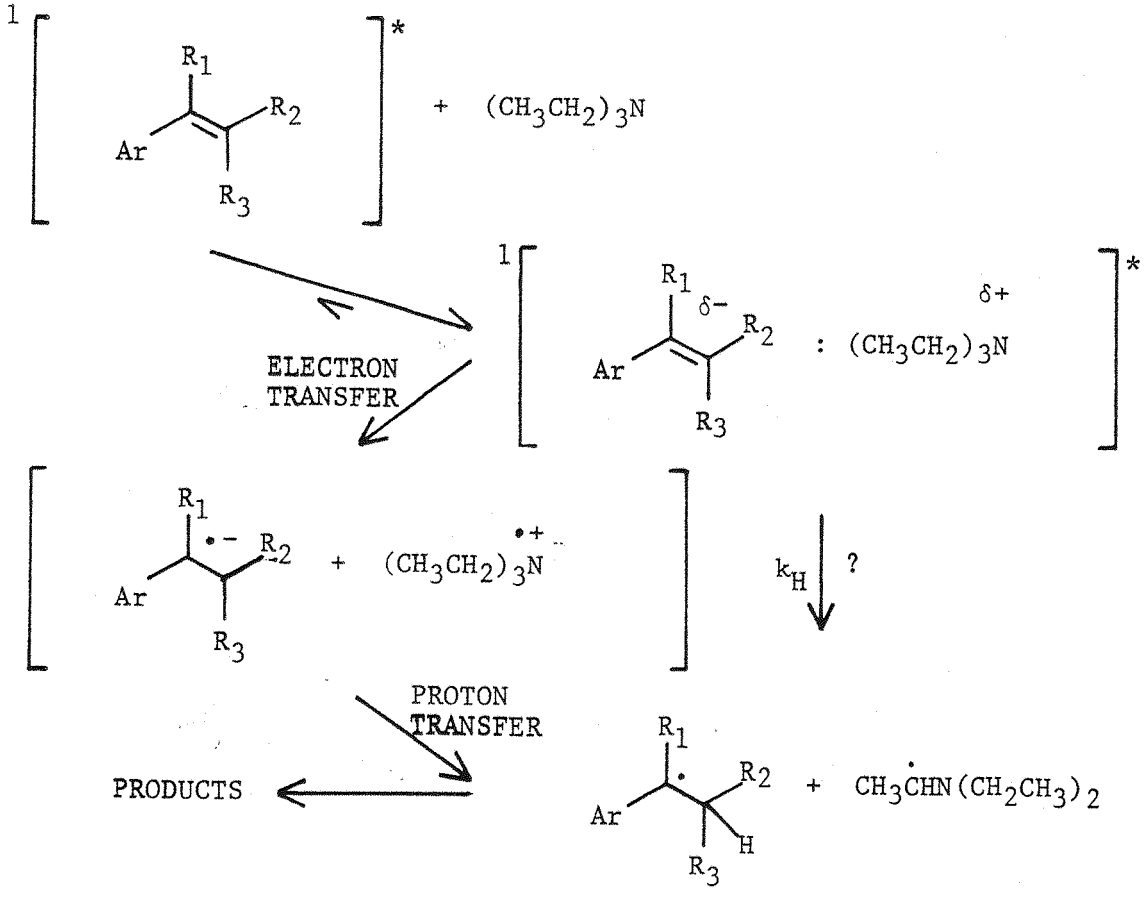

Figure 4.10: Scheme Depicting Product Formation via an Exciplex

Here again, the styryl/aminoalkyl radical pair would be formed prior to coupling or H-atom abstraction (from either an amine or solvent molecule) to yield the observed products. However, a rather different

pathway leading to this radical pair is suggested here, involving electron transfer via the exciplex intermediate. Such an electron transfer would give rise initially to a solvated radical ion pair, as shown in fig. 4.10. A subsequent proton transfer from the aminoalkyl radical cation to the styryl radical anion would then be required to form the corresponding pair of radicals.

This same mechanism has been proposed in the case of the closely related Stilbene/amine exciplex systems[5], although in that case, no photoproduct formation was observable with simple tertiary amines in nonpolar solvents. However, it was noted that for those systems, photoproducts due to addition to and reduction of the aromatic hydrocarbon were formed as the solvent polarity was increased (such that ε, the solvent dielectric constant was ≥ 4). Also, the quantum yield of product formation (Φ_{PROD}) was found to increase with ε at the expense of the exciplex fluorescence quantum yield. This increase in Φ_{PROD} was attributed to an increase in the probability of forming a radical ion pair (via electron transfer within the exciplex) at higher solvent polarities. From this it was inferred that:

a) Electron transfer to form the pair of radical ions must occur prior to formation of the radical pair; and

b) This full electron transfer is apparently necessary in order to render the α-C-H bond of the amine sufficiently acidic for the subsequent proton transfer to proceed.

Further support for product formation via radical ion intermediates was obtained from the Stilbene/Diisopropylmethylamine system. In this case, the exclusive addition product was found to be that arising from cleavage of the methyl α-C-H bond. This observation is compatible with proton transfer from the aminoalkyl radical cation but not a free radical abstraction mechanism. For the latter, it would be expected that abstraction of the H atoms attached to the tertiary α-carbons of the isopropyl groups would be preferred.

Radical and radical ion intermediates in exciplex decay, such as those proposed above, have been detected spectroscopically, e.g. using the techniques of CIDNP[8], CIDEP[9] and photoconductivity[10]. However, these studies have been confined to solvents of moderate to high polarity. In fact, it is interesting to note that, to date, photoionisation via exciplexes in nonpolar solvents has only been

observable for systems in which the radical ions may be generated biphotonically[11]. Calculations indicate that there is a large free energy difference between the dissociated radical ions ($^2A_s^{\cdot\ominus} + {}^2D_s^{\cdot\oplus}$) and the solvated radical ion pair ($^2A_s^{\cdot\ominus} \ldots {}^2D_s^{\cdot\oplus}$), which is assumed to be formed prior to the dissociation. Even for moderately polar solvents, having $\varepsilon \geqslant 10$, this energy difference is thought to be of the order of 0.2 eV, i.e. considerably larger than kT, at room temperature. Hence, it is expected that there will be a substantial energy barrier to formation of the dissociated radical ions in non-polar solvents. Thus if, as suggested by Lewis[5], radical ion pair formation is a necessary prerequisite for photoproduct formation, it is not too surprising that no such products were observed for the Stilbene/amine systems in nonpolar solvents. However, this limitation does not seem to apply to the styrene/Et_3N systems studied here, as photoproduct formation is readily observable for these systems in cyclohexane solution. Therefore it is suggested that in this case, formation of the required radical pair, as illustrated in fig. 4.10, is not dependent on formation of a dissociated radical ion pair.

The possibility of decay of the styrene/Et_3N exciplexes and subsequent photoproduct formation via the production of solvated radical ion pairs is not ruled out here. However, an alternative route to the styryl/aminoalkyl radical pair may be suggested. This would involve a proton transfer direct from the exciplex, as denoted by the rate constant, k_H in fig. 4.10. Such a process may well be feasible for these systems, where there is a high degree of CT character within the complexes. Also, as noted already (Section 3.4), there appears to be little perturbation of the interacting molecular orbitals of the reaction partners on exciplex formation. Thus, it may be that the distinction here between 'exciplex' and 'solvated radical ion pair' is a rather fine one; or in other words, it may be that there is only a relatively shallow energy barrier to formation of the latter. If this is so, then it is perhaps more appropriate in this case to regard the reactivity here as being analogous to the process of photoreduction of ketones by amines. Cohen suggests[7] that this process may still be thought of as occurring via an abstraction mechanism, but one in which "a substantial part of the

barrier to abstraction of hydrogen is overcome in the initial, efficient charge transfer interaction."

It may be of interest at this point to mention briefly calculations which have been made by Beens and Weller[12], in an attempt to characterise the geometrical structure of aromatic hydrocarbon/aromatic amine exciplexes. These studies provide some insight into the process of radical ion pair formation via the exciplex for these systems. In particular, it has been suggested that, for systems such as these which have a high degree of CT character, the equilibrium configuration for the exciplex will be that for which the energy of the CT state is minimised. Thus, the exciplex may be expected to adopt a geometry which corresponds to a maximum in the Coulombic energy of the system, while the contribution to exciplex stabilisation due to intermolecular overlap will tend to be rather small and of little importance in determining the complex equilibrium configuration.

These same comments are likely to apply to the styrene/Et_3N exciplexes also. Indeed the effects of intermolecular overlap may be expected to be even less important in stabilisation of these complexes for which there is no possibility of $\pi-\pi$ interactions occurring between the two reactants. Hence, it may be possible to suggest a preferred geometry for these exciplexes from an examination of the charge distributions within the radical anion of the aromatic hydrocarbon and the triethylamino radical cation. For the latter it is assumed that the net positive charge is essentially localised on the tertiary nitrogen atom, while in the case of the styryl radical anions, delocalisation of the charge would be expected. The calculated charge distribution within the tPP radical anion is in fact available from the literature[13], an INDO technique having suggested that this distribution takes the form:

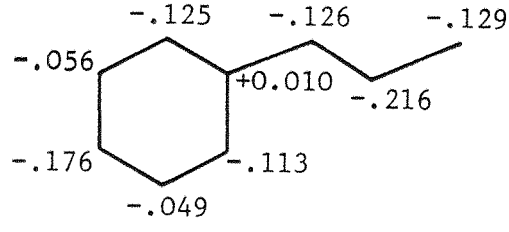

Figure 4.11: The Calculated Charge Distribution Within The tPP Radical Anion

From this it can be seen that the point charge density at the β carbon atom (C-8) of the side chain appears to be somewhat larger than that for any of the other positions. This therefore suggests that the equilibrium configuration for the tPP/Et_3N exciplex may be one in which the triethylamino-nitrogen is situated adjacent to the side chain of the styryl moiety.

Weller has carried the study of exciplex geometry further, in attempting to calculate the effects of intermolecular motion and solvent polarity on the free energy of aromatic hydrocarbon/amine exciplexes in the CT state. From this work, it has been suggested that a displacement of as little as 4Å in a direction perpendicular to the principal Z-axis of the complex will result in the formation of a solvated radical ion pair. The free energy barrier to such a displacement is calculated to be relatively low, even for solvents of low to moderate polarity ($\varepsilon \simeq 2$-10). Hence, it may be that, as postulated above for the styrene/Et_3N systems, conversion of the exciplex into a solvated radical ion pair is a relatively facile process when the exciplex has a high degree of CT character.

4.4 The Kinetics of Photoproduct Formation

As indicated already, the intermediacy of exciplexes has been proposed to account for photoproduct formation in a wide variety of systems[1]. However, in the main, only indirect evidence for their involvement has been presented, based on:

a) The observation of excited state quenching rates which correlate with donor or acceptor properties of the reaction partners[14].

b) Trapping experiments[2a),15].

c) The negative temperature dependence of quantum yields of product formation[2b),16].

d) Deuterium isotope effects[17].

Unfortunately, none of the above is in fact able to distinguish whether the exciplex is present as a true reaction intermediate or merely provides a competing pathway for deactivation of the excited monomer.

The most direct approach to making this distinction, which is of rather central importance to any study of exciplex photochemistry, would appear to be the technique of exciplex quenching. This technique,

as suggested by Caldwell[18], entails the discovery of some compound, which will quench at the same rate, both the exciplex fluorescence and photoproduct formation in a given system, without interfering in any way with the monomer. As may be imagined, this is by no means straightforward, however, such an investigation was attempted for the styrene/Et_3N exciplex systems, as outlined below.

A number of styrenes were irradiated, with Et_3N in cyclohexane solution, using an optical bench arrangement set up and calibrated as described briefly in the experimental section (5.3). Once again, the conditions under which the photolyses were carried out were chosen to reproduce as closely as possible those of the photophysical studies. It was of particular importance in this case to use relatively low concentrations of the styrenes throughout (typically 10^{-2} - 10^{-3} M) in order to minimise the possibility of polymer formation. The Et_3N-sensitised photopolymerisation of St itself has been reported in the literature[19] but monomer concentrations in excess of 3M were employed in that case. It was found here that photoproduct formation was readily observable, in the absence of photopolymerisation, in the case of the dilute IND/ and tPP/Et_3N systems in degassed cyclohexane. On irradiation at 280-290 nm., over a period of 2-3 hours, the percentage conversion of the styrenes was found to be in the preferred region of 5-10%. However, under these same conditions, very little photoproduct formation was observed in the case of the St/Et_3N system. This observation may be compared with the relatively low chemical yield of photoproduct formation of only 7%, reported by de Brito Costa[6] from photolysis of the St/Et_3N pair. This in turn, may be contrasted with the corresponding yield of 88% observed in the case of the IND/Et_3N system. From the kinetic studies of the previous Chapter, it has been shown that the value of the sum of rate constants depleting the exciplex state ($k_4 + k_p$) increases within the series St/ <tPP/<IND/Et_3N. Thus it appeared that, qualitatively at least, a correlation could be established between the photochemical reactivity of the styrene/Et_3N pairs and the stability of the exciplexes which have been shown to be formed on irradiation of these systems. However, in order to substantiate this point, a more detailed examination of the process of photoproduct formation was required. In particular, it was hoped that an investigation of the quantum yields of both product formation and monomer disappearance, in the presence of Et_3N, might complement

and further extend the kinetic studies of Chapter 3.

4.4.1 Indene/Triethylamine

The quantum yields of photoadduct Formation (Φ_A) and IND disappearance (Φ_{-IND}) were measured, over a range of quencher concentrations. The results obtained are presented below as Table 4.2 and as would be expected, the values of both these quantum yields were observed to increase with $[Et_3N]$.

Table 4.2

The Quantum Yields of Photoadduct Formation and Monomer Disappearance as a Function of Quencher Concentration for the IND/Et_3N System

$[Et_3N]$ (M)	Φ_{-IND}	Φ_A
0.05	0.16	0.08(5)
0.1	0.22	0.12
0.15	0.34	0.12(6)
0.2	0.35	0.13(8)

The standard exciplex kinetic scheme (presented as fig. 3.11) may now be used to derive expressions for the expected dependence of Φ_{-IND} and Φ_A on the quencher concentration, if it is assumed that photoproduct formation is occurring via the exciplex. If this is so and the exciplex is indeed a necessary reaction intermediate, then in the case of Φ_{-IND}, this expression takes the form:

$$\Phi_{-IND} = \frac{k_3[Et_3N]}{k_1 + k_2 + \frac{k_3 k_p [Et_3N]}{(k_4 + k_p)}} \cdot \frac{k_{PROD}}{(k_4 + k_p)} \qquad (1)$$

(where k_{PROD} denotes the rate constant for the exciplex decay process(es) leading to photoproduct formation). Equation (1) may be inverted to give:

$$(\Phi_{-IND})^{-1} = \frac{(k_1 + k_2)(k_4 + k_p)}{k_3 . k_{PROD} [Et_3N]} + \frac{k_p}{k_{PROD}} \qquad (2)$$

- and hence a plot of $(\Phi_{-IND})^{-1}$ vs. $[Et_3N]^{-1}$ is predicted to be linear. Fig. 4.12 illustrates the observation that the data of Table 4.2 plotted in this form does adhere reasonably well to a straight line. From equation (2) it can be seen that it should be possible to derive a value for the required rate constant, k_{PROD}, from both the slope and intercept of such a plot. In this case, it is found that the k_{PROD} values obtained thus are reasonably self-consistent and provide a value for the IND/Et_3N system of:

$$k_{PROD} = 4.2(\pm 0.9) \times 10^8 \ s^{-1}$$

The fact that there is this degree of consistency provides strong, albeit circumstantial evidence in support of the proposed mechanism of photoproduct formation via the exciplex in this case.

Having thus derived a value for the rate constant k_{PROD}, a more complete picture of the kinetics of exciplex decay within this system emerges. The spectroscopic studies of the previous Chapter provided values for the IND/Et_3N system of:

i) The exciplex radiative rate constant $k_5 = 1.9 \times 10^7 \ s^{-1}$; and

ii) k_p, the sum of the rate constants for the processes (other than reverse dissociation) depleting the exciplex state ($k_p = 8.0 \times 10^8 \ s^{-1}$).

It is interesting to note that the sum ($k_{PROD} + k_5$) fails to account completely for the observed value of k_p. From this, it would appear that there is at least one further non-radiative relaxation process by which the IND/Et_3N exciplex may revert to the ground state. As is the case with the primarily excited monomer, exciplex decay may be possible via both intersystem crossing and/or internal conversion processes. Although it is not clear whether either of these predominates in this case, it is apparent that the efficiency of this extra non-radiative decay route, as given by:

$$q_{NR} = \frac{k_p - (k_{PROD} + k_5)}{k_p} \qquad (3)$$

- is relatively high for the IND/Et_3N exciplex ($q_{NR} = 0.45$). This is especially notable when the comparison is made with the corresponding quantum efficiency term for the exciplex radiative decay ($q_5 = 0.02$ only).

So far, no reference has been made to the quantum yield for photoreduction (Φ_R) of IND under these conditions. Formation of the

Figure 4.12 Plots of Φ_{-IND}^{-1} and Φ_A^{-1} vs. Et_3N^{-1} for the IND/Et_3N System

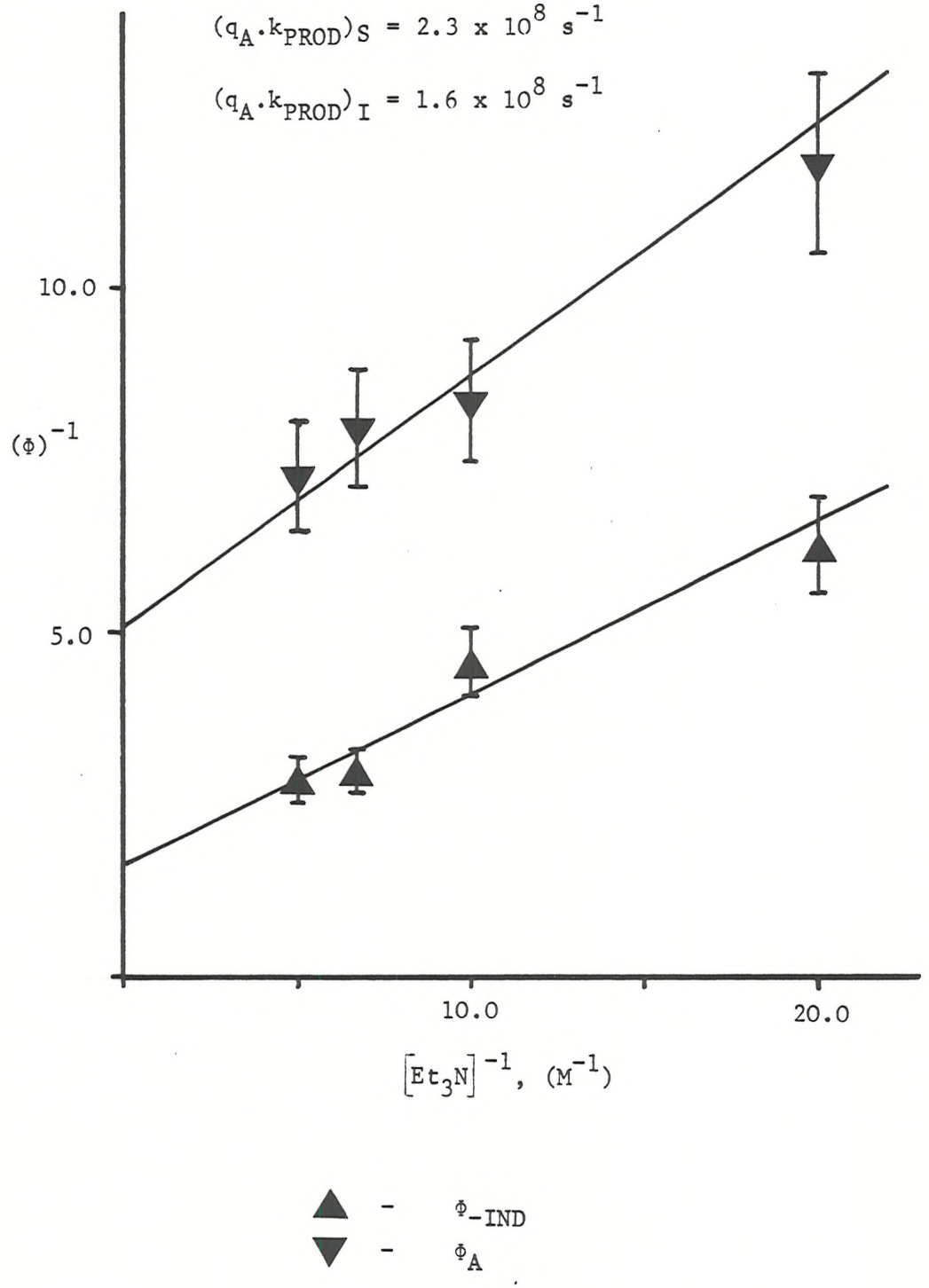

reduced hydrocarbon, Indane, was in fact observable over the range of quencher concentrations studied. Unfortunately though, Φ_R was difficult to quantify accurately as, under the conditions of the analytical g.l.c. technique used to monitor the reactions, the trace due to the Indane tended to be obscured by the solvent peak. However as indicated in Table 4.2 the corresponding values of Φ_A, the quantum yield of formation of the IND/Et_3N photoadduct were obtainable using this technique. If it is assumed that the sum ($\Phi_A + \Phi_R$) accounts for the total value of Φ_{-IND} at each quencher concentration, then an expression for Φ_A as a function of $[Et_3N]$ may be derived, which is equivalent to equation (2) above. The only difference here is that the expression for Φ_A involves, in addition, a quantum efficiency term, q_A. This denotes the probability with which the product-forming exciplex decay process gives rise to a photoadduct molecule. Hence, both the slope and intercept of a plot of Φ_A^{-1} vs. $[Et_3N]^{-1}$ should yield a value for the product ($q_A.k_{PROD}$). The Φ_A data of Table 4.2 is plotted in this form in fig. 4.12 and as was the case with Φ_{-IND} a reasonable linear relationship is apparent here. The values derived for ($q_A.k_{PROD}$) from this plot are also given in fig. 4.12 and again, they are seen to be reasonably self-consistent. From these, a value may be derived for the parameter q_A of 0.47 ($\pm$0.08). Thus, it would appear that approximately half of those complexes which decay to form products do so to produce the photoadduct, the other 50% presumably giving rise to the reduced hydrocarbon. Once again, it is interesting to note that a close comparison is revealed between the results of such a study of exciplex decay kinetics and the chemical yield values obtained by de Brito Costa[6] for this system. As indicated in fig. 4.1 , from this earlier work, yields of 45% and 43% were reported for the formation of Indane and the IND/Et_3N adduct, respectively.

4.4.2 Trans 1-Phenylprop-1-ene/Triethylamine

a) Geometric Isomerisation

The results of a similar study of the kinetics of photoproduct formation within the tPP/Et_3N system proved to be somewhat less straightforward to analyse than the above. This appears to be due to the fact that tPP monomer itself exhibits photochemical reactivity,

in the absence of any quencher. This reactivity takes the form of a geometrical isomerisation to produce cis Phenylprop-1-ene (cPP). During the course of this work, a value for the quantum yield of formation of cPP on irradiation of the trans isomer at 290 nm. in degassed cyclohexane, was measured as:

$$\Phi^{o}_{cPP} = 0.24\ (\pm 0.01)$$

- in good agreement with values reported in the literature[20]. From this, a value was derived for k^{M}_{cPP}, the rate constant for formation of the cis isomer via the tPP monomer, using the expression:

$$k^{M}_{cPP} = \frac{\Phi^{o}_{cPP}}{\tau^{o}_{F}} \qquad (4)$$

(where τ^{o}_{F} is the unquenched monomer fluorescence lifetime) and in this case it was found that:

$$k^{M}_{cPP} = 1.95 \times 10^{7}\ s^{-1}$$

Although the photoisomerisation of the tPP $\leftrightarrow$ cPP pair has been studied quite extensively[20,21], the more precise mechanistic details of this process are still open to question. In particular, it is still unclear as to the nature of the excited state(s) involved in the isomerisation. However, this aspect is discussed in more detail in Section 2.4 and it may be sufficient at this point to note that both singlet and triplet pathways are thought to be available for this process.

On the addition of successive amounts of the quencher, Et_3N, to dilute solutions of tPP, the value of Φ_{cPP} was observed to decrease as would be expected. This is illustrated in Table 4.3 and the dependence of Φ_{cPP} on quencher concentration is shown in fig. 4.13 in the form of a plot of $\Phi^{o}_{cPP}/\Phi_{cPP}$ vs. $[Et_3N]$. The comparison is made here with the observed fluorescence quenching efficiency for this system and as can be seen, the value of Φ_{cPP} is not reduced as rapidly as would be predicted from a simple Stern-Volmer quenching mechanism. In fact, the plot reproduced as fig. 4.13a) is apparently non-linear, an observation which, when taken with its shallow slope, strongly suggests

that for this system, it is possible for isomerisation of the tPP monomer to occur via the tPP/Et_3N exciplex. If this is the case, then the behaviour of this system is analogous to that reported by Aloisi[22] for a series of Styryl Naphthalene/N,N Diethylaniline exciplexes.

Table 4.3

The Observed Variation of Φ_{cPP} with Quencher Concentration and Calculated Contributions due to Isomerisation via the Monomer and Exciplex for the tPP/Et_3N System

$[Et_3N]$ (M)	Φ_{cPP}	Φ^{M}_{cPP}	Φ^{E}_{cPP}
0	2.24	0.24	-
0.02	0.16	0.11	0.047
0.03	0.13(5)	0.088	0.056
0.04	0.13	0.073	0.062
0.05	0.12(6)	0.062	0.066

It can be seen that, if photoisomerisation is invoked as a possible decay pathway within the exciplex, then the standard exciplex kinetic scheme may be used to derive an expression from the expected dependence of Φ_{cPP} on $[Et_3N]$. This expression involves the sum of the contributions to Φ_{cPP} due to the isomerisation routes via both the monomer and exciplex and takes the form:

$$\Phi_{cPP} = \frac{1}{k_1 + k_2 + \frac{k_3 k_p [Et_3N]}{(k_4 + k_p)}} \left[k^{M}_{cPP} + \frac{k_3 k^{E}_{cPP} [Et_3N]}{(k_4 + k_p)} \right] \qquad (5)$$

(where k^{E}_{cPP} represents the rate constant for cPP formation via the exciplex). Thus, from an examination of equations (4) and (5), it can be seen that a plot of $\Phi^{o}_{cPP}/\Phi_{cPP}$ vs. $[Et_3N]$ would not be expected to be linear. However, as pointed out in ref. 23, it should be possible to analyse the quantum yield data for this and similar systems in such a way as to enable a value for the rate constant for isomerisation via the exciplex (k^{E}_{cPP} in this case) to be derived. The treatment

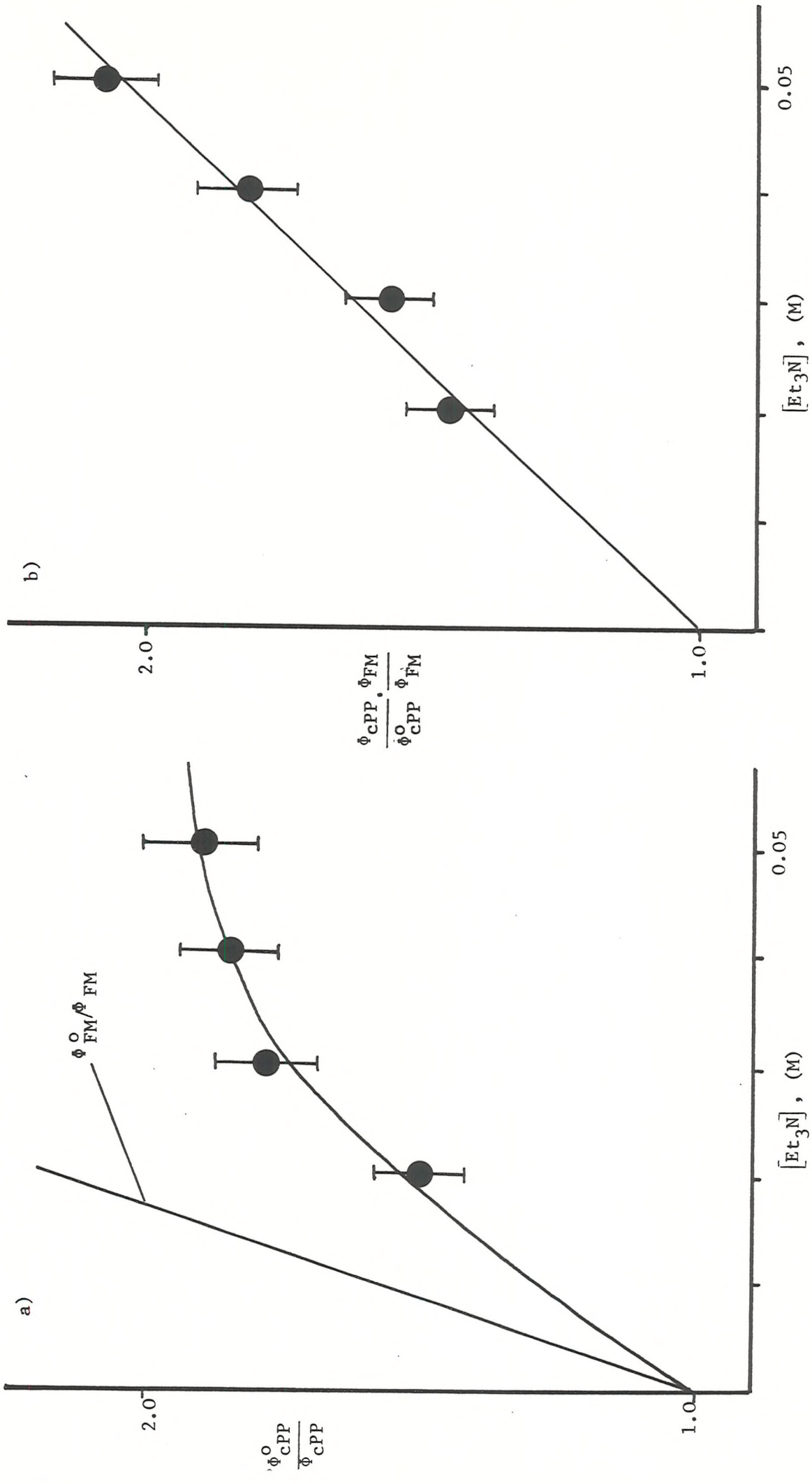

Figure 4.13 An Analysis of the Effect of Quencher Concentration on Φ_{cPP} for the tPP/Et_3N System

proposed involves the use of the inverted form of the normal Stern-Volmer ratio, i.e. $\Phi_{cPP}/\Phi^{o}_{cPP}$. It can be shown that when the value of this parameter, at a given quencher concentration, is multiplied by the ratio of the quantum yields of monomer fluorescence in the absence (Φ^{o}_{FM}) and presence of quencher at that same concentration (Φ_{FM}), then:

$$\frac{\Phi_{cPP}}{\Phi^{o}_{cPP}} \cdot \frac{\Phi^{o}_{FM}}{\Phi_{FM}} = 1 + \frac{k_3 k^{E}_{cPP} [Et_3N]}{k^{M}_{cPP}(k_4 + k_p)} \qquad (6)$$

Hence the Φ_{cPP} values of Table 4.3 were combined with the known fluorescence quenching efficiency terms for this system, to produce a plot of $(\Phi_{cPP}.\Phi^{o}_{FM})/(\Phi^{o}_{cPP}.\Phi_{FM})$ vs. $[Et_3N]$ and this is presented above as fig. 4.13b). As illustrated here, a good linear relationship was indeed apparent between these parameters with the 'best fit' straight line through the data points having the predicted intercept of 1.0. From the slope of fig. 4.13b) a value was derived for k^{E}_{cPP} by substitution of the known values of the appropriate rate constants into equation 5. Using this approach, the rate constant for formation of the cis isomer via the tPP/Et_3N exciplex was found to have a value of:

$$k^{E}_{cPP} = 1.0 \times 10^{7}\ s^{-1}$$

This value may now be taken in conjunction with equation (6) above, in order to separate out the contributions to Φ_{cPP} due to isomerisation via the monomer and exciplex (Φ^{M}_{cPP} and Φ^{E}_{cPP}, respectively) at each quencher concentration used. The results of such an analysis are presented in Table 4.3 and, as would be expected Φ^{E}_{cPP} is observed to increase with $[Et_3N]$, at the expense of Φ^{M}_{cPP}, which decreases according to standard Stern-Volmer kinetics (i.e. $\Phi^{o}_{cPP}/\Phi^{M}_{cPP}$ increases linearly with $[Et_3N]$.)

b) The Quantum Yields of Photoproduct Formation and Monomer Disappearance

The values of the quantum yields of monomer disappearance (Φ_{-tPP}) and photoadduct formation (Φ_A) were measured for the tPP/Et_3N system, over the range of quencher concentrations employed above. The results obtained are presented in Table 4.4 and it may be noted that a rather

unusual situation was observed in the case of Φ_{-tPP}, which was found to be essentially independent of $[Et_3N]$, within this range. This appears to be a consequence of the fact that photoproduct formation increases with quencher concentration at such a rate as to offset the observed decrease in the quantum yield of photoisomerisation noted in the preceding section.

Table 4.4

The Quantum Yields of Monomer Disappearance and Photoproduct Formation as a Function of the Quencher Concentration for the tPP/Et_3N System

Et_3N (M)	Φ_{-tPP}	Φ_A	Φ_{PROD}^{*}
0	0.24	-	-
0.02	0.24(3)	0.05(8)	0.083
0.03	0.24(2)	0.06(9)	0.107
0.04	0.24(3)	0.07(8)	0.113
0.05	0.26	0.08(7)	0.134

* Calculated using equation .

As a result of this lack of dependence of Φ_{-tPP} on the quencher concentration, it was not possible to derive a value for k_{PROD} from a plot of the inverse of the quantum yield of monomer disappearance vs. $[Et_3N]^{-1}$, as was done in the case of the IND/Et_3N system. Similarly, a plot of Φ_A^{-1} vs. $[Et_3N]^{-1}$ proved to be of little value for the determination of k_{PROD} here, since:

i) The Φ_A values recorded were rather small, such that the degree of accuracy to which these could be measured ($\sim \pm$ 10%) was not great enough to allow k_{PROD} to be extracted with any certainty from such a plot (i.e. the error bars generated here were rather large).

ii) Also, as pointed out above (Section 4.4.1) the slope and intercept of a plot of this type should yield the parameter $q_A \cdot k_{PROD}$. Hence, the relative efficiencies of photoreduction and photoadduct formation (at each quencher concentration studied) are required in order to derive k_{PROD}, since:

$$q_A = \frac{\Phi_A}{\Phi_A + \Phi_R} \qquad (7)$$

where ϕ_A is the quantum yield of formation of the reduced hydrocarbon (1-phenylpropane in this case).

Unfortunately, as was the case with the IND/Et_3N system, accurate determination of Φ_R (and hence q_A) was hampered here by the limitations of the g.l.c. analysis employed. Thus, the most reasonable route to the derivation of k_{PROD} for this system, appeared to be to use a combination of the rather more readily determined quantum yield values, Φ_{-tPP} and Φ_{cPP}. Using data given in Tables 4.3 and 4.4, the expected values of Φ_{PROD} (= $\Phi_A + \Phi_R$) at each quencher concentration, were calculated, on the assumption that:

$$\Phi_{PROD}^{CALC} = \Phi_{-tPP} - \Phi_{cPP} \qquad (8)$$

The Φ_{PROD}^{CALC} values calculated in this way are presented in Table 4.4, and graphically in the form of a plot of $(\Phi_{PROD}^{CALC})^{-1}$ vs. $[Et_3N]^{-1}$, as fig. 4.14. It can be seen that there is indeed a linear relationship between these parameters and using the slope and intercept of fig. 4.14 , it was possible to derive a value for k_{PROD} for this system. Using an expression analogous to equation (5) above, the value of k_{PROD} obtained for the tPP/Et_3N system was:

$$k_{PROD} = 1.85\ (\pm\ 0.38)\ \times\ 10^7\ s^{-1}$$

It can be seen that the ratio of the Φ_A and Φ_{PROD}^{CALC} values listed in Table 4.4, may now be used to calculate q_A, at each quencher concentration studied. An average value for q_A of 0.67 is derived thus, suggesting that, for those tPP/Et_3N complexes which decay to form photoproducts, adduct formation is preferred over photoreduction by a factor of approximately 2:1.

In the case of the IND/Et_3N system, it was shown that the sum of the rate constants ($k_{PROD} + k_5$) failed to account completely for the value of k_p, derived from transient studies on that system. It appears that this may also be true for the case of decay of the tPP/Et_3N exciplex. However, in order to make the comparison with k_p for this system, it is necessary to make certain assumptions regarding the process of geometric isomerisation via the exciplex. In particular, a value must be assumed

Figure 4.14 A Plot of $(\Phi_{PROD}^{CALC})^{-1}$ vs. $[Et_3N]^{-1}$ for the tPP/Et_3N System

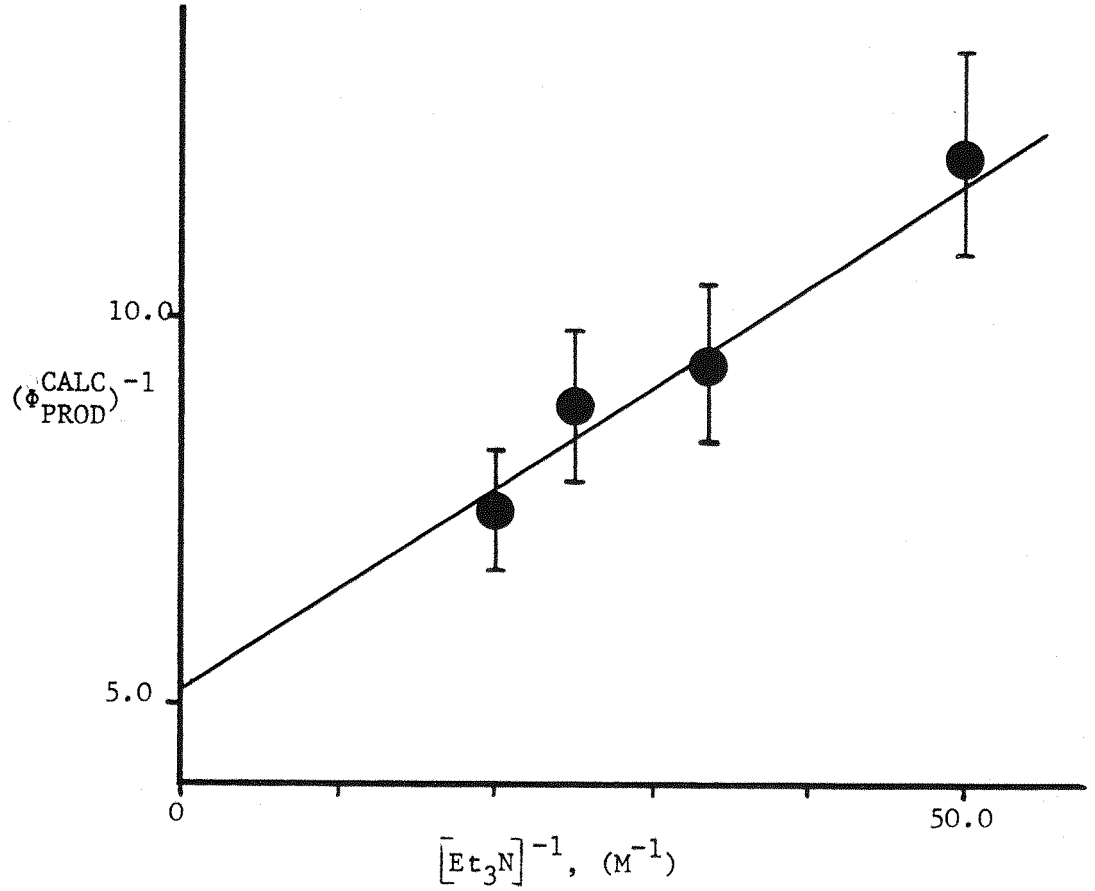

for the branching ratio associated with the formation of the cis and trans isomers, following this mode of exciplex decay. By analogy with the tPP monomer itself, it may be proposed that the 'isomerisation intermediates' formed via the exciplex should relax with equal efficiency to form the cis and trans isomers in this case. In other words, a branching ratio of 1.0 is assumed here, regardless of the nature of these intermediates. On the basis of this assumption, the total decay rate due to isomerisation via the exciplex should be twice the rate of formation of the cis isomer by this process. Hence, the comparison may be made here, between:

$$k_p = 1.13 \times 10^8 \ s^{-1}$$

and the sum:

$$(k_5 + k_{PROD} + 2k^E_{cPP}) = 5.14 \times 10^7 \ s^{-1}$$

and it can be seen from this that once again there appears to be an 'extra' non-radiative decay pathway available for the tPP/Et_3N complex.

4.5 Exciplex Decay Processes

The values of the rate constants associated with the various deactivation processes within the two exciplexes studied here, and the relative efficiencies of these processes are now summarised in Table 4.5.

Table 4.5

The Observed Values of the Rate Constants and Quantum Efficiencies* for the Decay Processes of the IND/ and tPP/Et_3N Exciplexes

Exciplex	k_5 $s^{-1}(x10^{-7})$	k_{PROD} $s^{-1}(x10^{-7})$	k^E_{ISOM} $s^{-1}(x10^{-7})$	k^E_{NR} $s^{-1}(x10^{-7})$
tPP	1.3	1.9	2.0	6.2
IND	1.9	42.0	-	36.0
	q_5	q_{PROD}	q^E_{ISOM}	q^E_{NR}
tPP	0.11	0.16	0.18	0.55
IND	0.02	0.53	-	0.45

* $q_i = \dfrac{k_i}{\Sigma k_i}$

From this data, a number of points of interest are apparent, namely:

a) For both these systems, the quantum efficiency of the exciplex fluorescence (q_5) is low and it can be seen that these complexes are characterised principally by their non-radiative decay.

b) As the electron accepting ability of the styrene monomer is reduced on going from tPP → IND, a 'weaker', less stable complex is formed. Associated with this reduction in stability, a dramatic increase in the absolute values of both k_{PROD} and k_{NR}^{E} is observed.

c) In terms of the relative efficiencies of these non-radiative processes, however, it may be noted that, while q_{PROD}^{IND} is substantially greater than q_{PROD}^{tPP}, the efficiency of the 'extra' radiationless decay process (denoted by q_{NR}^{E}) is such that in both cases, this pathway accounts for ∿50% of the total exciplex decay.

Thus, quite a detailed picture is now available, of the overall decay characteristics for these two exciplex systems, at room temperature in degassed cyclohexane. However, the nature of the non-radiative decay process(es) to which the rate constant k_{NR}^{E} has been assigned, is still open to question here. Unfortunately, little insight into this problem can be derived from the literature, since few systems have so far been studied in terms of both their photophysical characteristics and their photochemical reactivity. In fact, the observations reported for those systems, which have been studied in such detail, serve mainly to illustrate the diversity in the decay pathways available for the exciplexes concerned. Also, it is apparent that there can be a wide variation in the relative efficiencies of these processes and a number of examples which demonstrate these features are outlined below.

The Phenanthrene (P)/Dimethyl Fumarate (F) system has been the subject of detailed examination by both Farid[2c] and Caldwell[2d] and from these studies, it has been shown that decay of the P/F exciplex is characterised by the processes of:

1) Cycloaddition, leading to cyclobutane and oxetane formation.

2) Intersystem Crossing to form a triplet exciplex, which in turn may decay by a number of routes.

3) Exciplex fluorescence.

4) Energy transfer, leading to the formation of $^3F^*$.

5) A radiationless deactivation.

In this case, the quantum efficiencies of the processes 1) - 4) are relatively low, e.g. it has been reported that $q^E_{FL} = 0.003$ only. The major deactivation route for the P/F exciplex appears to be that of a non-product-forming non-radiative decay, which has been assumed to be an internal conversion (for which $q^E_{NR} = 0.82$).

In contrast to the above, the t-β-Styryl Naphthalene (StN)/ N,N Diethylaniline (DEA) exciplex[22], which has been mentioned briefly already, exhibits rather less complex behaviour. For this system, exciplex fluorescence provides the principal decay pathway (in nonpolar solvents), having a quantum efficiency, $q^E_{FL} = 0.72$. The only non-radiative decay process of any importance in this case, is found to be intersystem crossing, to form the triplet excited StN, which relaxes further via internal rotation, leading to geometric isomerisation of the StN monomer. The fact that relatively high efficiencies are attainable for product-forming exciplex decay pathways is demonstrated by a number of 1,2 Diarylethylene/Diene exciplexes, studied by Lewis[23]. In the case of the Diphenylvinylidene Carbonate/2,5 Dimethylhexadiene system, for example, the quantum efficiency of cycloadduct formation was observed to have a value of 0.93.

Thus, returning to the case of the tPP/ and IND/Et_3N systems, it can be seen that the values of the rate constants (k^E_{NR}) and quantum efficiencies (q^E_{NR}) observed for these systems are not, in themselves, characteristic of any particular mode of exciplex decay. However, it may be of interest at this point to refer back to the transient studies on the tPP/Et_3N exciplex, which have been outlined already in Section 3.2 . In particular, it may be recalled that a study was made of the effects of temperature and solvent polarity on the kinetics of exciplex formation and decay for this system. The results of this examination may be summarised in terms of the effects of these parameters on k_p, the total exciplex decay rate constant. In the case of a non-polar solvent system, k_p was found to decrease as the temperature was reduced, while an increase in the solvent polarity (at room temperature) was observed to lead to an increase in the value of k_p.

The observed variation in the sum of the rates of the non-radiative decay processes with temperature for the tPP/Et_3N exciplex, has been detailed in Table 3.19, in which this sum is denoted by the

rate constant, k_6. In this analysis, it has been assumed that the exciplex radiative rate constant, k_5, is temperature independent, such that at each temperature studied:

$$(k_6)_T = (k_p)_T - k_5 \qquad (9)$$

and it now becomes apparent that there are three processes contributing to the magnitude of k_6 here, i.e.

$$k_6 = k^E_{ISOM} + k^E_{PROD} + k^E_{NR} \qquad (10)$$

A plot of loge (k_6) vs. $(T)^{-1}$ was found to be linear over the temperature region studied (see fig. 3.24d)) implying that those components of k_6 which show a dependence on temperature, have rather similar activation energies. Hence, it is necessary at this point to examine the extent to which the rate constant for each of the three processes under consideration here, might be expected to vary with temperature.

A comparison of the data of Tables 3.19 and 4.5 reveals that the value of k^E_{NR} appears to decrease with temperature, since it can be seen that for $T \leqslant 270$ K, the value derived for k_6 falls below that recorded for k^E_{NR} at room temperature. In the case of geometric isomerisation via the exciplex, however, it may be argued that the rate constant for this process should not vary greatly with temperature. Although it is not clear as to the nature of the excited state(s) involved in the isomerisation here, it is to be expected that a strong temperature dependence of k^E_{ISOM} would be unlikely, especially if this process involves deactivation of the exciplex by a (vertical) intersystem crossing, to form ^{3}tPP*. On the other hand, it does seem likely that a product-forming exciplex decay pathway should be activated and this would appear to be so for the tPP/Et_3N system. If k^E_{PROD} is assumed to be temperature independent and the observed decrease in k_6 with temperature is ascribed to variation in k^E_{NR} alone, then a plot of loge $((k_6)_T - (k^E_{ISOM} + k^E_{PROD}))$ vs. $(T)^{-1}$ would be expected to be linear. This is clearly not the case here, even over the rather narrow temperature range examined.

Hence, it is suggested that, for this system, the processes of

exciplex fluorescence and geometric isomerisation via the exciplex are essentially temperature independent, while k^E_{PROD} and k^E_{NR} both decrease with temperature, the processes denoted by these latter rate constants both possessing similar activation energies. It should now be possible to derive values for these activation energies (assuming $\Delta E^{\ddagger}_{PROD} = \Delta E^{\ddagger}_{NR}$) from the slope of a plot of loge $(k^E_{NR} + k^E_{PROD})$ vs. $(T)^{-1}$ if the assumption is correct that for each temperature studied:

$$(k^E_{NR} + k^E_{PROD})_T = (k_6)_T - k^E_{ISOM} \qquad (11)$$

As illustrated in fig. 4.15, a plot of the type suggested is indeed linear over the range of temperature studied and the various activation parameters which have been extracted from this plot are presented in Table 4.6a) below.

Table 4.6a)

Activation Parameters* for the Temperature Dependent Decay Processes of the tPP/Et_3N Exciplex

Process	$\Delta E^{\ddagger}$ ($k_{cal}mol^{-1}$)	$\Delta H^{\ddagger}$ a) ($k_{cal}mol^{-1}$)	A b) (s^{-1})	$-\Delta S^{\ddagger}$ a),b) ($cal.deg^{-1}mol^{-1}$)
PROD	4.9	4.3	9.4×10^{10}	8.3
NR	"	"	3.1×10^{11}	5.9

* In degassed nonpolar solvents

a) Calculated for T = 293 K

b) Derived using the known room temperature values of k^E_{PROD} and k^E_{NR}

Table 4.6b)

Activation Energies and Arrhenius A Factors for the Unimolecular Decay Processes of Some Excited Aromatic Molecules*

Compound	$\Delta E^{\ddagger}$ ($k_{cal}mol^{-1}$)	A (s^{-1})
Toluene	4.1	8.0×10^{10}
cPP	3.5	9.1×10^{10}
tPP	0.9	9.8×10^{7}

Figure 4.15 An Analysis of the Temperature Dependence of the Non-Radiative Rate Constants for the tPP/Et_3N Exciplex

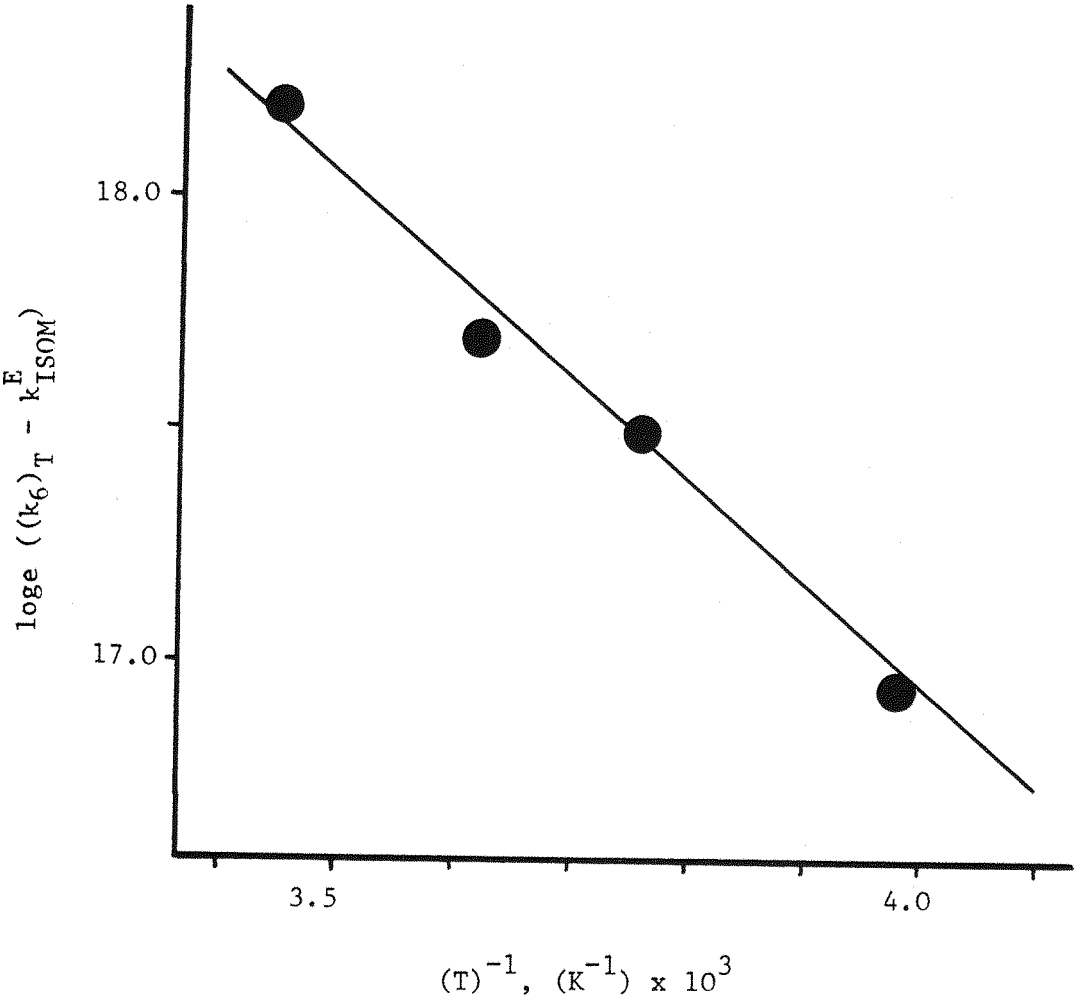

It is interesting to compare the data of Table 4.6a) with similar values reported for the temperature dependent unimolecular decay processes of excited aromatic molecules. The activation energies and A factors derived for toluene[24] and the isomeric styrenes cPP and tPP[20b)] are of particular interest in this context and these are presented, for comparison in Table 4.6b). Although the interpretation of activation parameters obtained from unimolecular reactions in solution is not straightforward, it may be noted that the values reported for toluene and cPP are typical of those observed for an allowed decay process, such as internal conversion. The close similarity between the data of Table 4.6b) and the values of $\Delta E^{\ddagger}_{NR}$ and A_{NR} derived for the tPP/Et_3N exciplex is noteworthy and the suggestion is that by analogy, the 'extra' non-radiative decay pathway available to the exciplex may also involve an internal conversion to the (repulsive) exciplex ground state. In the case of the singlet excited tPP monomer, in the absence of quencher, to which the data of Table 4.6b) is related, it is proposed that the temperature dependent decay process corresponds to a thermally activated inter-system crossing[20b)]. It can be seen that the activation parameters associated with this process are quite characteristic and differ markedly from those for the other monomers and also, those for decay of the tPP/Et_3N exciplex. Hence it would appear that the single most important physical consequence of formation of the tPP/Et_3N complex is that it provides a route (thought to be internal conversion) by which relaxation to form $^1tPP^o$ may occur, this route being unavailable to $^1tPP^*$ alone.

The observation that exciplex decay may occur via the processes of internal conversion and product formation and that these processes are both activated, having similar $\Delta E^{\ddagger}$ and $\Delta S^{\ddagger}$ values has also been made in the case of a series of aromatic hydrocarbon/olefin complexes[25]. For these systems, it was proposed that the exciplex decay processes were themselves closely related and the experimental results obtained were rationalised in terms of Transition State theory, following the work of Michl[26]. The results presented in Table 4.6a) suggest that in the case of the tPP/Et_3N exciplex also, a single, rate-determining energy barrier must be surmounted prior to relaxation of the exciplex

via decay pathways involving product formation and internal conversion. As mentioned earlier (Section 4.3), calculations on aromatic hydrocarbon/amine exciplexes predict that for these systems, there should exist a relatively shallow free energy barrier to formation of a solvated radical ion pair via the exciplex. It has also been suggested that as the polarity of the solvent is increased, the height of this barrier will be reduced[12]. This effect, if present, should be reflected in the observation of an enhancement of the rates of the non-radiative exciplex decay processes with increasing solvent dielectric. It is interesting to note, therefore, that such an observation has been made in the case of the tPP/Et_3N system (see Table 3.18). Thus, although the nature of the Transition State(s) involved here remains unclear, it may be that for this system, it is the requirement for the formation of a solvated radical ion pair, which is providing the energy barrier to the principal non-radiative decay routes via the exciplex.

4.6 Exciplex Quenching Studies Involving the tPP/Et_3N System

In the foregoing sections, product-forming exciplex decay pathways have been postulated in the analysis of the kinetics of exciplex formation and decay for the styrene/Et_3N systems. The experimental results, in terms of the measured quantum yields of photoproduct formation and their dependence on quencher concentration, are compatible with the suggestion that these routes are available to the exciplexes studied. However, as has been noted already, perhaps the most direct approach available for determining whether or not an exciplex is in fact a necessary intermediate in a given photochemical reaction, is the technique of exciplex quenching. This technique has been used to great effect by Caldwell,[2d),18,27] whose work has shown that for a variety of aromatic hydrocarbon/olefin systems, the products observed on irradiation of these systems are indeed formed via the fluorescent exciplexes, known to be present in solution. The styrene/Et_3N systems provide another series in which both photoproduct formation and exciplex emission are observable and thus, it was hoped that a similar study might prove rewarding here. Naturally, the first objective was to attempt to discover, if possible, a number of compounds which would efficiently quench the exciplex fluorescence from these systems. From Caldwell's work[18c)], general guidelines were available to aid this

search. In particular, it appears that such quenching is expected to occur preferentially when the quenching interaction occurs with the exciplex component of lower singlet energy (i.e. the initially excited species). This therefore suggested that for efficient quenching of the styrene/Et_3N exciplexes, strong CT acceptors might be most useful. In fact, this did prove to be the case and as is detailed in Table 4.7, a range of olefin acceptors were found to quench, with varying degrees of efficiency, the exciplex fluorescence in the case of the tPP/Et_3N system.

Table 4.7

Rate Constants for Fluorescence Quenching of the Monomer and Exciplex in the tPP/Et_3N System

Quencher	k_q^M ($l.mol^{-1}s^{-1}$) ($x10^{-9}$)	k_q^E ($l.mol^{-1}s^{-1}$) ($x10^{-9}$)
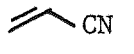	4.9	12.0
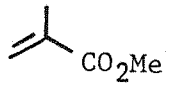	3.0	12.0
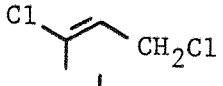	0.15	0.40
	0.37	0.22

It can be seen that, as might be expected, the fluorescence quenching rate constant, k_q^E, was observed to decrease as the electron accepting ability of the quenchers was reduced. The most efficient quenching was found to occur using Acrylonitrile (ACN) and Methylmethacrylate, both of which have powerful electron withdrawing groups attached to the olefinic double bond. For these compounds, the quenching of the tPP/Et_3N exciplex fluorescence was found to be diffusion controlled, which ties in well with predictions made by Caldwell, based on an FMO rationalisation of exciplex quenching. It has been suggested already that on formation of the tPP/Et_3N exciplex, there is in fact little perturbation of the various molecular orbitals involved. If this is so, then the important interaction in the exciplex quenching process

can be thought of as being that between 'LUMO'$_{A*}$ of the excited ^{1}tPP* monomer and LUMO$_{Q}$ of the ground state quencher. The energies of these orbitals may be approximated to ($I_A - E_S$), the difference between the Ionisation Potential and the Singlet Excitation Energy for each of the two compounds. Taking the tPP/Et_3N/ACN system as an example here, it may be noted that in this case, the energy difference between these orbitals (ΔEQ) is calculated to be of the order of 1.4 eV[28]. This value falls rather neatly within the range predicted by Caldwell[29], who suggests that for diffusion controlled exciplex quenching to be observed for such a system, a value of approximately 1.0 - 1.5 eV is required for ΔE_Q. Unfortunately, as is apparent from Table 4.7, none of those quenchers examined was in fact ideal in that, although efficient exciplex quenching could be achieved, quenching of the monomer fluorescence was also observed in each case. This lack of discrimination is probably a further indication that, for the tPP/Et_3N system, there is only a relatively small energy difference (ΔE_3, see fig. 3.5) between 'LUMO'$_{A*}$ and the corresponding exciplex orbital derived from it. However, due to the fact that at the time, purified samples of ACN were readily available, this quencher was chosen for study in somewhat greater detail. Quenching of the fluorescence of the ^{1}tPP* monomer by ACN alone, was observed to follow familiar Stern-Volmer kinetics, although no fluorescence which might have been associated with a tPP/ACN excited state complex was detected. The effects of addition of ACN on the fluorescence spectrum of the tPP/Et_3N system in degassed cyclohexane solution are clearly demonstrated in fig. 4.16. It can be seen that, by using a sufficiently large concentration of the primary quencher, Et_3N, the conditions could be chosen such that quenching of the monomer fluorescence appeared to be relatively insignificant by comparison to that of the exciplex. However, as is discussed later, it seems that for this system, it is still necessary to take into account the effects of monomer quenching, when attempting to derive values for the various rate constants involved in the exciplex quenching process, from steady state data.

A further complicating factor which may be encountered in studies such as this is the possibility that the kinetics of the system may be affected by attenuation of the absorption of the incident light,

Figure 4.16 The Effects of Addition of Acrylonitrile on the Fluorescence Spectrum of the tPP/Et_3N (0.2 M) System in Degassed Cyclohexane

	[ACN] (M)
I	0
II	0.005
III	0.015

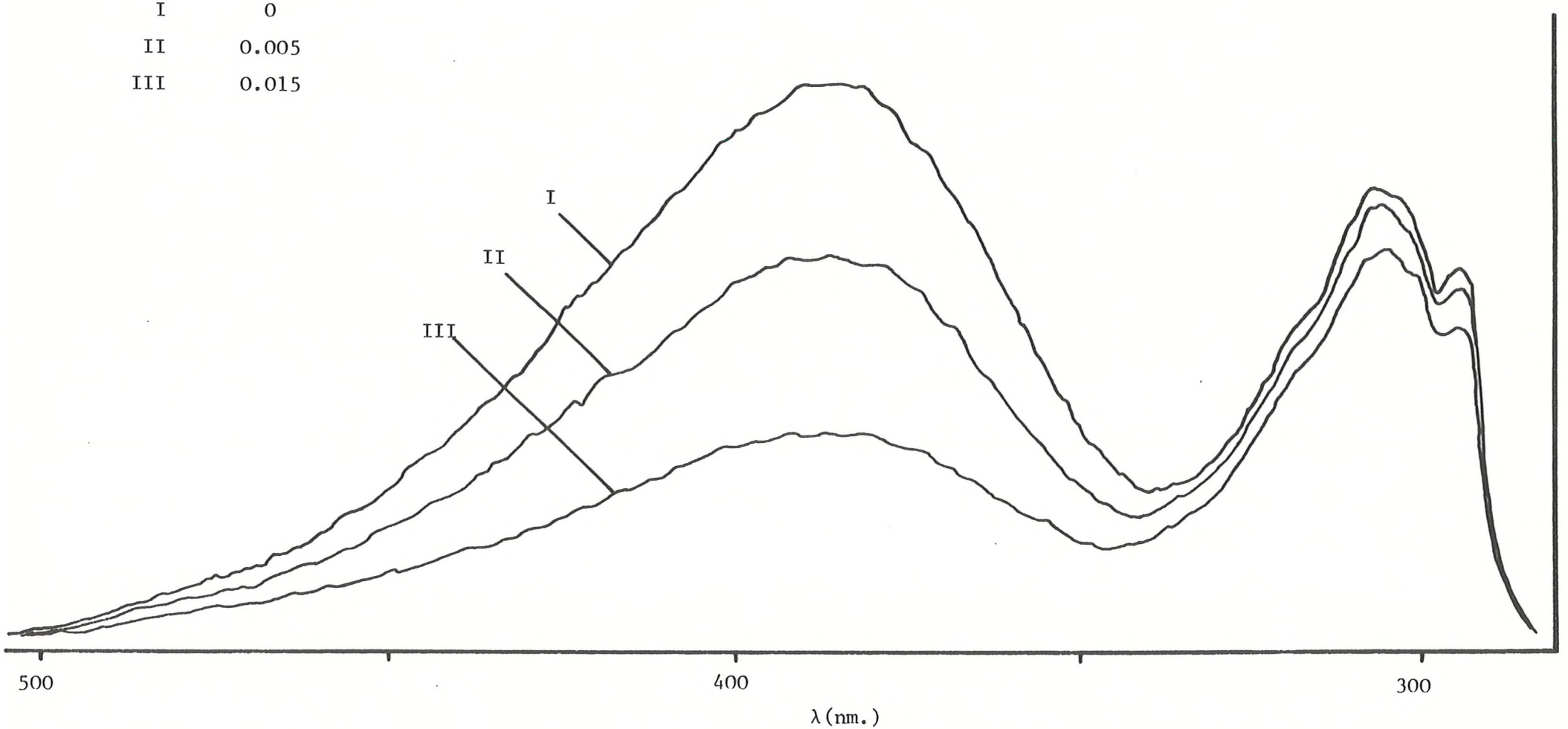

due to the presence of ground state Charge Transfer complexes. In the case of the tPP/Et_3N/ACN system, there was no evidence for the formation of such complexes between tPP and either of the quenchers present. There was however, a suggestion that an interaction of some sort was occurring between Et_3N and ACN in their ground state, in that a slight broadening of the Et_3N absorption band was observed on the addition of ACN. That this in fact has a negligible effect on the exciplex kinetics for this system, was demonstrated by a transient study of the fluorescence lifetime of the exciplex as a function of the concentration of added ACN. As is illustrated in fig. 4.17, the interaction between ACN and the tPP/Et_3N exciplex does indeed provide an additional decay pathway for the exciplex, as the exciplex fluorescence lifetime (τ^E) is observed to decrease in the presence of ACN, following standard Stern-Volmer kinetics.

Figure 4.17: The Observed Reduction in the tPP/Et_3N Exciplex Fluorescence Lifetime with Added ACN

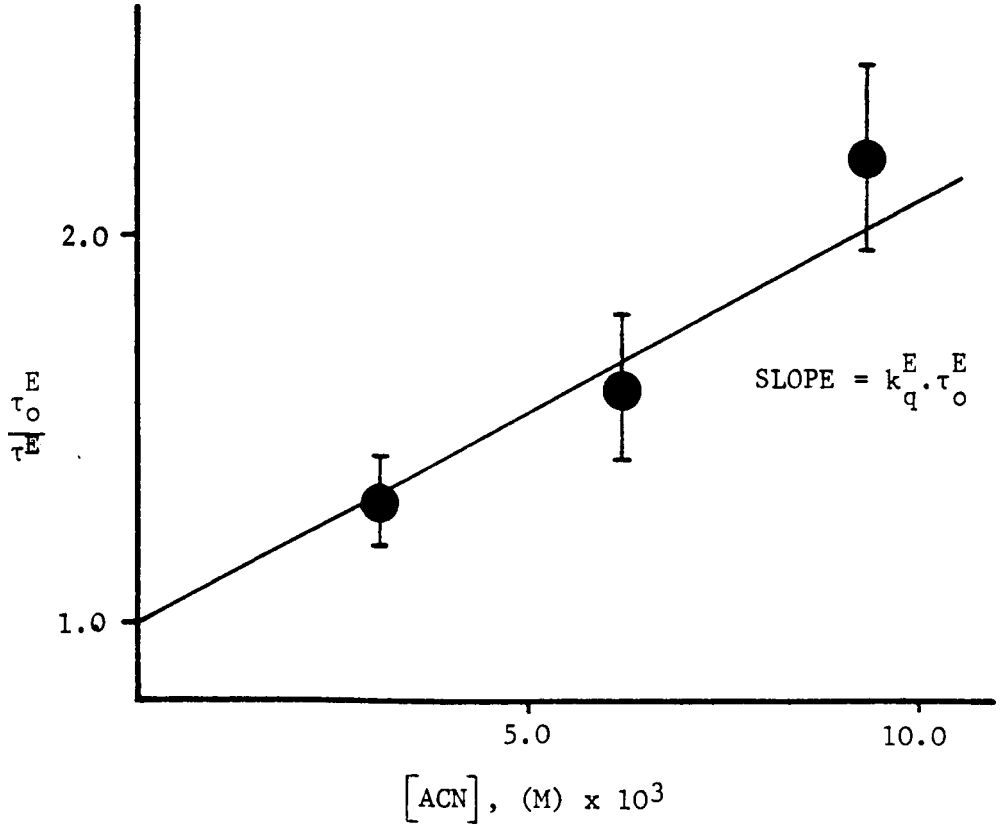

The slope of fig. 4.17 provides a value for the quenching rate constant k_q^E of 1.2×10^{10} $l.mol^{-1}s^{-1}$, which is identical to that derived from steady state data. It may be that this quenching is occurring via the formation of a stable, excited termolecular complex, although such a complex, if formed does not appear to be emissive in this case. Such an observation is not uncommon however, and it may be noted that fluorescence which could be assigned to the decay of an 'exterplex' has been reported for relatively few systems.[18b),30)]

Having thus established that the fluorescence of the tPP/Et_3N exciplex may be quenched by the addition of ACN, an examination was required of the effects of this quenching on the quantum yields of the photoproduct-forming processes. As noted already, there were difficulties associated with the measurement of Φ_R, the quantum yield of photoreduction, however Φ_A and Φ_{cPP}, the quantum yields of photo-adduct formation and photoisomerisation respectively were accessible for the tPP/Et_3N/ACN system. The results of a study of the effects of ACN on Φ_A and Φ_{cPP} are presented in Table 4.8 below, from which it may be noted that at a fixed concentration of the primary quencher, Et_3N, both these quantum yields are observed to decrease as [ACN] is increased.

Table 4.8

The Quantum Efficiency of Exciplex Formation and Quantum Yields of Photoproduct Formation for the tPP/Et_3N System as a Function of the Concentration of Added ACN

[ACN] (M) $\times 10^2$	a) q_{EX}	b) Φ_A	c) Φ_{cPP}
0	0.81	0.087	0.12(6) (0.066)
0.61	0.72	0.03(8) (0.043)	0.09 (0.038)
1.54	0.62	0.02(2) (0.029)	0.07 (0.027)

a) Calculated according to equation 13

b) 'Corrected' values in parentheses.

c) " " (of Φ_{cPP}^E) in parentheses

However, in order to establish whether or not, for this system, the exciplex is directly involved in formation of the observed photo-products, the comparison must be made between the efficiencies with which the processes of product formation and exciplex fluorescence are quenched by ACN. From the foregoing it has been shown that quenching of the tPP/Et_3N exciplex fluorescence by ACN is diffusion controlled. Unfortunately, a Stern-Volmer type analysis of the experimental data for Φ_A and Φ_{cPP} presented in Table 4.8, yielded values for the rate constants for quenching of photoadduct formation (k_q^A) and isomerisation (k_q^{cPP}) which were considerably in excess of k_{diff}. In other words, the observed reduction in these quantum yields on addition of ACN was rather too large to be accounted for by the exciplex quenching alone. However, it seems likely that this is simply a consequence of the fact that, under the conditions chosen for this study, quenching of the $^1tPP^*$ monomer by ACN is significant in this context and should not be neglected. It can be seen that the effect of this monomer quenching will be to cause a decrease in the quantum efficiency of exciplex formation (q_{EX}) within the system. In the case of photoadduct formation, if as is suggested here, the adduct is being formed exclusively via the exciplex, then Φ_A will be reduced in the presence of ACN, not only by quenching of the exciplex but also as a consequence of this decrease in q_{EX}, since:

$$\Phi_A = q_{EX} \cdot q_A \qquad (12)$$

(where q_A is the quantum efficiency for the adduct-forming exciplex decay process).

From fluorescence quenching studies, the rate constant for quenching of the $^1tPP^*$ monomer by ACN (k_q^M) was known and hence, it was possible to calculate the expected value of q_{EX} at each quencher concentration studied, using an expression of the form:

$$q_{EX} = \frac{k_3[Et_3N]}{k_1 + k_2 + \frac{k_3 k_p[Et_3N]}{(k_4 + k_p)} + k_q^M[ACN]} \qquad (13)$$

The values calculated thus for q_{EX} are presented in Table 4.8 as are the values of Φ_A and Φ^E_{cPP} "corrected" for the effects of monomer

quenching, by the use of the ratio of the quantum efficiencies of exciplex formation in the absence and presence of ACN. As is evident from Table 4.8, these corrections are quite significant and fig. 4.18 illustrates the observation that the quantum yield data plotted in the form Φ^{o}/Φ^{CORR} vs. $[Et_3N]$ now adheres reasonably well to a straight line of slope $k_{diff}.\tau_o^E$. In other words, it appears that for this system, the fluorescence of the tPP/Et_3N exciplex, formation of the tPP/Et_3N photoadduct and photoisomerisation via the exciplex are all quenched with the same efficiency by ACN. This therefore strongly suggests that the exciplex is indeed a precursor to formation of the observed photoproducts.

Figure 4.18: The Dependence of the Corrected Quantum Yields of Photoproduct Formation on [ACN] for the tPP/Et_3N System

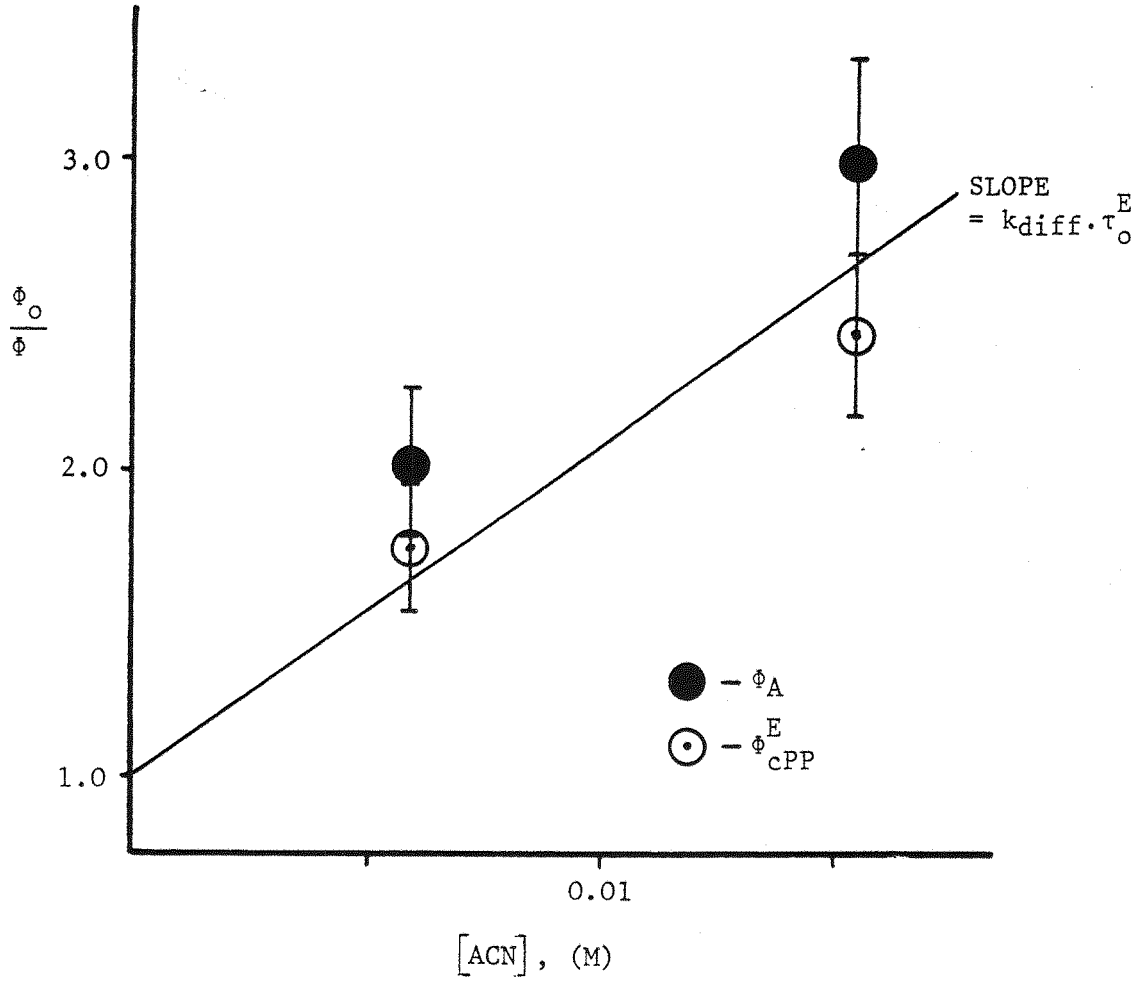

REFERENCES - CHAPTER 4

1a) A. Lablache-Combier
Bull. Soc. Chim. Fr., 4791 (1972)

1b) 'Molecular Association', vol. 1 (R. Foster Ed.)
R.S. Davidson
Academic Press N.Y. (1975)

2a) K. Mizuno, C. Pac and H. Sakurai
J. Amer. Chem. Soc., 96, 2993 (1974)

2b) T. Sugiroka, C. Pac and H. Sakurai
Chem. Lett., 667 (1972)

2c) S. Farid, S.E. Hartman, J.C. Doty and J.L.R. Williams
J. Amer. Chem. Soc., 97, 3697 (1975)

2d) D. Creed, R.A. Caldwell, M. McK. Ulrich
J. Amer. Chem. Soc., 100, 5831 (1978) and references therein.

3. R.C. Cookson, S.M. de B. Costa and J. Hudec
Chem. Comm., 753 (1969)

4a) N.C. Yang, D.M. Shold and B. Kim
J. Amer. Chem. Soc., 98, 6587 (1976)

4b) J. Saltiel, D.E. Townsend, B.D. Watson, P. Shannon and S.L. Finser
J. Amer. Chem. Soc., 99, 884 (1977)

5. F.D. Lewis
Acc. Chem. Res., 12, 152 (1979)

6. S.M. de B. Costa
Ph.D. (Southampton) 1969

7. S.G. Cohen, A. Parola and G.H. Parsons
Chem. Rev., 73, 141 (1973)

8. H.D. Roth and M.L. Manion
J. Amer. Chem. Soc., 97, 6886 (1975)

9. K.A. McLauchlan and R.C. Sealy
Chem. Phys. Lett., 39, 310 (1976)

10. M. Ottolenghi
Acc. Chem. Res., 6, 153 (1973)

11. A. Alcholal, M. Tamir and M. Ottolenghi
J. Phys. Chem., 76, 2229 (1972)

12. 'Organic Molecular Photophysics', chap. 4 (J.B. Birks Ed.)
H. Beens and A. Weller

13. H. Tylli and F. Sundholm
Acta. Chem. Scand., 27, 47 (1973)

14a) T.R. Evans
J. Amer. Chem. Soc., 93, 2081 (1971)

14b) D.A. Labianca, G.N. Taylor and G.S. Hammond
J. Amer. Chem. Soc., 94, 3679 (1972)

14c) I.H. Kochevar and P.J. Wagner
J. Amer. Chem. Soc., 92, 5742 (1970)

14d) N.E. Schore and N.J. Turro
J. Amer. Chem. Soc., 97, 2482 (1975)

14e) F.D. Lewis and R.H. Hirsch
J. Amer. Chem. Soc., 98, 5914 (1976)

15. R.M. Bowman, T.R. Chamberlain, C-W Huang and J.J. McCullough
J. Amer. Chem. Soc., 96, 642 (1974)

16. J. Saltiel, J.T. D'Agostino, O.L. Chapman and R.D. Lura
J. Amer. Chem. Soc., 93, 2804 (1971)

17. R.A. Caldwell, G.W. Sovocool and R.P. Gajewski
J. Amer. Chem. Soc., 95, 2549 (1973)

18a) R.A. Caldwell
J. Amer. Chem. Soc., 95, 1690 (1973)

18b) D. Creed and R.A. Caldwell
J. Amer. Chem. Soc., 96, 7369 (1974)

18c) R.A. Caldwell, D. Creed and H. Ohta
J. Amer. Chem. Soc., 97, 3247 (1975)

19. K. Yokota, H. Tomioka and K. Adachi
Polymer, 14, 561 (1973)

20a) C.S. Nakagawa and P. Sigal
J. Chem. Phys., 58, 3529 (1973)

20b) P.M. Crosby
Ph.D. (Southampton) 1979

21a) A.A. Lamola and G.S. Hammond
J. Chem. Phys., 43, 2129 (1965)

21b) R.A. Caldwell, G.W. Sovocool and R.J. Peresie
J. Amer. Chem. Soc., 93, 779 (1971)

21c) M.G. Rockley and K. Salisbury
J.C.S. Perkin II, 1582 (1973)

22. G.G. Aloisi, U. Mazzucato, J.B. Birks and L. Minuti
J. Amer. Chem. Soc., 99, 6340 (1977)

23. F.D. Lewis and C.E. Hoyle
J. Amer. Chem. Soc., 99, 3779 (1977)

24. R.B. Cundall, L.C. Perreira and D.A. Robinson
J.C.S. Faraday II, 701 (1973)

25. D. Creed, P.H. Wine, R.A. Caldwell and L.A. Melton
J. Amer. Chem. Soc., 98, 621 (1976)

26. J. Michl
Photochem. Photobiol., 25, 141 (1977)

27. R.A. Caldwell, N.I. Ghali, C-K Chien, D. De Marco and L. Smith
J. Amer. Chem. Soc., 100, 2857 (1978)

28. Using IP(ACN) = 10.8 eV
R.P. Blaunstein and L.G. Christophoron
Radn. Res. Rev., 3, 69 (1971)

29. D. Creed, R.A. Caldwell, H. Ohta and D. De Marco
J. Amer. Chem. Soc., 99, 277 (1977)

30a) H. Beens and A. Weller
Chem. Phys. Lett., 2, 140 (1968)

30b) J. Saltiel, D.E. Townsend, B.D. Watson and P. Shannon
J. Amer. Chem. Soc., 97, 5688 (1975)

CHAPTER 5

EXPERIMENTAL

5.1 Time Correlated Single Photon Counting

The fluorescence lifetimes (τ_F) reported in this work were determined using the Single Photon Counting (SPC) technique. The basic principle of this technique[1] is that it involves the building up of a fluorescence decay profile in a time correlated manner, according to the probability of detecting a photon emitted at a given time after the sample has been excited by a pulsed light source. The component parts of the apparatus are illustrated in the block diagram presented below as fig. 5.1. The apparatus, constructed in this laboratory[2] was conventional in design, incorporating many of the features recommended[3] for the successful acquisition of lifetime data in the nanosecond time domain.

The central component in any system such as this is the biased Time to Amplitude Convertor (TAC), the model employed in this case being an ORTEC 457. As its name suggests, this is basically an electronic timing device, which measures the interval between the time of arrival of START and STOP pulses. These are provided to the TAC respectively by the r.f. radiation generated by the lamp discharging and by the appearance at the Photomultiplier Tube (PMT) of an emitted photon. Each time the lamp fires, a START pulse (typically of amplitude $\geq$650 mV.) is delivered via an inductive pick-up, fixed adjacent to the lamp (approximately 5 cm. from the electrode tips) to the 100 MHz Leading Edge Discriminator (ORTEC 436). The START pulse is then passed on via the calibrated variable delay unit (ORTEC 425) to the START channel of the TAC, thus initiating a voltage ramp within the TAC. This voltage ramp may then be terminated by the arrival of an emitted photon at the Phillips 56 DUVP fast PMT, which in turn causes a STOP pulse to be delivered via the Constant Fraction Discriminator (ORTEC 463) to the STOP channel of the TAC.

Figure 5.1 - A Block Diagram Showing the Components of the S.P.C. Apparatus

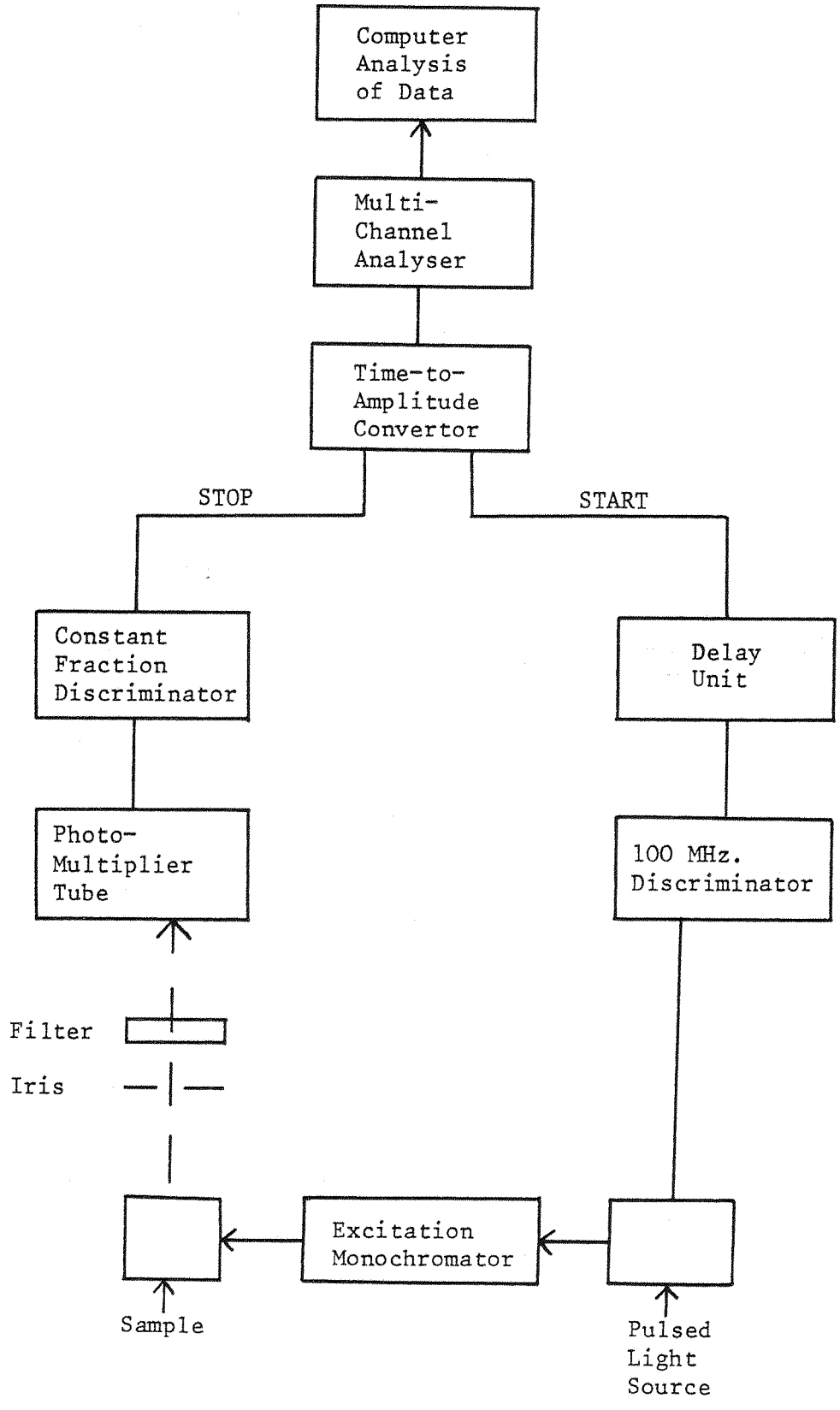

This process is illustrated in fig. 5.2, which also shows that if no STOP pulse is received from the PMT during the time sweep, the TAC is reset to await the next START pulse from the lamp.

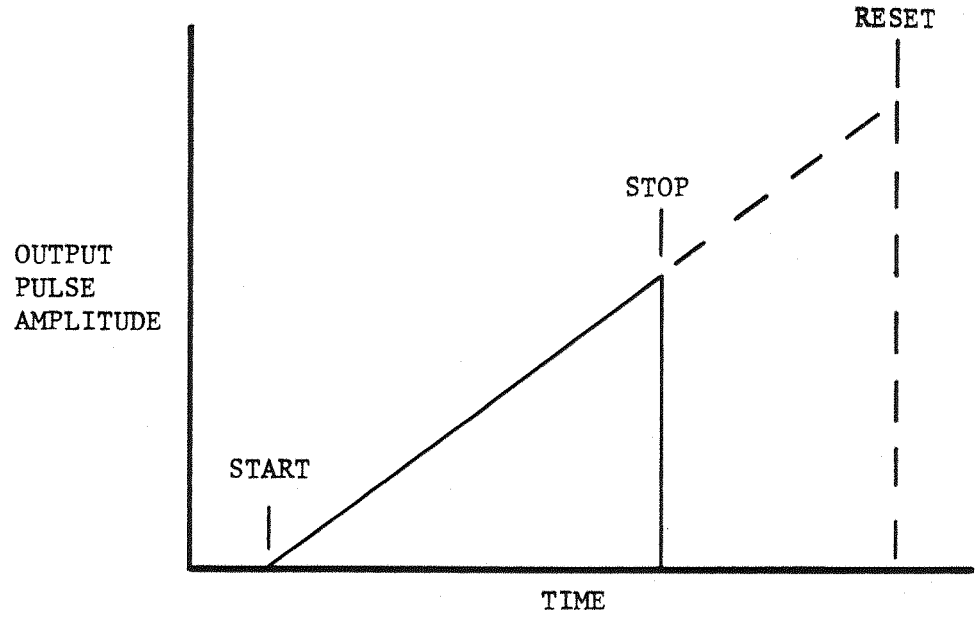

Figure 5.2 - The Principle of Operation of the TAC

The output pulses from the TAC are fed out to an Ino-Tech S/5000 Multi-Channel Pulse Height Analyser (MCA) and sorted and stored as counts, according to their amplitude. The 200 channels of the MCA memory thus represent time increments, with the 'channel width' being determined by the time range chosen on the TAC (typically 0.05, 0.1 or 0.2 μsec. from START to RESET). Calibration of the TAC ranges was effected using the ORTEC 425 variable delay unit. A BNC T-piece was

connected to the negative output of the 100 MHz discriminator so that each lamp pulse could be fed both directly to the START channel and also, via the delay unit to the STOP channel of the TAC. Altering the length of time by which the stop pulse was delayed thus caused a shift of the output to the MCA. The known delay (in nsec.) thus introduced was then divided by the number of channels between successive output peaks and the values obtained averaged to provide a value for the 'channel width'.

It was generally found to be necessary to attenuate the emitted light beam by placing an (adjustable) iris in front of the PMT. This ensured that only a relatively small, central area of the PMT was exposed, as has been recommended[5] and also that the condition was fulfilled, that $\leq 5\%$ of the exciting light pulses resulted in a photon being detected at the PMT, such that the importance of multi-photon events could be minimised. In order that fluorescence could be observed in the absence of any scattered light at the excitation wavelength, suitable cut-off filters were also placed in front of the PMT. The transmission characteristics of the filters principally used, are illustrated in fig. 5.3, from which it can be seen that filters A and B were particularly suitable for the measurement of τ_F for the styrenes, using excitation wavelengths in the region of 260-280 nm. Fluorescence decay profiles were recorded for the styrene/Et_3N exciplexes, in the absence of any emission due to the quenched monomers, using filters C or D. The measurement of the quenched monomer fluorescence lifetimes for these systems, presented greater difficulty however, in that a rather narrow window of transmission was required in order to allow observation of the styryl emission alone. As illustrated in fig. 5.3, this requirement was fulfilled using the filter system E, which transmits $\geq 10\%$ of the incident light over a wavelength region from 280-350 nm. Filter E was in fact a combination of the glass filter, A, with a chemical filter, comprising an aqueous solution of $CoSO_4.7H_2O$(0.09M) with $NiSO_4.H_2O$(0.19M), contained in a quartz cell of path length 1 cm. A test of the efficiency of this combination at removing both scattered light and exciplex emission in a system in which both are present is illustrated in fig. 5.4. This shows the fluorescence spectra recorded in the absence and presence of filter system E for a

Figure 5.3

Transmission Characteristics of Filters Used with the SPC Apparatus

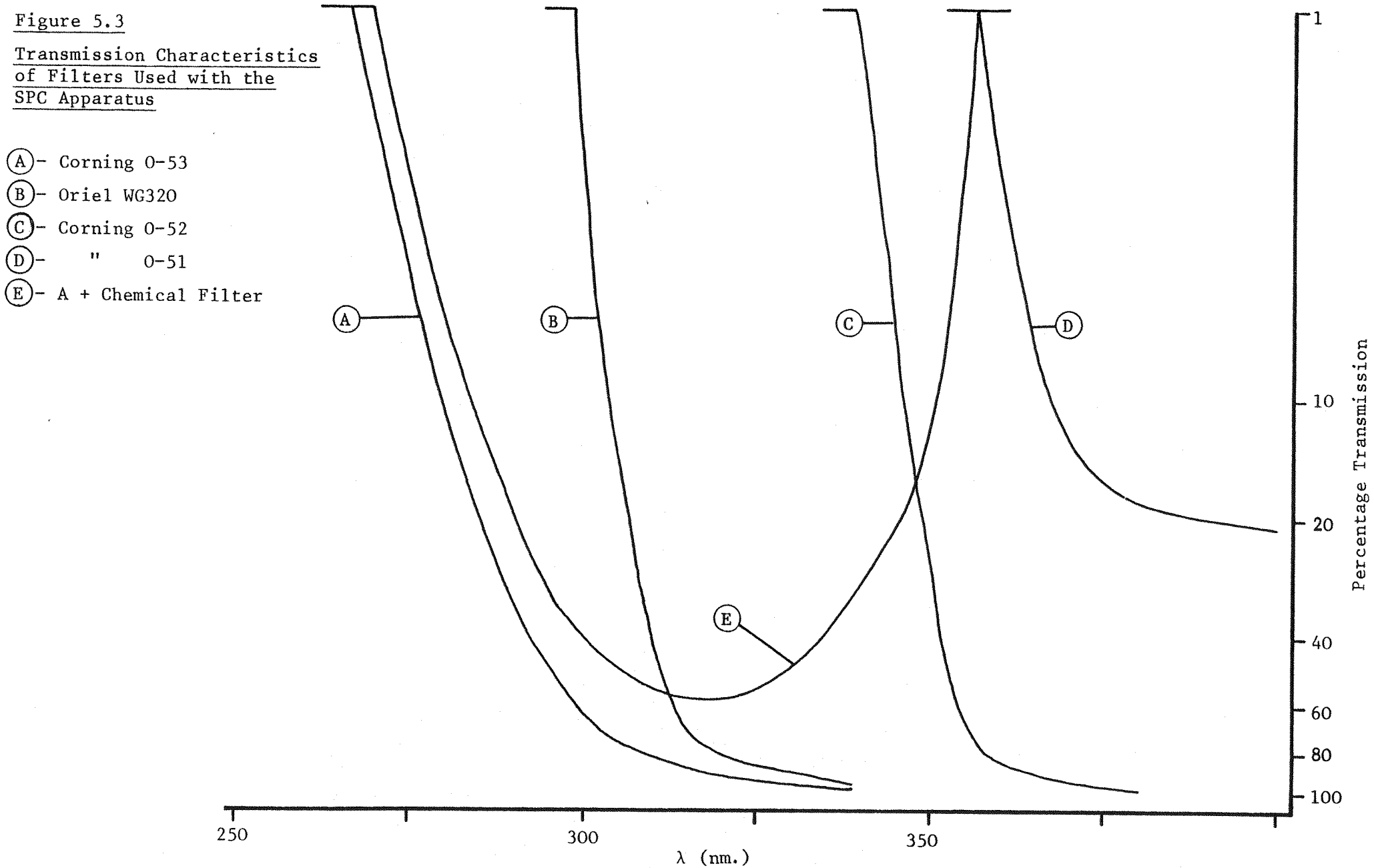

Figure 5.4 - Emission Spectra for the tPP/Et_3N (0.02 M) System Recorded in the Absence and Presence of Filter E

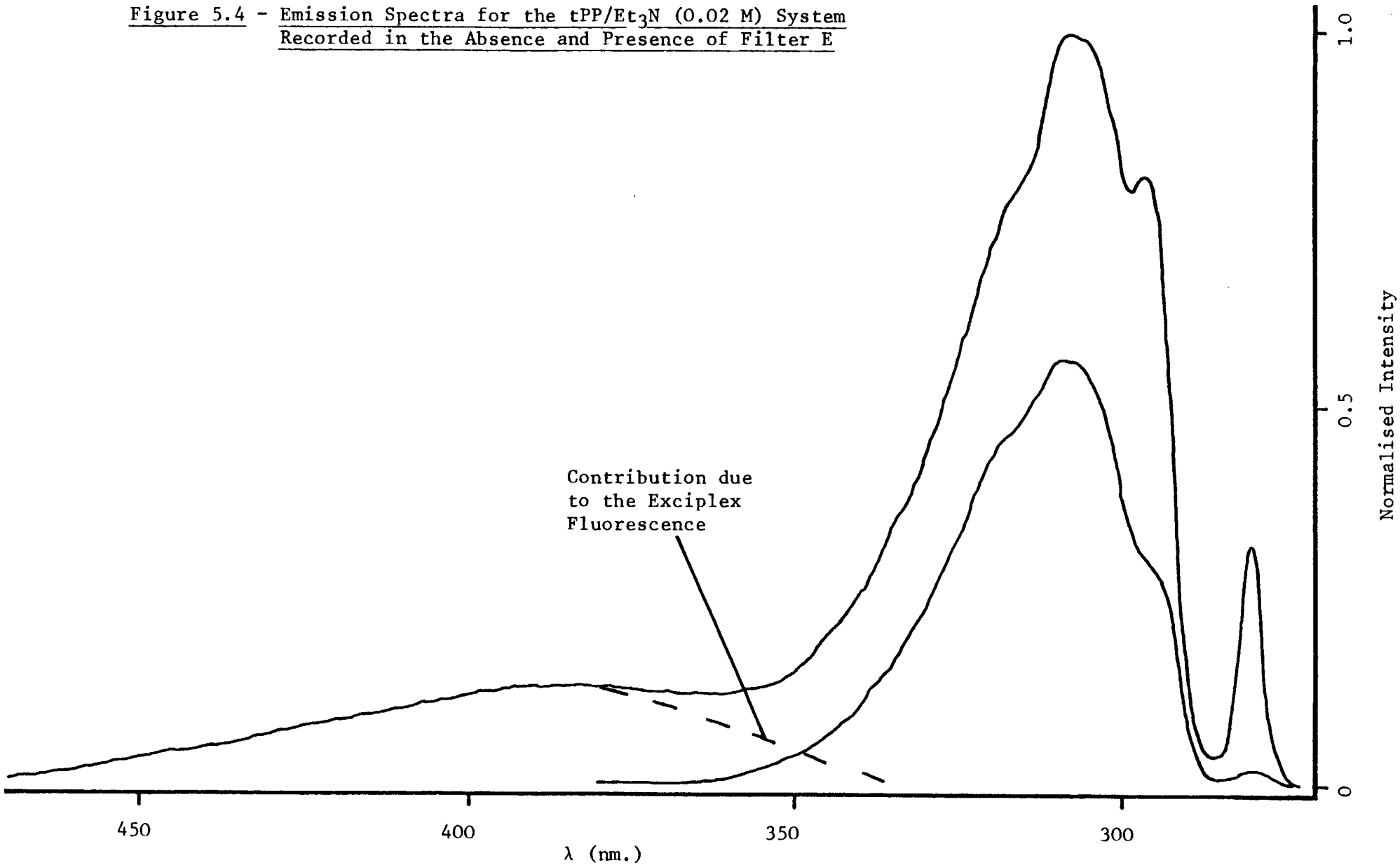

solution of trans phenylprop-1-ene (tPP) in cyclohexane, containing Et_3N (0.02M). It can be seen that, in the presence of these filters, the contribution to the total intensity of light reaching the PMT, which is due to either emission from the tPP/Et_3N exciplex or light scattered at the excitation wavelength (280 nm.) is in fact negligible.

For the purposes of computational analysis, an instrument response function or 'lamp profile' was required for each decay collected. Typically, a fluorescence decay profile was accumulated to the statistically required 10^4 counts in the maximum channel[4] and stored in one memory of the MCA. The sample was then replaced by a piece of aluminium foil, positioned in the cell holder, at 45° to the incident beam. A lamp profile was then collected in the second memory of the MCA, by reflection of the incident light, either:

a) at the excitation wavelength used for the sample, with the filter removed, or

b) through the filter, by alteration of the excitation monochromator to the emission maximum of the sample.

No significant differences were noted in the lifetime data recovered from a) and b) above, i.e. there were no apparent effects due to the variation in response of the PMT with wavelength[5]. Sets of lamp and decay profile data were then transferred from the MCA memories, using an ASR 33 teletype, onto punched paper tape for analysis using the SXFIT and DXFIT programmes kindly supplied by W.R. Ware[6] and modified slightly for use with the ICL 1907 and 2970 computers available

5.1.1 The Pulsed Light Source

The majority of the lifetime data reported here was obtained using a free-running low pressure H_2 flash-lamp as the pulsed light source, the normal operating conditions for which are detailed below in fig. 5.5. A Foster high power (10 W) resistor was used for R, while the capacitance C was simply that stray capacitance associated with the lamp power input connections and the brass box (8.5 x 14.5 x 30 cm) in which the lamp was housed. Under free-running conditions the lamp was allowed to discharge to earth via the Brandenburg 0-30 kV power supply used to provide Vapp. In the free-running configuration,

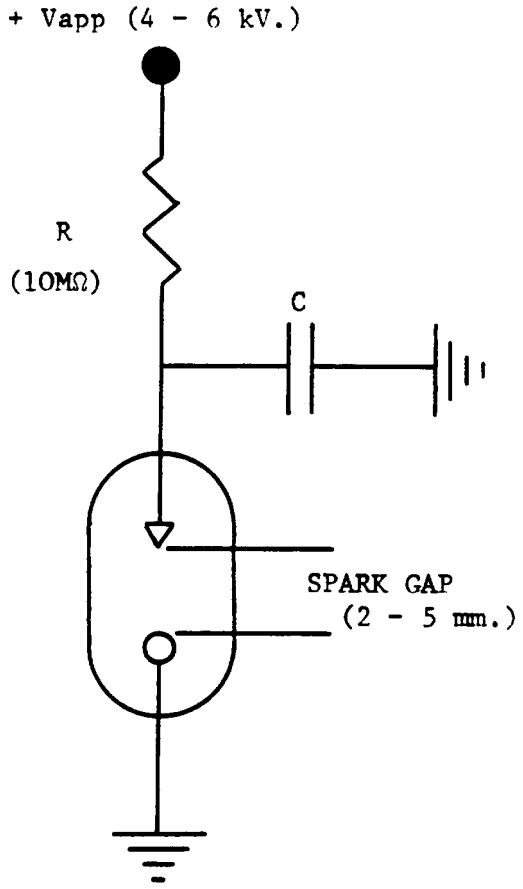

Figure 5.5 - A Representation of the H_2 Flashlamp In the Free-Running Mode

the charging resistor, R, and the capacitance, C, make up a relaxation oscillator in that C charges until the breakdown voltage of the lamp is reached, at which point the lamp fires and the process repeats. The lamp itself was of conventional design, having moveable, tungsten electrodes to allow adjustment of the spark gap and easy access for cleaning and refilling the lamp. Using a low pressure of H_2 as the flashing gas, cleaning was found to be necessary after $\sim$50 hours of operation as black deposits formed on the electrodes, leading to a loss of intensity and broadening of the observed lamp profile. For a given RC time constant, the spark gap, applied voltage and gas pressure could all be varied readily. The dependence of the lamp parameters (i.e. intensity, pulse repetition rate, Full Width at Half Maximum (FWHM), breakdown voltage, etc.) on these variables was found to be as reported elsewhere[7] for lamps of similar design. In

practice, an optimum gas pressure was chosen as 400 $N.cm^{-2}$ of hydrogen and with this parameter fixed, the effects of increasing the distance between the electrodes and the applied voltage are summarised in Table 5.1

Table 5.1

The Effects of Increasing the Spark Gap and Applied Voltage on Various Lamp Parameters, in the Free-Running Mode

Increasing	Breakdown Voltage	Pulse Repetition Rate	FWHM	Count Time
Spark Gap	+	-	+	-
Vapp	0	+	0	-

0 indicates no significant change
+ indicates an increase in that parameter
- indicates a decrease in that parameter

The count time recorded here is the time taken to accumulate a lamp profile, under equivalent conditions (to 10^4 counts in the maximum channel) and as such is an indication of the energy released per pulse. It is interesting to note that widening the spark gap, whilst reducing the pulse repetition rate, actually decreases the count time. This is presumably a result of the fact that there is an increase in the breakdown voltage, which leads to the generation of pulses of greater intensity.

5.1.2 Thyratron Gating of the Lamp

An added refinement, introduced during the course of this work was the provision of a facility for gating the lamp[4]. In this mode, instead of the lamp discharging directly to earth as soon as the breakdown voltage is reached, Vapp may be held off by placing a thyratron between the cathode and earth (see fig. 5.6). Application of a suitable high voltage pulse at the grid of the thyratron will

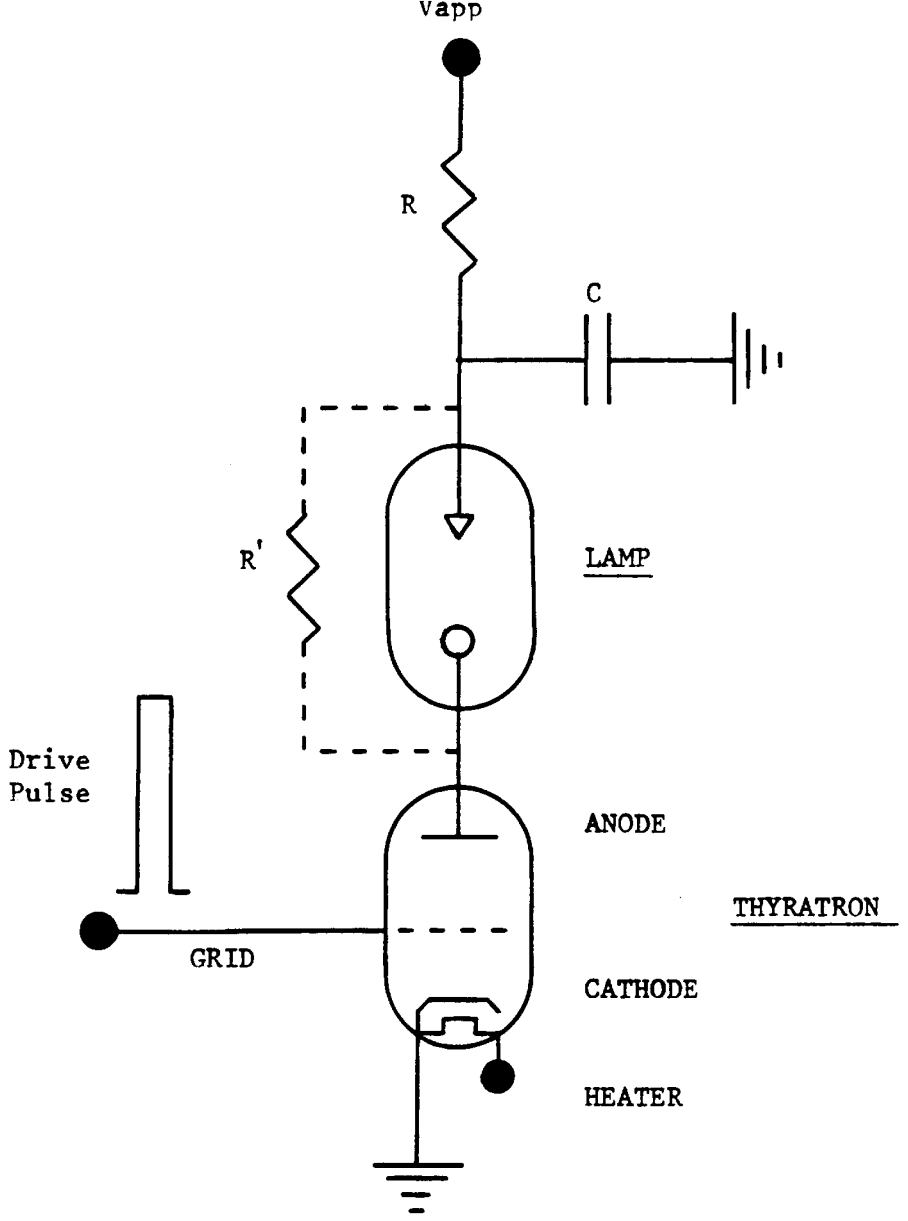

Figure 5.6 - Thyratron Gating of the Low Pressure H_2 Flashlamp

cause it to conduct and at this point, the lamp is free to discharge the held off voltage (now up to ∿3 times the breakdown voltage of the filler gas) through the thyratron to earth.

The thyratron used here was an English Electric model FX2517 positive grid hydrogen thyratron, capable of holding off a maximum of 10 kV. The requirements for the grid pulse needed to cause conduction were:

a) A minimum unloaded grid drive pulse voltage of 175 V;

b) A rate of rise of the grid pulse of >160 $V.\mu s^{-1}$;

c) A grid pulse duration of >2μs.

Figure 5.7a) - Power Supply Circuitry for the Thyratron

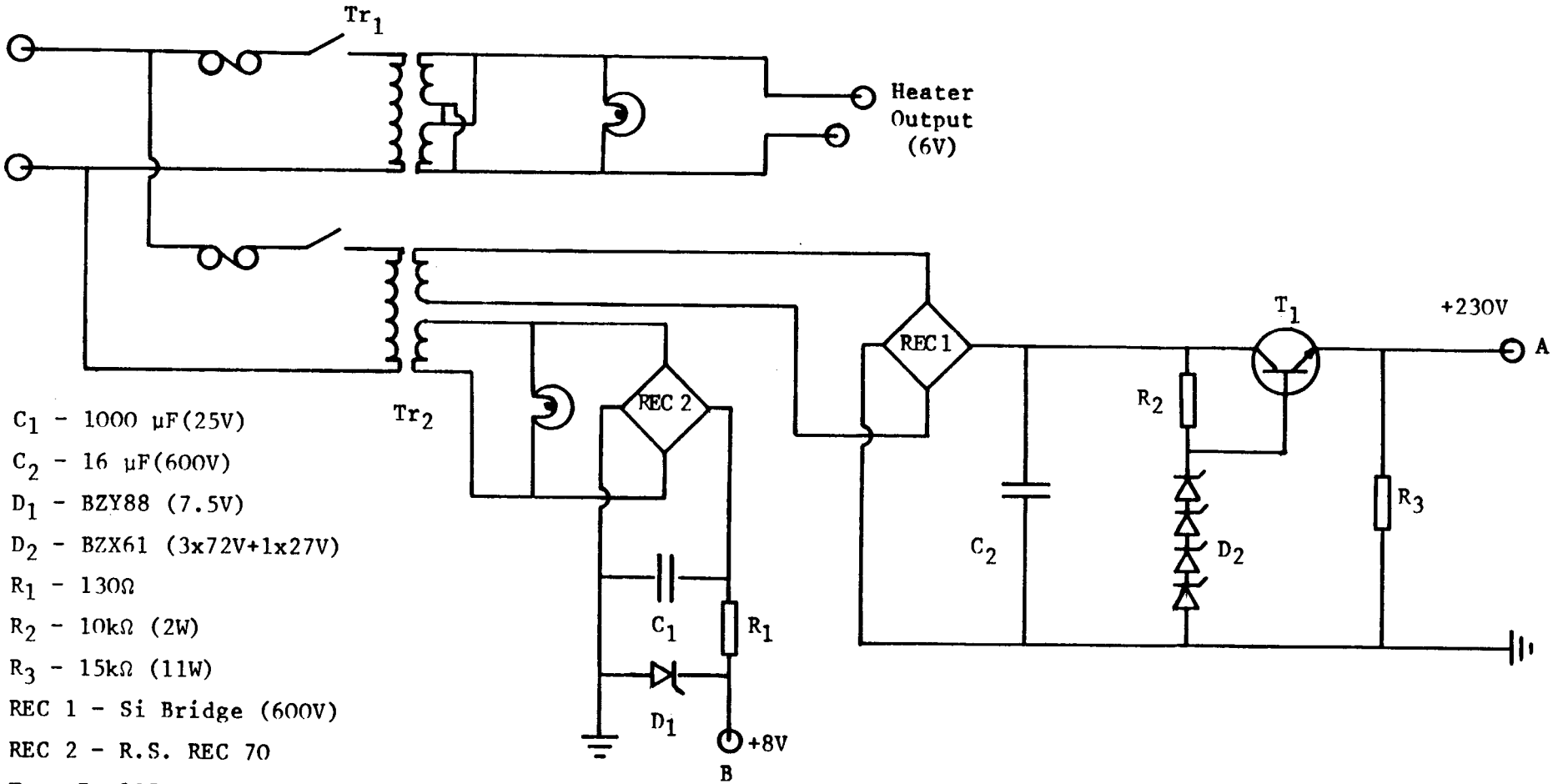

C_1 - 1000 µF(25V)
C_2 - 16 µF(600V)
D_1 - BZY88 (7.5V)
D_2 - BZX61 (3x72V+1x27V)
R_1 - 130Ω
R_2 - 10kΩ (2W)
R_3 - 15kΩ (11W)
REC 1 - Si Bridge (600V)
REC 2 - R.S. REC 70
T_1 - Bu 105
Tr_1 - R.S.50VA
Tr_2 - R.S.h.t.

Figure 5.7b) - The Circuitry used to Provide Thyratron Grid Drive Pulses

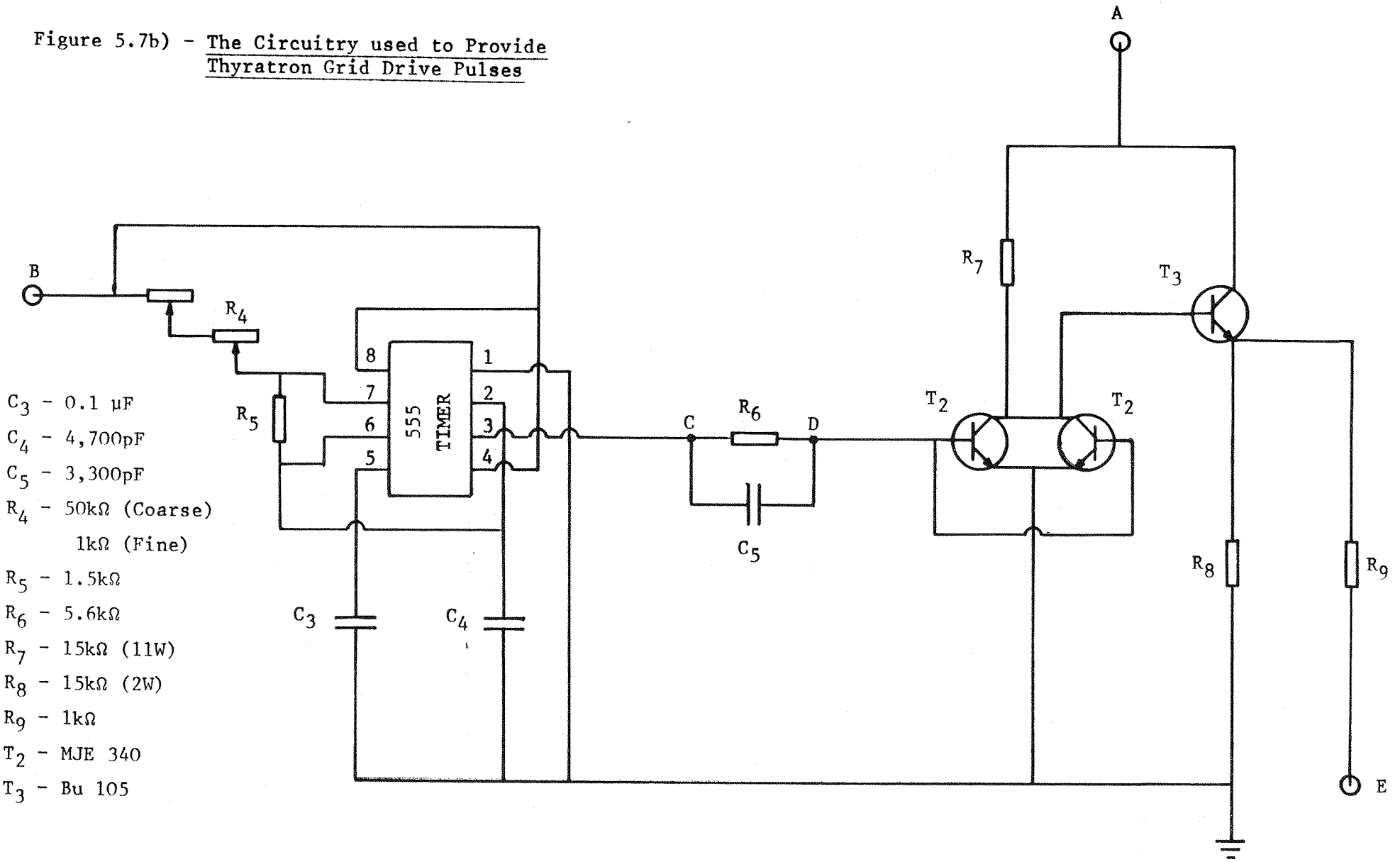

C_3 - 0.1 µF
C_4 - 4,700pF
C_5 - 3,300pF
R_4 - 50kΩ (Coarse)
1kΩ (Fine)
R_5 - 1.5kΩ
R_6 - 5.6kΩ
R_7 - 15kΩ (11W)
R_8 - 15kΩ (2W)
R_9 - 1kΩ
T_2 - MJE 340
T_3 - Bu 105

These conditions were fulfilled utilising the circuits shown above[8] as figs. 5.7 a) and b), based around the Radio Spares 555 timer, acting as an astable oscillator.

The heater voltage for the (titanium hydride) hydrogen reservoir of the thyratron, was provided by the 6 V a.c. output of an R.S. 50VA transformer (Tr_1), while the 250 V and 6.3 V outputs of an R.S. h.t. transformer (Tr_2) were used to supply the grid pulse voltage and the driving voltage for the timer, respectively. The magnitude of the high voltage output at point A was governed by the zener diodes (D2) of the power supply circuit. Pulse shapes, sampled at various points in the circuit, using an oscilloscope, are shown in fig. 5.8 below.

Figure 5.8 - Pulse Shapes Sampled at Various Points in the Thyratron Grid Drive Circuit

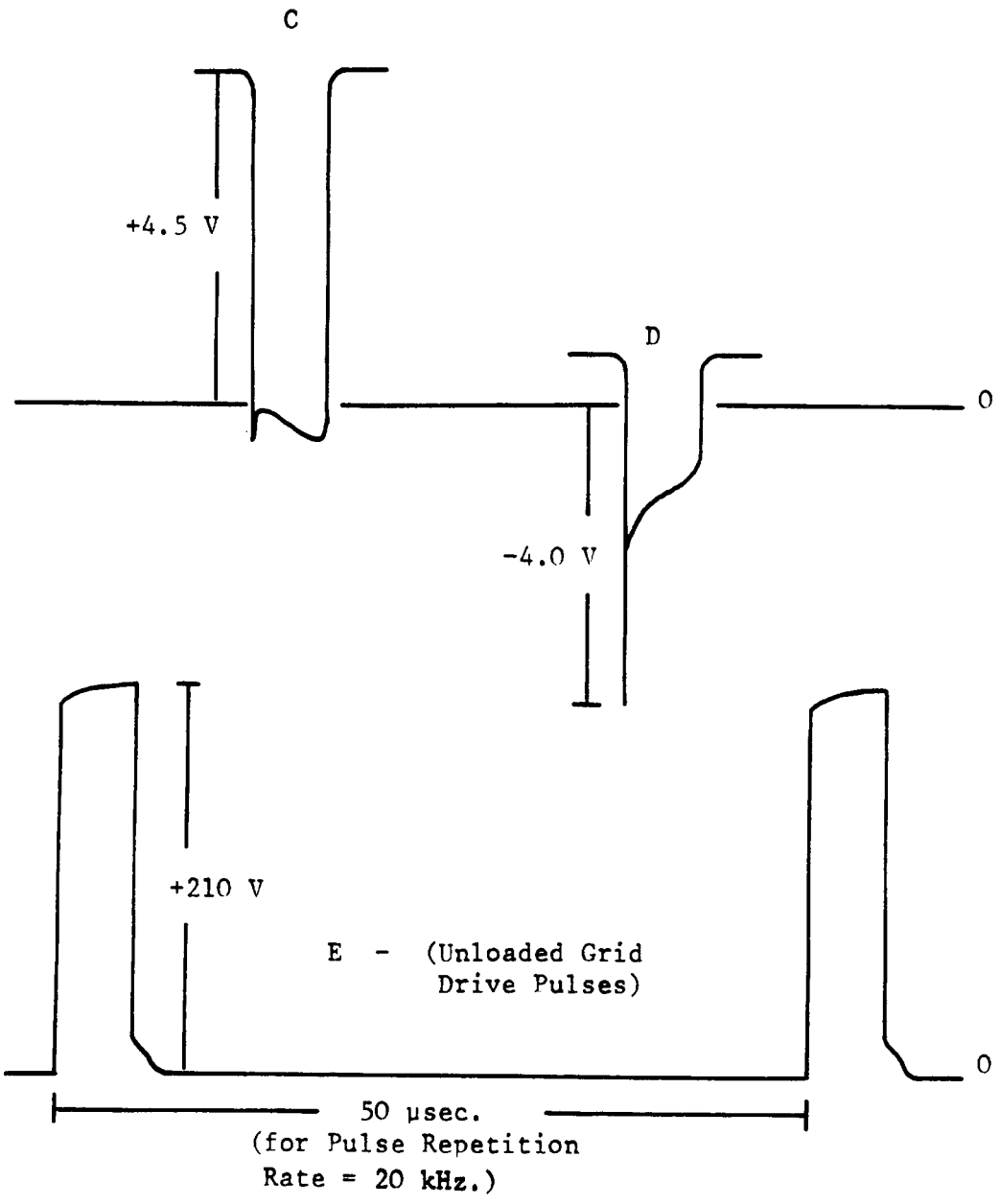

Output pulses from the timer at point C were a.c. coupled to produce negative-going pulses at the base of transistors T_2, (point D). These pulses were thus used to switch off T_2, which in turn allowed pulses to be delivered to the base of T_3, switching the 230 V power output through T_3, to produce the required grid drive pulses at the output E. The pulse repetition rate and grid pulse duration were controlled by R_4 and R_5 respectively. The variable resistors, R_4, allowed coarse and fine adjustments of the repetition rate to be made over the range from 5 to 500 kHz, while R_5 was fixed at 1.5 kΩ, to give a pulse width of ∿5μs (at FWHM).

The thyratron was initially housed in a brass box (8.5 x 12.5 x 20 cm in dimension) adjacent to the lamp housing, with the anode of the thyratron connected via screened u.h.f. cable to the lamp cathode. In this configuration (as illustrated in fig. 5.6) the high voltage applied across the lamp (Vapp) could be held off until grid pulses were delivered to the thyratron, at which point the lamp would commence firing. The thyratron was thus acting as an electronic switch, remaining in a non-conducting state, with a positive voltage at the anode, until such time as a pulse, which was positive with respect to its cathode potential, was applied to the grid. The principle of operation of positive grid hydrogen thyratrons[9], such as the FX2517 used here, is that on application of such a grid drive pulse, a grid-cathode discharge is initiated. Under these conditions the grid 'loses control' and this allows the electrons emitted by the cathode to be accelerated by the anode voltage thus producing a conducting, ionised column of gas, within the thyratron. The tube will then return to a non-conducting state only when the anode voltage has been removed or reversed for a length of time sufficient to allow this charge density to decay below a certain threshold value. At this point the grid is capable of regaining control such that it can once more electrically separate the anode and cathode regions of the thyratron.

Unfortunately, it was found that, with the lamp parameters fixed as outlined in fig. 5.5, although Vapp could indeed be held off initially, as soon as drive pulses were delivered to the grid, the lamp commenced firing at a rate which was in excess of the pulse

repetition rate selected, using R_4 (see fig. 5.7b)). This is illustrated in fig. 5.9a) below, in which an oscilloscope trace of the lamp START pulse profile under these conditions is presented. It can be seen that, while the gating pulse repetition rate had been set at 20 kHz, the lamp was in fact discharging at a rate of around 100 kHz. In other words, it appeared that the thyratron switch was ON (conducting) continuously such that the lamp was allowed to revert to a free-running state. This suggested that after the initial thyratron/lamp discharge, recovery of the tube was incomplete before the breakdown voltage of the lamp had been reached and that this voltage was therefore being re-applied at the anode of the thyratron before the grid was able to regain control.

It can be seen that a lamp discharge rate of 100 kHz represents a time for charging up to the breakdown voltage of the lamp of only 10 μsec. This may be compared to the maximum recovery time of 25 μsec. (for a peak anode current of 100A and re-applied voltage of 1 kV.) quoted[9] in the specifications of the FX2517 thyratron, in the absence of any negative bias at the grid. Thus, it was found to be necessary either to reduce the recovery time of the thyratron or to increase in some way the time taken for the lamp to charge up to its breakdown voltage. The application of a negative bias voltage to hold the grid at a negative potential between pulses would have assisted recovery[9], by helping to reduce the plasma density at the grid. However in practice, it was found to be more convenient to alter the various lamp parameters in order to decrease the lamp pulse repetition rate and thus give the thyratron more time to recover.

For a given gas pressure and applied voltage, this therefore necessitated an increase in the breakdown voltage of the lamp, which could be effected by increasing the spark gap and/or the RC time constant of the system. As noted earlier, increasing the spark gap tends to breaden the lamp profile recorded and this same effect was observed when added capacitance in the form of 2 x 10 pF disk ceramic capacitors (each rated at 6 kV) were introduced in series, between the lamp anode and earth. For the study of relatively short fluorescence lifetimes in the region of 1 ns, a minimum FWHM of the lamp profile was desirable. Initially therefore it was decided simply to increase the value of the charging resistor, R, to 20 MΩ since it was known that this would reduce the pulse repetition rate as required, without

affecting the shape of the lamp profile. An alternative approach however was to connect a resistor across the lamp as suggested by Malmberg[10a]. This resistor (R' in fig. 5.6) prevents the lamp from discharging at all unless it fires within a few microseconds of the thyratron firing and suitable values of R' were found to be capable of preventing the lamp from breaking down prematurely, in the case of the high Vapp required. The value of R' was chosen as 4.1 MΩ, in the form of 5 x 820 kΩ, 2W resistors, as this configuration allowed the lamp to fire at a rate determined by the thyratron over a range of applied voltage from 7 to 10 kV. Figs. 5.9 show oscilloscope traces of the START pulses derived from the lamp under the same conditions in the absence (a)) and presence (b)) of R', with the gating pulse repetition rate set at 20kHz, in each case.

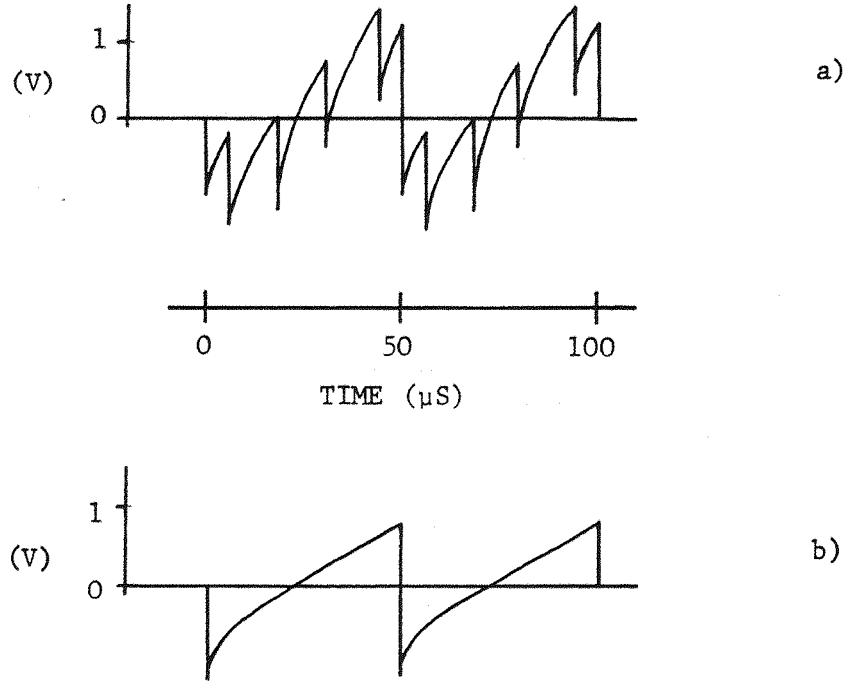

Figure 5.9 - Oscilloscope Traces of the Lamp START Pulses in the Absence and Presence of the Added Resistance R'

As noted already, with the thyratron gating pulse repetition rate set at 20 kHz, in the absence of R', the thyratron was not in control and a lamp pulse repetition rate of 100 kHz was recorded. However with R' in position, it can be seen that, it was only possible for the lamp to discharge the held-off voltage at the rate governed by the thyratron.

The range of applied voltage over which the thyratron was in control of the lamp was found to depend on the value of R'. For lower values of R', e.g. 500 kΩ or 1 MΩ, as used in other similar systems[10a,b]) it was found that in this case, the lamp would not fire at all for Vapp < 10 kV as apparently, the high voltage was being discharged to earth preferentially through R' rather than across the lamp. Also for values of R' greater than approximately 5 MΩ, the effect of this resistor was negated and the lamp reverted to its essentially free-running configuration, which would seem to indicate that the resistance associated with the lamp itself, at the point of breakdown is of a similar order. Thus the value of R' = 4.1 MΩ was chosen as being the optimum value for successful operation of the lamp in the gated mode.

5.2 Fluorescence Spectroscopy

5.2.1 Apparatus

Fluorescence excitation and emission spectra were recorded using either a Farrand MkI spectrofluorimeter, fitted with 'Corrected Excitation and Emission' modules or using a spectrofluorimeter constructed in this laboratory and described in detail in ref. 2. In the case of the latter, a powerful Wotan 450 W high pressure Xenon arc lamp provided the excitation source, the desired excitation wavelength being selected using a Bausch and Lomb High Intensity Monochromator. This permitted the study of systems exhibiting relatively low fluorescence quantum yields ($\Phi_F \gtrsim 10^{-3}$) although the intensity of the output from this source was found to diminish quite rapidly, with decreasing wavelength in the region of ∿300-250 nm. An RCA 935 photodiode was fixed behind the sample holder and in line with the excitation source, to allow measurement of the percentage of light transmitted by the sample solution, relative to the solvent alone. This photodiode also provided a means for correction of excitation spectra, recorded

using this instrument, for the observed variation in the intensity of the lamp output, with wavelength. Radiation emitted by the sample was detected, via a driven Hilger and Watts D330 monochromator (with variable slits) fixed at an angle of 90° to the excitation source, using a Phillips IP28 photomultiplier tube. Using the photodiode noted above, it was ensured that in all cases, the concentration of samples for which the emission spectra were recorded, were such that >80% of the light incident on the sample was in fact transmitted, in order to avoid so-called inner filter effects[11].

5.2.2 Fluorescence Quantum Yield Measurements

The quantum yields of fluorescence (Φ_F) reported in Chapter 2 for the various styrenes studied, were obtained by comparison of the integrated areas beneath the fluorescence spectra of the styrenes with that observed for a reference solution of p-methoxy toluene (MeOT). This compound was chosen as a fluorescence standard here, as it was known that the emission band envelope of MeOT lies in the same spectral region as that of the styrenes, under consideration. Any requirement for correction of the spectra of the sample and reference for variation in the response of the detection system with wavelength, was thus eliminated. These spectra were recorded using two optically matched, degassable 1 cm^2 quartz cells, one of which contained the standard solution of MeOT in cyclohexane, diluted to give an absorbance of approximately 0.1 at the wavelength of excitation (λ_{EXC} = 270 nm). A solution of the styrene under consideration, again in cyclohexane, would be placed in the second cell and diluted until its absorbance at λ_{EXC} matched that of the standard. It was found to be possible to match these absorbances to within an error of $\sim\pm$0.5% by using the photodiode attached to the spectrofluorimeter. Both solutions would then be degassed, using at least three freeze-pump-thaw cycles, (typically pumping down to as low as $\sim 10^{-5}$ $N.cm^{-2}$, using an oil diffusion pump). The fluorescence quantum yield of MeOT in degassed cyclohexane solution, has been reported[11] to have a value of: $\Phi_F = 0.26$. Hence, it was possible to extract the values of Φ_F for the styrenes, using the ratio of the integrated areas beneath the sample and reference fluorescence spectra, according to:

$$\Phi_F(\text{SAMPLE}) = \frac{I_F(\text{SAMPLE})}{I_F(\text{REFERENCE})} \cdot 0.26 \qquad (1)$$

5.3 Photoproduct Formation in the Styrene/Et_3N Systems

5.3.1 Preparative Scale Photolyses

Photolysis of cyclohexane solutions of a number of styrenes, in the presence of Et_3N, was carried out in an immersion well, using a Hanovia 400 Watt, medium pressure Mercury lamp as the excitation source. Cooling for the lamp was provided by circulating, between the lamp and the sample to be irradiated, a cooled filter solution (0.12M Copper (II) Sulphate), the path length of which was 0.5 cm. This enabled the conditions employed for the photophysical studies to be duplicated as closely as possible, in that absorption by the amine present was minimised, as only radiation of wavelength >280 nm. was transmitted by the filter.

The general procedure for the photolyses involved irradiating solutions of the freshly purified styrenes ($\sim 10^{-2}$ - 10^{-3}M) and Et_3N (0.1 - 0.2M) in cyclohexane, which was degassed by bubbling through it dry, oxygen-free nitrogen. The progress of the reactions was monitored using analytical g.l.c. (column E - see Section 5.5a)) and it was found that in general, irradiation times of the order of 1 hour were required to provide an adequate build-up of the various products. In the examples outlined below, significant yellowing of the samples, together with the formation of insoluble, polymeric material was observed on prolonged irradiation. However, it was possible to remove this material by filtration and thus allow the soluble photoproducts to be isolated by preparative scale g.l.c., following evaporation of the solvent and excess amine. In the case of three styrene/Et_3N systems studied here, the results of a structural analysis of the 1:1 photoadducts isolated in this way are given below, in terms of the n.m.r. and mass spectra recorded for these compounds. It may be noted that a more detailed assignment of the n.m.r. data has already been presented for the tPP/ and 2PP/Et_3N adducts, in Section 4.2.

a) Indene/Et_3N

A solution of IND (0.12 g, 7×10^{-3}M) and Et_3N (3.03 g, 0.2M) in degassed cyclohexane (150 ml) was irradiated under the conditions outlined above, for a period of 1 hr. After this time, and following

solvent removal, the product fraction was shown to consist of three major components, present in a ratio of approximately 0.86 : 0.14 : 1.0 (by weight). These were respectively, unreacted IND, Indane (the product of photoreduction of the IND) and the photoadduct, N,N diethyl-1-(1-indanyl) ethylamine. This latter compound was isolated (using Column C) as a clear, colourless liquid (B.pt. = 130°, 1 mm. , Hg.) and was characterised by:

'H n.m.r. 9.12 - 8.4, m, 9H;
8.5 - 6.6, m, 10H;
3.0 - 2.68, m, 4H

M.S.

m/e	Assignment
217	Parent ion (m)
117	m-$\dot{C}H_3CHNEt_2$
116	
101	
100	m - 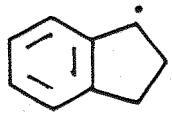 , base
99	
98	

b) Trans-1-phenylprop-1-ene/Et_3N

On irradiation of tPP (0.28 g, 1.2 x 10^{-2}M) in degassed cyclohexane (200 ml), with Et_3N (2.02 g, 0.1M) for 45 min., g.l.c. analysis indicated the presence of four principal components in a ratio of approximately 0.43 : 0.17 : 0.07 : 1.0. These were shown to be respectively unreacted tPP, the corresponding cis isomer (cPP), 1-phenylpropane and the photoadduct 2-diethylamino-3-phenylpentane. Again, the addition product here was analysed, after isolation by preparative g.l.c. (Column C), using n.m.r. and mass spectroscopy.

'H n.m.r. 9.45 - 8.82, m, 11H;
8.8 - 8.0, m, 2H;
7.9 - 6.9, m, 7H;
3.0 - 2.8, m, 5H.

M.S.	m/e	Assignment
	219	Parent ion (m)
	119	m-$CH_3\dot{C}HNEt_2$
	118	
	101	
	100	m - 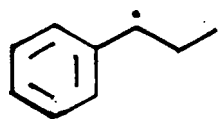 , base
	99	
	98	

c) 2-phenylpropene/Et_3N

On irradiation of 2PP (0.16 g, 7 x 10^{-3}M) in degassed cyclohexane (200 ml), in the presence of Et_3N (4.04 g, 0.2M) for 1 hr., 2-diethylamino-3-methyl-3-phenylbutane was formed, in low yield (∿4% overall), together with a trace amount of 2-phenylpropane. The 1 : 1 photoadduct was characterised in this case by:

^{1}H n.m.r.	
	9.22, d, 3H;
	9.05, t, 6H;
	8.64, s, 6H;
	7.72, q, 4H;
	7.28, q, 1H;
	2.9 - 2.5, m, 5H.

M.S.	m/e	Assignment
	219	Parent ion (m)
	119	m - $CH_3\dot{C}HNEt_2$
	118	
	101	
	100	m - 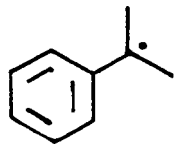 , base
	99	
	98	

u.v. (C_6H_{12})	λ (nm.)	ε
	268	370
	264	500
	257	690
	251	870
	238	1,320

5.3.2 The Measurement of Quantum Yields of Product Formation and Loss of Starting Material

The results, reported in the preceding Chapter, concerning the quantum yields of photoadduct formation (Φ_A), loss of starting material (Φ_{-IND}, Φ_{-tPP}) and photoisomerisation (Φ_{cPP} - derived in the case of the tPP : cPP pair), were obtained using an optical bench irradiation apparatus. This consisted of a Wotan 200W high pressure Mercury lamp as excitation source, a Bausch and Lomb high intensity excitation monochromator and a light-tight box, enclosing the sample cell holder and a photodiode. All irradiations were carried out in a cylindrical, 1 cm. path length, degassable quartz cell and the photodiode was used to monitor sample absorbances and any lamp intensity variations.

An absolute value for the intensity of the lamp output (I_C) was obtained by calibration of the photodiode, using Potassium Ferrioxalate actinometry. Using the technique and solutions described by Murov[12], a value of $I_C = 7.4 \times 10^{16}$ Photons min^{-1} μA^{-1} was derived in this case, at the excitation wavelength employed (λ_{EXC} = 280 nm). This allowed the number of photons absorbed, min^{-1}, (N) under a given set of experimental conditions, to be calculated, according to:

$$N = I_C \cdot I_{SOLV} \left(1 - \frac{I_{SOLN}}{I_{SOLV}}\right) \qquad (2)$$

- where I_{SOLV} and I_{SOLN} represent the transmittances of the solvent and solution respectively. The various quantum yields quoted in Chapter 4 were derived using the familiar expression:

$$\Phi = \frac{\text{Number of Molecules Produced (or Lost), } min^{-1}}{N} \quad (3)$$

By adding an unreactive internal standard, prior to the photolyses, a value for the number of molecules produced (or lost) in each case, was obtained by comparison of the integrated areas under g.l.c. traces of the product and/or starting material, with that of the standard (before and after the irradiation). A convenient g.l.c. standard, for use with Columns E, F and G, was found to be n-Pentadecane and irradiation times were arranged in all cases such that the percentage conversion of starting material was relatively low ($\lesssim 10\%$).

5.4 Sample Purification

a) The Styrenes

Koch Light or BDH 'Reagent Grade' samples of the various styrenes examined (together with N,N dimethylaniline and p-Methoxytoluene) were purified by distillation under nitrogen followed by preparative g.l.c. immediately prior to their use. Columns A and B were found to be particularly useful in this respect, in that conditions could be chosen in which impurities which could not be removed by distillation alone, were readily separable. For example, it was possible to remove traces of Indane from samples of Indene and to separate the commercially supplied 'β-Methyl Styrene' readily into its component cis and trans isomers (cPP and tPP respectively). Although the purity of the samples thus prepared, was examined rather closely using u-v and n.m.r. spectroscopy and analytical g.l.c., no impurities were detected. In a number of cases, the preparative scale g.l.c. was followed by semi-micro vacuum distillation but as this had no apparent effect on the fluorescence decay times of these compounds, this procedure was thought not to be required.

b) The Fluorescence Quenchers

The Triethylamine used in the course of this work as a fluorescence quencher, was again either BDH or Koch Light 'Reagent Grade' material. Purification of the Et_3N was effected by fractional distillation from KOH, under dry, oxygen-free nitrogen, through a fractionating column (46 cm x 2.5 cm, diameter) packed with Fenske helices. Solutions of

the Et_3N thus purified showed negligible absorption and no detectable emissive impurities when irradiated at the wavelengths (280-300 nm) and over the concentration ranges (0.01-0.4M) of interest in the photophysical studies reported here.

Acrylonitrile (BDH) and the other related compounds examined as quenchers of the exciplex fluorescence, were also purified by fractional distillation, prior to their use.

c) Solvents

The solvents used throughout this work were carefully purified, where necessary. The criteria for 'purity' were that they should exhibit 100% transmission (for a 1 cm path length) at wavelengths >250 nm and that there should be no detectable fluorescence from the solvents, at the chosen excitation wavelengths.

Cyclohexane - Cambrian Chemicals cyclohexane was purified in batches of 2½ l. by passing twice through chromatography columns (30 cm x 2.5 cm, diameter), packed with silica (100/200 mesh), discarding the first 250 ml fraction in each case.

Methylcyclohexane - BDH 'Special for Fluorimetry' methylcyclohexane was generally used as supplied.

2-methylbutane (i-Pentane) - BDH 'Special for Fluorimetry' solvent was again generally acceptable as supplied.

Methylene Chloride - Aldrich 'Gold Label' grade solvent was found to be of sufficient purity to be used as supplied.

Perfluoromethylcyclohexane - 'Flutec PPII' solvent grade was used, fluorescent impurities being removed by passing once through an activated alumina column, discarding the initial 10% collected.

Acetonitrile - Aldrich 'Gold Label' acetonitrile was used as supplied, although it was found to be advisable to take care to store the solvent under anhydrous conditions.

N,N dimethylformamide (DMF) - BDH 'Reagent Grade' solvent was purified by distillation twice from P_2O_5, immediately prior to use.

5.5 Other Techniques

a) Gas Liquid Chromatography (g.l.c.)

Analytical and preparative g.l.c. was carried out using a standard Pye-Unicam 104 chromatograph. Glass columns of various lengths and

having internal diameters of 3 mm. (analytical) and 5 mm. (preparative) were used throughout. 'Chromosorb G' was the column support in each case and the liquid phases of the various columns referred to in the text are listed below.

Preparative:

A - 20% QF1/14% XE-60, 7.6 m.

B - 20% SE-30, 4.6 m.

C - 14% XE-60, 1.5 m.

D - 12% FFAP, 1.5 m.

Analytical:

E - 2% QF1, 2.4 m.

F - 5% Carbowax, 1.5 m.

G - 3% XE-60, 6.1 m.

b) Nuclear Magnetic Resonance Spectroscopy (n.m.r.)

The proton n.m.r. spectra reported here were obtained in $CDCl_3$ solution using either a Perkin Elmer R.12 (60 MHz) or Varian XL-100 (100 MHz) spectrometer, the latter operated by Mrs. J.M. Street. Chemical shift data is given in the text as the value in p.p.m. on the τ-scale, relative to Tetramethyl Silane as internal standard (τ = 10p.p.m.). The abbreviations employed to denote the multiplicities of the various absorbances are: s, singlet; d, doublet; t, triplet; q, quartet and m, multiplet.

c) Ultraviolet (u.v.) Spectroscopy

Electronic absorption spectra in the near u.v. region were recorded on Pye-Unicam SP.800 or SP.1800 spectrometers, using optically matched 1 cm. path length quartz cells.

d) Mass Spectroscopy (M.S.)

Mass spectra were obtained, by Mr. A. Wallbridge, using an AEI MS12 spectrometer, with g.l.c./M.S. facility. It may be noted that in order to observe the parent ion peaks for the various styrene/Et_3N photoadducts examined, it was found to be necessary to operate at a low electron energy (15 eV, compared to the standard energy of 70 eV)

e) Photoelectron Spectroscopy (PES)

The photoelectron spectrum of 1,2 dihydronaphthalene was recorded by Mr. J.H. Briggs, using a Perkin Elmer PS 18 spectrometer, with a

sample pressure of 5×10^{-5} N.cm^{-2}.

f) Cyclic Voltammetry

The assistance of Dr. S. Pons was greatly appreciated in obtaining the half-wave reduction potentials, $E_{A^{\ominus}/A}$ (listed in Table 3.2) using the technique of cyclic voltammetry on solutions of the styrenes in purified DMF. Tetrabutyl Ammonium tetrafluoroborate was employed as the supporting electrolyte and the $E_{A^{\ominus}/A}$ values were derived at a Pt electrode (which was flamed prior to each measurement) relative to a Standard Calomel Electrode, as reference.

REFERENCES - CHAPTER 5

1. L.J. Cline Love and L.A. Shaver,
Analyt. Chem., 48, 364 (1976)

2. P.M. Crosby
Ph.D. Thesis, Southampton, (1979)

3a) C. Lewis, W.R. Ware, L.J. Doemeny and T.L. Nemzek,
Rev. Sci. Instrum., 44, 107 (1973)

3b) A.E.W. Knight and B.K. Selinger,
Austral. J. Chem., 26, 1 (1973)

4. W.R. Ware
'Creation and Detection of the Excited State', Vol. 1A
(A.A. Lamola, ed.),
Marcel Dekker, N.Y. (1971)

5. For discussions of this and other proposed sources of instrumental error in the S.P.C. technique, see e.g.

a) Ph. Wahl, J.C. Auchet and B. Donzel,
Rev. Sci. Instrum., 45, 28 (1974).

b) D.K. Wong and A.M. Halpern,
Photochem. Photobiol., 24, 609 (1976).

c) B. Leskorar, C.C. Lo, P.R. Hartig and K. Sauer,
Rev. Sci. Instrum., 47, 1113 (1976)

d) P.R. Hartig, K. Sauer, C.C. Lo and B. Leskovar,
Rev. Sci. Instrum., 47, 1122 (1976).

e) G. Hazan, A. Grinvald, M. Maybach and I.Z. Steinberg,
Rev. Sci. Instrum., 45, 1602 (1974).

6. W.R. Ware,
University of London, Ontario.

7a) J.B. Birks, T.A. King and I.H. Munro
Proc. Phys. Soc., 80, 355 (1962)

7b) I.B. Berlman, O.J. Steingraber and M.J. Benson,
Rev. Sci. Instrum., 39, 54 (1968)

7c) S.S. Brody,
Rev. Sci. Instrum., 28, 1021 (1957).

8a) G. Beddard,
Royal Institution, London,
Personal Communication.

8b) D.J.S. Birch,
Mol. Photochem., 8, 273 (1977)

8c) The assistance of Mr. F.V. Goodfellow is gratefully acknowledged.

9. 'Hydrogen Thyratrons - Preamble',
English Electric Valve Co. Ltd., (1972)

10a) J.H. Malmberg,
Rev. Sci. Instrum., 28, 1027 (1957)

10b) D.J.S. Birch and R.E. Imhof,
J. Phys. E, 10, 1044 (1977).

11. I.B. Berlman,
'Handbook of Fluorescence Spectra of Aromatic Molecules'
(2nd. Ed., A.P., 1971).

12. S.L. Murov,
'Handbook of Photochemistry',
(Marcel Dekker, 1977).